AN AILERON DESIGN TO COUNTER ADVERSE YAW

By

GARY LEE KREPS

Bachelor of Science

Oklahoma State University

Stillwater, Oklahoma

1970

Submitted to the Faculty of the
Graduate College of the
Oklahoma State University
in partial fullfillment of
the requirements for
the Degree of
MASTER OF SCIENCE
July, 1985

AN AILERON DESIGN TO COUNTER

ADVERSE YAW

Thesis Approved:

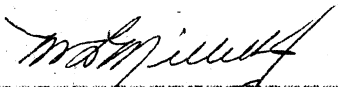

Thesis Adviser

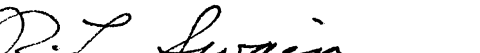

Dean of the Graduate College

PREFACE

The thesis project was chosen to represent an original idea to avoid being an assistant on someone's research project. This research explores an idea developed several years ago but with no suitable opportunity to test. The fact that the idea worked under test has been very satisfying because the idea can be justified completely from the standpoint of aviation safety. An interest in aviation and aeronautical engineering made the subject of this research an appropriate choice for a thesis.

The design proposed is intended for light general aviation aircraft flown by pilots with low experience. The basic principle of this design is to add parasite drag to replace lost induced drag on the aircraft wing when ailerons are displaced. Originally it was predicted that the design would have to be optimized for a narrow speed range. The wind tunnel testing showed that the idea works and can be optimized over a large speed range due to a self modulating effect of the drag. The lift and drag characteristics of the wind tunnel model tested showed that it has promise as a glide path control device also. The design has merit over others used to counter adverse yaw because it is basically a control surface replacement and

could be retrofitted to existing aircraft.

Numerous difficulties were encountered along the way and the success of the project is due in large part to the assistance of others. Special credit must be given to my major adviser, Dr. M. L. Millett, Jr. Dr. Millett is a full time employee of Boeing Military Airplane Co. of Wichita, Kansas. He teaches an aircraft design course at Oklahoma State University in the spring. The time demands of commuting so far to teach a course indicate tremendous dedication to education. Agreeing to be a major adviser for a graduate student placed even greater demands on his time. Having taught aeronautical engineering at Iowa State University for twenty five years, in addition to working in industry, gives Dr. Millett the highest credentials for serving as a thesis adviser on an aeronautical research project.

My other committee members, Dr. Robert L. Swaim and Dr. Flint O. Thomas provided advice, guidance, and encouragement.

Recognition must be given to Wichita State University for making the low speed wind tunnel available at a very reasonable cost.

Marvin Davidson and Hugh Crane of the Walter H. Beech Memorial Wind Tunnel gave valuable advice and assistance in carrying out the experimental phase.

TABLE OF CONTENTS

LIST OF TABLES

LIST OF FIGURES

NOMENCLATURE

Alpha	Angle of attack
AR	Aspect ratio
b	Wing span
Cd	Coefficient of drag
Cd	Coefficient of induced drag
Cd	Coefficient of parasite drag
Cl	Coefficient of lift
Cm	Coefficient of moment
D	drag
e	Oswald wing efficiency factor
f	Equivalent parasite area
L	Lift
L/D	Lift to drag ratio
q	Dynamic pressure
S	Reference area
V	Airspeed
W	Weight
ρ	Air density

CHAPTER I

INTRODUCTION

Adverse yaw is a phenomenon that occurs when ailerons are deflected to turn an airplane in one direction while the nose of the aircraft tends to yaw in the opposite direction. It is an undesirable control response and must be countered. Many methods have been developed but all have shortcomings. The classical solution requires the pilot to overcome the adverse yaw by appropriate rudder deflections. The objective of this research is to examine a means of eliminating the adverse yaw characteristic from the aircraft.

Eliminating adverse yaw would make aircraft control an easier task for the pilot. However there are more compelling reasons for eliminating this undesirable control characteristic. One of the lesser reasons is that failure to counter adverse yaw results in uncoordinated flight and unnatural inertial forces which cause discomfort to passengers.

Enhancement of flying safety alone is adequate to justify determined efforts to eliminate adverse yaw. The stall/spin accident still remains one of the leading types of aviation accident. The pilot inadvertently stalls

the aircraft and fails to recover before striking the ground. In some cases the stall progresses to a spin from which recovery is difficult or impossible. Excessive adverse yaw may result in a spin while the plane is in a stalled condition. Many aircraft roll when entering a stall. Efforts by the pilot to recover level flight by large aileron inputs without coordinated rudder can aggravate the situation and lead to the spin. As will be explained later, an aircraft entering a stall is in the set of conditions which result in the greatest adverse yaw and, at the same time, the pilot is least able to counter it by rudder inputs. Intentional spins performed during flight training are usually entered by a different technique. However this method of spin entry is easy to demonstrate. Eliminating adverse yaw from an aircraft's natural behavior will enhance safety.

Another safety problem involves the common situation of a pilot without instrument flight skills flying into poor weather conditions and losing visual reference. When a person in an aircraft does not have visual reference his sense of orientation is totally unreliable. The human sense of balance functions properly only when in a stationary reference frame. The inertial accelerations of an aircraft in flight result in incorrect attitude sensations. Disorientation on the part of a pilot is referred to as vertigo. If the pilot is disoriented he will make incorrect control inputs in an effort to maintain

level flight. If the pilot is not trained for instrument flight, he may easily panic and make incorrect decisions. The typical accident sequence is one in which the noninstrument pilot inadvertently gets caught in bad weather, becomes disoriented, loses control of the aircraft, and crashes. Such accidents are usually fatal. Uncoordinated flight resulting from adverse yaw is a prime contributor to vertigo. The pilot would have a much better chance of maintaining level flight after losing visual reference if his aircraft was incapable of producing adverse yaw.

The elimination of adverse yaw would therefore be desirable from a safety standpoint. A stall proof aircraft without adverse yaw would be a major improvement over most current general aviation aircraft.

Before being able to counter adverse yaw it is necessary to understand the mechanism that causes it. Quantitative analysis requires the use of rather complex fluid theories. Qualitative study of the mechanism of adverse yaw can be accomplished by a much more straight forward process using physical laws.

An aircraft is supported in level flight by symmetrical distribution of lift on the wings. It is necessary to bank the aircraft to effect a coordinated turn. (Coordinated flight is flight in which all inertial accelerations are perpendicular to the floor of the aircraft.) The bank tilts the lift vector in the desired

direction of turn. The corresponding horizontal component of the lift force provides the horizontal acceleration necessary to accomplish the turn. This is illustrated in Figure 1. Some means are necessary to cause the aircraft to roll about the lateral axis. This is done by altering the lift distribution of the wing to a nonsymmetrical state. This creates unbalanced moments about the longitudinal axis and the aircraft rotates about that axis until symmetry is restored. The Wright brothers initially accomplished this by twisting the wings in flight. Warping the wing structure had many disadvantages. The primary disadvantage was the difficulty of building adequate flexibility for in flight wing warping and at the same time obtaining adequate structural strength and resistance to warping under load. At the higher speeds at which aircraft now operate, wing flutter would be a serious problem. Moveable surfaces (ailerons) were developed to alter the lifting characteristics of the wing. The movement of the ailerons is a differential type of motion to increase lift on one wing while decreasing lift on the other. The ailerons are displaced in opposite directions from their neutral position.

An aircraft in flight experiences drag forces resulting from its movement through the atmosphere. For steady flight to be maintained the drag forces must be maintained in a state of symmetry. Unfortunately, when symmetrical lift is disturbed to roll the aircraft the

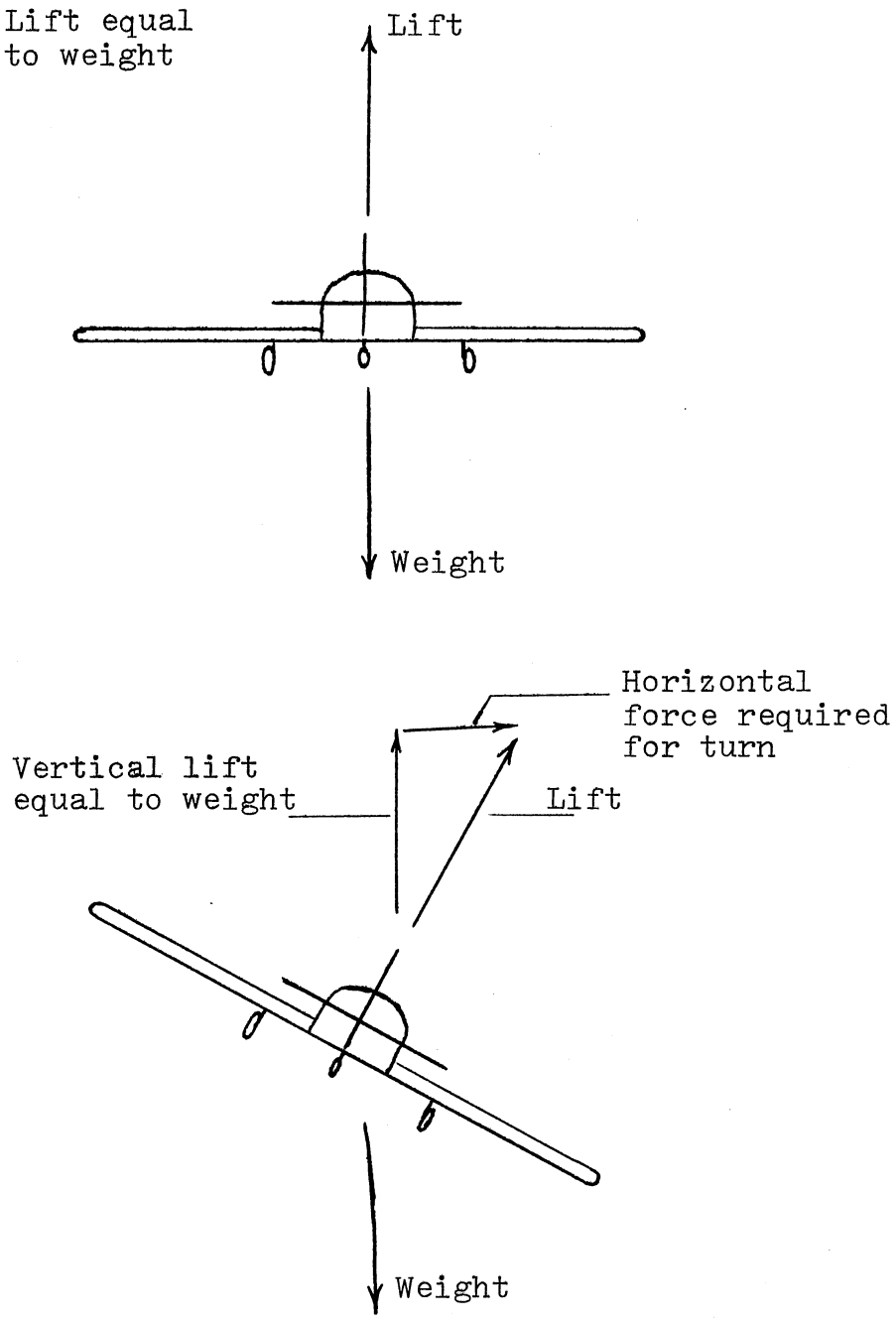

Figure 1. Forces Acting on an Aircraft in Level Flight and in a turn

symmetrical drag is also disturbed opposite to the desired direction of turn. This is the mechanism of adverse yaw. Figure 2 illustrates the lift and drag forces for an aircraft with the controls displaced to cause a roll to the right. Maintaining drag symmetry during a roll would eliminate adverse yaw.

Drag experienced by an aircraft is categorized into parasite drag and induced drag. Parasite drag is the drag that results from resistance to motion through the atmosphere and increases with increasing speed. Induced drag is drag caused by the production of lift. Induced drag is high at low speed and low at high speed. It is not intuitively obvious that induced drag should be inversely proportional to velocity. Further explanation of the functional relationship of drag and velocity is provided in chapter two. Figure 3 illustrates the parasite, induced, and total drag of an aircraft as a function of velocity. Since induced drag plays a key role in the mechanism of adverse yaw it can be seen that adverse yaw will be more pronounced under conditions of high lift and slow speed, the conditions that create high induced drag. This is why an aircraft approaching a stall is in a condition where adverse yaw forces are high. Since dynamic pressures are low at the low speed associated with the stall the aircraft control surfaces have the least capability to counter adverse yaw when the adverse yaw forces are greatest.

Induced drag is a function of lift on the wing.

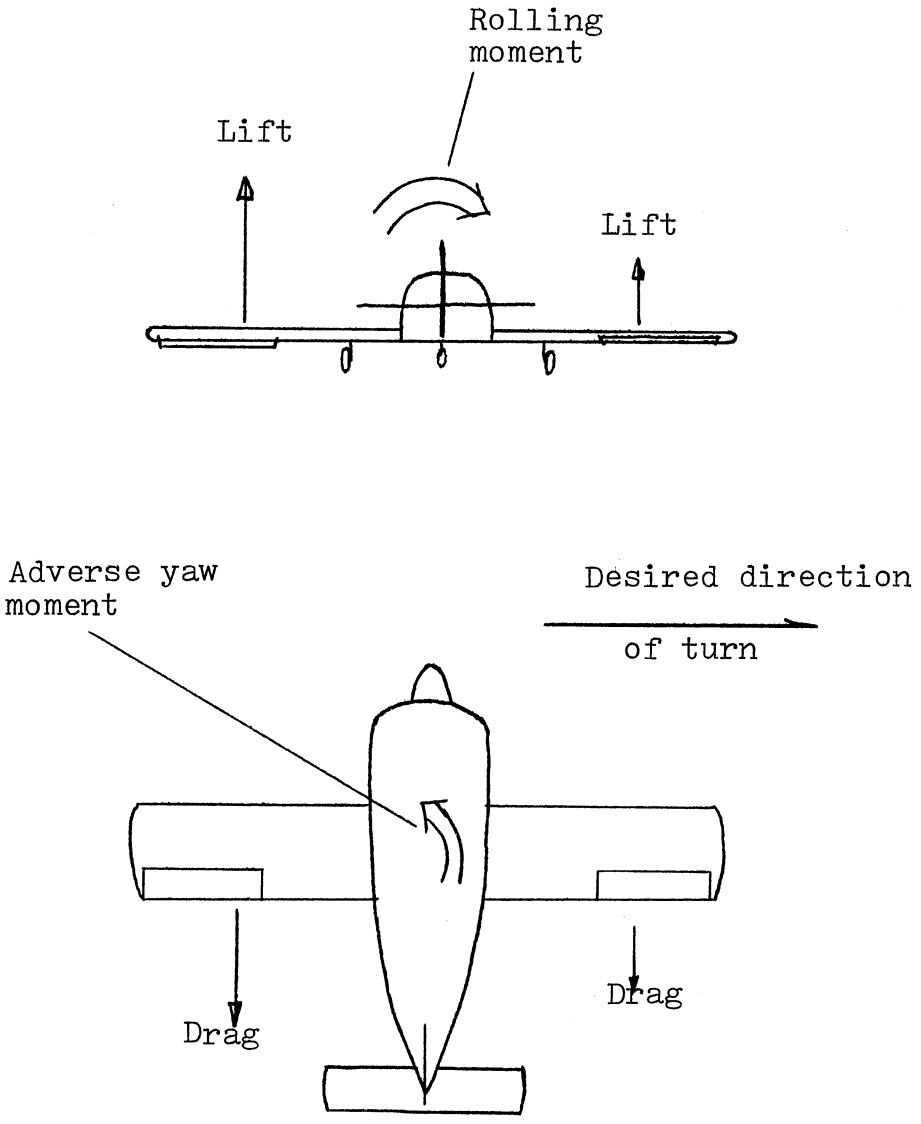

Figure 2. Lift and Drag Forces on an Aircraft with Ailerons Displaced for a Turn to the Right

$$\text{Total Drag} = f\frac{\rho}{2}V^2 + \left(\frac{L}{b}\right)^2 \frac{1}{\pi \frac{\rho}{2} e} \frac{1}{V^2}$$

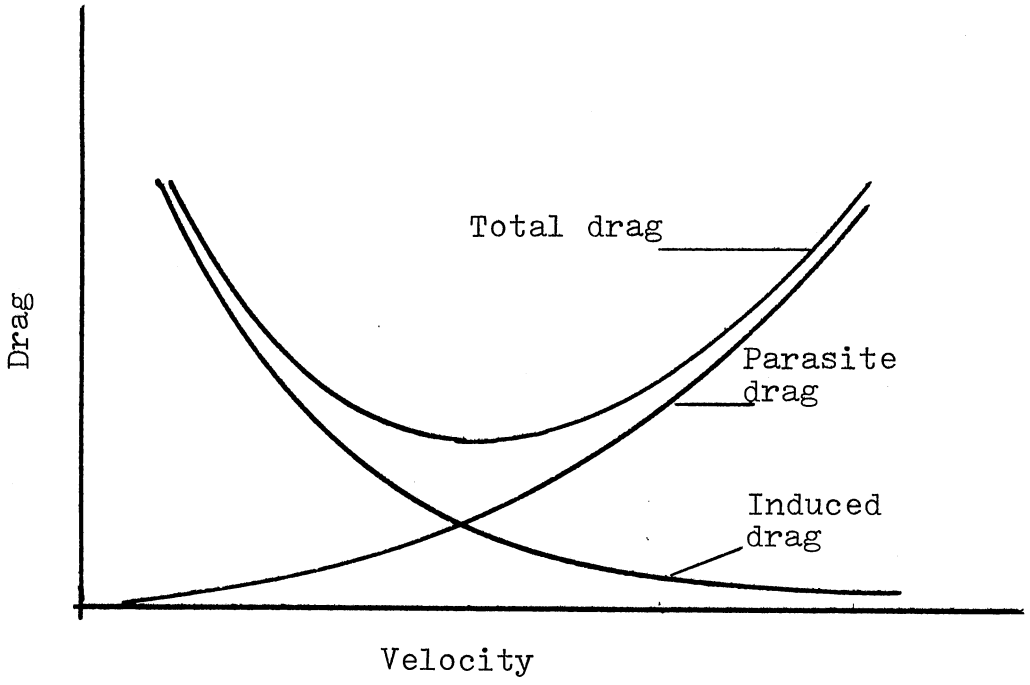

Figure 3. Drag of an Aircraft for Low Subsonic Velocities

Therefore any change in lift will result in a change in the induced drag of the wing. The differential aileron action effects the roll necessary for a turn by modifying the lift distribution of the wing and the drag distribution is altered as a consequence. Unfortunately the drag distribution is altered in such a fashion that it is not symmetrical and the aircraft tends to yaw. If the yaw were in the desired direction of turn it would give a favorable yaw roll coupling. Unfortunately it is in the opposite direction and opposes the turn. This is the situation illustrated in Figure 2. In some situations it can be the dominant factor and result in the aircraft turning in the opposite direction. Ultralight aircraft sometimes experience this condition and they must be turned by the use of wingtip drag devices instead of ailerons. The man powered aircraft recently developed by Paul McCready experienced this difficulty (6). Being able to turn was one of the greatest challenges to the development of the man powered aircraft. The early experimental aircraft built by the Wright brothers also proved difficult to turn because of the effects of adverse yaw. The problem was so great that the aircraft would turn in the direction opposite of the attempted turn due to an unfavorable yaw-roll coupling. It is a mark of their insight and genius that they were able to identify the cause of the problem and provide a solution (4).

Aircraft of the size generally used by individuals for

private flying are not dominated by adverse yaw and can provide satisfactory control by the use of ailerons. However the adverse yaw is still present and a significant consideration for aircraft flown by novice pilots.

Adverse yaw is not considered a problem for large aircraft, such as those used for commercial operations. Large aircraft generally fly at higher speeds where the higher dynamic pressures on the stabilizing surfaces give more resistance to yaw. These aircraft are typically flown by highly experienced and well trained pilots who are not likely to have difficulty controlling the aircraft when adverse yaw forces exist. Large aircraft have autopilots and control augmentation systems capable of overcoming undesirable control characteristics. However, designers of commercial aircraft built for V/STOL operations must still be concerned about the problems of adverse yaw.

The result is that efforts to eliminate adverse yaw from an aircraft's control response are directed at lower speed aircraft piloted by less skilled pilots, i.e., light general aviation aircraft. The economics of these aircraft preclude the use of automated control augmentation systems such as used on large aircraft.

An effective and economical method of eliminating adverse yaw will improve the safety of light aircraft being operated by novice pilots. The design developed in this

research is intended to meet this objective. As will be explained in the following chapters, this design shows the potential to meet the objective of improving flight safety through improved aircraft control.

CHAPTER II

DEVELOPMENT OF THEORY

Classical aerodynamic analysis methods employ the use of coefficients for force measurement. The coefficient is a nondimensional number chosen to fit the following equation:

$$F = C\ q\ S$$

F is the force being measured.

C is the coefficient for the force.

q is the dynamic pressure of the airstream.

S is a reference area.

The type of aircraft considered for this design proposal fly at low subsonic speeds where compressibility is not a factor. For incompressible flow dynamic pressure can be calculated by $q = \rho V^2/2$ where ρ is the air density and V is the speed of the undisturbed airstream relative to the airfoil.

For drag measurements the equation becomes

$$Drag = Cd\ q\ S$$

where Cd is the coefficient of drag. For lift measurements the equation becomes

$$Lift = Cl\ q\ S$$

where Cl is the coefficient of lift.

A similar system can be used for moments by the addition of a length term to the equation.

$$\text{Moment} = Cm\ q\ S\ l$$

where Cm is the coefficient of moment and l is a reference length.

Drag is usually analyzed in two categories. Induced drag is the drag resulting from the production of lift. Parasite drag includes all other sources of drag.

Parasite drag is proportional to the square of velocity and can be expressed as

$$\text{Parasite Drag} = Cd_p\ q\ S$$

where Cd_p is the coefficient of parasite drag. It is desirable to express induced drag in the same way.

$$\text{Induced Drag} = Cd_i\ q\ S$$

where Cd_i is the coefficient of induced drag. Whereas Cd_p remains essentially constant for different angles of attack, Cd_i is totally a function of angle of attack. As indicated in an earlier discussion induced drag is inversely proportional to velocity. Cd_i is a function of angle of attack and angle of attack for an aircraft in flight is related inversely to the velocity.

Classical aerodynamic theory shows that

$$Cd_i = Cl^2 / \pi\ AR\ e$$

where AR is the wing aspect ratio and e is as an efficiency factor to relate lift distribution to the ideal elliptic lift distribution. Therefore as Cl increases the induced drag coefficient increases

exponentially. Since the function of an aileron is to change the Cl of the wing actuation of the aileron will change the induced drag of the wing. This will have the greatest effect when Cl is high, or in other words at high angle of attack or low speeds.

Shevell (12) provides a good development of the lift and drag relationships. The total drag (parasite plus induced) is given by the following equation:

$$D = f \frac{\rho}{2} V^2 + \frac{1}{\pi \frac{\rho}{2} e} \left(\frac{L}{b}\right)^2 \frac{1}{V^2}$$

where f= equivalent parasite area

L= lift

b= wing span.

Collecting constant terms together the equation becomes:

$$D = C_1 V^2 + C_2 / V^2$$

where

$$C_1 = f \frac{\rho}{2}$$

and $$C_2 = \frac{1}{\pi \frac{\rho}{2} e} \left(\frac{L}{b}\right)^2$$

This is the equation illustrated in Figure 3.

The principle of this proposal is an aileron design intended to counter adverse yaw. For conventional aileron design one aileron is displaced downward to roll the aircraft. Lift is increased and the total drag increases due to increased induced drag. The other aileron is displaced upward to reduce lift and the total drag decreases. This unbalances the drag symmetry of the wing and results in a yaw moment. Figure 2 shows the effect for a roll to the right. The

figure also shows that the yaw is to the left, opposite or adverse to the desired direction of turn.

Another type of aileron is proposed to overcome this result of aileron displacement. It is designed to have an upper and lower surface that can be moved independently. The two surfaces move together when displaced downward. This action is identical to that of a conventional aileron. When moved upward, however, only the upper surface is displaced, leaving the lower surface in the neutral position. This results in a split action and the aileron is referred to as a split aileron. Figure 4 illustrates the concept.

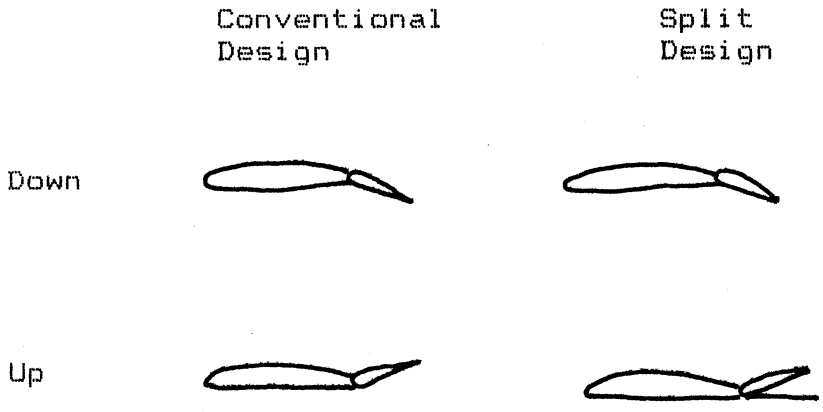

Figure 4. Aileron Profiles.

The split aileron is used on the wing on which the aileron is displaced upward. The deflection of the split aileron increases the parasite drag to balance the loss of induced drag and the increase of drag on the opposite wing. Since induced drag decreases as the square of velocity and parasite drag increases as the square of velocity it is expected that the design must be optimized for a specific velocity. This situation is typical of design activity. Wind tunnel testing of this design has shown that this split aileron design can actually be optimized over a much broader range than might be expected. This is explained in Chapter Six.

CHAPTER III

OTHER METHODS OF COUNTERING ADVERSE YAW

Numerous other methods have been used in the past to deal with adverse yaw. The purpose here is to review other methods and point out their deficiencies, thereby substantiating the need for an improved design.

The most common method has been to train the pilot to input appropriate rudder displacements at the same time ailerons are displaced. This can work fairly well if the pilot is sufficiently skilled. It has the obvious disadvantage of increasing pilot workload. It does not work if the pilot fails to make appropriate inputs. A pilot with low experience cannot be depended upon at times of high stress to make all appropriate inputs consistently. It was pointed out in the introduction that a pilot who is spatially disoriented is at high risk. Another disadvantage is that some situations require the pilot to use the rudder for other purposes. The inputs to counter adverse yaw must be superimposed on the inputs required.

Some aircraft have been designed with the aileron and rudder controls interconnected in such a way that they move at the same time to counter adverse yaw. The pilot displaces the ailerons to effect a turn and the rudder

moves automatically with the ailerons. While this method has some distinct advantages it has been poorly received by pilots. Pilots have been unwilling to give up control of the rudder because they cannot use it for other purposes. This design can only be optimized for a narrow range of speed. The aircraft will be operating off design at any other speed. Interconnecting rudder and ailerons eliminates the capability of making crosswind landings by conventional methods.

Wing spoilers have been used with some success for roll control. Ailerons may not be installed on the aircraft. An upper surface spoiler is displaced to effect a roll by reducing lift on that wing, causing it to sink. The spoiler also increases drag on that wing. One disadvantage is that it alters lift on one wing instead of both. Another problem is that overall wing lift of the aircraft is reduced during the roll since there is no increase of lift on the other wing. The most serious problem with using spoilers is the highly nonlinear control characteristics of spoilers. Without automatic control augmentation systems it is difficult to obtain acceptable flying qualities using spoilers. For small displacements the spoiler gives little control response, but the response can become very pronounced at higher spoiler angles. This would give the pilot a "stuck drawer" effect.

One very interesting design can be found on the Helio aircraft. This aircraft is designed for short field

operation and operates under the conditions which give the greatest adverse yaw forces. The wing has flaps and leading edge slats which enable it to fly at high Cl or low airspeeds. The wings have a large span and the ailerons are on the outer portions of the wing to permit essentially full span flaps. The yaw forces have a large moment arm to create yaw moments. The fact that adverse yaw is a problem on this aircraft is evidenced by the manufacturer adding a device to counter it. A spoiler type device is deflected on the upper surface in front of the aileron. This system may even increase roll rate with positive G loading. This solution would require structural design to carry the loads across the cutouts for the spoilers. Since most aircraft use stressed wing skins for structural integrity these slots would weaken the wing. It would be difficult to retrofit existing aircraft since a major wing redesign would be required. If adequate drag is provided at low speed it would predictably be excessive at high speed. This system will not work under negative G loading. The extra mechanical complexity might also be viewed as a drawback.

Another method is the use of differential displacement of the ailerons. The aileron displaced up is displaced more than the aileron displaced down. This is usually referred to as differential aileron action. The extra displacement of the upward aileron is intended to suffer parasite drag due to the departure from the basic airfoil

shape. This method has proved to be ineffective.

Another method of dealing with adverse yaw is with automated control systems or yaw dampener systems. The cost, weight, and complexity of such systems preclude use on small aircraft where they would be needed most.

CHAPTER IV

WIND TUNNEL TESTING

It was desirable to conduct wind tunnel tests to carefully measure the split aileron performance compared to conventional aileron performance. Since the aileron functions by modifying the wing airfoil it would at first seem appropriate to use two dimensional airfoil testing techniques. Airfoil data is usually determined by two dimensional testing techniques to eliminate wing tip effects. The test wing completely spans the space between two parallel walls oriented perpendicular to the span. Lift and drag values are determined with pitot static probe measurements and application of momentum theory. Rae and Pope (10) point out that this method is invalid for any flow with separation. An aileron operates in the area of the wing where some separation exists and the split aileron concept is intended to cause additional separation. Therefore two dimensional testing will not provide proper data.

Direct force measurement in two dimensional testing is difficult because the wing must touch the end plate walls. Even very small gaps at the wing tips cause large measurement errors (10). It is difficult to separate

forces acting on the wing from forces acting on the end plates.

Two dimensional testing of this concept is not desirable in any case. The reason for the difference between two dimensional and three dimensional airfoil performance is the alteration of flow characteristics caused by the wingtips. The flow in the region of the wingtips is drastically different from two dimensional behavior and this is the very region in which the ailerons operate. Additionally each aileron has two wingtips of its own. Therefore meaningful testing must be done in a three dimensional mode with proportions similar to the type of aircraft intended to incorporate this concept.

Lift and drag performance is also sensitive to Reynolds number (RN). Previous wind tunnel experience has shown that results obtained at RN of one million are valid up to about twenty five million (10). Since the aircraft of interest for this design operate at Reynolds numbers between two and seven million, it is important that the testing be accomplished at RN of one million or higher. This rules out the use of small slow speed wind tunnels.

For this test the Walter H. Beech Memorial Wind Tunnel at Wichita State University was chosen. This tunnel has a 7 X 10 foot test section and can operate at Reynolds number in excess of one million at the test section. This tunnel is highly automated and computerized to provide corrections for wind tunnel errors, i.e., blockage, buoyancy, etc. The

data produced by this tunnel is of the highest quality and well suited to the requirements of this test. A complete description of the test facility can be found in reference two.

A model simulating a small general aviation aircraft was constructed to obtain realistic results. A NACA 23015 airfoil section was chosen for the model. Although the actual airfoil section selected is not relevant to the purpose of the test, it is important that the airfoil chosen have no unusual characteristics. This eliminates the possibility of obtaining unusual test results due to some unique feature of the airfoil. The NACA 23015 airfoil is typical of that used on general aviation aircraft.

Although airflow over a fuselage is not normally influenced by ailerons, a fuselage does cause interference on the wing flow characteristics and separation at the fuselage wing junction. Therefore the test model wing was equipped with a fuselage to simulate the real world environment. An empennage was not used because it has no bearing on wing performance and is difficult to simulate realistically in the wind tunnel. Since the tunnel walls alter the downwash behind the wing, the tunnel environment is not the same as the free stream flow case unless the model is small for the test section. This in turn will result in a low Reynolds number. Use of an empennage for wing testing can therefore cause distortion of the results.

Since a wind tunnel is bounded flow there are many

limitations to the use of wind tunnel data. Wind tunnel data must be corrected for many sources of error and these sources must be minimized by careful model design and testing procedure. Reference nine gives a good development for low speed wind tunnel corrections. One of the advantages of the Walter H. Beech memorial wind tunnel is the capability to remove the errors and produce corrected output for the experimenter. This data output is produced on line by computer and the experimenter can observe results as the test is in progress.

The experimenter provides the tunnel operator with a list of correction parameters before the test is started. These parameters are entered into the computer data reduction program. The details of data reduction and error removal can be found in references five and nine. The parameters calculated for this test are found on the first page of Appendix B. The details of the test model construction can be found in Appendix A.

Ideally the test sequence might be set up with the wing at a certain angle of attack and then test data could be taken for all possible control surface configurations. Since this data is needed for many angle of attack settings it would require that this sequence be repeated for each angle of attack. Since the wind tunnel must be shut down to change model configuration this would be very time consuming.

The actual test was run by setting a specific control

surface configuration and then cycling the test model through all angles of attack of interest. Since the angle of attack could be altered by remote control with the tunnel in operation this sequence resulted in considerable time savings.

Since performance at a negative angle of attack is of interest for a control surface some testing at negative angle of attack is required. Also performance in the stall mode must be tested to determine any unusual behavior that may occur. A range of minus six degrees to stall (approximately 18 degrees) was chosen for the test to meet these objectives. The control surfaces were built for deflections from fifteen degrees down to eighteen degrees up in three degree increments. The upward deflection was available in both normal and split mode.

Run 1 was made with the ailerons in normal position to obtain basic model characteristics. Run 2 was made with both ailerons down fifteen degrees. Subsequent runs were made with the ailerons elevated at increments of three degrees until full deflection of eighteen degrees was obtained. Run 13 was made with the left aileron full down and the right aileron full up. This measured the maximum rolling moment capability in normal mode. On run 14 the left aileron was remained down but the right aileron was now split to full open position. This measured maximum rolling moment capability in split mode operation. Runs 15 through 20 were then made with increments of split opening

on both from three degrees to eighteen degrees. This provided a data base for comparing conventional versus split mode lift and drag characteristics. Table I shows the testing sequence.

The test data output is in numerical and graphical form. Appendix B contains the numerical output which shows force and moment coefficients as a function of angle of attack. Dynamic pressure, mach number, and effective Reynolds number are listed for each run. Appendix C contains computer generated plots for coefficients of lift, drag, pitching moment, and rolling moment as a function of angle of attack.

Although care was taken to set angles of attack to consistent values, i.e., 2,4,6, etc., it can be seen in the numerical output that the actual angles of attack vary from one run to another. Angle of attack is one of the parameters in wind tunnel testing that requires correction. The values shown in the numerical output are corrected values.

This creates a slight inconvenience in the use of the data. Since the data points in the listings are not at a consistent set of angles of attack interpolations must be made. Linear interpolation is not suitable because the plots show substantial curvature at places.

A computer program was written to interpolate using the cubic spline technique of numerical methods. This is a classical mathematical approach which gives good results

TABLE I

WIND TUNNEL TESTING SEQUENCE

60 PSF dynamic pressure

RUN NUMBER	CONFIGURATION
1	Clean
2	15 down
3	12 down
4	9 down
5	6 down
6	3 down
7	3 up
8	6 up
9	9 up
10	12 up
11	15 up
12	18 up
13	Left 15 down Right 18 up
14	Left 15 down Right 18 split
15	3 split
16	6 split
17	9 split
18	12 split
19	15 split
20	18 split

Note: On runs 1-12 and 15-20, both ailerons have identical deflections.

when the explicit functional form for a data set is not known. The interpolation program was used to produce coefficients for nonvarying angles of attack. Due to length and complexity the computer routine is not published with this thesis. It is, however, available from the author.

The interpolated data sets are used primarily for making comparisons of multiple test runs. The graphical plots are used for qualitative interpretations on specific runs.

CHAPTER V

RESULTS OF TESTING

The wind tunnel tests produced some very useful data. Examination of the graphical coefficient plots (found in the appendices) shows the characteristics of the model and analysis of the numerical data reveals the information sought from the test.

Table I of chapter four shows the wind tunnel testing sequence. Run number one is the basic model performance with no control deflections. The Cl versus angle of attack curve is typical for wing airfoils. The curve is essentially linear until near the stall. A very slight nonlinearity occurs around twelve degrees angle of attack. The stall portion occurs over a fairly large range of angle of attack. If this curve represented an actual aircraft it would indicate excellent flying qualities because the stall is gradual with sufficient warning to the pilot that the stall is imminent.

The Cd versus angle of attack is typical with a minimum drag at just under zero degrees angle of attack. For the NACA 23015 airfoil used this is expected. A noticeable discontinuity occurs at around twelve degrees

angle of attack and a small discontinuity in the stall region.

The fuselage acts as a lifting body and contributes to lift until it stalls. It is a streamline body with low fineness ratio. One characteristic of such streamline bodies is a positive pitching moment whereas the airfoil has a very slight negative pitching moment. The pitching moment curve shows that Cm is positive but takes a drop to near zero at about twelve degrees angle of attack. This is good evidence of a change of flow characteristics on the lifting body. It is obvious that something is happening in the region of twelve degrees angle of attack. Examination of all of the plots shows that this occurred on all twenty runs and at approximately the same angle of attack. The curve discontinuity can be found on the plots for lift, drag, pitching moment, and rolling moment. Very convincing evidence can be found in the moment coefficient curves to indicate that wing root separation is occurring here along with separation on part of the fuselage body.

When the lifting body stalls it would be expected that wing root separation would occur at the same time. This would cause a slight change in wing lift and pitching moment. The rolling moment changes at twelve degrees angle of attack and the right wing root separation is greater than the left wing root separation.

This accounts for a slight loss in the lift as the angle of attack is increased through this region, for the

sudden increase in drag, and for moment curve fluctuations. Since the expected results of wing root separation are found in all of the curves, this is the likely explanation for the behavior in the twelve degree angle of attack region.

The cause of the fluctuation in the stall region can be found in the rolling moment curves. It is impossible to build an aircraft so that both wings stall precisely at the same time. Rolling moments change significantly when a nonsymmetrical stall occurs. The rolling moment curves indicate this change. The first drop in the lift curve is small and represents another indication that the stall transition is gradual.

Plots of drag coefficient versus aileron deflection were prepared for several wing angles of attack to examine the results of the aileron performance (Figures 4 through 10). These plots show the drag characteristics of the split aileron along with the conventional aileron. At small negative angles of attack there is no significant difference. At small positive angles of attack there is a small increase in drag with the split configuration. For high angles of attack the drag increase is progressively higher. Figure 9 shows some erratic behavior. This plot is at twelve degrees angle of attack where drag characteristics are changing due to lifting body and wing root flow separation. A mutual interference is apparently occurring where the upward aileron deflections are

influencing the fuselage and wing root separations. Remnants of this behavior are still apparent at fifteen degrees angle of attack (Figure 10).

The lift to drag ratio (L/D), is a useful parameter for indicating aircraft performance and is the glide ratio of the aircraft. A high L/D implies an aerodynamically clean aircraft capable of a long glide at a shallow angle and low L/D implies a steep glide angle. Figure 11 was prepared to show the affect of the split ailerons on the L/D ratio for the model.

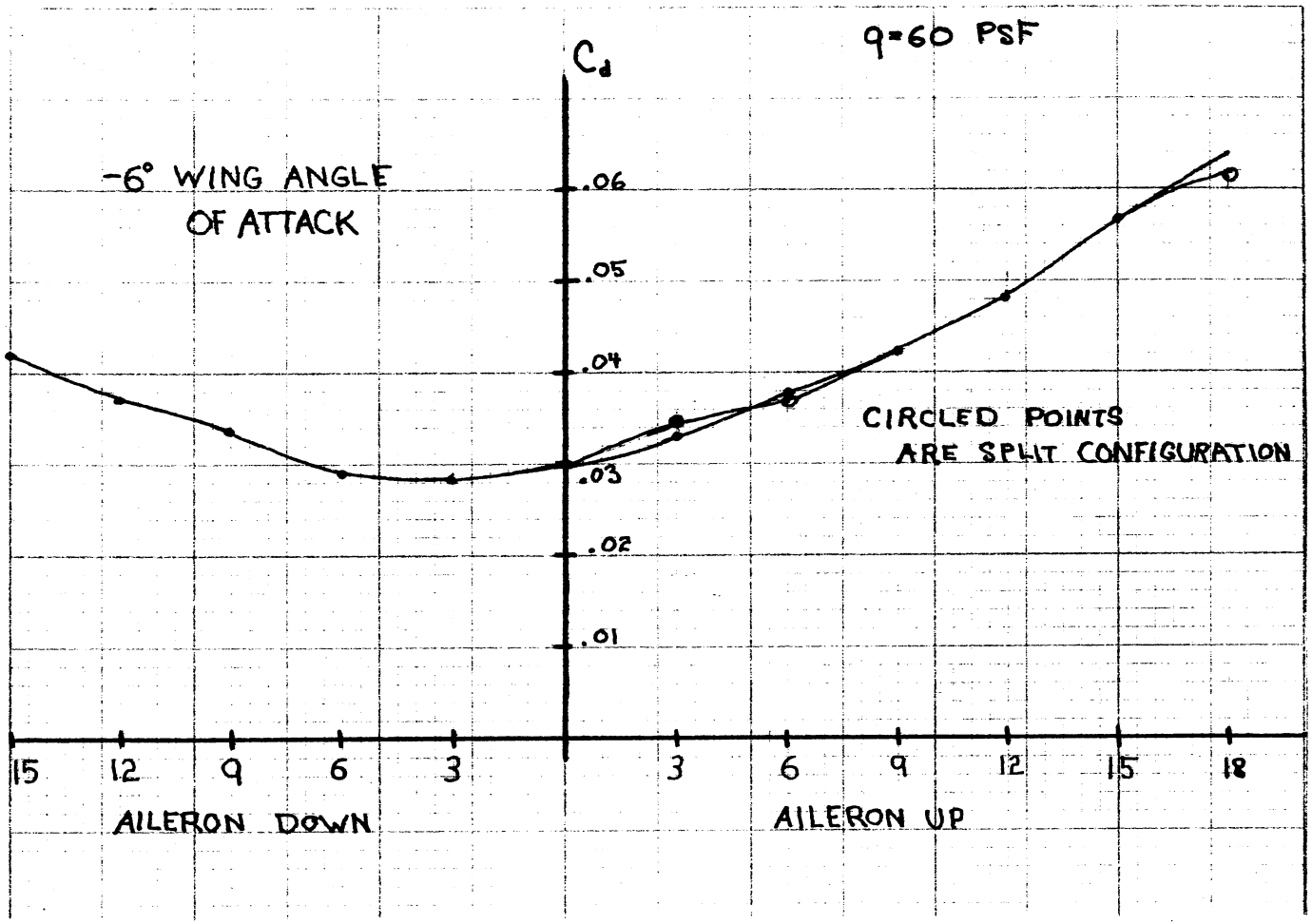

Figure 5. Drag Curves at -6 Degrees Angle of Attack

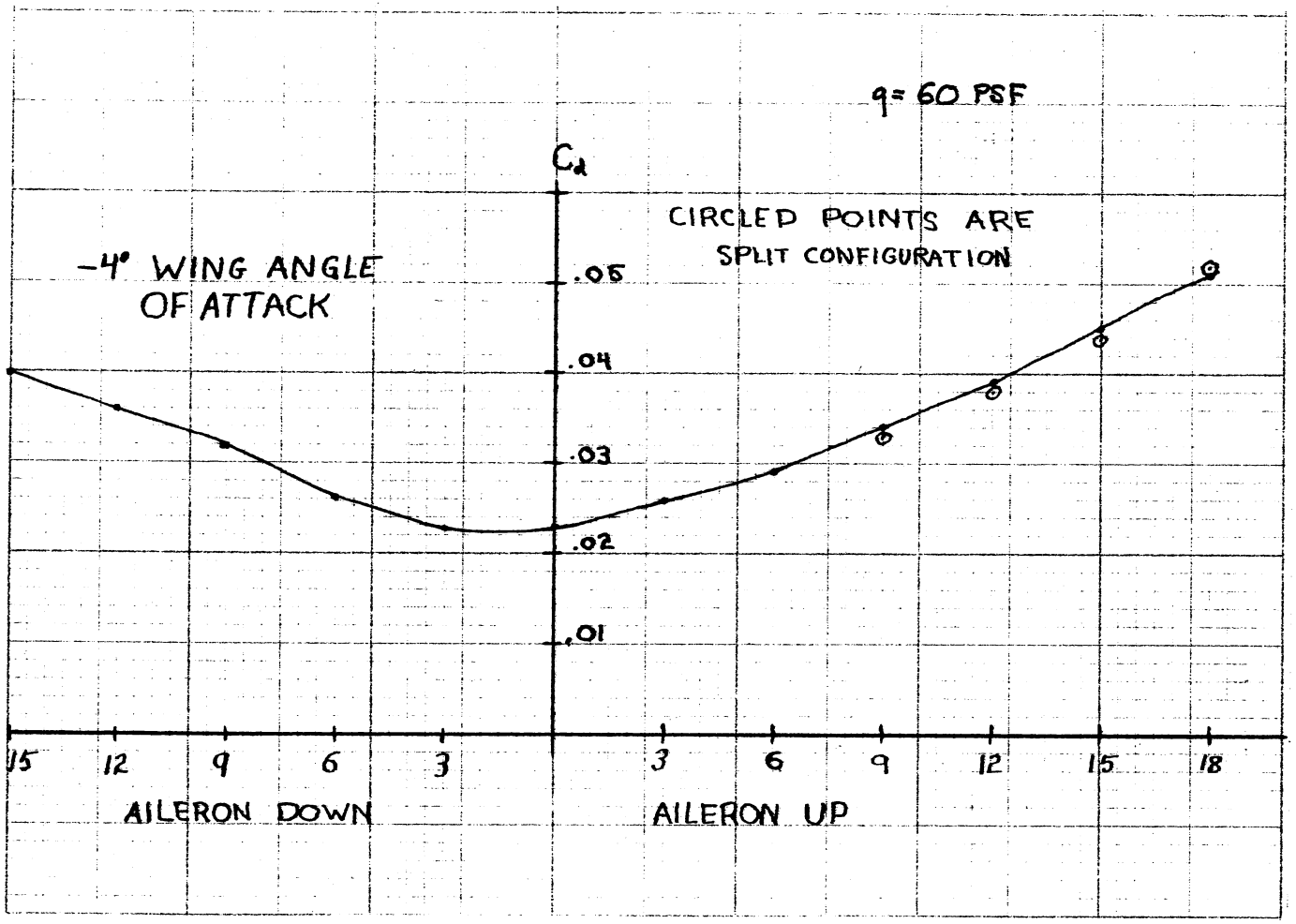

Figure 6. Drag Curves at -4 Degrees Angle of Attack

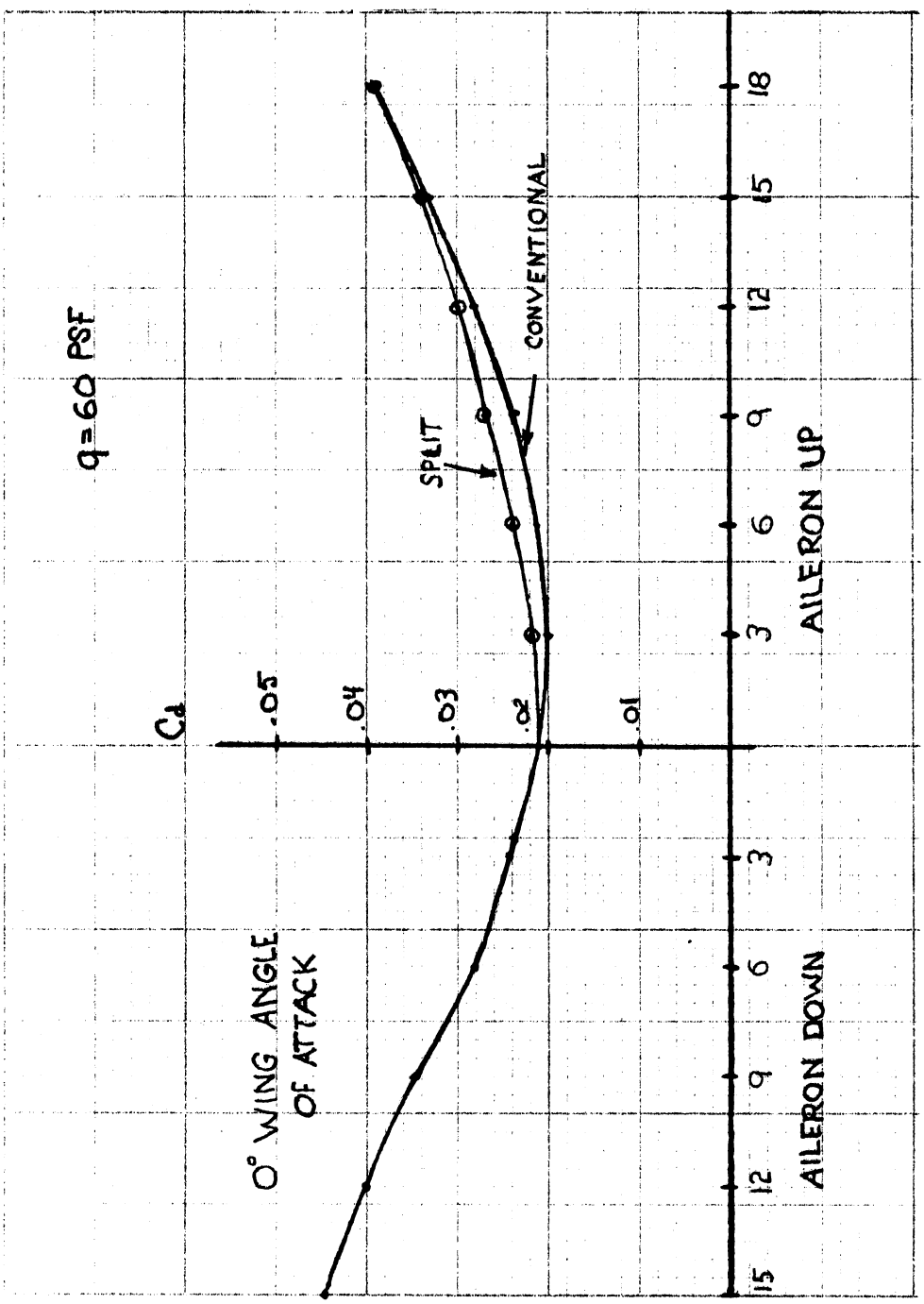

Figure 7. Drag Curves at 0 Degrees Angle of Attack

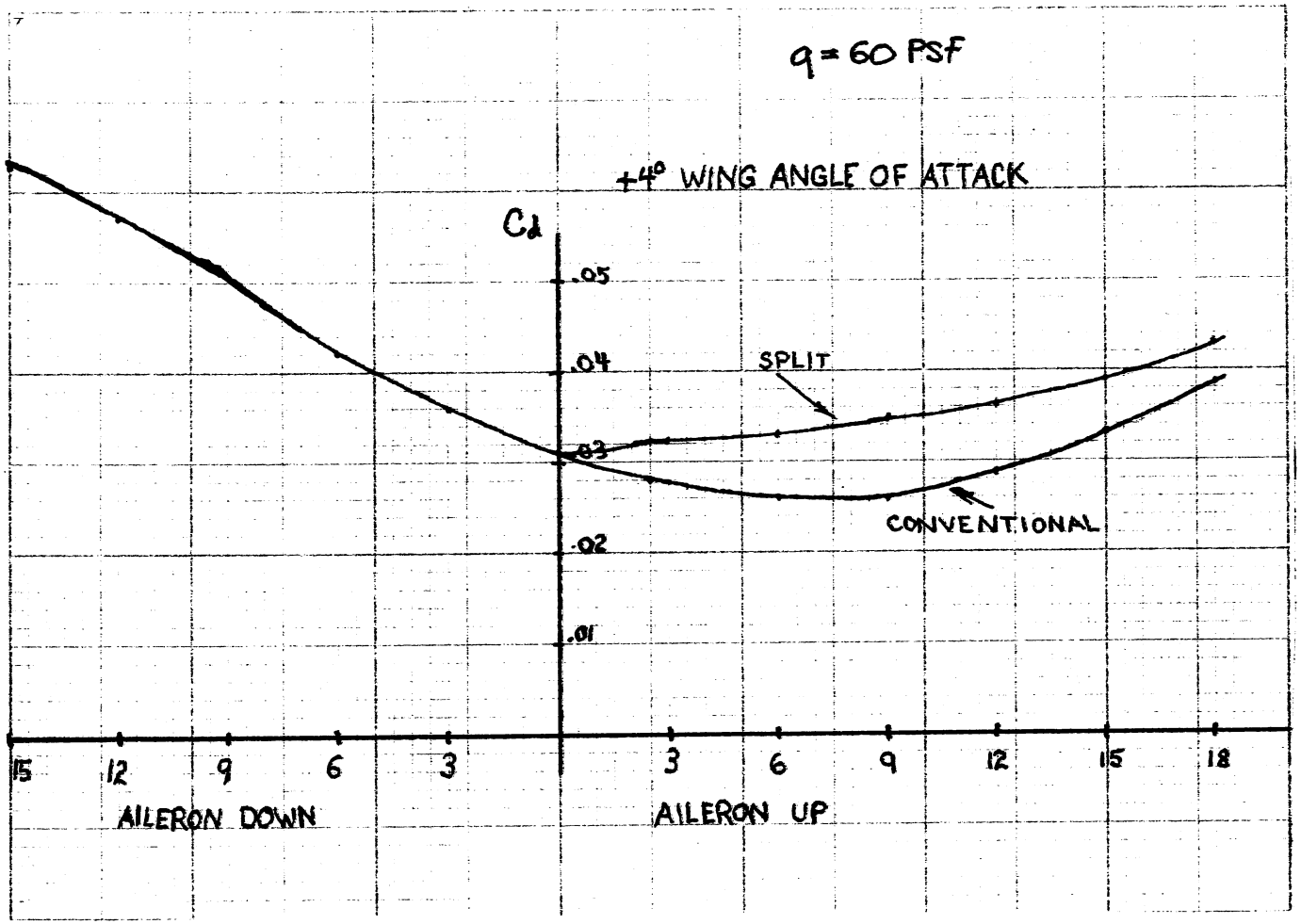

Figure 8. Drag Curves at 4 Degrees Angle of Attack

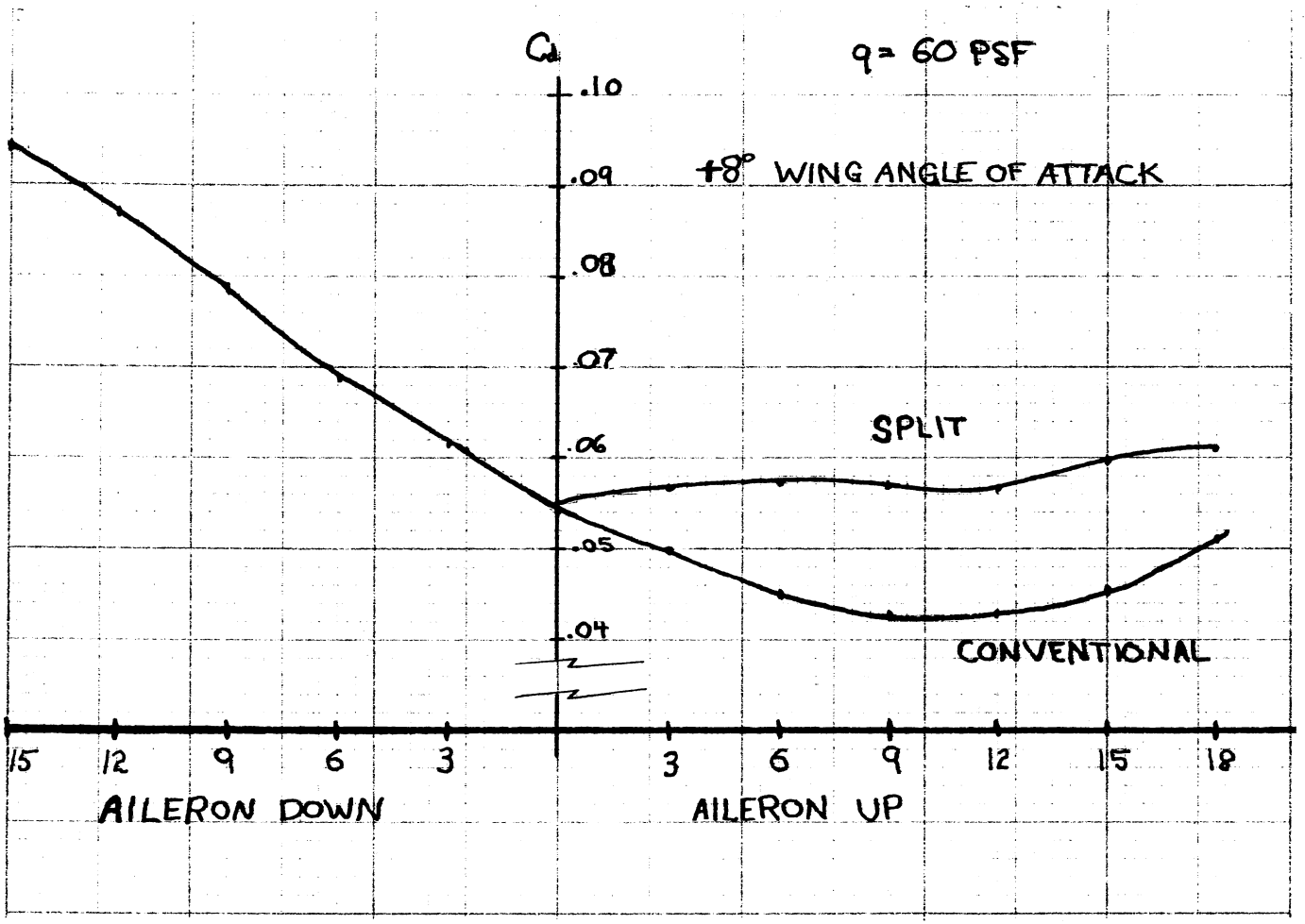

Figure 9. Drag Curves at 8 Degrees Angle of Attack

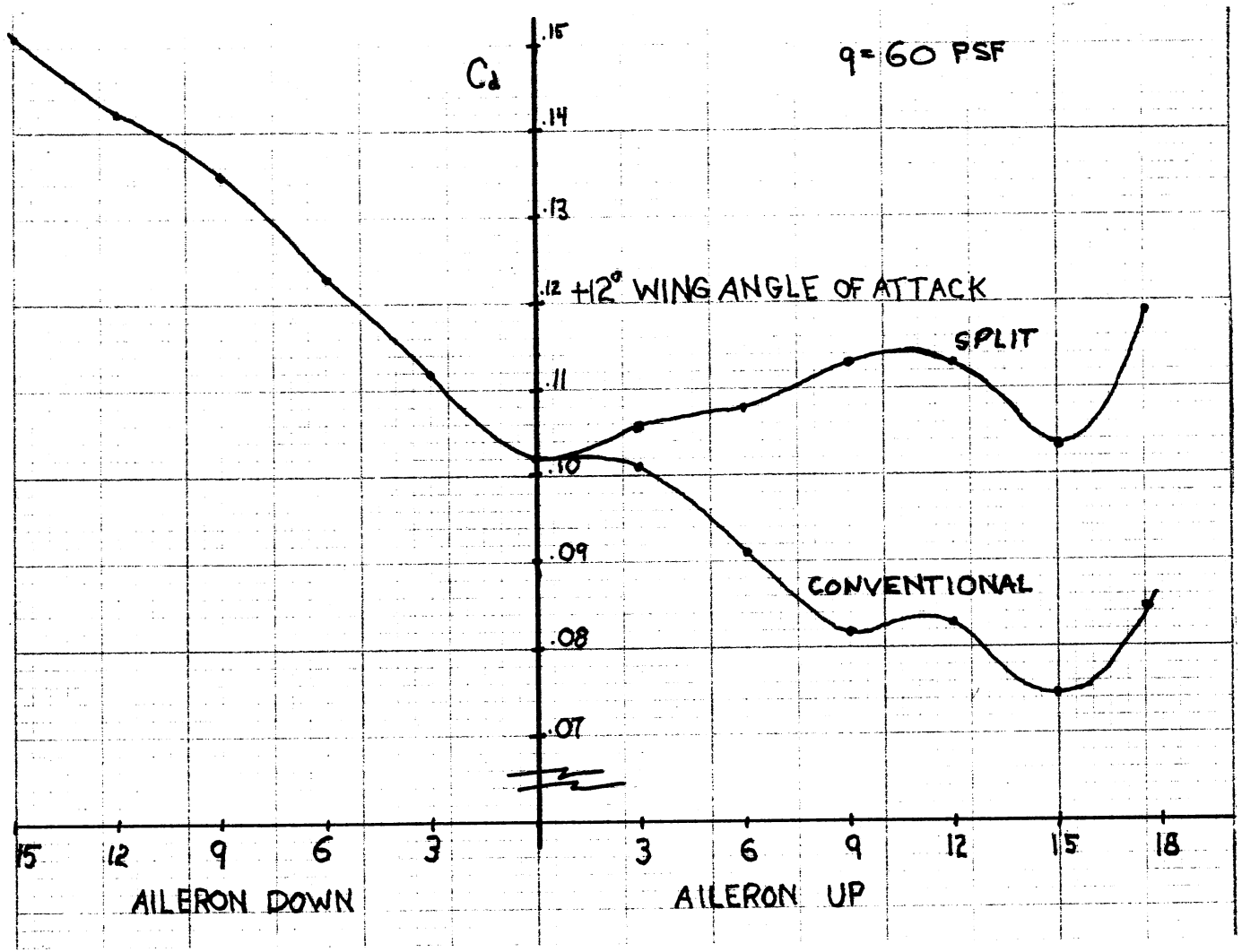

Figure 10. Drag curves at 12 Degrees Angle of Attack

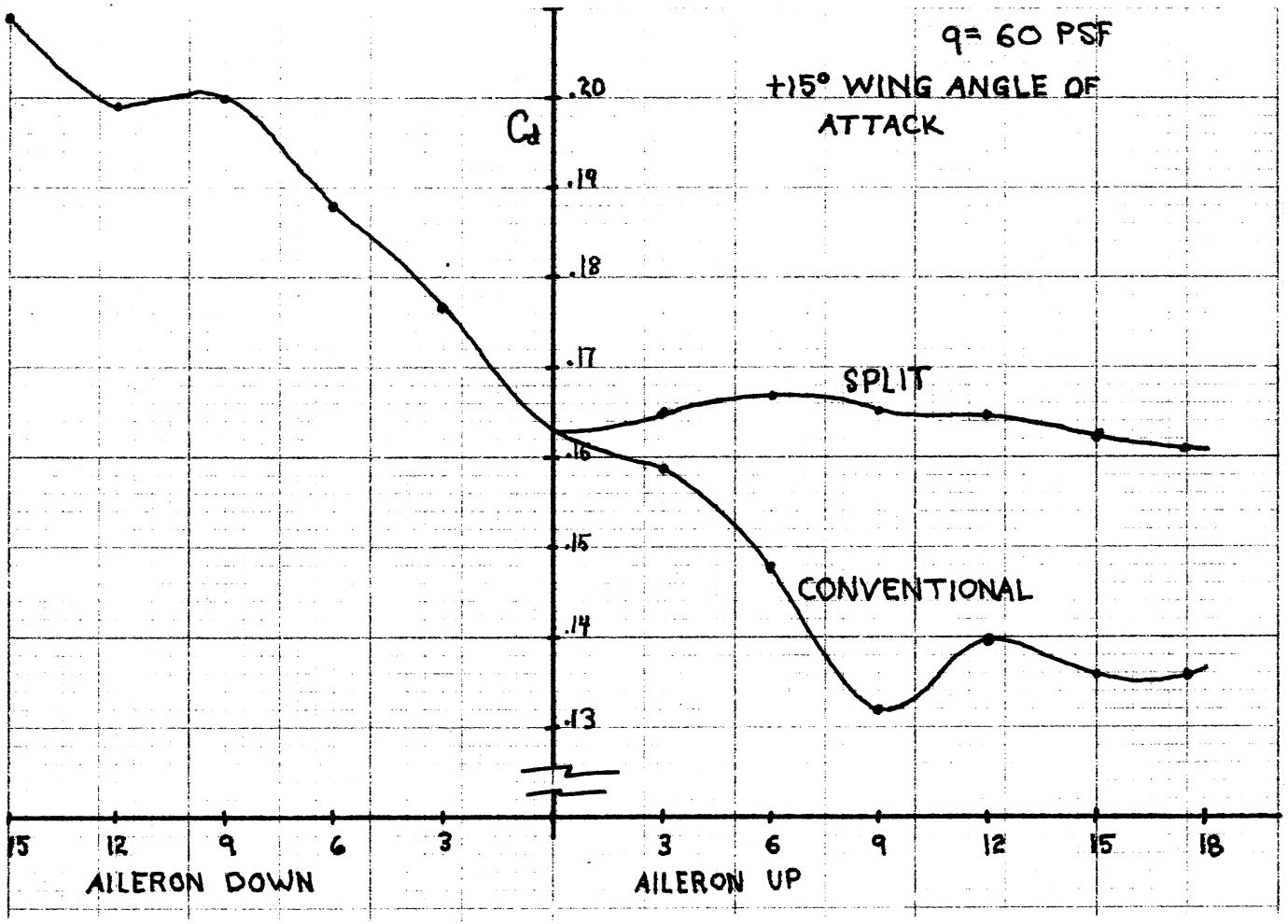

Figure 11. Drag Curves at 15 Degrees Angle of Attack

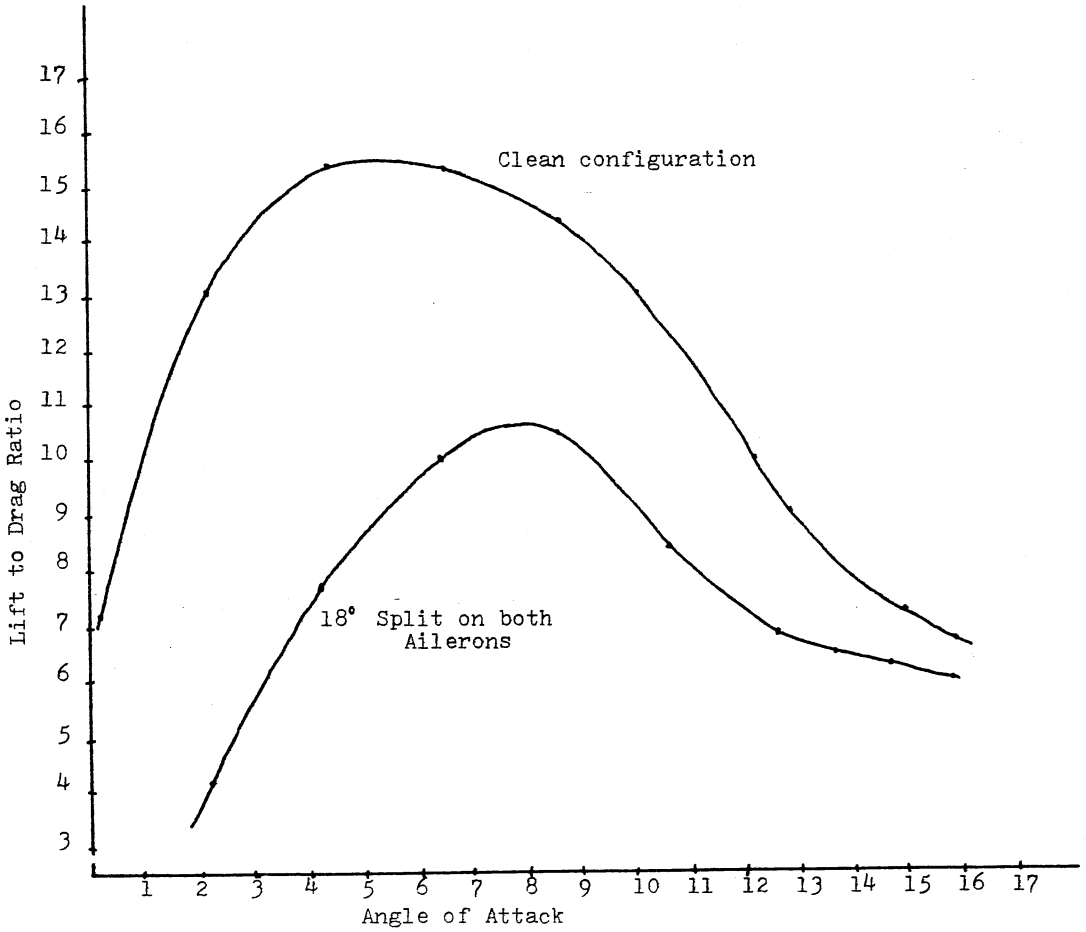

Figure 12. Lift/Drag Plots

CHAPTER VI

DISCUSSION OF RESULTS

The purpose of the split aileron is to add parasite drag at the same time induced drag is being lost. Parasite drag addition ideally should be equal to the induced drag reduction plus the parasite and induced drag increase of the opposite wing. (See Figures 4 through 10).

As was mentioned earlier, a problem of design optimization could be expected. Since parasite drag and induced drag vary in an opposite manner for changes in flight airspeed it would be expected that a balance can only be found for one airspeed.

When aircraft airspeed is changed the angle of attack is increased or decreased to change the lift coefficient to maintain a balance between lift and weight of the aircraft. At low speed a high angle of attack results to achieve high Cl. Under this condition the forces contributing to adverse yaw are great. Since parasite drag is lower at low speed, intuition would indicate that a large aileron split angle would be required. An aircraft operating at high speed is operating at low Cl and the forces contributing to adverse yaw are small. Since parasite drag is high at high

speed it would seem that a small split angle would be required.

These factors imply that the adverse yaw can be countered at only one airspeed and/or one split aileron deflection. Inspection of Figures 4 through 10 show that this is not the situation. At low angle of attack where little drag increase is desired, there is little difference between the conventional aileron and split aileron performance. At moderate angle of attack, there is a slight increase in drag for the split concept. At high angle of attack, where high drag increase is desired, there is a larger increase in drag for the split aileron over the conventional aileron. The split aileron design would appear to modulate the drag contribution according to demand. It is contrary to expectation but is the behavior desired for such a control device. The implication is that an optimization can be performed over a much broader range of operating conditions than originally anticipated. Even if the design could only be optimized over a narrow range, it would be an improvement over conventional control design where no optimization was possible. In fact, conventional design does little, if anything, to counter adverse yaw. The fact that optimization is possible over a broad range increases the utility of this concept significantly.

At negative angle of attack another interesting result is noted. A device designed to counter adverse yaw for positive angle of attack would be adding to adverse yaw for

negative angle of attack if it continued to function. The figures for negative angle of attack show identical drag characteristics for split and conventional aileron designs. The maximum difference of the curves is .001 which is the level of round off. No difference is measurable, and is a convenient result. Test data was not taken at deflections below negative six degrees angle of attack so operation below negative six degrees cannot be predicted. However only an experienced pilot with an aerobatic type airplane would purposely operate at such negative angles.

One area of concern for a control surface is the stall region. One must insure that no unusual characteristics are present because a pilot must have good control response for stall recovery. The data shows that the lift and drag curves are of the same form for both the split and the conventional aileron mode. Deep stall operation was not tested in this experiment so that region remains unknown. Only T-tail aircraft experience the deep stall and airplanes are not normally flown in the deep stall region. Thus it does not represent an area of concern.

Runs 13 and 14 were accomplished to compare the rolling moment capabilities of the model for the two modes of operation. The rolling moment curves have approximately the same form. However the split mode curve shows a loss of rolling moment of 20 percent at low angle of attack and about 50 percent at stall. Since these curves were made for identical aileron deflection angles

the implication is that the designer would have to provide greater deflection angles to maintain the same rolling moment. Large rudder deflection is required to counter the large adverse yaw during a stall with a conventional aileron configuration. Adverse yaw induces a rolling moment in the opposite direction to the aileron induced moment. This counters part, or perhaps all, of the aileron moment. The split mode aileron could be depended on to maintain rolling moment in the desired direction. It is necessary that the downward deflection angle be matched with the proper split mode angle to achieve a proper balance of drag forces. This functional relationship could vary for different angles of attack. The proper match of angles for a given angle of attack can be found from plots such as those in Figures 4 through 10. A horizontal line can be made intersecting the downward deflection curve on the left and the split mode curve on the right. The intersection indicates the appropriate angles. Inspection of the curves indicates that the split mode opening angle on the up going aileron must be significantly larger than the down going aileron. Since the split mode curves tend to be essentially flat and then start to increase, it can be seen that it would have been useful to have data points beyond the eighteen degree maximum tested. Most of the effectiveness is realized at higher split aileron deflections.

The match between angles for control deflection

appears to be essentially independent of angle of attack of the wing. This is significant from the design standpoint in that optimization can be achieved over a broad operating range.

The L/D curves (see Figure 11) are fairly typical for an aircraft. The significant feature is the displacement between the curves. Even though the ailerons span only a portion of the wing, deployment of eighteen degrees of split aileron lowers the overall aircraft L/D significantly. This implies that the split control could be used as a glide path control device.

Some aircraft have ailerons that can be lowered simultaneously to augment flap action. Differential deflections for rolling moments are superimposed on this aileron droop. In a similar manner a symmetrical split could be applied to both ailerons to provide additional drag to act as a speed brake or to provide a steep landing approach without gaining speed. The differential action for roll control can be superimposed on this symmetrical split. Such a symmetrical split is not limited to raising the upper surface alone while leaving the lower surface in normal position. It could be accomplished by moving both surfaces apart from neutral or by displacing only the lower surfaces in an action similar to that of a split flap. This would increase the mechanical complexity of the control system. This is merely a design problem, however, and similar systems are already in use on STOL aircraft.

As an example, an aircraft flying on approach without flaps would have a Cl of 0.8. In the clean configuration the L/D is approximately 14.5. At the same lift coefficient with eighteen degree split deployment the L/D drops to about 8.5, a reduction of over forty percent. This is sufficient for glide path control. As another example, an aircraft at high speed would have a Cl of 0.3. For this situation L/D drops from 12.5 to 7.5, again a loss of forty percent. This would serve nicely for a high speed penetration maneuver such as performed in some instrument flying procedures or when descending through a small opening in a cloud layer.

Spoilers have been used successfully as glide path control devices in the past. However few small aircraft have them and a major wing redesign is required to install them. The split aileron design maintains the advantage of serving as a control surface replacement item.

CHAPTER SEVEN

CONCLUSIONS AND RECOMMENDATIONS FOR FURTHER STUDY

The wind tunnel testing and data analysis show that the split aileron concept provides a simple device to counter adverse yaw. It has the unexpected property of a modulated drag affect that permits it to be optimized over a broad range of operating conditions. One of the strengths of this design is that it could be easily retrofitted to existing aircraft designs without changing the wing design. It would amount to a control surface change with some modification of existing actuator linkages.

The test data showed that it can be used as an effective glide path control device. Although this was not the original objective, it is a bonus.

Since this was the first test of this idea, the wind tunnel tests were designed to establish the validity and any unusual behavior of the concept. Consequently some areas were not investigated.

Additional testing could be done to experiment with greater control surface deflection angles. From this testing a detailed optimization profile for downward and

upward aileron settings could be established. This would provide design of an operating linkage concept.

Another area for further research would be to determine why the drag increment is modulated with angle of attack. This result was not expected and cannot be explained. Flow visualization techniques will probably be required here.

Further research should be accomplished with other airfoil sections to determine if the performance of the split aileron is independent of the airfoil section. Modern airfoils such as the GAW series should be investigated.

Investigations of deep stall and extreme negative wing angle of attack should be performed to discover any undesirable or limiting characteristics. This research could be performed with the original test model.

Hinge moment testing should be accomplished. This will insure that a hinge design can be made to permit the pilot to easily operate the ailerons with unpowered controls. It must be insured that there are no sudden changes or reversals of hinge moment which would create control problems for the pilot.

A design should be made for retrofitting an existing aircraft with this concept. The cost of producing and marketing the design should then be determined. This will permit assessing the financial feasibility of the concept.

A SELECTED BIBLIOGRAPHY

(1) Abbott, Ira H. and Albert E. von Doenhoff. Theory of Wing Sections. New York, McGraw-Hill 1949.

(2) Davidson, M. L. Facility Description of the 7 X 10 Foot Walter H. Beech Memorial Wind Tunnel. Aeronautical Engineering Department, Wichita State University, Wichita, Kansas, 1979.

(3) Dole, Charles E. Flight Theory and Aerodynamics. John Wiley & Sons, 1981.

(4) Garber, Paul E. "Warped Wings." Evolution of Aircraft Wing Design, American Institute of Aeronautics and Astronautics, 1980.

(5) Habluetzel, Tracy. Three-Dimensional Force Data Acquisition and Reduction Routine For The Walter H. Beech 7 x 10 Foot Low Speed Wind Tunnel. Aeronautical Engineering Department, Wichita State University, Wichita, Kansas, 1980.

(6) Lissaman, P. B. S. "Wings For Human Powered Flight." Evolution of Aircraft Wing Design, American Institute of Aeronautics and Astronautics, 1980.

(7) McCormick, Barnes W. Aerodynamics, Aeronautics, and Flight Mechanics. John Wiley & Sons, 1979.

(8) Perkins, Courtland D. and Robert E. Hage. Airplane Performance Stability and Control. John Wiley & Sons,1949.

(9) Pope, Alan and John J. Harper. Low Speed Wind Tunnel Testing. John Wiley & Sons, 1966.

(10) Rae, William H. and Alan Pope. Low Speed Wind Tunnel Testing. John Wiley & Sons, 1981.

(11) Riegels, Friedrich W. Aerofoil Sections, London, Butterworths, 1961.

(12) Shevell, Richard S. Fundamentals of Flight. Prentice-Hall, Inc., 1983.

(13) Torenbeek, Egbert. Synthesis of Subsonic Airplane Design. Delft University Press, Delft,Holland and Martinus Nijhoff Publishers, The Hague, Holland, 1982.

(14) Warner, Edward P. Airplane Design Performance. New York, McGraw-Hill, 1936.

APPENDIXES

APPENDIX A

MODEL CONSTRUCTION

Details of the wind tunnel test model construction are provided as a matter of record. The wing section chord and span were chosen to be consistent with the wind tunnel test section dimensions. Based on past experience the wind tunnel operators recommend that wing span should not exceed 70% of the test section span. This limitation minimizes errors from wall interference. This limited span to seven feet or less due to the ten foot test section width of the Walter H. Beech Memorial Low Speed Wind Tunnel. A reasonably thick wing is desired to obtain structural strength and provide space for actuating systems. A thick wing requires a long chord for a given airfoil section. For a given span, a long chord leads to a low aspect ratio. A high aspect ratio is desired to reduce wingtip effects. Thus airfoil thickness and aspect ratio require a compromise. An aspect ratio of seven was chosen as a reasonable value to represent light general aviation aircraft. This results in a wing chord of one foot and a wing area of seven square feet.

Dimensional tolerances must be very close for wind tunnel models to achieve reliable test data. Structural

strength is important because the aerodynamic loads of the wind tunnel can be large compared to the model size. If the model deforms under load it is impossible to predict the actual angle of attack and control settings for a given set of data. For the data to be reliable the deformations under load must be small. Therefore it is necessary to build in rigidity. Dimensional accuracy and rigidity are major considerations for model construction. The model design was based on these considerations, available material, and equipment.

The main structural member of the wing is a simple vertical spar at 25% chord. The spar is a continuous seven foot length of 0.132 inch stainless steel milled to 1.400 inch height. The stainless was chosen for its high strength. Ribs were placed at one foot intervals along the span. Aluminum alloy 6061-T651 of 0.375 inch thickness was chosen for the ribs. This thickness permitted the wing skin to be attached by rivets driven into the ribs without the use of flanges. Rectangular sections were cut and milled to high dimensional tolerance to construct the one piece ribs. All interior cutouts and holes were made before the ribs were milled further because it was easier to accurately locate positions for the cuts while the rib blanks were still rectangular. Two reference holes at two and seven inch positions of 0.1875 inch diameter were cut along the chord line. These holes were later used to hold the ribs in a jig fixture by use of steel dowel pins.

After all interior cuts were machined a carefully made wooden airfoil was attached to the rib blank with dowel pins and the airfoil shape was scribed onto the rectangular aluminum rib blank. An approximation of the airfoil was then cut by use of straight line cuts made on a vertical milling machine. This series of cuts was made to within a few thousandths of an inch of the airfoil shape. This airfoil approximation was then bolted into a wooden jig illustrated in Figure 13. A metal cutting tool was installed in a router and used to cut the airfoil shape. By geometrical techniques developed by the author this wooden jig was cut in a manner such that when the router base was guided along the outer curves, the cutting tool edge scribed the airfoil shape on the inside. This left a slightly rough surface which was then smoothed by hand by a single cross cut file.

This procedure was experimental in nature and was necessary due to a lack of profile milling equipment. The greatest concern was dimensional consistency. Although it was not necessary that the airfoil be a perfect representation, it was necessary that all eight ribs produce identical airfoils. The maximum deviation of any airfoil from any other airfoil is approximately 0.002 inch. Figure 14 shows all eight ribs bolted through the reference holes and the good fit is evident.

Figure 14 also illustrates a circular cutout at the front of each rib. This was finish cut on the vertical

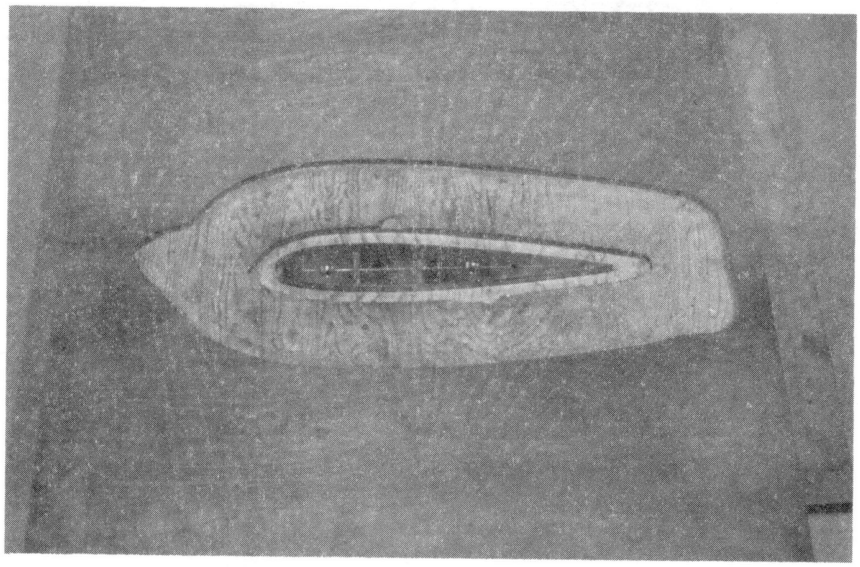

Figure 13. Rib Profiling Fixture

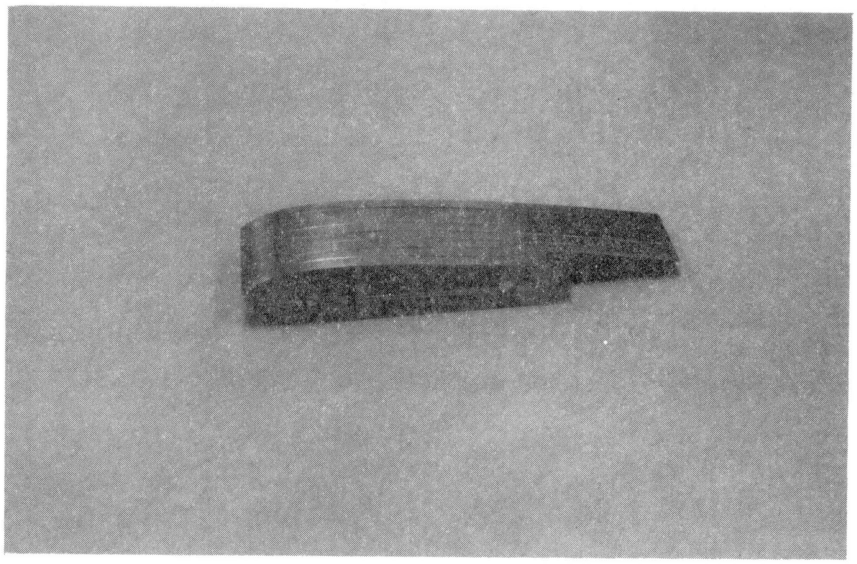

Figure 14. Rib Sections

mill with all ribs bolted together to insure consistent location. This cutout was used to install an aluminum rod along the leading edge to establish the leading edge radius curve when the sheet metal covering was installed.

Figure 15 illustrates the spring loaded mounting mechanisms for the two wing mounting points. A second spar is placed between the mounting fixtures to prevent the lift loading from twisting the main spar. This secondary spar was made of aluminum and is not primary structure. Actuation of the mounting device was provided through small slots in the lower wing surface.

The ailerons were constructed for high torsional strength so that a single point attachment could be used for setting deflections. The upper and lower aileron parts were milled from single pieces of 6061-T651 aluminum. Figure 16 shows the aileron parts.

Some means to set aileron deflections was necessary. An internal mechanism is more streamlined but the shallow airfoil thickness at the aileron hinge point provides poor mechanical advantage. "Blow down" of control surfaces is a common problem of wind tunnel models. The aerodynamic loads tend to cause the surfaces to deflect somewhat from the static setting. External brackets were used with an indexing arrangement for bolting the aileron surfaces rigidly in place. The index permitted three degree increments of aileron position. The indexing bracket was attached externally to the wing structure and the upper

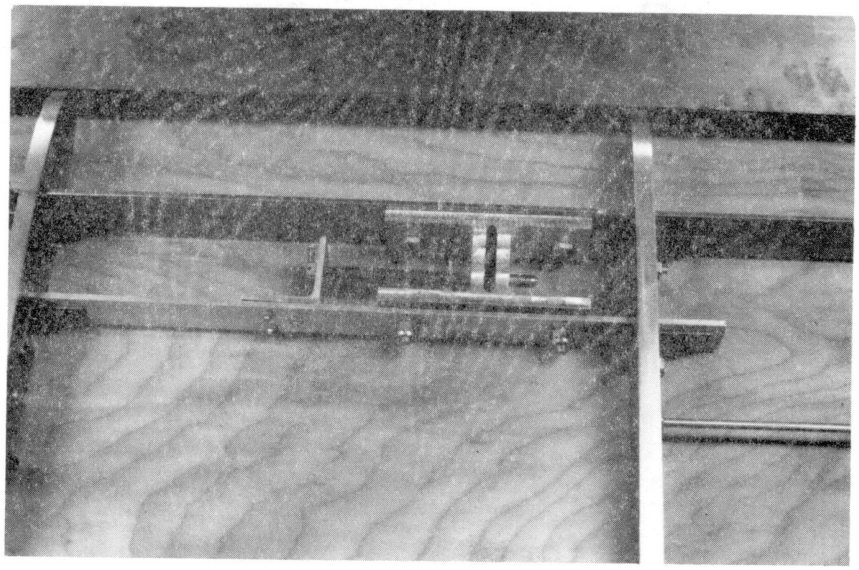

Figure 15. Tunnel Mounting Fixture

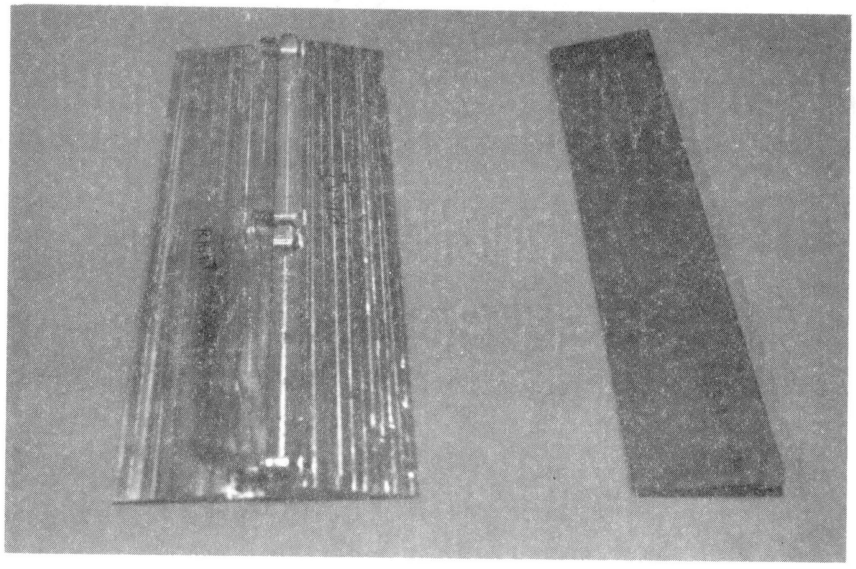

Figure 16. Milled Aileron Components

aileron surface was secured to the indexing bracket. A single small bolt at the trailing edge attached the lower aileron surface to the upper surface. When the split mode operation was desired this small bolt was removed and two small drive pins in the indexing bracket were driven forward to capture the lower surface at the zero deflection position. The axis of the drive pins was tapered slightly to eliminate all slack from the ailerons. See Figure 17 for an illustration of this arrangement.

The ailerons were sized to cover two feet of span on each wing tip. The chord length of the ailerons was chosen at 30% chord or 3.6 inches. This is a figure typical of control surface design.

Small rods threaded on both ends were placed between ribs and used for rigging purposes only. The structure was rigged into alignment using a precision straight edge along the leading edge (see Figure 18). Figure 19 shows the structural assembly ready for the surface skin.

The surface skin was made from 0.040 inch thick aluminum sheet metal. This thickness was used to provide rigid surfaces between ribs to prevent deflection under dynamic loading. A tail sting of 11/16 inch aluminum tubing was attached securely to the main spar to provide the third mounting point. Additional structural support of the tail sting can be seen in Figure 20.

A fuselage was provided for the test model to simulate the wing-fuselage flow interference of an actual aircraft.

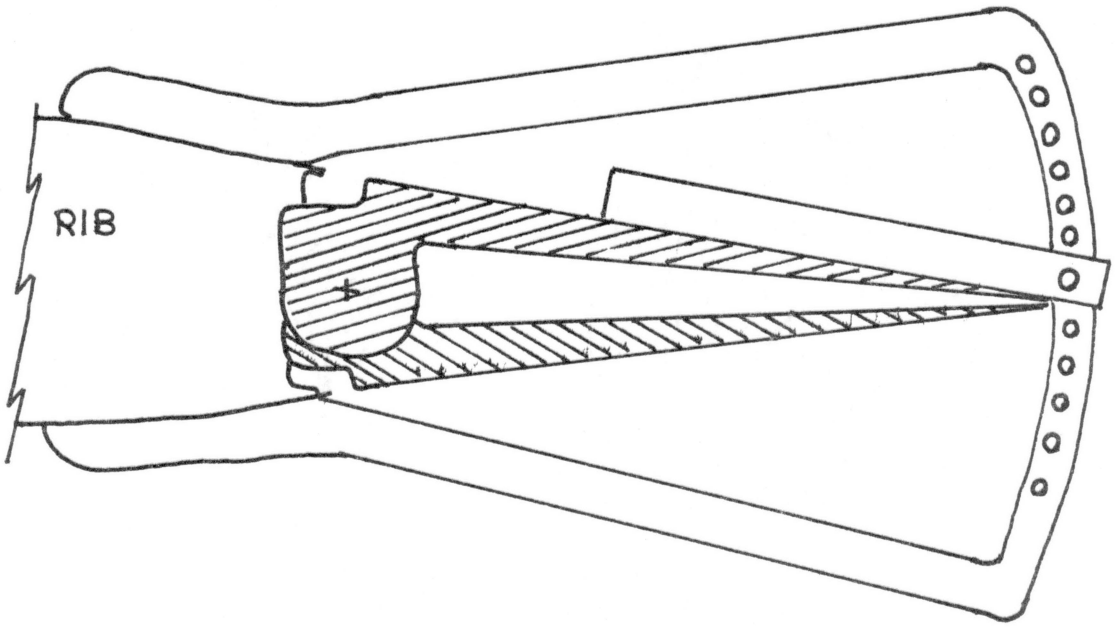

Figure 17. Aileron Indexing Brackets

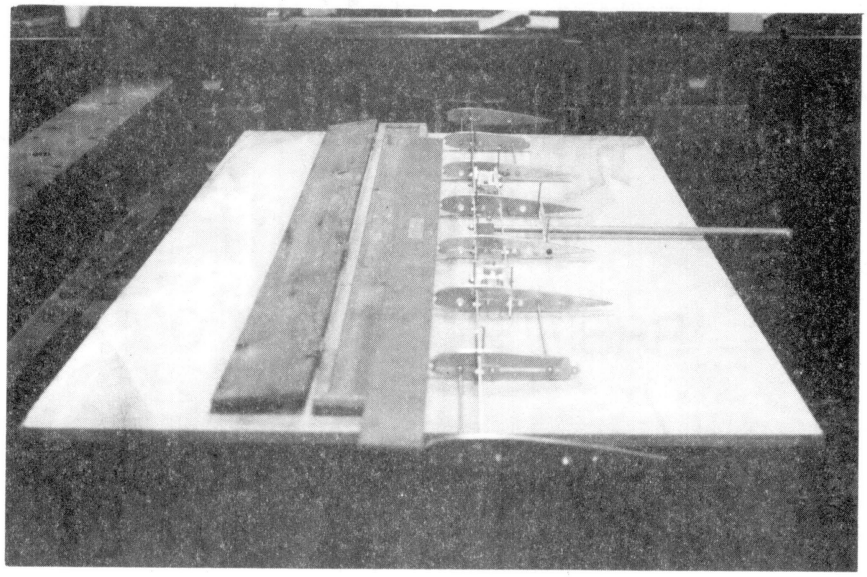

Figure 18. Rigging Structure

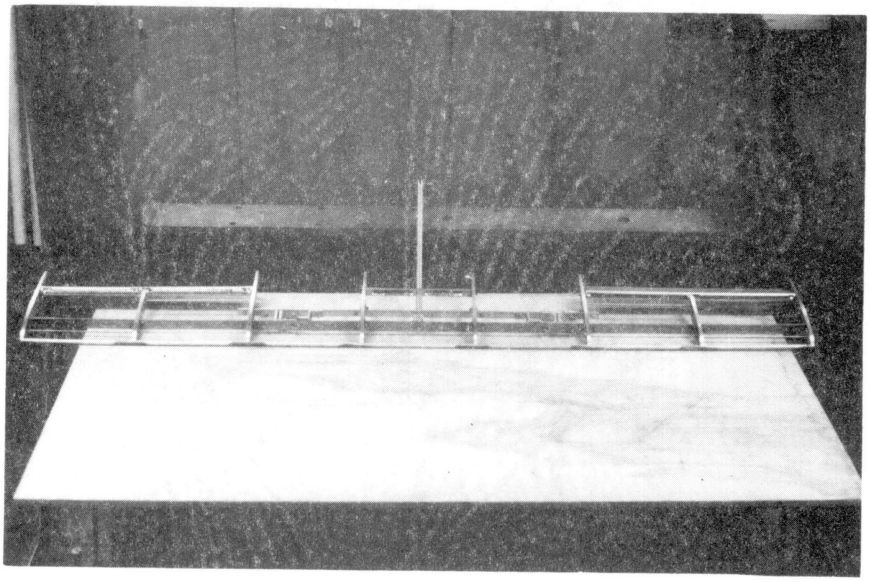

Figure 19. Complete Structure Prior to Covering

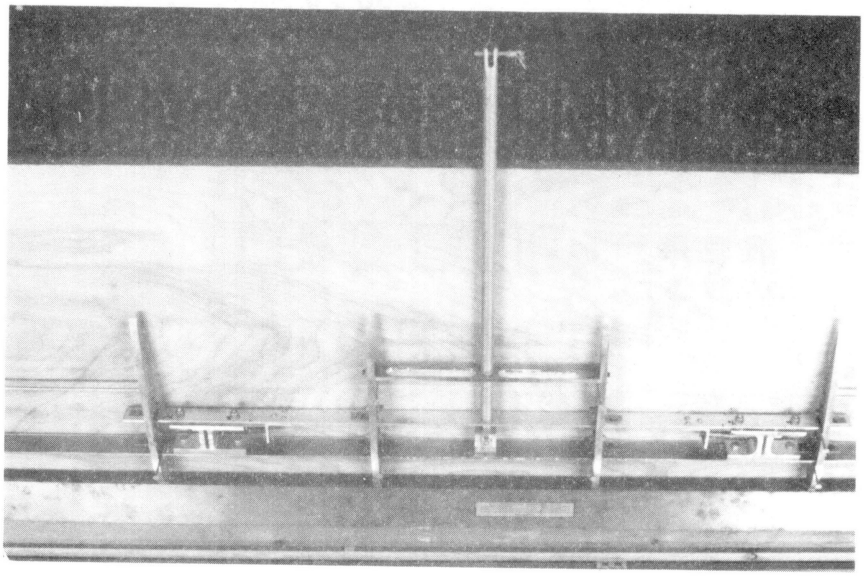

Figure 20. Tail Sting Components

This arrangement provided the best simulation of actual aircraft flow conditions to enhance the applicability of the results. The fuselage was constructed by bonding planks of wood under pressure and turning to final dimension on a lathe. The upper and lower parts of the fuselage were provided with an internal slot to fit tightly on the tail sting. This increased the rigidity of the tail sting to prevent flexing of the tail sting and change of the angle of attack under load.

Figure 21 shows the complete model installed in the wind tunnel for testing with the ailerons in neutral positions. Figure 22 shows the model in the tunnel with maximum split on the ailerons.

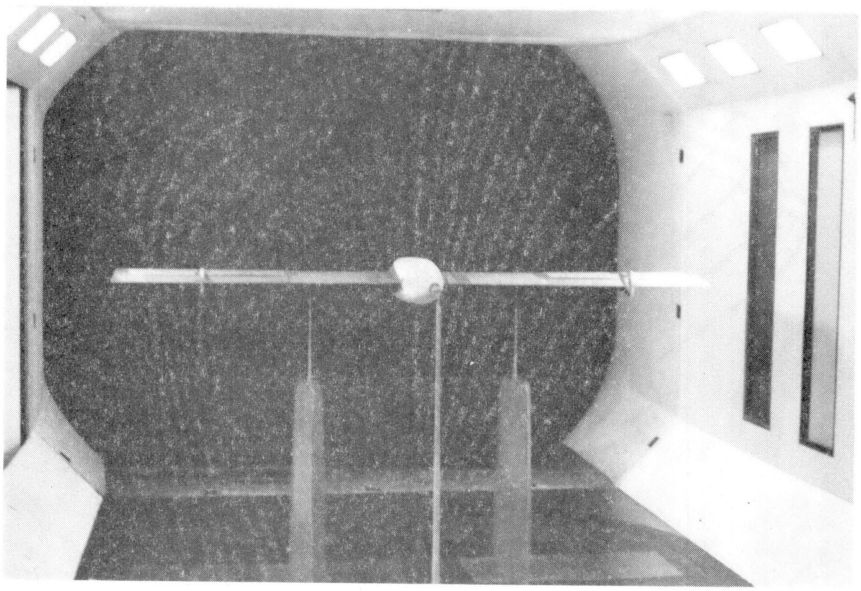

Figure 21. Test Model Installed in Wind Tunnel with Ailerons in Neutral Positions

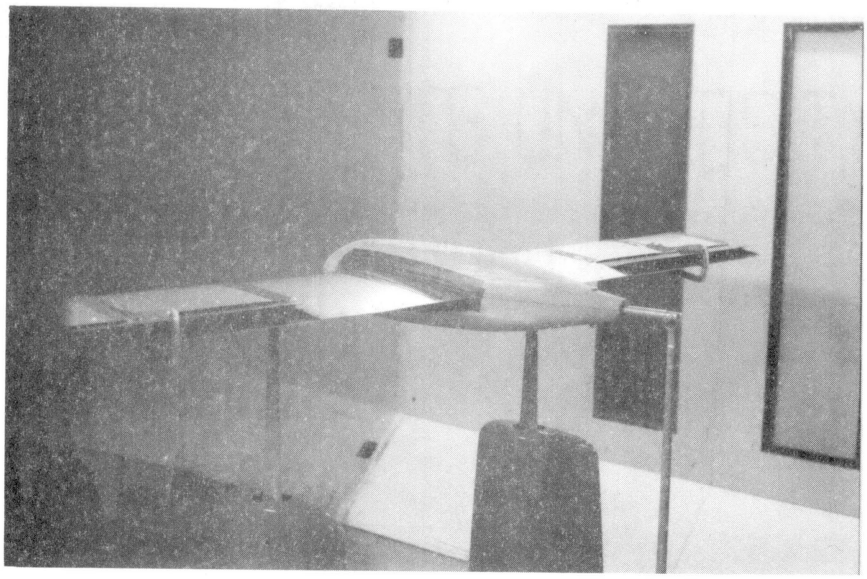

Figure 22. Maximum Split on Ailerons

APPENDIX B

WIND TUNNEL NUMERICAL DATA

REMARKS Program CBS3D::-20 (G.D.II)

WICHITA STATE UNIVERSITY
7x10 FOOT LOW SPEED WIND TUNNEL

TEST OF Wing - Body w/ Ailerons RUN NO. 1 - 20
FOR Gary Kreps - Okla. State Univ DATE March 1985
CONFIGURATION Wing - Body on 3 PT. Mount

DATE	RUN	FUND	TYPE RUN	UP/INV	MC	ST	DT	RAW T	RAW F	FINAL T	FINAL F	α	ψ	δ_A	REMARKS
3-21	2000	0	ST	UP	1	-	-	D19	2	CBSF1	=	VAR	0	-	STRUT STATIC TARE
	3000	60	DT	UP	1	2000	-		3		2	VAR	0	-	STRUT DYNAMIC TARE
	1000	0	ST	UP	1	-	-	↓	4	↓	-	VAR	0	0	MODEL STATIC TARE
3-21	1	60	F	UP	1	1000	3000	D19	5	CBSF1	3	VAR	0	0	BASIC MODEL
	2	60	F	UP	1	1000	3000		6		4	VAR	0	-15	
	3	60							7		5			-12	
	4	60							8		6			-9	
	5	60							9		7			-6	
	6	60							10		8			-3	
	7	60							11		9			+3	
	8	60							12		10			+6	
	9	60							13		11			+9	
	10	60							14		12			+12	
	11	60							15		13			+15	
	12	60							16		14			+18	
	13	60							17		15			~~+16 +18~~	
	14	60							18		16			~~+15 +18~~	SPLIT AILERONS
	15	60							19		17			+3	↓
	16	60							20		18			+6	
	17	60							21		19			+9	
	18	60							22		20			+12	
	19	60							23		21			+15	
	20	60							24		22			+18	
			↓	↓	↓	↓	↓	↓		↓		↓	↓		

WICHITA STATE UNIVERSITY
7 X 10 FOOT LOW-SPEED WIND TUNNEL

const. table 1

Static Tare 1000

MARCH 21, 1985
GARY KREPS - THESIS PROJECT
OKLAHOMA STATE UNIVERSITY
model upright

Static Tare Counts

ALPHA	PSI	lift	drag	pitch	roll	yaw	sideforce
-80	0	0	0	-3	1	0	0
-40	0	0	1	-4	0	0	0
0	0	0	1	0	-1	0	0
40	0	0	1	7	-2	0	0
80	0	0	1	19	-3	0	0
120	0	0	1	36	-4	0	0
160	0	0	1	57	-5	0	0
200	0	0	1	82	-6	0	0

WICHITA STATE UNIVERSITY
7 X 10 FOOT LOW-SPEED WIND TUNNEL

const. table 1

Static Tare 2000

MARCH 21, 1985
GARY KREPS - THESIS PROJECT
OKLAHOMA STATE UNIVERSITY
model upright

Static Tare Counts

ALPHA	PSI	lift	drag	pitch	roll	yaw	sideforce
-80	0	0	0	-3	2	0	0
-40	0	0	0	-3	1	0	0
0	0	0	0	0	0	0	0
40	0	0	0	7	-1	0	0
80	0	0	-1	19	-2	0	0
120	0	0	0	35	-4	0	0
160	0	0	1	56	-4	0	0
200	0	0	1	81	-6	0	0

WICHITA STATE UNIVERSITY
7 X 10 FOOT LOW-SPEED WIND TUNNEL

const. table 1
Dynamic Tare 3000 Static Tare 2000

MARCH 21, 1985
GARY KREPS - THESIS PROJECT
OKLAHOMA STATE UNIVERSITY
model upright

wind axes data about trunnion

ALPHA (deg)	PSI (deg)	CL	CD	CM	CRM	CYM	CY	q (psf)
-8	0	.0012	.0305	-.0546	0	0	.002	59.45
-4	0	.0012	.029	-.0528	0	-.0001	.002	59.44
0	0	.0013	.0277	-.0521	-.0001	-.0001	.0022	59.34
4	0	.0013	.0265	-.0515	-.0001	0	.0022	59.43
8	0	.0014	.0253	-.0501	-.0001	-.0001	.0022	59.33
12	0	.0014	.0239	-.0485	-.0002	0	.0022	59.33
16	0	.0014	.0227	-.0468	-.0001	0	.0023	59.23
20	0	.0014	.0215	-.045	-.0002	0	.0023	59.42

REYNOLDS NUMBER/FOOT= 1.44597E+06
MACH NUMBER= .2043

MODEL CONSTANT TABLE 1

7	1	7	7	0	
.4	.6	.4167	0	.0064	
2.2	1.04	.88	.95	.12	
0	0	0	.8	0	.7188

WICHITA STATE UNIVERSITY
7 X 10 FOOT LOW-SPEED WIND TUNNEL

Run number 1

Static Tare 1000
Dynamic Tare 3000
const. table 1

MARCH 21, 1985
GARY KREPS - THESIS PROJECT
OKLAHOMA STATE UNIVERSITY
model upright

Wind Axes Data

ALPHA (deg)	PSI (deg)	CL	CD	CM	CRM	CYM	CY	q (psf)
-6.27	0	-.3786	.0308	-.0258	-.0026	-.0002	.0004	59.32
-4.15	0	-.2102	.0238	-.0194	-.0029	-.0001	.0004	59.32
-2.02	0	-.0321	.0203	-.0115	-.0028	-.0001	.0003	59.32
.1	0	.148	.0206	-.0041	-.0025	-.0001	.0001	59.22
2.23	0	.3199	.0244	.0034	-.0031	-.0002	.0002	59.21
4.35	0	.4948	.0321	.01	-.0032	-.0002	.0001	59.21
6.47	0	.6643	.0434	.0168	-.0029	-.0001	-.0001	58.91
8.59	0	.8361	.058	.0224	-.0028	-.0001	.0001	58.91
10.7	0	.988	.0757	.0283	-.0024	-.0001	0	58.62
12.76	0	1.0715	.1184	.0099	-.0054	-.0001	.0008	58.52
13.79	0	1.1134	.1339	.0083	-.0069	-.0002	.0016	58.35
14.82	0	1.1556	.1492	.0051	-.008	-.0002	.0033	58.28
15.82	0	1.1655	.1738	-.004	-.0062	0	.0024	58.06
16.81	0	1.1457	.1969	-.0152	-.0075	-.0021	-.0035	57.94
17.81	0	1.1447	.2166	-.0212	-.0123	-.0031	-.0037	57.6
18.83	0	1.1751	.2364	-.025	-.0063	-.003	-.0048	57.65
19.83	0	1.1693	.2696	-.0439	.0075	-.002	-.005	57.55
20.82	0	1.1521	.2871	-.0524	.0186	-.0002	-.0055	57.51

REYNOLDS NUMBER/FOOT= 1.40282E+06
MACH NUMBER= .201

WICHITA STATE UNIVERSITY
7 X 10 FOOT LOW-SPEED WIND TUNNEL

Run number 2

Static Tare 1000
Dynamic Tare 3000
const. table 1

MARCH 21, 1985
GARY KREPS - THESIS PROJECT
OKLAHOMA STATE UNIVERSITY
model upright

Wind Axes Data

ALPHA (deg)	PSI (deg)	CL	CD	CM	CRM	CYM	CY	q (psf)
-6.11	0	-.1619	.0419	-.0811	.0024	-.0006	.0004	59.28
-4	0	-.0045	.0398	-.0726	.002	-.0006	.0005	59.28
-1.88	0	.1645	.0413	-.0627	.0026	-.0008	.0009	59.08
.24	0	.3377	.0462	-.0543	.0023	-.001	.0008	59.28
2.36	0	.5078	.0546	-.0464	.0022	-.0011	.0006	59.18
4.48	0	.6795	.0664	-.0397	.0021	-.0012	.0005	59.08
6.6	0	.8471	.0815	-.0321	.0019	-.0013	.0005	58.88
8.72	0	1.0107	.1002	-.0266	.0019	-.0013	.0004	58.79
10.83	0	1.1676	.1225	-.0208	.0015	-.0015	.0001	58.59
12.88	0	1.2441	.1727	-.041	-.0029	-.0018	.0021	58.22
13.91	0	1.2923	.1895	-.0419	-.0034	-.0017	.0037	58.45
14.94	0	1.335	.2083	-.0451	-.0039	-.0016	.0057	58.09
15.93	0	1.3191	.2367	-.056	.0008	-.002	.0025	57.88
16.91	0	1.2865	.2632	-.0683	-.0118	-.006	-.0025	57.88

REYNOLDS NUMBER/FOOT= 1.39808E+06
MACH NUMBER= .2017

WICHITA STATE UNIVERSITY
7 X 10 FOOT LOW-SPEED WIND TUNNEL

Run number 3

Static Tare 1000
Dynamic Tare 3000
const. table 1

MARCH 21, 1985
GARY KREPS - THESIS PROJECT
OKLAHOMA STATE UNIVERSITY
model upright

Wind Axes Data

ALPHA (deg)	PSI (deg)	CL	CD	CM	CRM	CYM	CY	q (psf)
-6.14	0	-.1995	.0382	-.0736	.0015	-.0003	.0007	59.56
-4.03	0	-.0381	.0355	-.0649	.0013	-.0003	.0006	59.46
-1.91	0	.1251	.0363	-.0553	.002	-.0005	.0008	59.17
.21	0	.3012	.0407	-.0467	.0018	-.0006	.0008	59.36
2.34	0	.4741	.0483	-.0394	.0014	-.0008	.0008	59.36
4.46	0	.6467	.0599	-.0328	.0013	-.0009	.0009	59.27
6.58	0	.8132	.0743	-.0254	.0009	-.0009	.0009	59.07
8.69	0	.9786	.0922	-.0189	.0008	-.0008	.001	59.07
10.8	0	1.1318	.1137	-.0132	.0006	-.0009	.001	58.88
12.86	0	1.2086	.1619	-.0318	-.0035	-.0013	.0022	58.6
13.89	0	1.2625	.1792	-.0351	-.0045	-.0013	.0035	58.53
14.92	0	1.304	.197	-.0369	-.0054	-.0013	.0055	58.56
15.94	0	1.3235	.2194	-.0438	-.0039	-.001	.0056	58.42
16.94	0	1.3321	.2443	-.05	-.0023	-.0009	.0053	58.3
17.9	0	1.2697	.2721	-.0623	-.0111	-.0049	-.0021	58.21

REYNOLDS NUMBER/FOOT= 1.38590E+06
MACH NUMBER= .2023

WICHITA STATE UNIVERSITY
7 X 10 FOOT LOW-SPEED WIND TUNNEL

Run number 4

Static Tare 1000
Dynamic Tare 3000
const. table 1

MARCH 21, 1985
GARY KREPS - THESIS PROJECT
OKLAHOMA STATE UNIVERSITY
model upright

Wind Axes Data

ALPHA (deg)	PSI (deg)	CL	CD	CM	CRM	CYM	CY	q (psf)
-6.17	0	-.2368	.035	-.0648	.0003	-.0002	.0003	59.55
-4.05	0	-.0758	.0318	-.0562	.0001	-.0001	.0004	59.55
-1.94	0	.0883	.0319	-.0468	.0003	-.0002	.0006	59.25
.19	0	.267	.0353	-.038	.001	-.0005	.0005	59.25
2.31	0	.4394	.0424	-.0307	.0007	-.0006	.0006	59.15
4.43	0	.6111	.0531	-.0239	.0003	-.0007	.0006	59.05
6.55	0	.783	.0673	-.0168	.0003	-.0006	.0006	58.96
8.67	0	.9452	.0845	-.0102	.0004	-.0006	.0009	58.86
10.78	0	1.1	.1053	-.004	.0006	-.0008	.0009	58.67
12.83	0	1.1773	.1534	-.0228	-.0033	-.0011	.0025	58.39
13.87	0	1.2233	.1703	-.0252	-.0049	-.0011	.0036	58.22
14.83	0	1.1766	.1962	-.0395	-.0073	-.0044	-.0003	58.12
15.85	0	1.2048	.2158	-.0437	-.0108	-.0049	-.0015	58.07
16.86	0	1.218	.2403	-.0512	-.0122	-.0052	-.0013	57.84
17.88	0	1.2368	.2596	-.0528	-.0111	-.0053	-.001	57.79

REYNOLDS NUMBER/FOOT= 1.37593E+06
MACH NUMBER= .2015

WICHITA STATE UNIVERSITY
7 X 10 FOOT LOW-SPEED WIND TUNNEL

Run number 5

Static Tare 1000
Dynamic Tare 3000
const. table 1

MARCH 21, 1985
GARY KREPS - THESIS PROJECT
OKLAHOMA STATE UNIVERSITY
model upright

Wind Axes Data

ALPHA (deg)	PSI (deg)	CL	CD	CM	CRM	CYM	CY	q (psf)
-6.2	0	-.2769	.0304	-.0551	0	-.0001	0	59.43
-4.08	0	-.1138	.0263	-.0471	-.001	-.0001	0	59.33
-1.96	0	.0508	.0258	-.0377	-.0006	-.0001	.0002	59.14
.16	0	.2264	.0283	-.0281	-.0004	-.0003	.0002	59.23
2.28	0	.3987	.0343	-.02	-.0001	-.0005	.0003	59.33
4.4	0	.5706	.0441	-.0127	-.0001	-.0005	.0002	59.13
6.52	0	.7406	.0575	-.0055	.0001	-.0005	.0002	58.84
8.64	0	.9069	.0739	.0004	-.0004	-.0005	.0001	59.04
10.75	0	1.0576	.0941	.0059	-.0004	-.0004	-.0004	58.85
12.81	0	1.1404	.1408	-.0124	-.0051	-.0005	.0014	58.56
13.83	0	1.1755	.1587	-.0179	.0032	-.0004	-.0001	58.5
14.84	0	1.1815	.1843	-.0273	.0005	-.0003	.0016	58.48
15.83	0	1.1713	.2015	-.0346	-.0113	-.0042	-.0029	58.44
16.83	0	1.1779	.2247	-.0399	-.0126	-.0045	-.0027	58.31
17.84	0	1.1853	.255	-.0532	-.009	-.0013	-.0017	58.1

REYNOLDS NUMBER/FOOT= 1.36739E+06
MACH NUMBER= .2021

WICHITA STATE UNIVERSITY
7 X 10 FOOT LOW-SPEED WIND TUNNEL

Run number 6

Static Tare 1000
Dynamic Tare 3000
const. table 1

MARCH 21, 1985
GARY KREPS - THESIS PROJECT
OKLAHOMA STATE UNIVERSITY
model upright

Wind Axes Data

	ALPHA (deg)	PSI (deg)	CL	CD	CM	CRM	CYM	CY	q (psf)
	-6.23	0	-.3205	.0291	-.0421	-.0009	0	.0001	59.43
	-4.11	0	-.1534	.0237	-.0352	-.0011	0	.0003	59.32
	-1.98	0	.0218	.022	-.0267	-.0011	0	.0003	59.22
	.14	0	.1961	.0239	-.0182	-.0008	-.0001	.0003	59.32
	2.26	0	.368	.0291	-.0102	-.0012	-.0002	.0004	59.32
*	4.38	0	.5376	.038	-.0026	-.0012	-.0002	.0004	59.12
*	6.5	0	.7076	.0505	.0047	-.0009	-.0002	.0006	59.02
	8.62	0	.8698	.0661	.0113	-.0008	-.0001	.0007	58.83
	10.72	0	1.0187	.0872	.0159	-.0009	-.0001	-.0001	58.64
	12.78	0	1.0977	.1283	-.0005	.0036	-.0003	.0015	58.34
	13.8	0	1.1259	.1494	-.0072	.0022	-.0002	.0015	58.3
	14.81	0	1.1375	.1734	-.0147	-.0004	.0001	.0028	57.97
	15.82	0	1.1585	.1902	-.0193	-.0025	-.0013	.0002	57.81
	16.81	0	1.1471	.2135	-.0289	-.012	-.0039	-.0015	57.59
	17.81	0	1.144	.2439	-.0449	-.0083	-.0004	-.0008	57.48
	18.82	0	1.1575	.2634	-.0487	-.0055	.0002	-.0006	57.34
	19.85	0	1.1992	.2889	-.0579	-.0009	.0004	.0037	57.3
	20.85	0	1.1989	.3057	-.0578	-.0003	.0009	.0081	57.25

REYNOLDS NUMBER/FOOT= 1.36872E+06
MACH NUMBER= .2006

WICHITA STATE UNIVERSITY
7 X 10 FOOT LOW-SPEED WIND TUNNEL

Run number 7

Static Tare 1000
Dynamic Tare 3000
const. table 1

MARCH 21, 1985
GARY KREPS - THESIS PROJECT
OKLAHOMA STATE UNIVERSITY
model upright

Wind Axes Data

ALPHA (deg)	PSI (deg)	CL	CD	CM	CRM	CYM	CY	q (psf)
-6.3	0	-.4267	.0345	-.0128	-.0023	-.0002	.0002	59.43
-4.18	0	-.2574	.026	-.0048	-.0031	-.0001	.0004	59.42
-2.06	0	-.0855	.0213	.0037	-.0031	0	.0004	59.22
.07	0	.0963	.0199	.0115	-.0028	0	.0004	59.22
2.2	0	.2777	.0227	.0186	-.0026	-.0001	.0005	59.21
4.32	0	.4551	.0293	.0248	-.0028	-.0001	.0007	59.21
6.45	0	.6291	.0399	.0309	-.0027	0	.0009	59.21
8.56	0	.7949	.0541	.0362	-.0025	.0001	.0012	59.21
10.66	0	.9342	.0754	.0362	-.0008	-.0001	.0026	59.13
12.72	0	1.0238	.1122	.0219	.0025	-.0001	.0022	58.92
13.76	0	1.0778	.1265	.0194	.0038	0	.0015	58.94
14.76	0	1.0745	.1541	.0092	-.003	-.0001	.0041	58.53
15.8	0	1.1264	.1715	.0056	.0023	-.0003	.0029	58.46
16.76	0	1.0735	.1966	-.0093	-.0123	-.0018	.0003	58.46
17.76	0	1.0697	.223	-.0179	-.009	.0001	.0007	58.34

REYNOLDS NUMBER/FOOT= 1.36201E+06
MACH NUMBER= .2025

WICHITA STATE UNIVERSITY
7 X 10 FOOT LOW-SPEED WIND TUNNEL

Run number 8

Static Tare 1000
Dynamic Tare 3000
const. table 1

MARCH 21, 1985
GARY KREPS - THESIS PROJECT
OKLAHOMA STATE UNIVERSITY
model upright

Wind Axes Data

ALPHA (deg)	PSI (deg)	CL	CD	CM	CRM	CYM	CY	q (psf)
-6.32	0	-.4577	.0391	.0009	-.0019	-.0003	.0008	59.44
-4.21	0	-.2952	.0303	.0085	-.0024	-.0002	.0008	59.23
-2.09	0	-.1251	.0241	.0179	-.0026	-.0002	.0008	59.23
.03	0	.0443	.0211	.0266	-.0023	-.0003	.0006	59.32
2.16	0	.22	.0217	.0349	-.0027	-.0004	.0007	59.41
4.28	0	.3962	.0269	.041	-.003	-.0004	.0008	59.21
6.4	0	.5698	.0358	.0473	-.0032	-.0003	.0009	59.31
8.52	0	.7367	.0487	.0523	-.0031	-.0002	.0011	59.31
10.62	0	.873	.0683	.053	-.002	-.0003	.0025	59.23
12.69	0	.9735	.103	.0383	.0014	-.0003	.0022	59.1
13.72	0	1.0153	.1201	.0327	.0016	-.0003	.0017	59.24
14.74	0	1.0502	.1439	.0242	0	-.0003	.0001	59
15.78	0	1.0957	.1597	.0209	.0013	-.0005	-.0001	58.84
16.75	0	1.0644	.1795	.0109	-.0116	-.0024	-.0014	58.81
17.77	0	1.0846	.1964	.0054	-.0105	-.0027	-.0017	58.75
18.76	0	1.0694	.2182	-.0047	-.0022	-.0012	-.0016	58.63

REYNOLDS NUMBER/FOOT= 1.35343E+06
MACH NUMBER= .203

WICHITA STATE UNIVERSITY
7 X 10 FOOT LOW-SPEED WIND TUNNEL

Run number 9

Static Tare 1000
Dynamic Tare 3000
const. table 1

MARCH 21, 1985
GARY KREPS - THESIS PROJECT
OKLAHOMA STATE UNIVERSITY
model upright

Wind Axes Data

ALPHA (deg)	PSI (deg)	CL	CD	CM	CRM	CYM	CY	q (psf)
-6.35	0	-.5009	.0454	.0094	-.0041	-.0005	.0008	59.45
-4.24	0	-.3323	.0352	.0184	-.0041	-.0005	.0011	59.34
-2.12	0	-.1669	.0283	.0279	-.0037	-.0005	.001	59.54
0	0	.0041	.0243	.0376	-.003	-.0005	.0011	59.33
2.12	0	.1702	.0234	.0466	-.0032	-.0006	.0011	59.42
4.25	0	.3478	.0269	.054	-.0033	-.0007	.0012	59.42
6.37	0	.5165	.0341	.0604	-.0039	-.0005	.0011	59.31
8.48	0	.6813	.045	.0661	-.0049	-.0003	.0006	59.21
10.6	0	.841	.0593	.0708	-.0053	-.0002	.0006	59.31
12.67	0	.947	.0942	.0566	-.0079	-.0001	.0001	59.28
13.7	0	.983	.11	.051	0	-.0002	.0015	59.22
14.74	0	1.0394	.1251	.0483	.0012	-.0003	-.0004	59.25
15.73	0	1.0351	.1532	.0316	-.0053	.0001	.0018	59.14
16.74	0	1.0389	.1702	.0261	-.0071	-.0006	.0002	58.89
17.73	0	1.03	.1978	.0114	-.0035	.0012	.0008	58.78

REYNOLDS NUMBER/FOOT= 1.34750E+06
MACH NUMBER= .2032

WICHITA STATE UNIVERSITY
7 X 10 FOOT LOW-SPEED WIND TUNNEL

Run number 10

Static Tare 1000
Dynamic Tare 3000
const. table 1

MARCH 21, 1985
GARY KREPS - THESIS PROJECT
OKLAHOMA STATE UNIVERSITY
model upright

Wind Axes Data

ALPHA (deg)	PSI (deg)	CL	CD	CM	CRM	CYM	CY	q (psf)
-6.38	0	-.5356	.0509	.0187	-.0055	-.0007	.0007	59.26
-4.26	0	-.3646	.0399	.0277	-.0051	-.0006	.001	59.35
-2.14	0	-.1959	.0327	.0373	-.0048	-.0006	.0012	59.25
-.02	0	-.0267	.0283	.0484	-.0031	-.0006	.001	59.34
2.1	0	.1356	.027	.0585	-.0026	-.0008	.0009	59.34
4.22	0	.308	.0299	.0657	-.003	-.0008	.0007	59.43
6.33	0	.4717	.0358	.0725	-.0037	-.0007	.0007	59.33
8.45	0	.6361	.0449	.0787	-.004	-.0006	.0009	59.32
10.56	0	.791	.0574	.0837	-.004	-.0005	.0008	59.32
12.62	0	.8744	.0928	.0657	-.0005	-.0007	.0022	59.2
13.67	0	.9457	.1053	.065	.0003	-.0004	.0008	59.02
14.66	0	.9394	.1322	.0504	-.0041	.0001	.0008	59.01
15.67	0	.9522	.1524	.0411	-.0022	.002	.0019	58.77
16.7	0	.9828	.1731	.034	-.0004	.0038	.0046	58.52
17.71	0	1.0067	.1931	.0224	-.0008	.0027	.0048	58.48

REYNOLDS NUMBER/FOOT= 1.33873E+06
MACH NUMBER= .2027

WICHITA STATE UNIVERSITY
7 X 10 FOOT LOW-SPEED WIND TUNNEL

Run number 11

Static Tare 1000
Dynamic Tare 3000
const. table 1

MARCH 21, 1985
GARY KREPS - THESIS PROJECT
OKLAHOMA STATE UNIVERSITY
model upright

Wind Axes Data

ALPHA (deg)	PSI (deg)	CL	CD	CM	CRM	CYM	CY	q (psf)
-6.41	0	-.5783	.058	.0287	-.0059	-.0008	.0012	59.57
-4.29	0	-.4111	.0468	.0368	-.0052	-.0006	.0013	59.37
-2.16	0	-.2321	.0382	.0474	-.0048	-.0005	.0015	59.26
-.04	0	-.0615	.0333	.0581	-.0035	-.0005	.0014	59.26
2.06	0	.0905	.0316	.0678	-.0025	-.0006	.0014	59.35
4.19	0	.2677	.0335	.0769	-.0021	-.0008	.0017	59.44
6.3	0	.4266	.0386	.0838	-.0021	-.0007	.0017	59.34
8.42	0	.5901	.0472	.09	-.0024	-.0008	.0018	59.24
10.53	0	.746	.0591	.0959	-.0029	-.0008	.0019	59.24
11.58	0	.821	.0667	.0977	-.0032	-.001	.002	59.44
12.6	0	.8517	.0891	.0844	-.0061	-.0007	.0012	59.3
13.64	0	.9019	.1052	.0787	-.0083	-.0009	.0021	59.13
14.64	0	.9011	.1263	.0681	-.0002	-.001	.0004	58.9
15.64	0	.9041	.1511	.0558	-.0012	.0005	.0021	58.88
16.65	0	.9224	.1705	.0456	-.0001	.0017	.0029	58.73
17.67	0	.946	.192	.0336	-.0031	.0003	.0034	58.59
18.66	0	.9285	.2106	.0249	-.008	-.0013	.0004	58.36

REYNOLDS NUMBER/FOOT= 1.32449E+06
MACH NUMBER= .2025

WICHITA STATE UNIVERSITY
7 X 10 FOOT LOW-SPEED WIND TUNNEL

Run number 12

Static Tare 1000
Dynamic Tare 3000
const. table 1

MARCH 21, 1985
GARY KREPS - THESIS PROJECT
OKLAHOMA STATE UNIVERSITY
model upright

Wind Axes Data

ALPHA (deg)	PSI (deg)	CL	CD	CM	CRM	CYM	CY	q (psf)
-6.42	0	-.5963	.0646	.037	-.0076	-.001	.0012	59.59
-4.31	0	-.4383	.0533	.0449	-.0068	-.0008	.0014	59.48
-2.19	0	-.2632	.0443	.0547	-.0067	-.0006	.0013	59.38
-.06	0	-.0909	.039	.065	-.0056	-.0006	.0011	59.37
2.05	0	.0712	.0374	.0751	-.0044	-.0007	.0011	59.27
4.17	0	.2351	.0392	.0834	-.0037	-.0009	.0013	59.37
6.28	0	.3917	.0435	.0913	-.0028	-.001	.0013	59.36
8.39	0	.5502	.0511	.0979	-.0029	-.0009	.0013	59.16
10.5	0	.7094	.0622	.1039	-.0029	-.001	.0015	59.36
12.57	0	.8111	.0929	.0899	-.0065	-.0008	.0004	59.22
13.61	0	.8582	.1061	.0862	-.0079	-.0008	.0013	59.05
14.61	0	.8666	.1273	.0754	-.0002	-.0013	.0006	58.92
15.61	0	.8655	.1504	.0645	-.0009	.0003	.0015	58.79
16.63	0	.8882	.1714	.0538	-.0012	.0005	.0019	58.65
17.64	0	.9058	.1905	.0442	-.0038	.0001	.0022	58.4
18.65	0	.9192	.2094	.0347	-.0041	-.0009	.001	58.36

REYNOLDS NUMBER/FOOT= 1.32114E+06
MACH NUMBER= .2025

WICHITA STATE UNIVERSITY
7 X 10 FOOT LOW-SPEED WIND TUNNEL

Run number 13

Static Tare 1000
Dynamic Tare 3000
const. table 1

MARCH 21, 1985
GARY KREPS - THESIS PROJECT
OKLAHOMA STATE UNIVERSITY
model upright

Wind Axes Data

ALPHA (deg)	PSI (deg)	CL	CD	CM	CRM	CYM	CY	q (psf)
-6.27	0	-.379	.0546	-.0254	.073	.0034	.0026	59.5
-4.15	0	-.2157	.0481	-.0171	.0726	.0016	.0027	59.49
-2.03	0	-.038	.0447	-.0069	.0725	-.0006	.0032	59.49
.1	0	.1361	.0452	.0022	.0742	-.0028	.0036	59.49
2.21	0	.3018	.049	.0121	.0766	-.005	.004	59.29
4.34	0	.4773	.0566	.0199	.0776	-.0073	.0042	59.29
6.46	0	.6441	.0676	.0272	.0784	-.0096	.0042	59.19
8.57	0	.8031	.0812	.033	.0784	-.0116	.0042	59.29
10.68	0	.9591	.0987	.0375	.0777	-.0138	.004	59.29
12.74	0	1.0395	.1386	.02	.0722	-.0157	.0031	58.99
13.77	0	1.0866	.1539	.0154	.0698	-.0165	.0041	58.82
14.76	0	1.0667	.1822	.0038	.073	-.0175	.0043	58.62
15.73	0	1.0355	.2057	-.0097	.0649	-.0216	.0005	58.6
16.73	0	1.0373	.2283	-.0194	.0621	-.0217	-.0009	58.37
17.74	0	1.0498	.2461	-.0236	.0607	-.0219	-.001	58.32
18.75	0	1.0614	.2626	-.0282	.0591	-.0225	-.0021	58.17

REYNOLDS NUMBER/FOOT= 1.31333E+06
MACH NUMBER= .2022

WICHITA STATE UNIVERSITY
7 X 10 FOOT LOW-SPEED WIND TUNNEL

Run number 14

Static Tare 1000
Dynamic Tare 3000
const. table 1

MARCH 21, 1985
GARY KREPS - THESIS PROJECT
OKLAHOMA STATE UNIVERSITY
model upright

Wind Axes Data

ALPHA (deg)	PSI (deg)	CL	CD	CM	CRM	CYM	CY	q (psf)
-6.26	0	-.363	.0538	-.0284	.0703	.0031	.0023	59.5
-4.14	0	-.194	.0469	-.0211	.0672	.0012	.0026	59.59
-2.02	0	-.0288	.0439	-.0143	.0655	-.0007	.0031	59.49
.11	0	.16	.0442	-.0068	.0638	-.0027	.0034	59.39
2.24	0	.3435	.049	.0001	.0618	-.0046	.0036	59.29
4.37	0	.5252	.058	.006	.0605	-.0062	.0037	59.29
6.49	0	.6972	.0704	.0114	.0585	-.0078	.0033	59.29
8.61	0	.8681	.0862	.0167	.0565	-.0091	.003	59.29
10.73	0	1.0257	.1058	.0202	.0538	-.0104	.0023	59.19
12.79	0	1.1166	.1491	-.0009	.0474	-.0118	.0014	58.99
13.82	0	1.1582	.1657	-.0034	.0443	-.0126	.0017	58.83
14.82	0	1.1516	.1943	-.0175	.049	-.0132	.0006	58.62
15.84	0	1.1877	.2133	-.0239	.0516	-.0136	-.0005	58.66
16.79	0	1.1151	.243	-.0399	.0372	-.0161	-.0027	58.39
17.8	0	1.1301	.2635	-.0456	.0348	-.0162	-.0033	58.34
18.81	0	1.1436	.28	-.0491	.0302	-.0162	-.0037	58.19

REYNOLDS NUMBER/FOOT= 1.30688E+06
MACH NUMBER= .2022

WICHITA STATE UNIVERSITY
7 X 10 FOOT LOW-SPEED WIND TUNNEL

Run number 15

Static Tare 1000
Dynamic Tare 3000
const. table 1

MARCH 21, 1985
GARY KREPS - THESIS PROJECT
OKLAHOMA STATE UNIVERSITY
model upright

Wind Axes Data

ALPHA (deg)	PSI (deg)	CL	CD	CM	CRM	CYM	CY	q (psf)
-6.29	0	-.4126	.0348	-.0141	-.0022	-.0003	-.0002	59.43
-4.17	0	-.2431	.0269	-.0089	-.0027	-.0002	.0001	59.43
-2.04	0	-.0562	.0223	-.0025	-.003	-.0003	0	59.42
.1	0	.135	.0221	.0032	-.0032	-.0003	.0001	59.42
2.23	0	.3242	.0264	.0087	-.0033	-.0005	.0002	59.32
4.35	0	.5009	.0342	.0148	-.003	-.0005	.0002	59.22
6.47	0	.6709	.046	.0206	-.0024	-.0005	.0006	59.22
8.59	0	.835	.061	.0256	-.0018	-.0005	.0014	59.32
10.7	0	.9869	.0797	.03	-.003	-.0005	.0002	59.23
12.76	0	1.0736	.1211	.0115	-.0066	-.0006	-.0005	58.92
13.8	0	1.1248	.1367	.0099	-.0077	-.0005	.0004	58.95
14.8	0	1.1367	.1605	-.0023	-.0033	.0018	.0017	58.72
15.8	0	1.1235	.1859	-.0131	-.0009	.0005	.0006	58.71
16.8	0	1.1345	.2116	-.025	.0036	.004	.0028	58.58
17.77	0	1.0896	.2328	-.0299	-.0111	.0005	-.0024	58.37

REYNOLDS NUMBER/FOOT= 1.30797E+06
MACH NUMBER= .2025

WICHITA STATE UNIVERSITY
7 X 10 FOOT LOW-SPEED WIND TUNNEL

Run number 16

Static Tare 1000
Dynamic Tare 3000
const. table 1

MARCH 21, 1985
GARY KREPS - THESIS PROJECT
OKLAHOMA STATE UNIVERSITY
model upright

Wind Axes Data

ALPHA (deg)	PSI (deg)	CL	CD	CM	CRM	CYM	CY	q (psf)
-6.31	0	-.442	.0385	-.0039	-.0017	-.0004	.0003	59.44
-4.19	0	-.2699	.0301	.0014	-.0022	-.0003	.0003	59.43
-2.06	0	-.0886	.0254	.007	-.0024	-.0004	.0002	59.33
.07	0	.1017	.0243	.0123	-.0026	-.0005	.0003	59.43
2.21	0	.2927	.0274	.0175	-.003	-.0006	.0005	59.32
4.33	0	.4706	.0344	.0221	-.0032	-.0006	.0007	59.42
6.46	0	.6544	.0459	.0263	-.0029	-.0006	.0012	59.12
8.58	0	.8209	.0604	.0301	-.0033	-.0006	.0011	59.12
10.69	0	.9753	.0789	.0335	-.0033	-.0007	.0004	59.03
12.72	0	1.0218	.1256	.0111	.0011	-.001	.0005	58.76
13.75	0	1.0557	.1464	.003	.0006	-.0011	-.0004	58.71
14.78	0	1.096	.1633	-.0022	.001	-.0011	-.0008	58.55
15.81	0	1.1442	.1802	-.0045	.0024	-.0012	-.0014	58.58
16.75	0	1.0623	.2103	-.0232	-.0108	-.0006	-.0029	58.31
17.76	0	1.0785	.2302	-.0276	-.0112	-.0003	-.0029	58.26

REYNOLDS NUMBER/FOOT= 1.30079E+06
MACH NUMBER= .2023

WICHITA STATE UNIVERSITY
7 X 10 FOOT LOW-SPEED WIND TUNNEL

Run number 17

Static Tare 1000
Dynamic Tare 3000
const. table 1

MARCH 21, 1985
GARY KREPS - THESIS PROJECT
OKLAHOMA STATE UNIVERSITY
model upright

Wind Axes Data

ALPHA (deg)	PSI (deg)	CL	CD	CM	CRM	CYM	CY	q (psf)
-6.34	0	-.4809	.0442	.0043	-.0032	-.0006	.0004	59.55
-4.21	0	-.2986	.0341	.0099	-.0037	-.0006	.0004	59.25
-2.08	0	-.1143	.0284	.0163	-.0039	-.0005	.0005	59.34
.05	0	.0763	.0267	.0222	-.0039	-.0005	.0004	59.24
2.18	0	.256	.0293	.0274	-.0045	-.0006	.0006	59.33
4.31	0	.4378	.0361	.032	-.0045	-.0007	.0006	59.23
6.44	0	.6183	.0465	.0355	-.0048	-.0006	.0008	59.23
8.56	0	.7942	.0608	.0385	-.0047	-.0005	.0006	59.23
10.67	0	.9425	.0806	.0393	-.0061	-.0004	-.0007	59.05
12.71	0	.9995	.1301	.0104	-.0045	-.0005	0	58.68
13.73	0	1.0357	.146	.0089	-.0036	-.0007	-.0002	58.62
14.77	0	1.089	.1609	.0061	-.0003	-.0009	-.0017	58.45
15.8	0	1.1283	.1792	-.0007	.0025	-.0004	-.0024	58.49
16.73	0	1.037	.2094	-.0159	-.0111	-.0006	-.0025	58.32
17.75	0	1.0608	.229	-.0212	-.0116	-.0006	-.0038	58.17

REYNOLDS NUMBER/FOOT= 1.29695E+06
MACH NUMBER= .2022

WICHITA STATE UNIVERSITY
7 X 10 FOOT LOW-SPEED WIND TUNNEL

Run number 18

Static Tare 1000
Dynamic Tare 3000
const. table 1

MARCH 21, 1985
GARY KREPS - THESIS PROJECT
OKLAHOMA STATE UNIVERSITY
model upright

Wind Axes Data

ALPHA (deg)	PSI (deg)	CL	CD	CM	CRM	CYM	CY	q (psf)
-6.36	0	-.509	.0494	.0133	-.0041	-.0007	.0006	59.46
-4.24	0	-.3373	.0392	.0179	-.0042	-.0006	.0008	59.55
-2.11	0	-.1507	.0323	.0245	-.0044	-.0005	.0007	59.35
.03	0	.0421	.0295	.0309	-.0044	-.0005	.0005	59.35
2.16	0	.2281	.0314	.036	-.0048	-.0005	.0005	59.24
4.29	0	.4038	.0374	.0413	-.0051	-.0006	.0005	59.34
6.41	0	.5836	.0472	.0454	-.0058	-.0006	.0001	59.34
8.54	0	.7613	.0608	.0485	-.0061	-.0004	.0001	59.14
10.63	0	.8889	.0904	.0373	-.0036	-.0006	.0016	58.99
12.69	0	.9804	.125	.0233	-.001	-.0006	.0004	58.97
13.72	0	1.0186	.1431	.017	-.0018	-.001	-.0004	58.81
14.76	0	1.0684	.161	.0102	-.0019	-.0009	-.0008	58.65
15.78	0	1.1053	.1799	.0055	.0017	-.0001	-.0011	58.5
16.73	0	1.0348	.2073	-.0098	-.0067	0	-.0002	58.31
17.74	0	1.051	.2255	-.0137	-.0108	-.0005	-.0014	58.26

REYNOLDS NUMBER/FOOT= 1.29428E+06
MACH NUMBER= .2023

WICHITA STATE UNIVERSITY
7 X 10 FOOT LOW-SPEED WIND TUNNEL

Run number 19

Static Tare 1000
Dynamic Tare 3000
const. table 1

MARCH 21, 1985
GARY KREPS - THESIS PROJECT
OKLAHOMA STATE UNIVERSITY
model upright

Wind Axes Data

ALPHA (deg)	PSI (deg)	CL	CD	CM	CRM	CYM	CY	q (psf)
-6.38	0	-.5368	.0562	.0213	-.0041	-.0009	.0004	59.57
-4.26	0	-.3685	.0454	.0263	-.0042	-.0007	.0005	59.27
-2.13	0	-.1799	.0372	.0327	-.0047	-.0007	.0005	59.36
.01	0	.0104	.0338	.0386	-.0043	-.0007	.0004	59.36
2.13	0	.1892	.035	.0442	-.0045	-.0006	.0004	59.36
4.26	0	.3718	.0404	.0493	-.0049	-.0007	.0004	59.35
6.39	0	.5503	.0499	.0537	-.0051	-.0007	.0004	59.35
8.51	0	.7265	.0629	.0571	-.0048	-.0007	.0009	59.35
10.63	0	.883	.0806	.058	-.0054	-.0007	.0007	59.26
12.7	0	.9853	.1186	.0385	-.0095	-.0006	.0012	59.25
13.69	0	.9744	.1436	.026	-.0024	-.0007	.0009	59.13
14.73	0	1.0319	.1591	.0224	-.0012	-.001	.0004	59.06
15.76	0	1.0782	.1744	.0173	.0005	-.0009	-.0005	58.89
16.73	0	1.0266	.2058	-.0007	-.0047	.0013	.0008	58.81
17.73	0	1.025	.2229	-.0068	-.0107	-.0005	-.0018	58.66

REYNOLDS NUMBER/FOOT= 1.29348E+06
MACH NUMBER= .203

WICHITA STATE UNIVERSITY
7 X 10 FOOT LOW-SPEED WIND TUNNEL

Run number 20

Static Tare 1000
Dynamic Tare 3000
const. table 1

MARCH 21, 1985
GARY KREPS - THESIS PROJECT
OKLAHOMA STATE UNIVERSITY
model upright

Wind Axes Data

ALPHA (deg)	PSI (deg)	CL	CD	CM	CRM	CYM	CY	q (psf)
-6.4	0	-.5661	.0645	.0286	-.0042	-.001	.0012	59.3
-4.28	0	-.397	.0529	.0334	-.0042	-.0009	.0012	59.49
-2.15	0	-.2184	.0441	.0392	-.0045	-.0007	.0009	59.38
-.01	0	-.0206	.0392	.0454	-.0045	-.0006	.0008	59.38
2.11	0	.1602	.0394	.0511	-.0047	-.0005	.0006	59.37
4.24	0	.3379	.044	.0561	-.0052	-.0006	.0007	59.27
6.37	0	.5187	.0525	.0609	-.0052	-.0005	.0003	59.27
8.49	0	.6869	.0652	.0646	-.0053	-.0004	-.0002	59.17
10.57	0	.802	.0946	.0541	-.006	-.0007	.0002	59.23
12.63	0	.8894	.1285	.0392	-.003	-.0007	.0001	59.01
13.67	0	.9431	.1429	.0344	-.0018	-.0008	-.0005	58.94
14.7	0	.9925	.1572	.0321	-.0016	-.0008	-.0014	58.87
15.74	0	1.046	.1742	.0264	.0001	-.0007	-.0019	58.7
16.75	0	1.0571	.2023	.0109	.0034	.0025	-.0003	58.58
17.74	0	1.043	.2249	-.0009	-.003	.0013	-.0019	58.36

REYNOLDS NUMBER/FOOT= 1.28525E+06
MACH NUMBER= .2025

APPENDIX C

WIND TUNNEL COEFFICIENT PLOTS

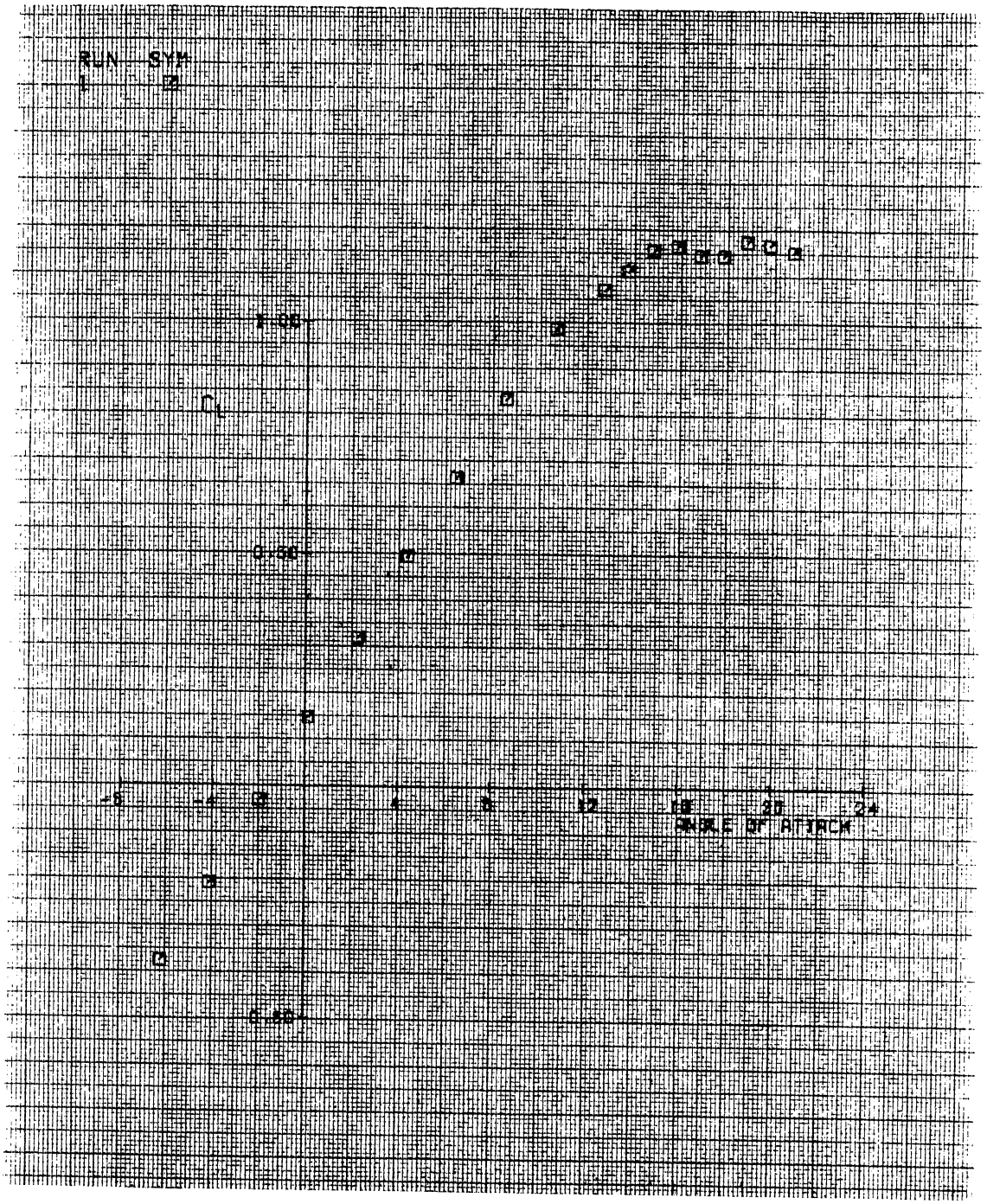

Figure 23. Run 1. Cl vs Alpha

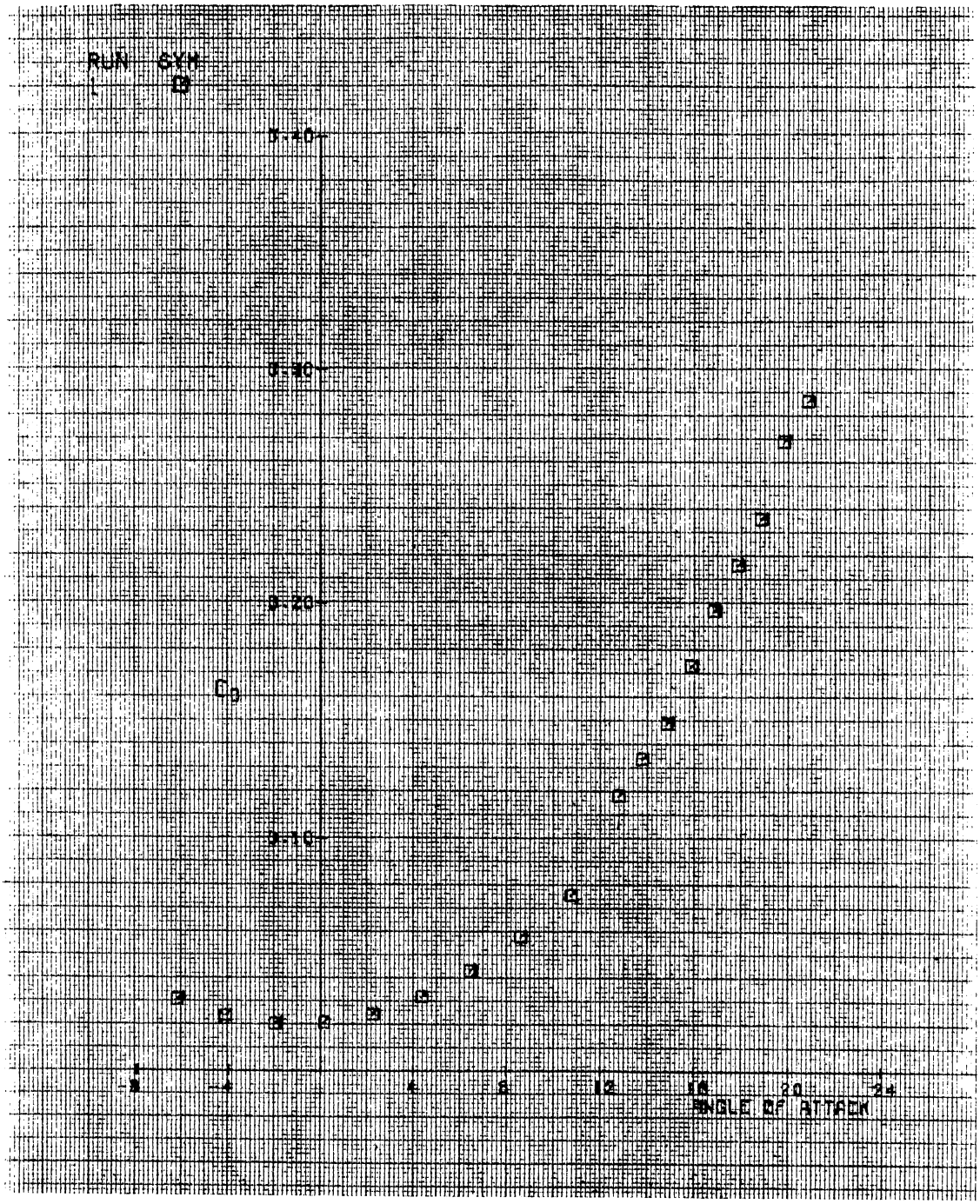

Figure 24. Run 1. Cd vs Alpha

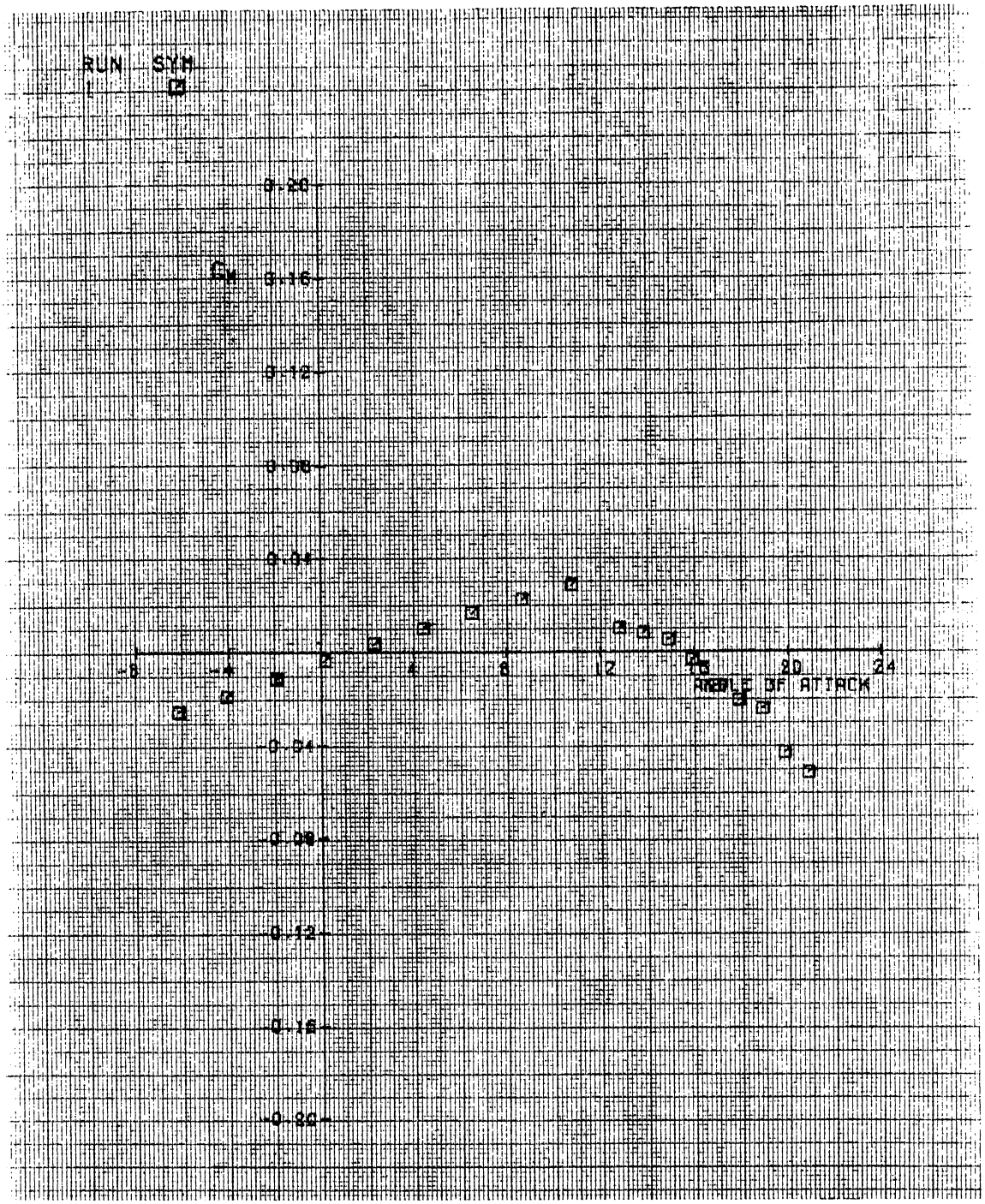

Figure 25. Run 1. Cm vs Alpha

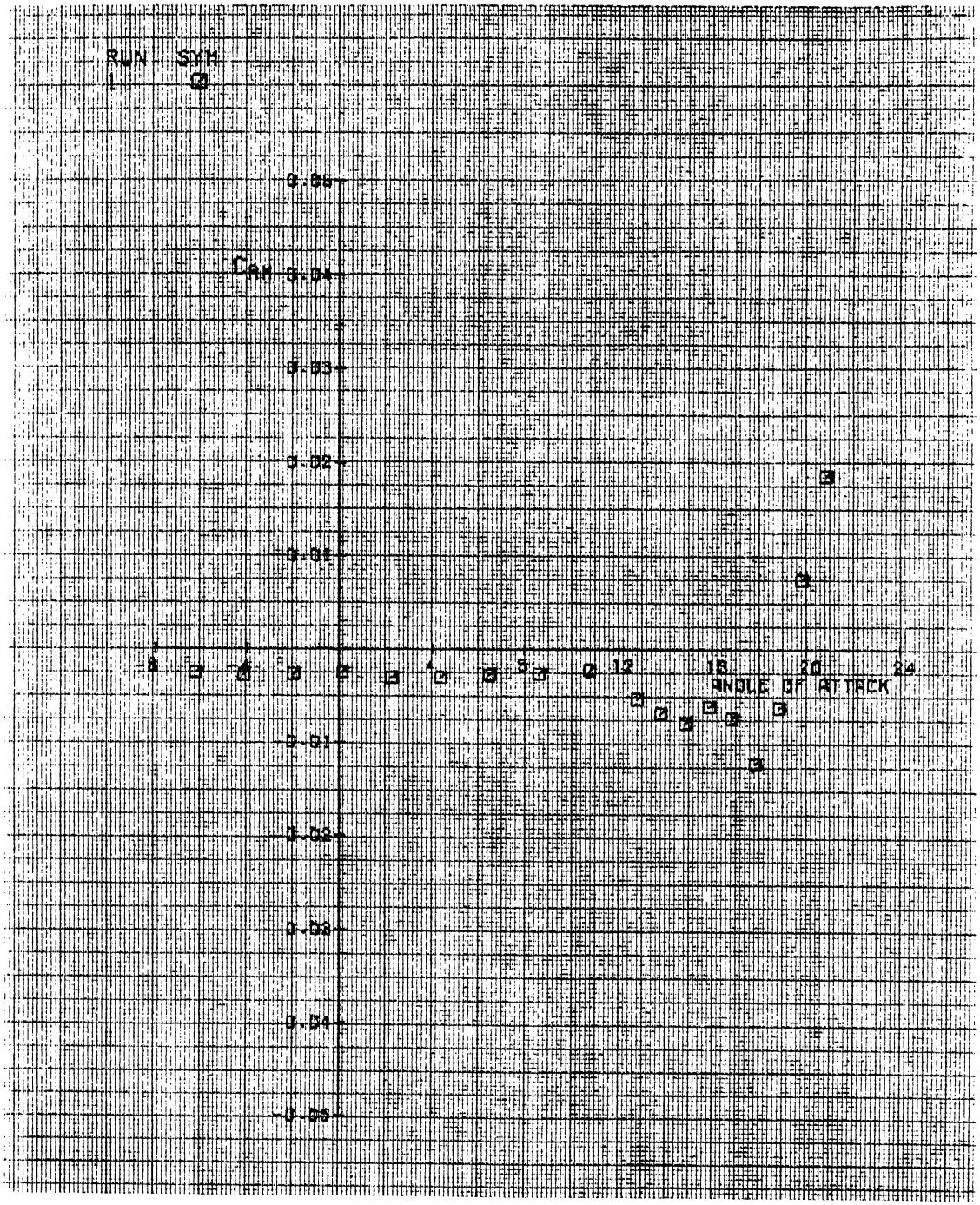

Figure 26. Run 1. Crm vs Alpha

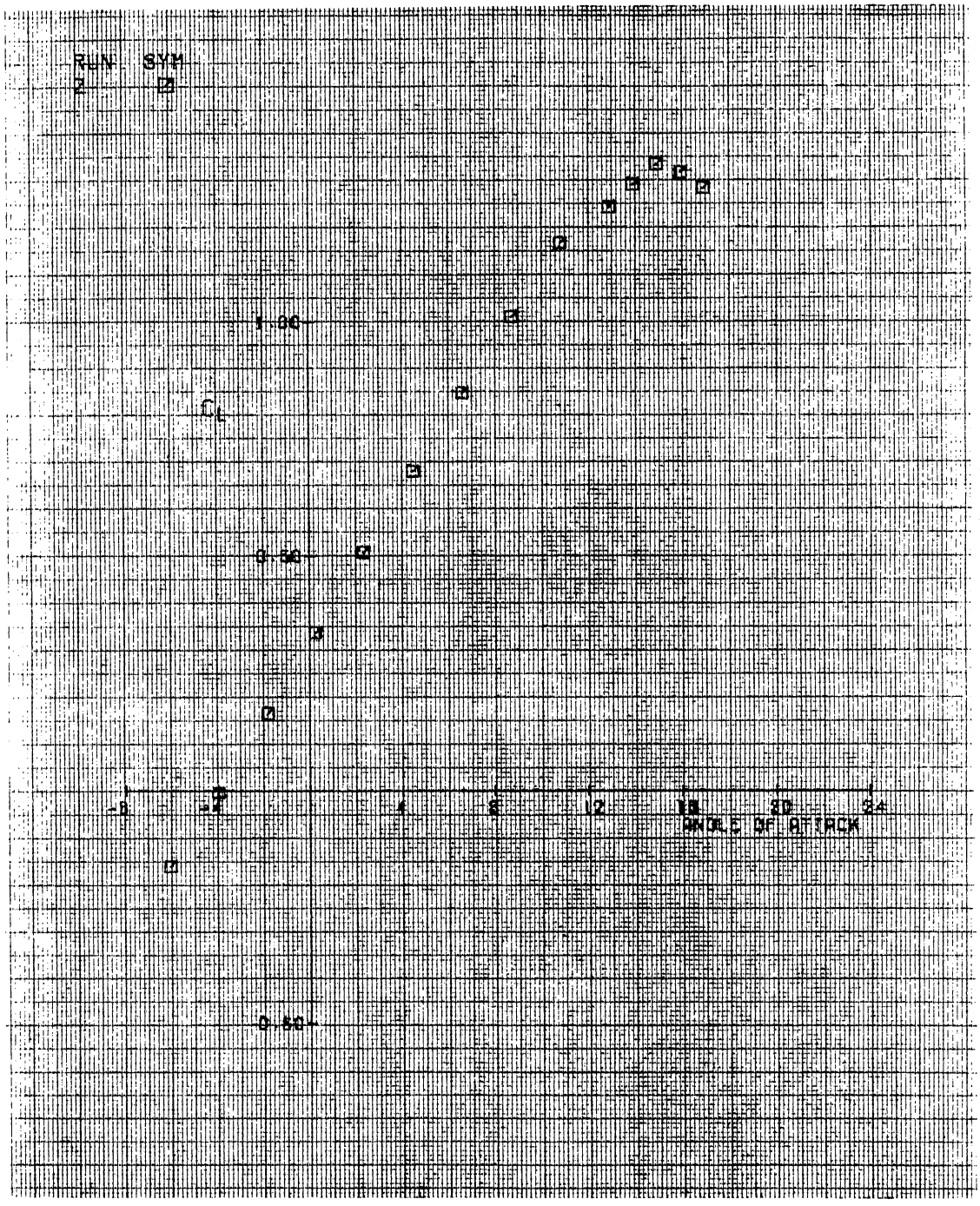

Figure 27. Run 2. Cl vs Alpha

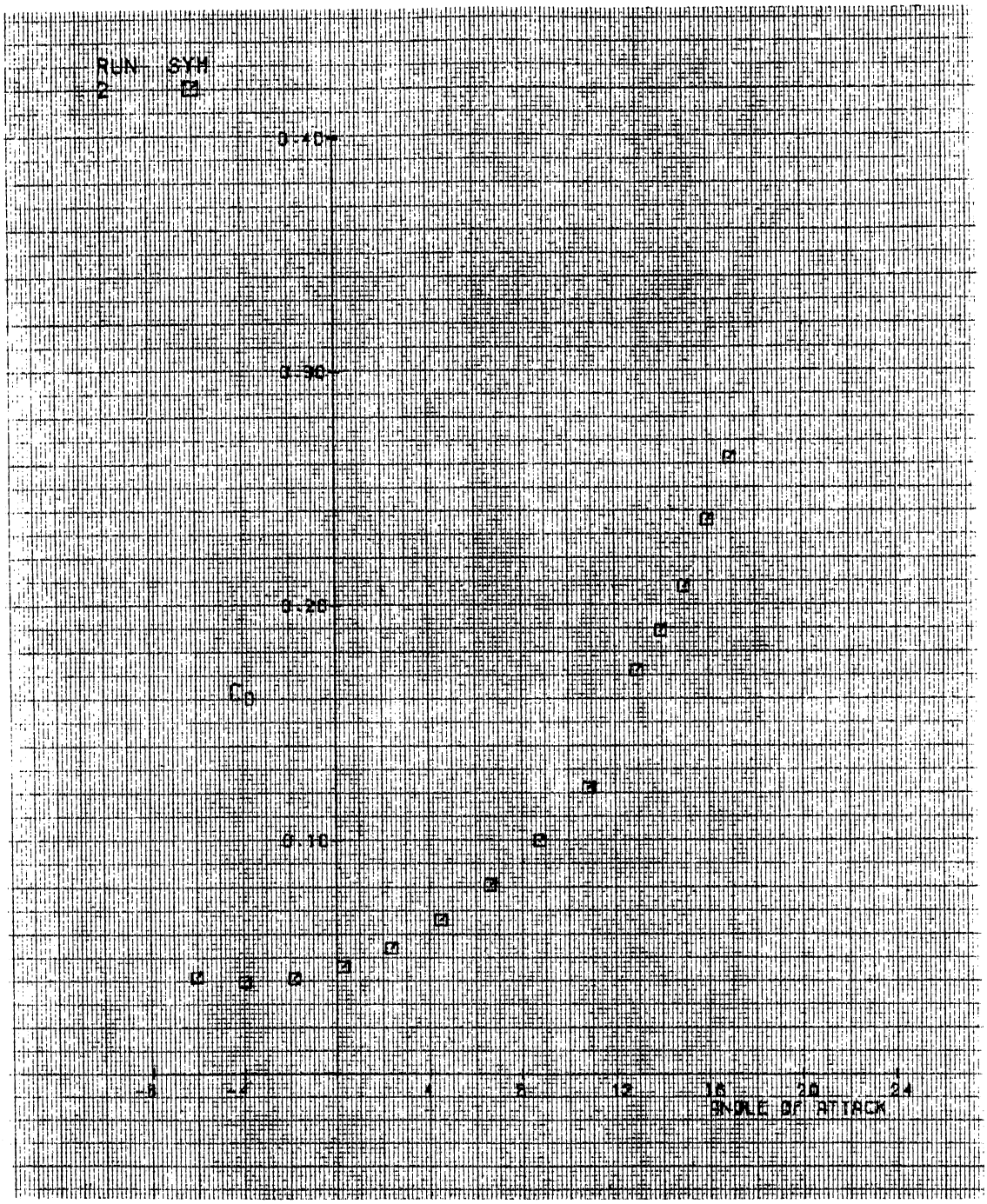

Figure 28. Run 2. Cd vs Alpha

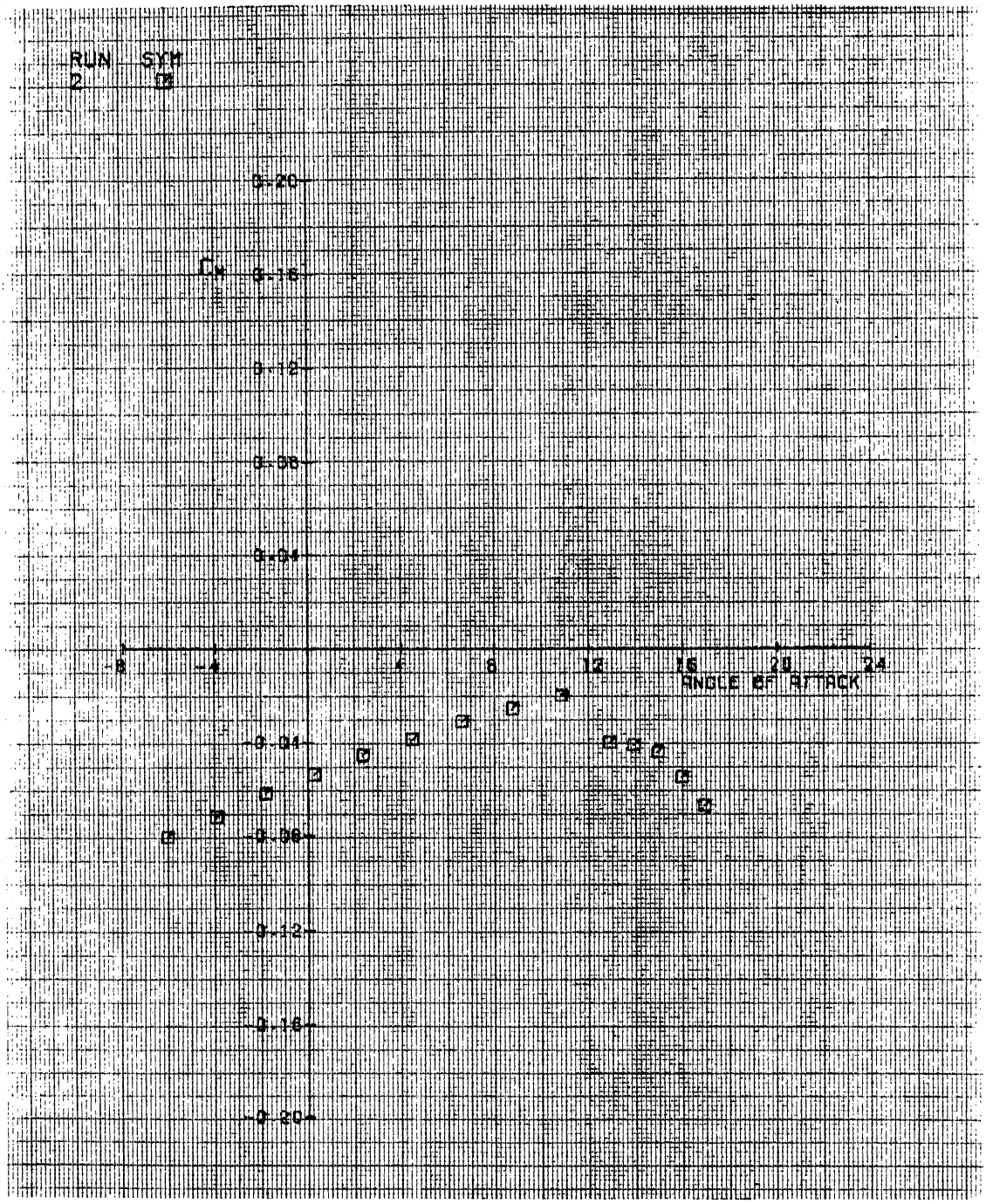

Figure 29. Run 2. Cm vs Alpha

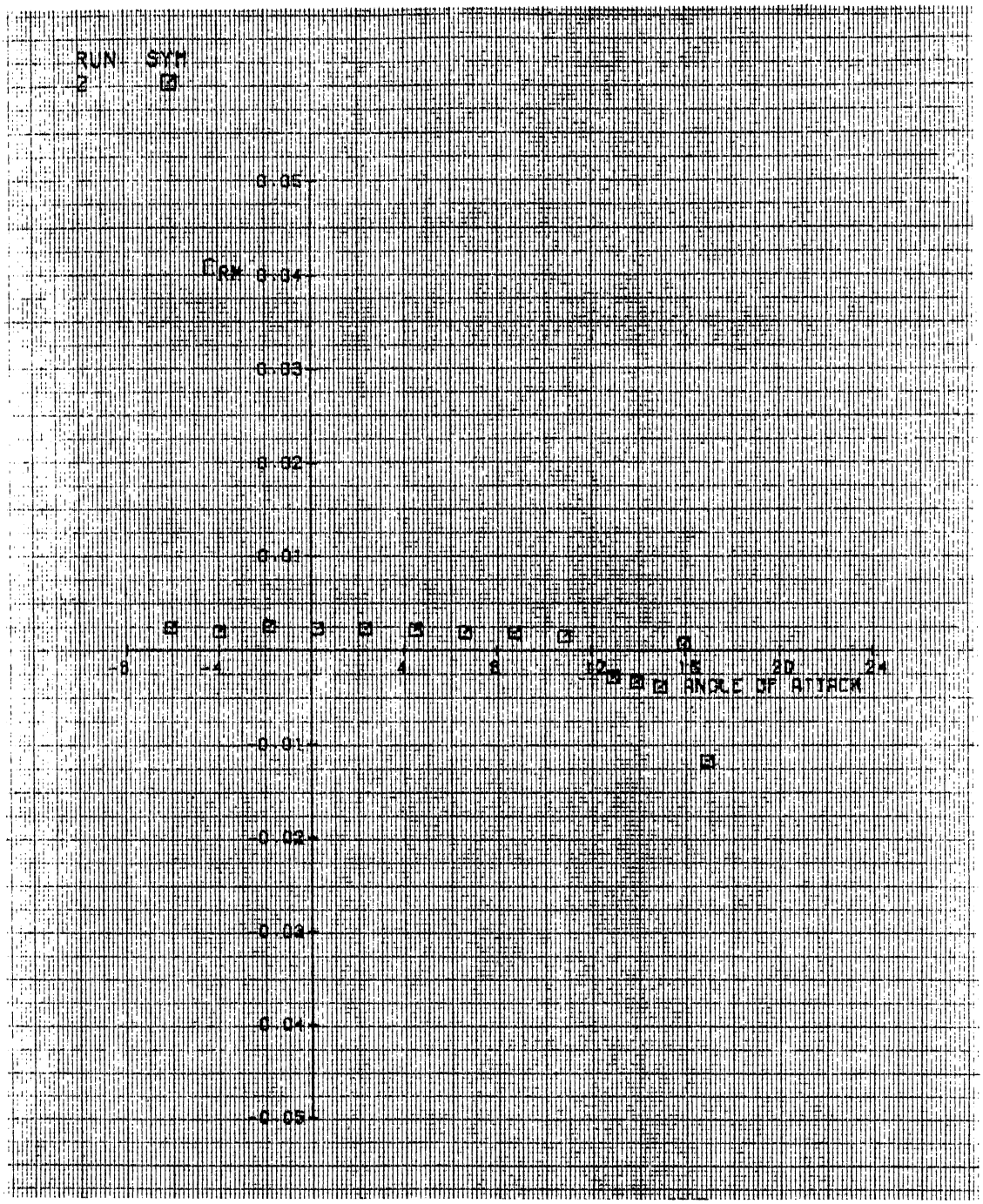

Figure 30. Run 2. Crm vs Alpha

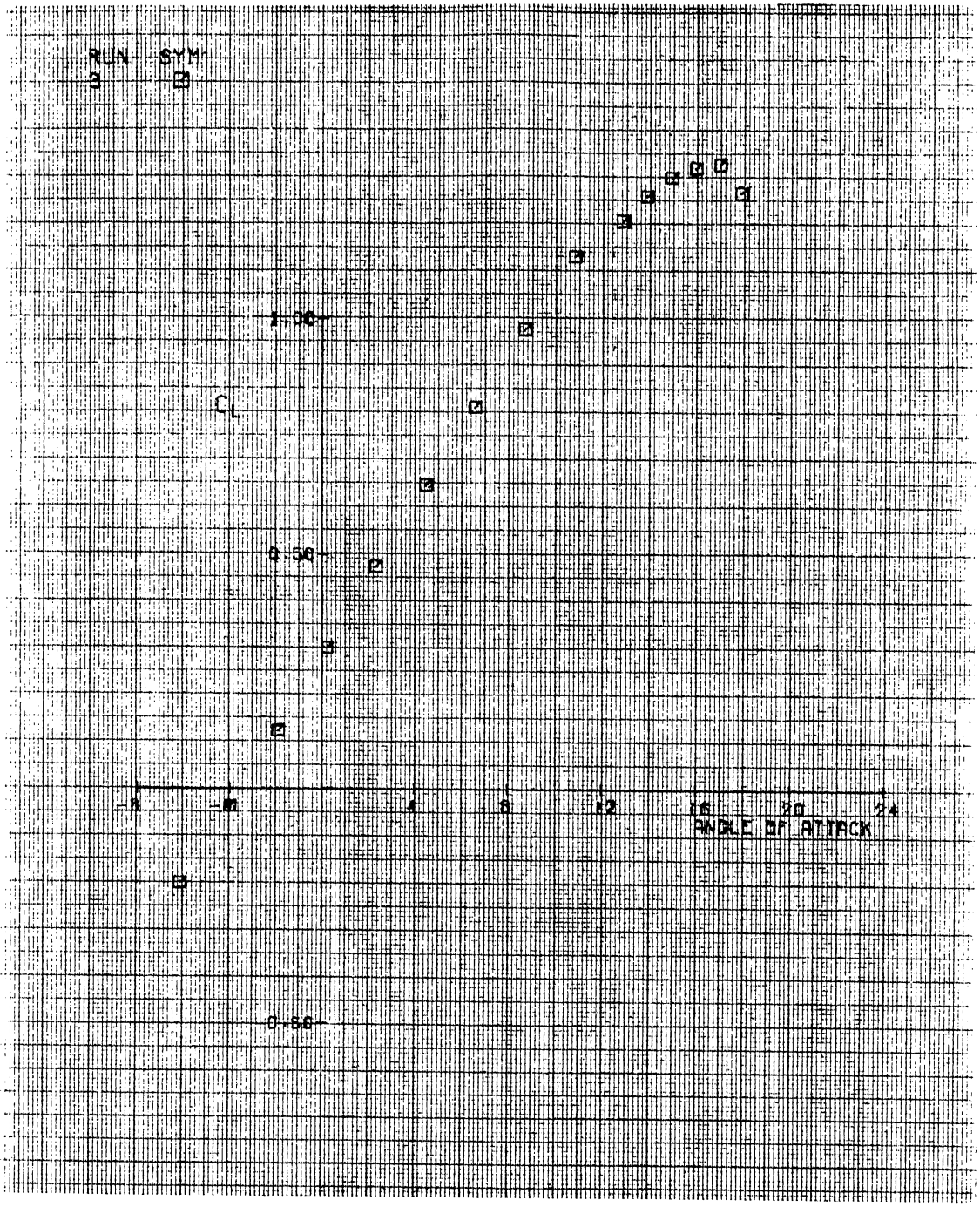

Figure 31. Run 3. Cl vs Alpha

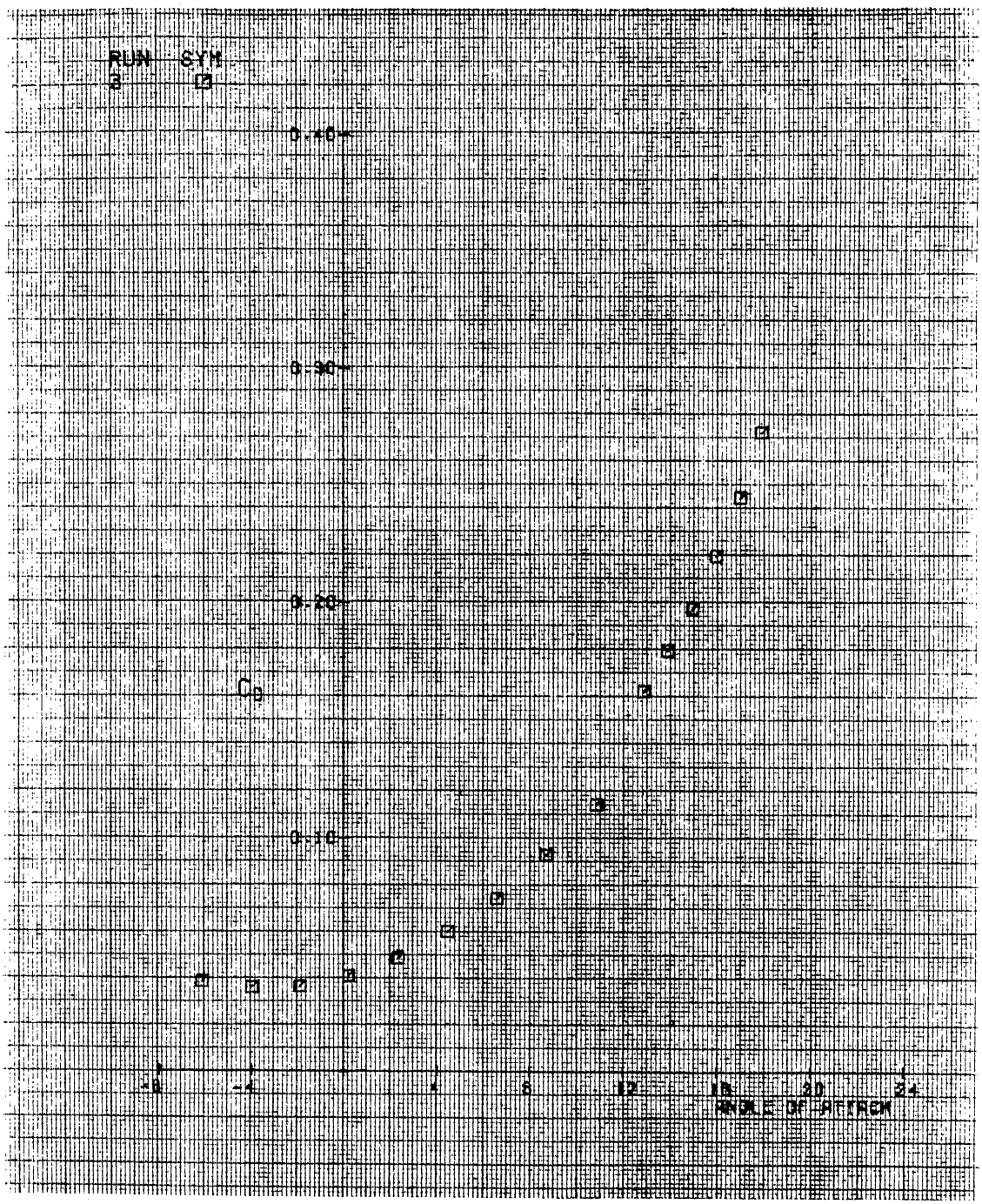

Figure 32. Run 3. Cd vs Alpha

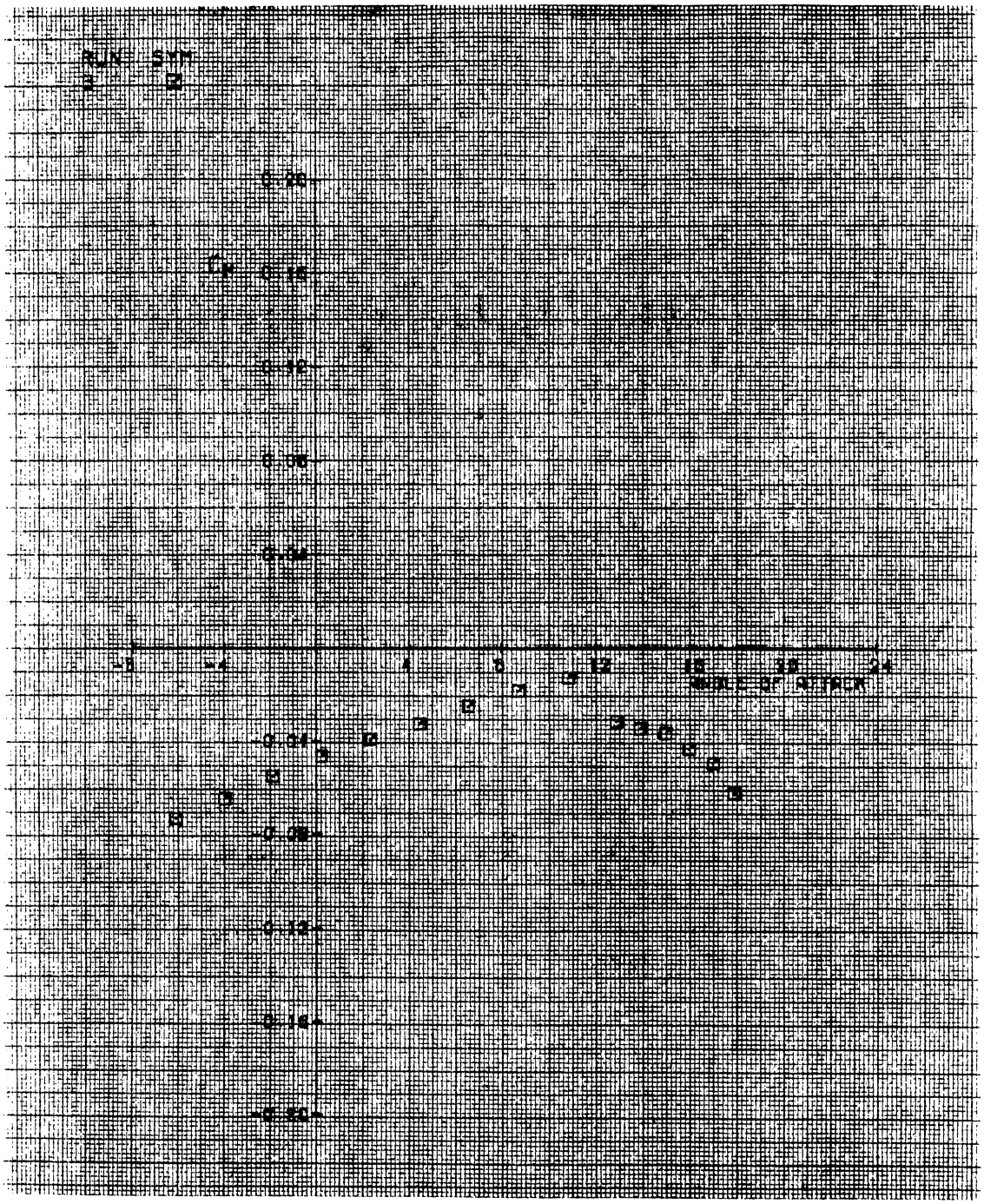

Figure 33. Run 3. Cm vs Alpha

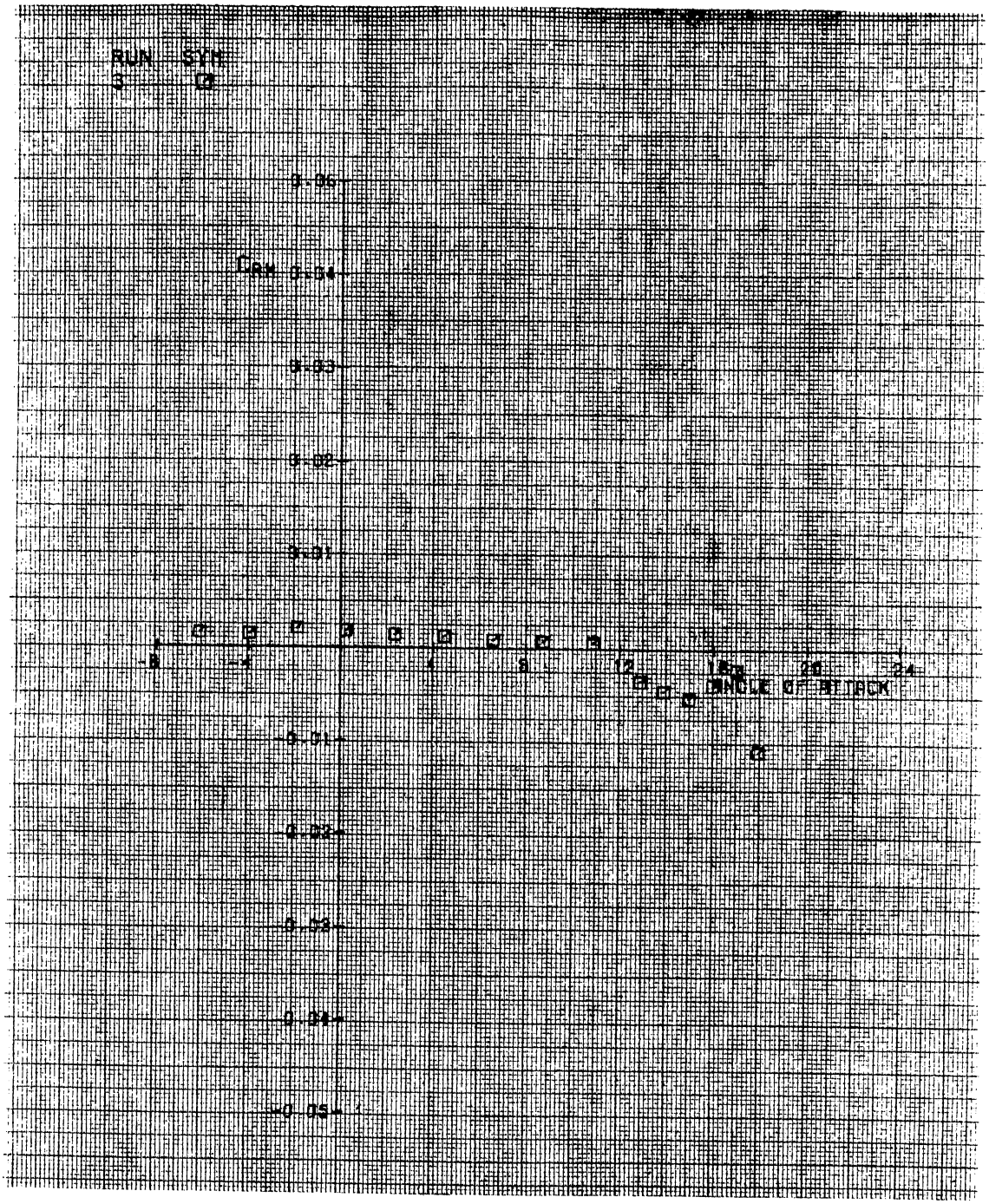

Figure 34. Run 3. Crm vs Alpha

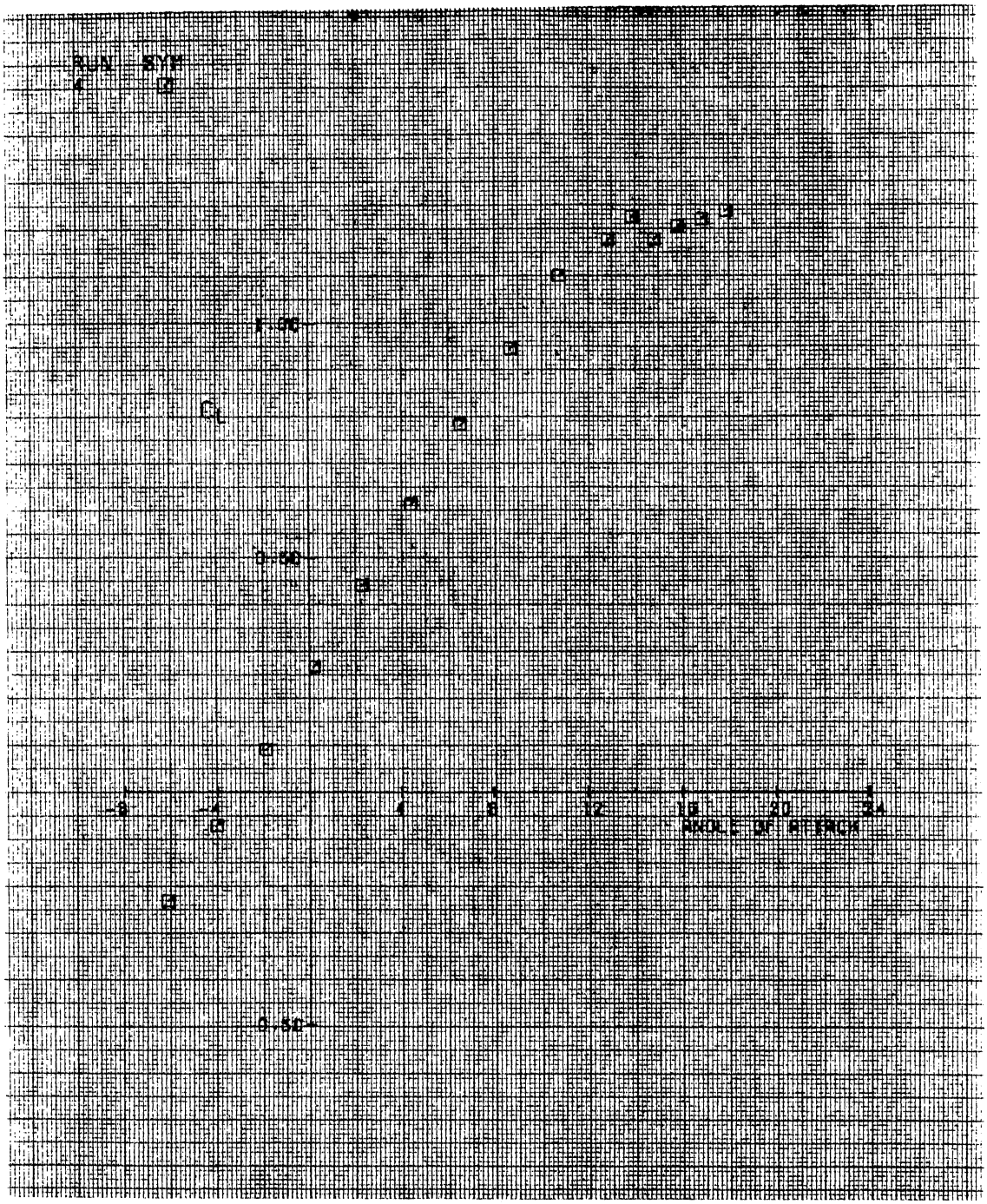

Figure 35. Run 4. Cl vs Alpha

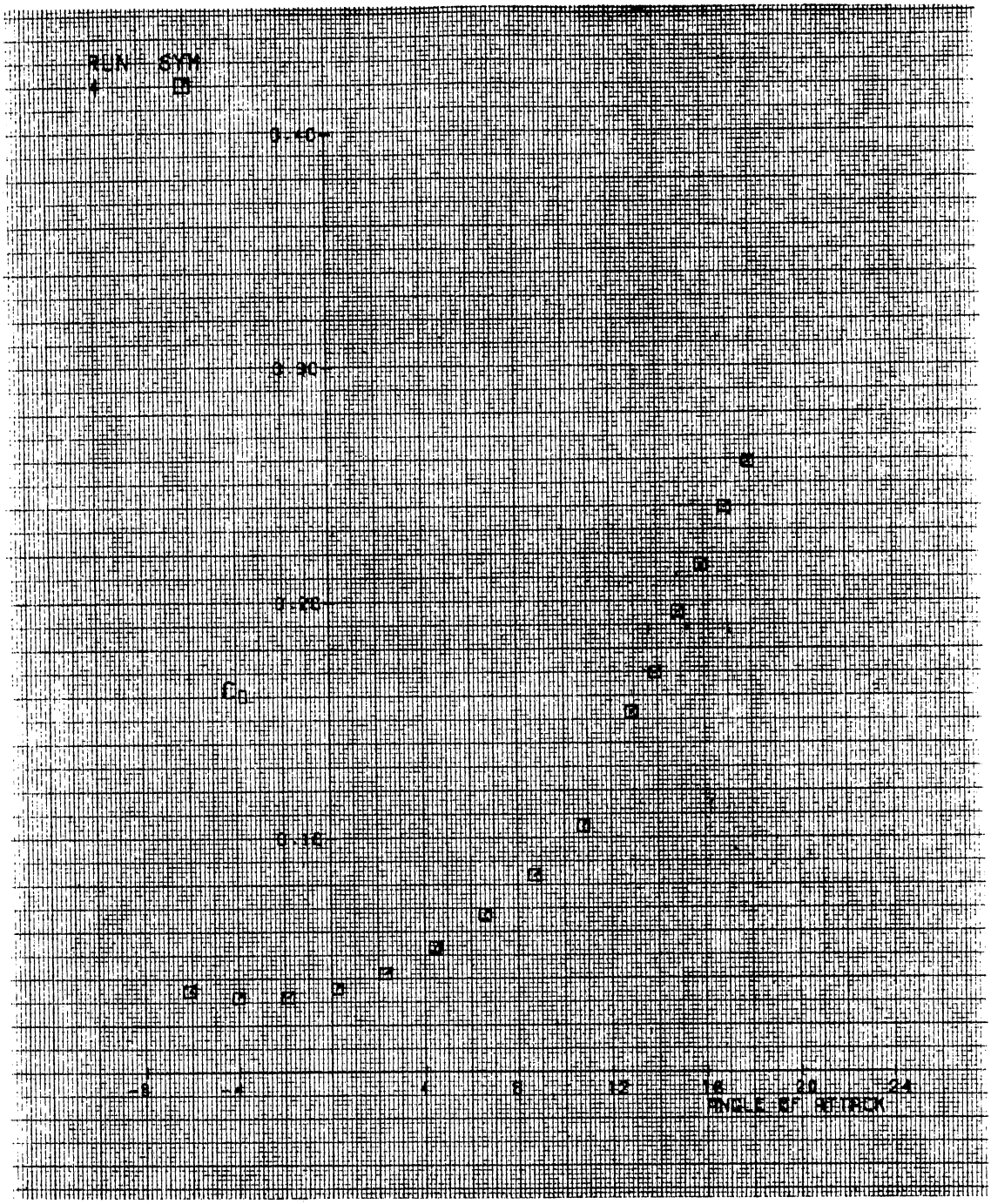

Figure 36. Run 4. Cd vs Alpha

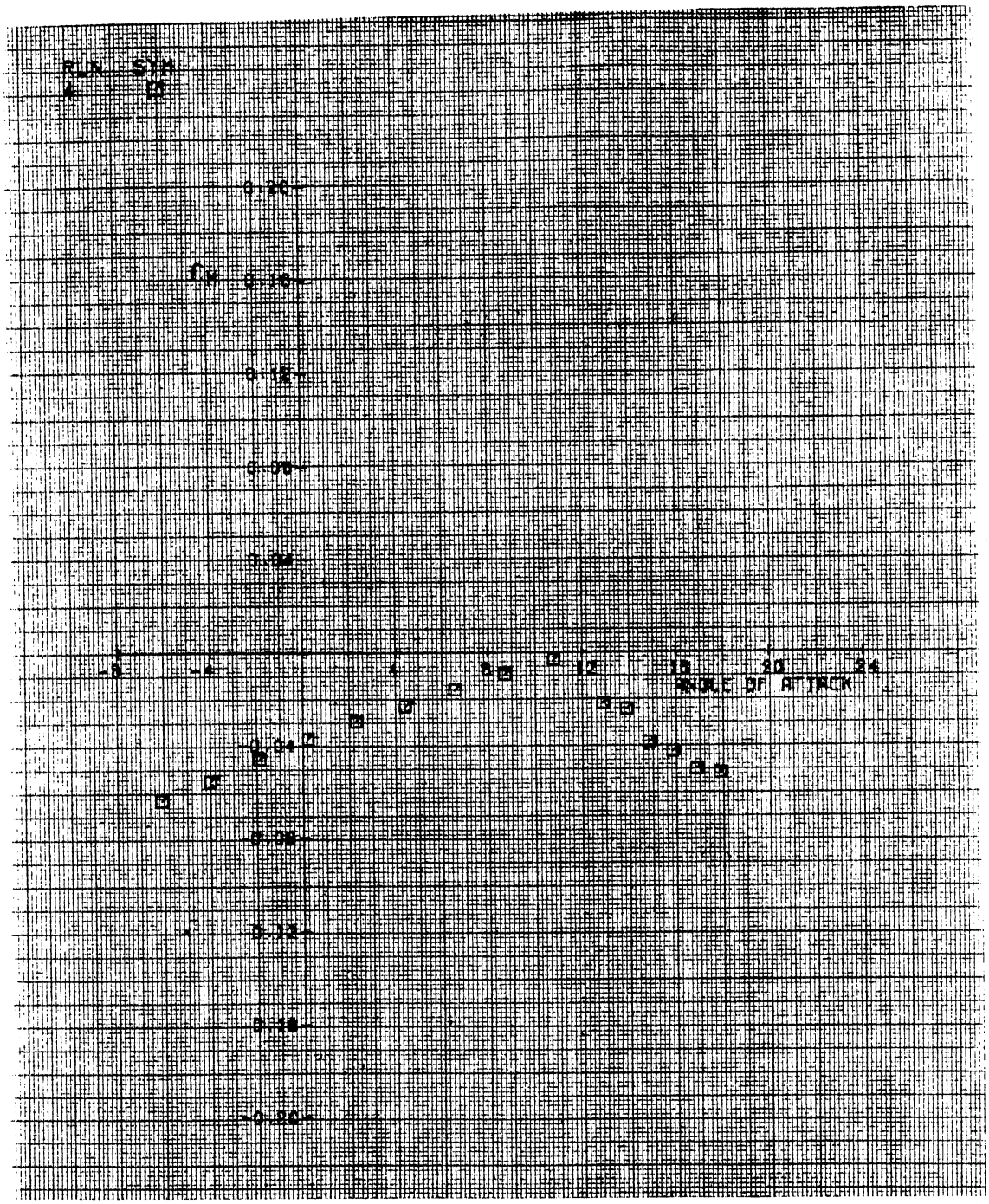

Figure 37. Run 4. Cm vs Alpha

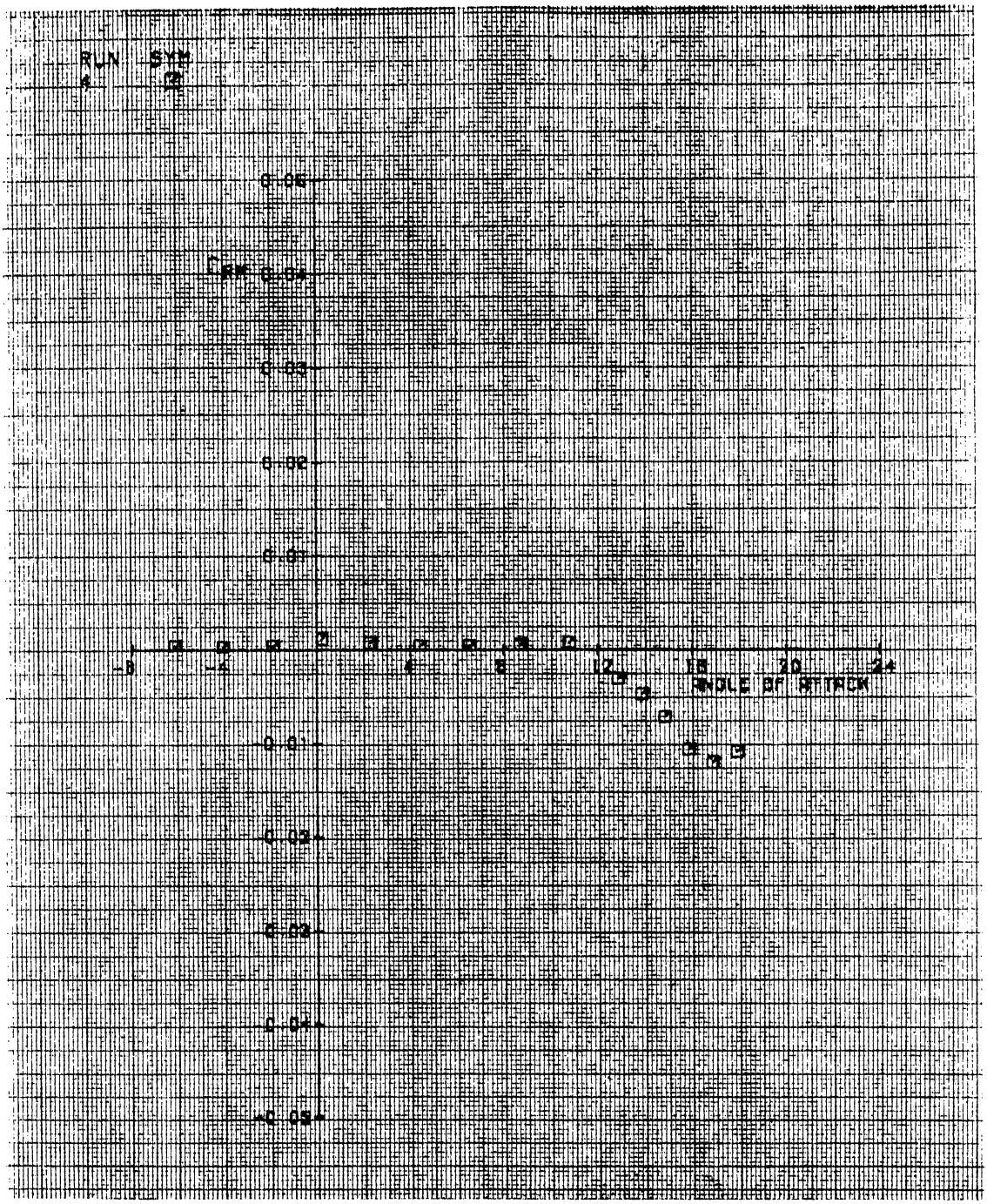

Figure 38. Run 4. Crm vs Alpha

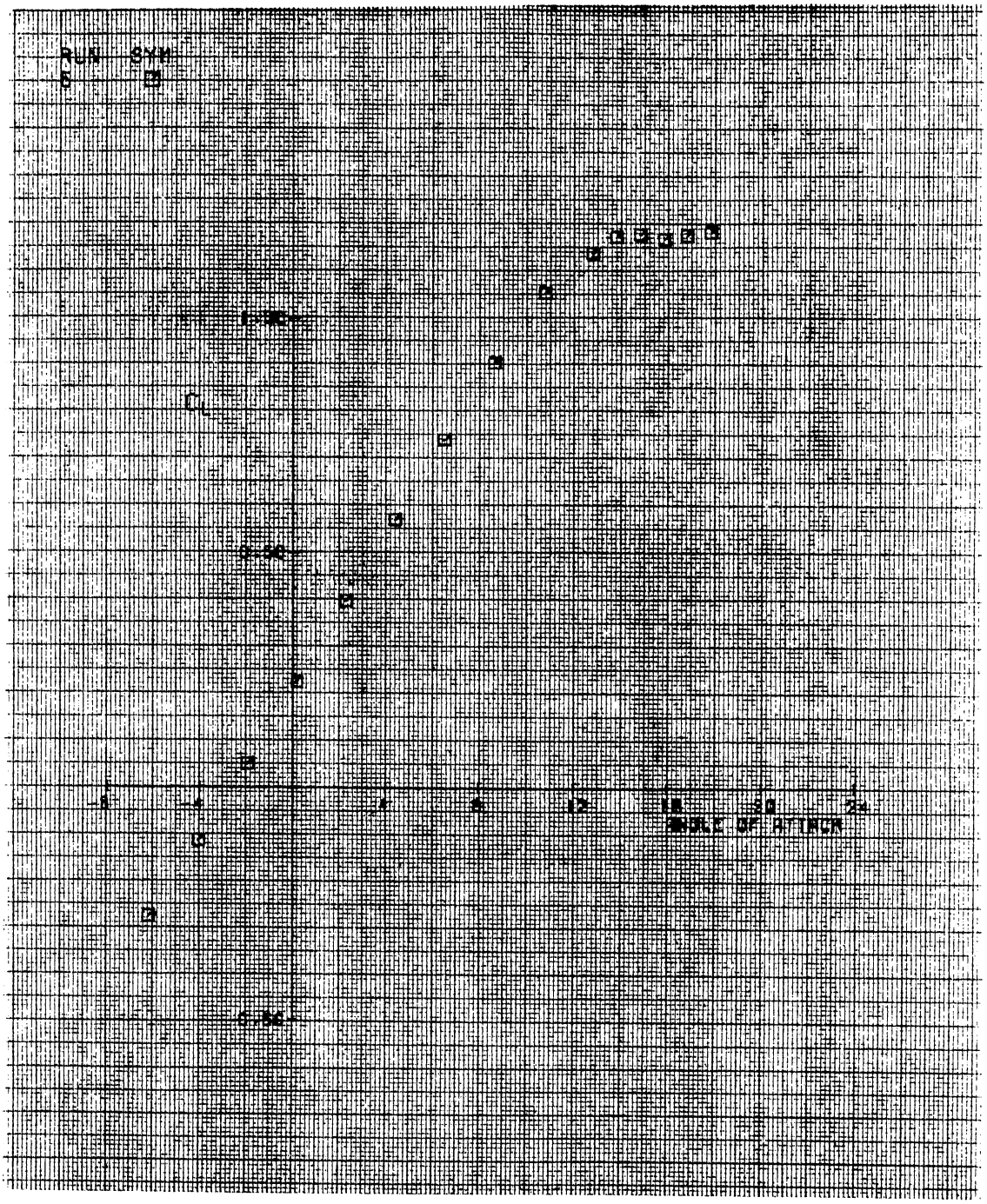

Figure 39. Run 5. Cl vs Alpha

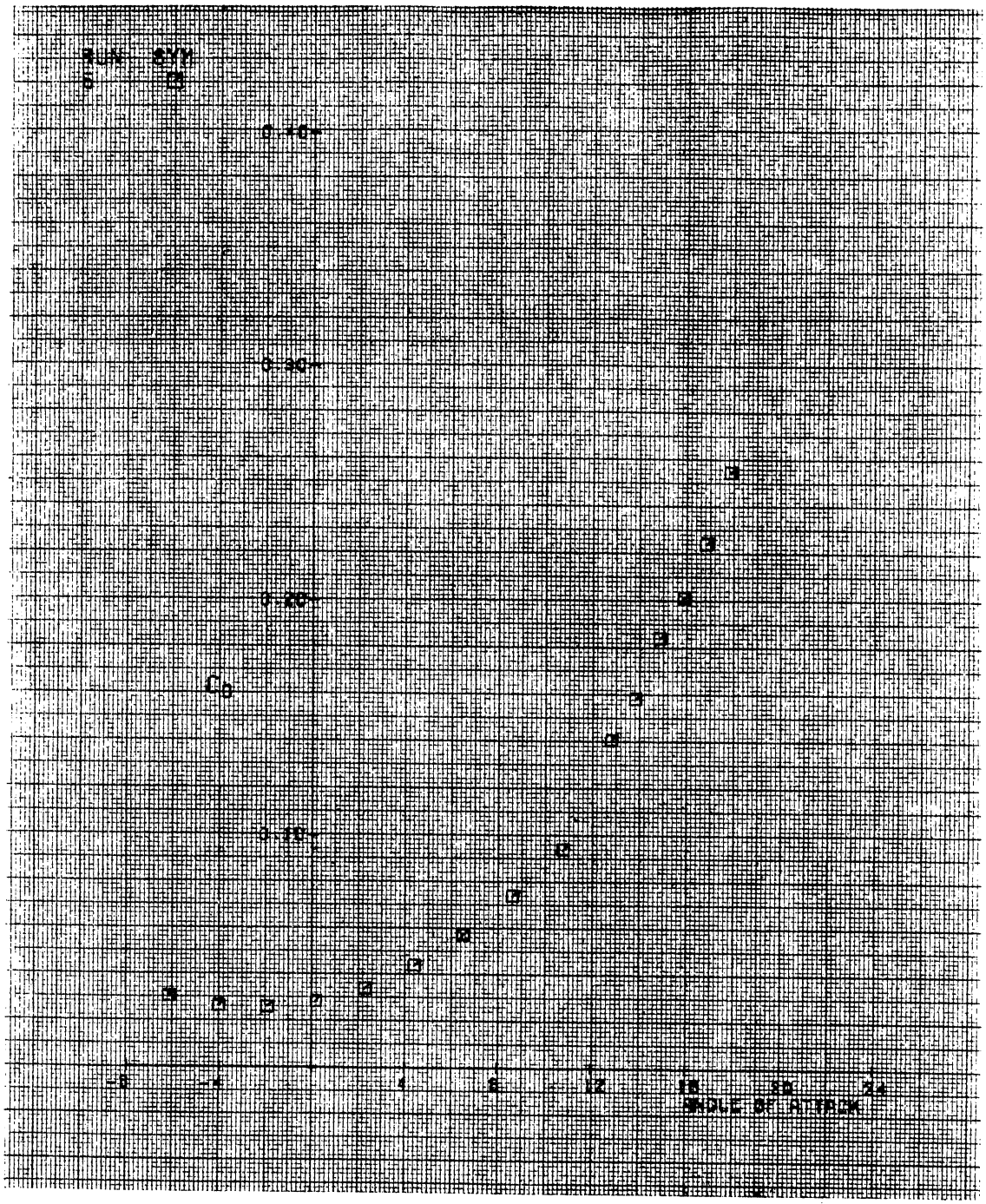

Figure 40. Run 5. Cd vs Alpha

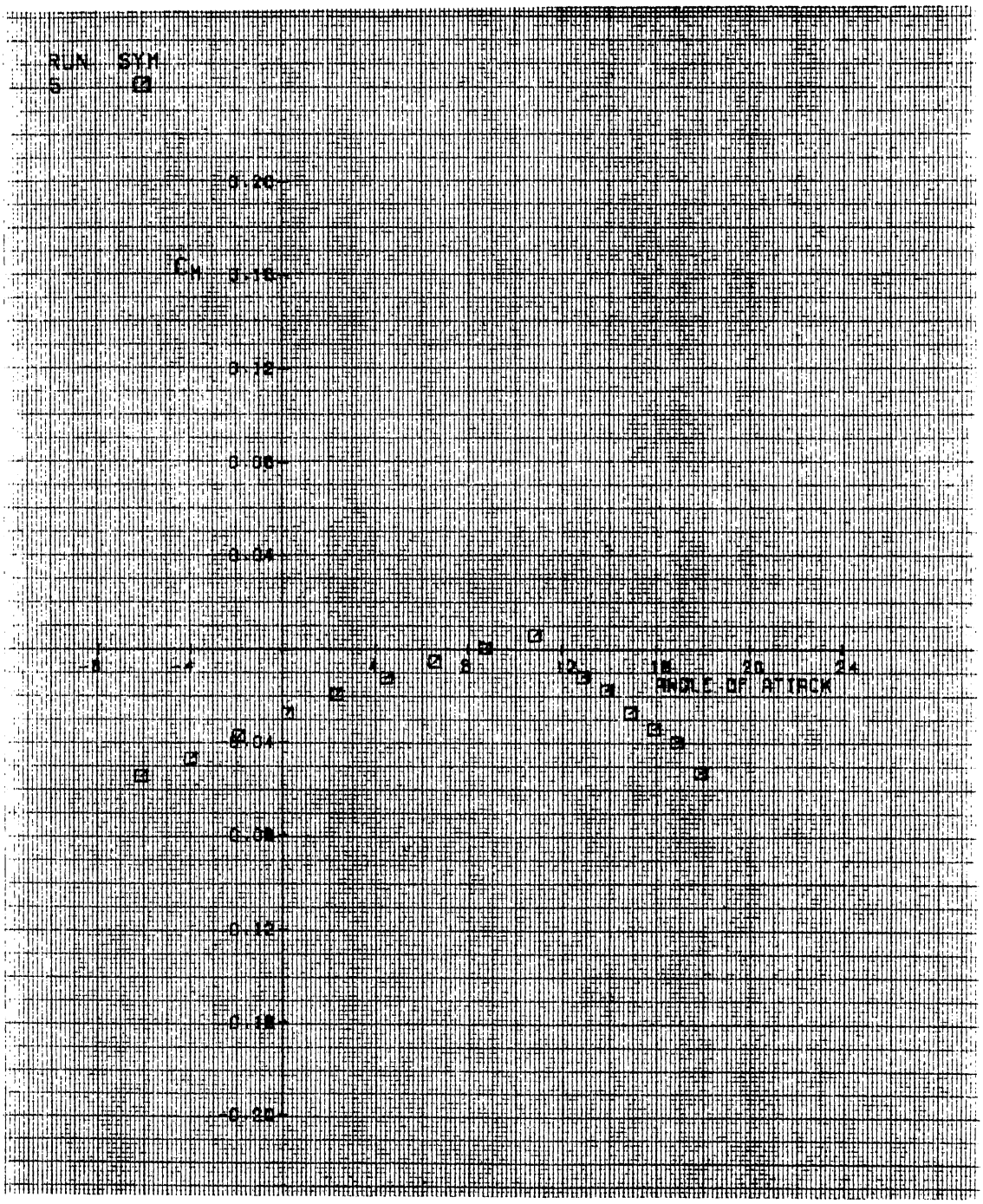

Figure 41. Run 5. Cm vs Alpha

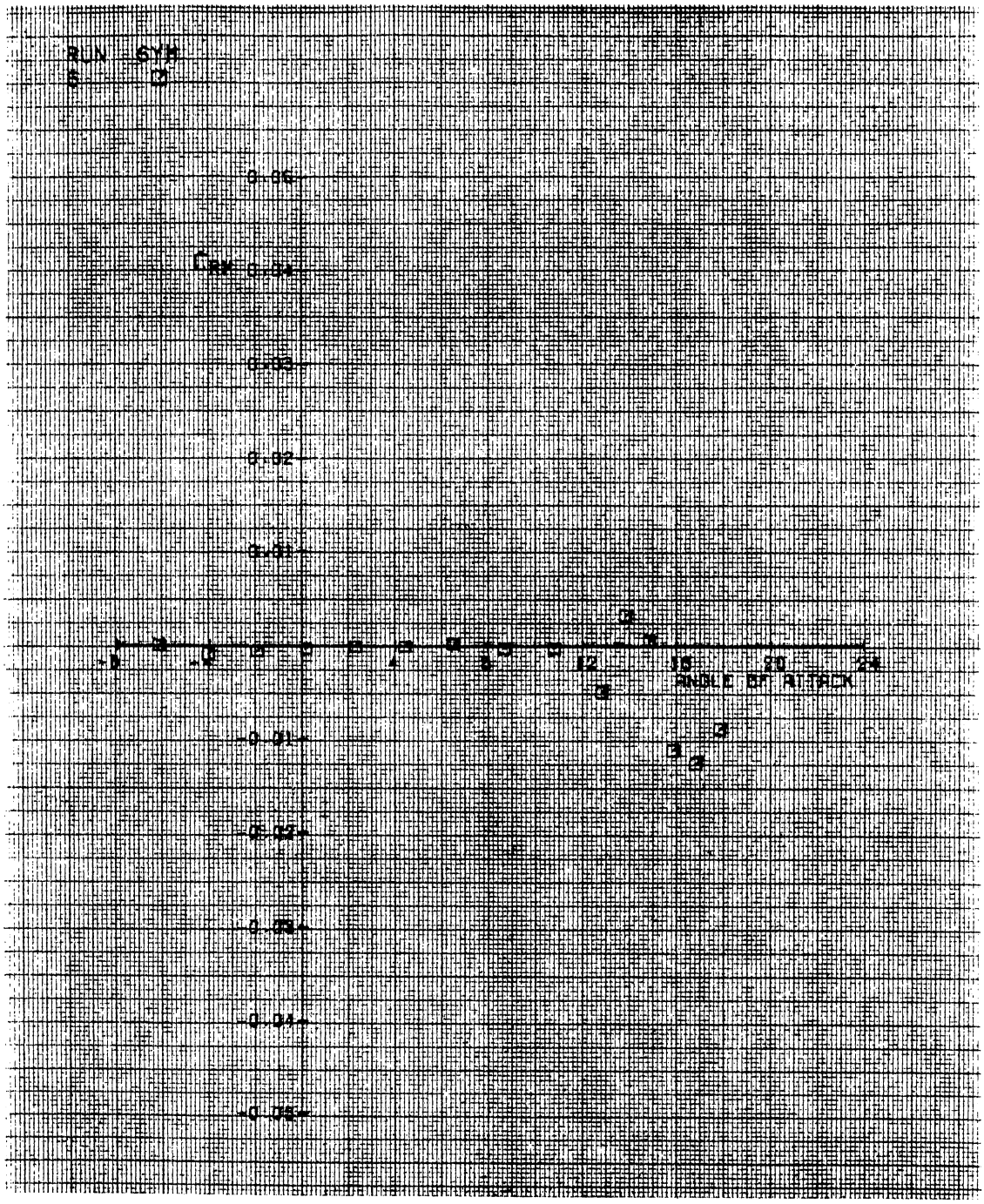

Figure 42. Run 5. Crm vs Alpha

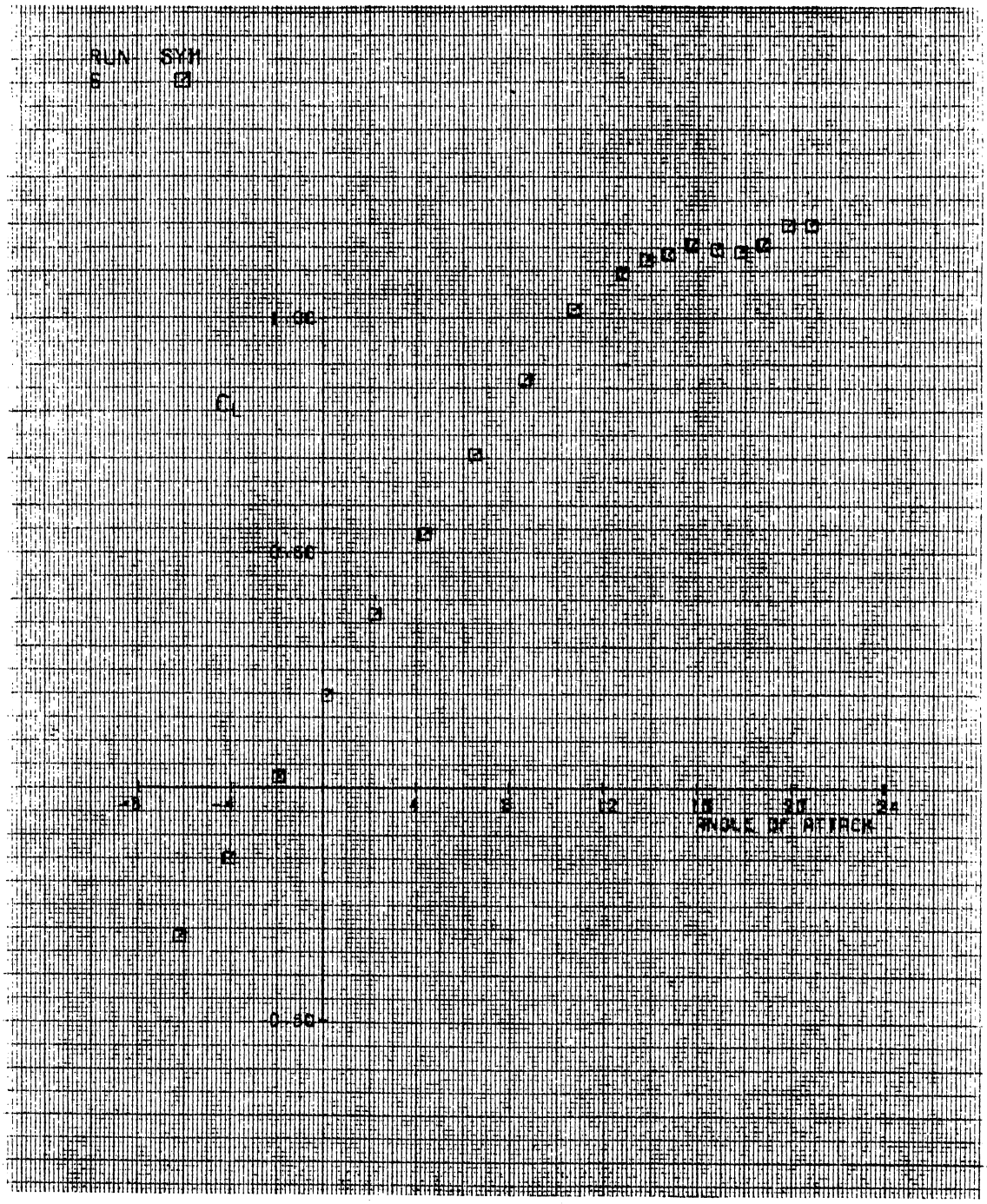

Figure 43. Run 6. Cl vs Alpha

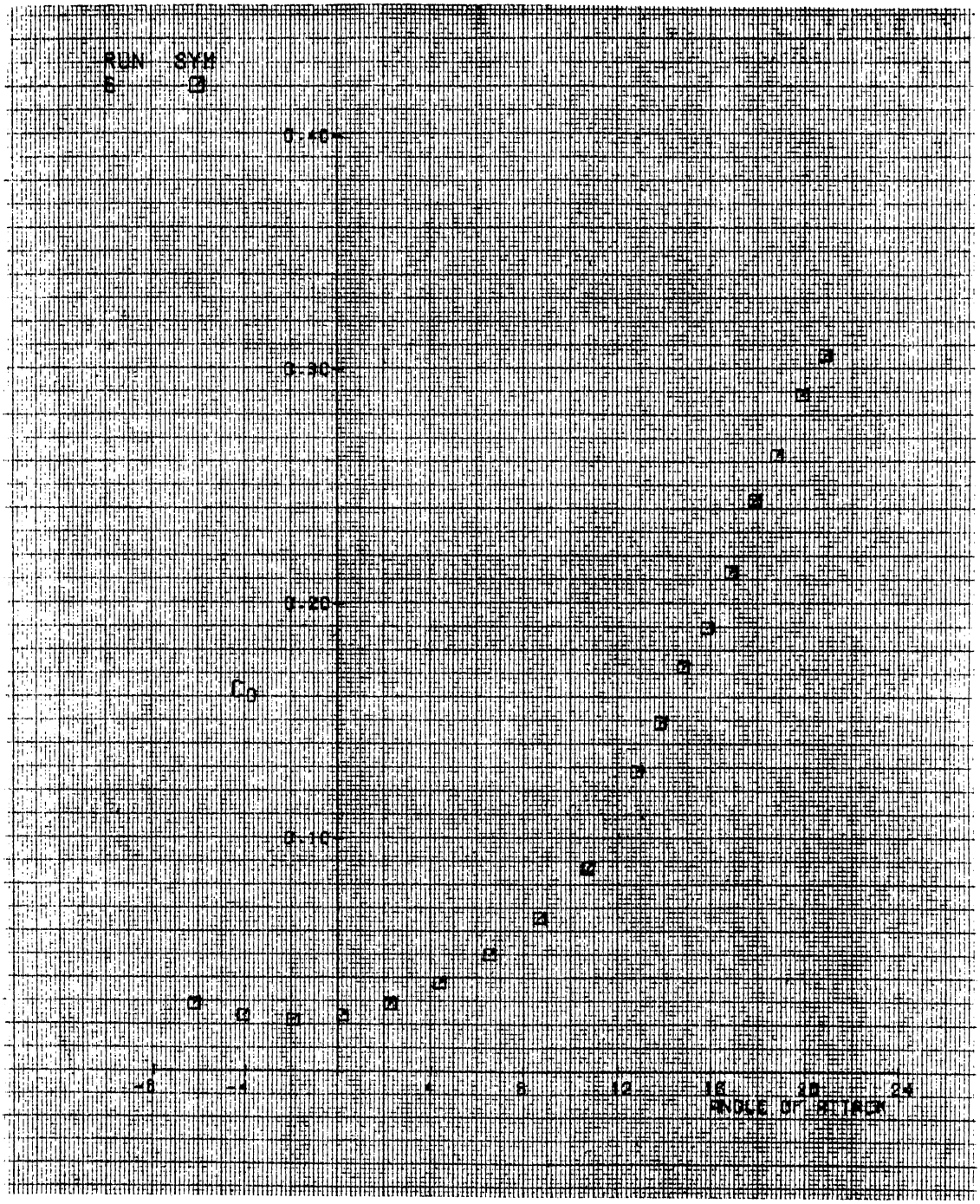

Figure 44. Run 6. Cd vs Alpha

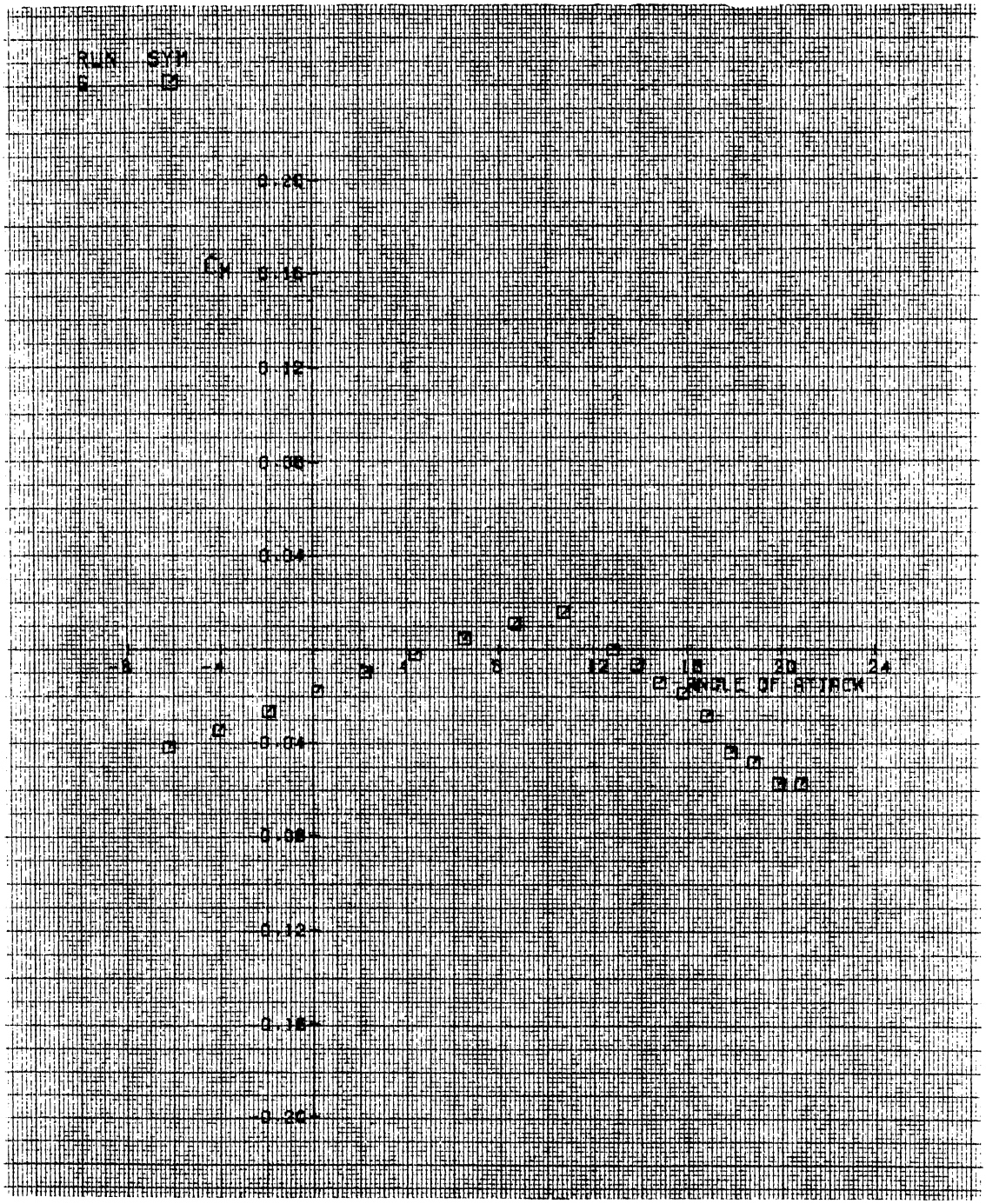

Figure 45. Run 6. Cm vs Alpha

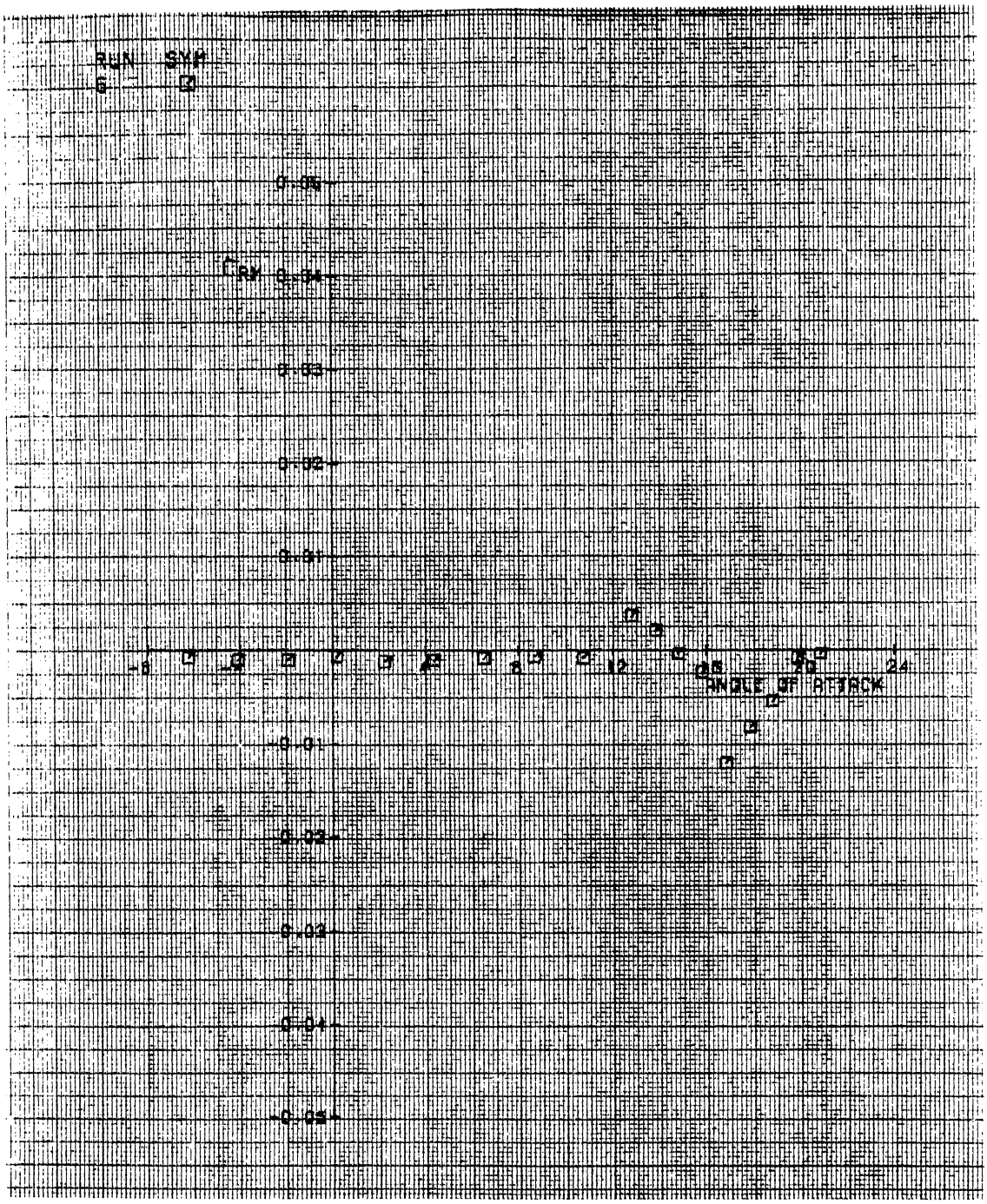

Figure 46. Run 6. Crm vs Alpha

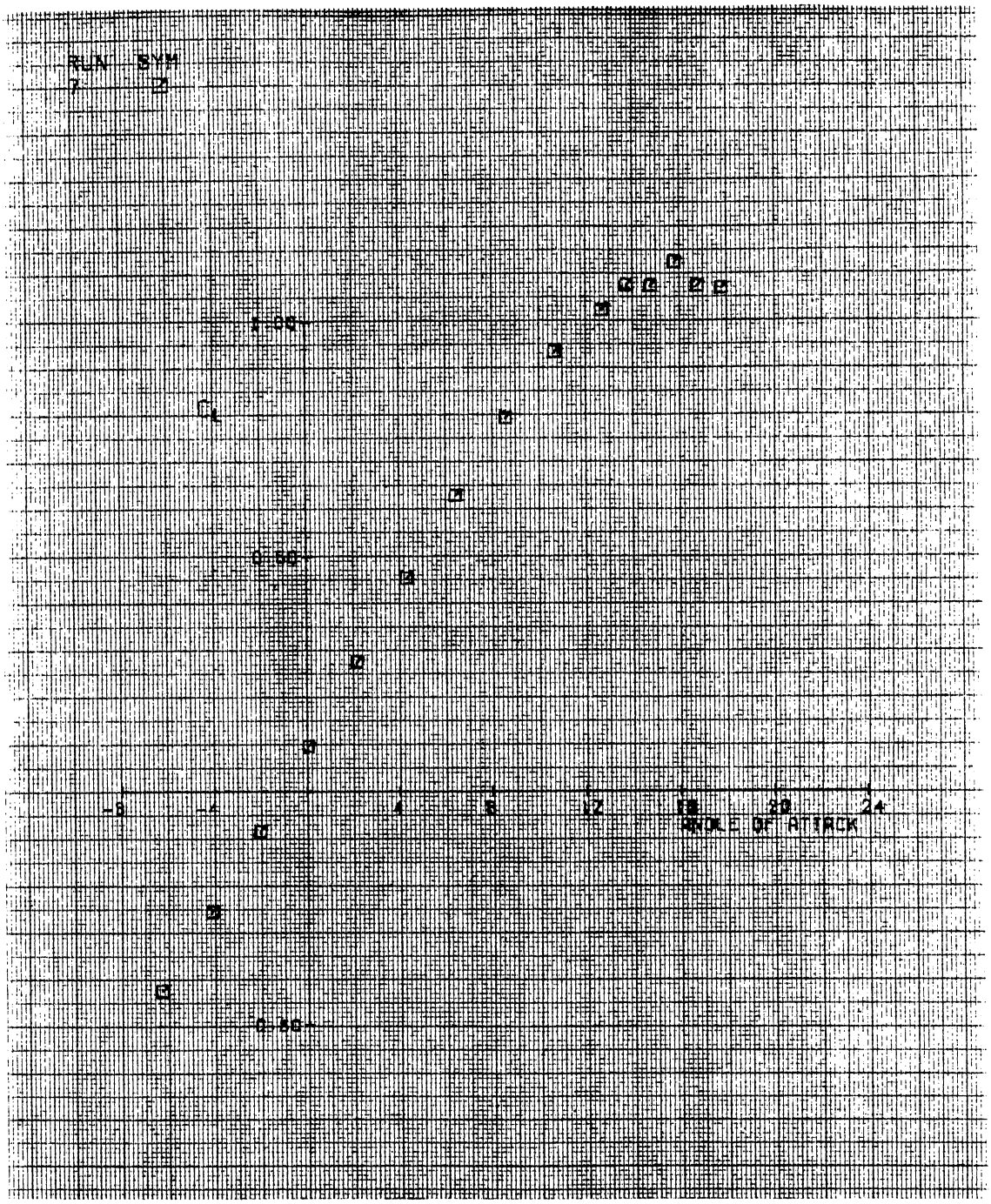

Figure 47. Run 7. Cl vs Alpha

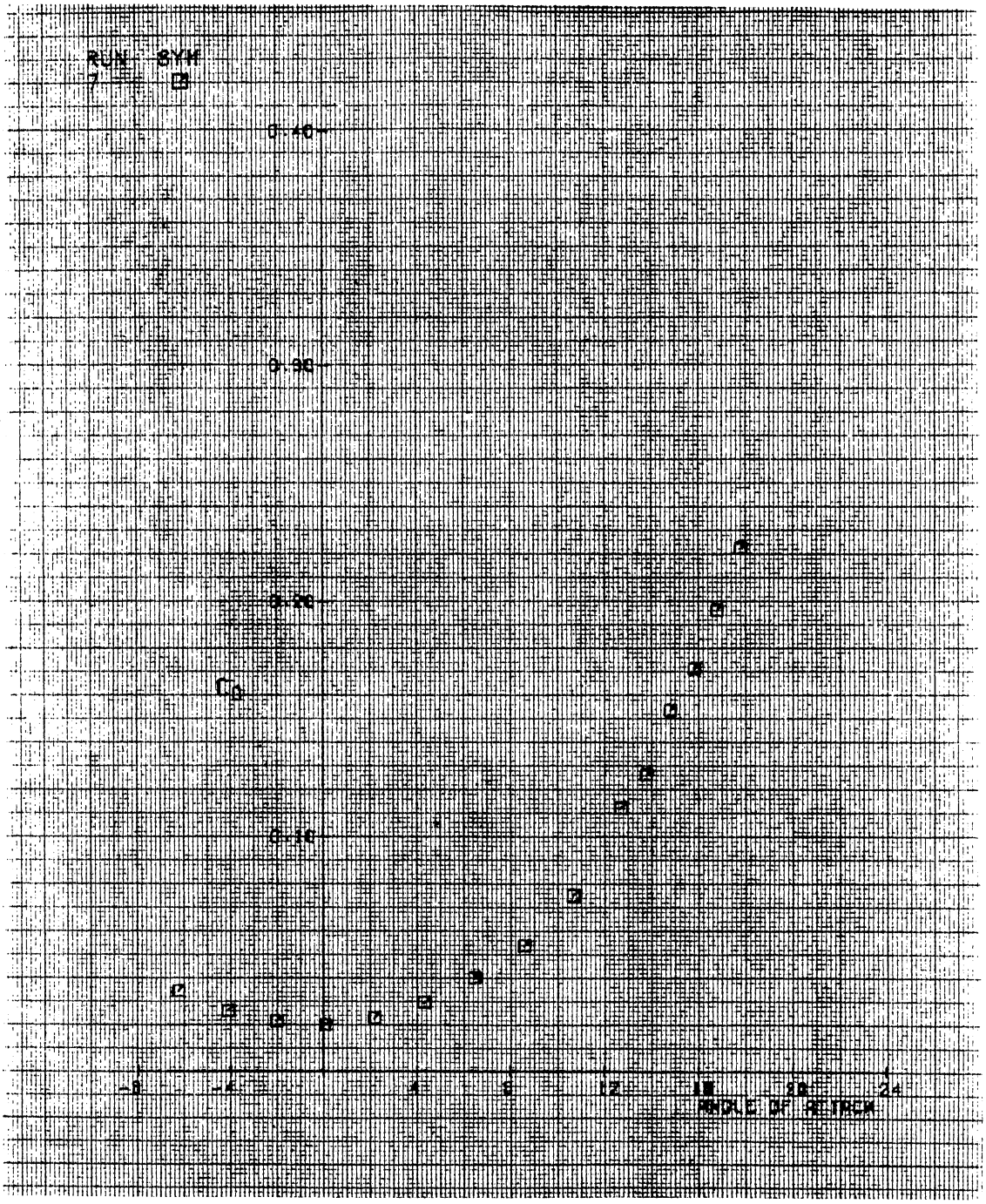

Figure 48. Run 7. Cd vs Alpha

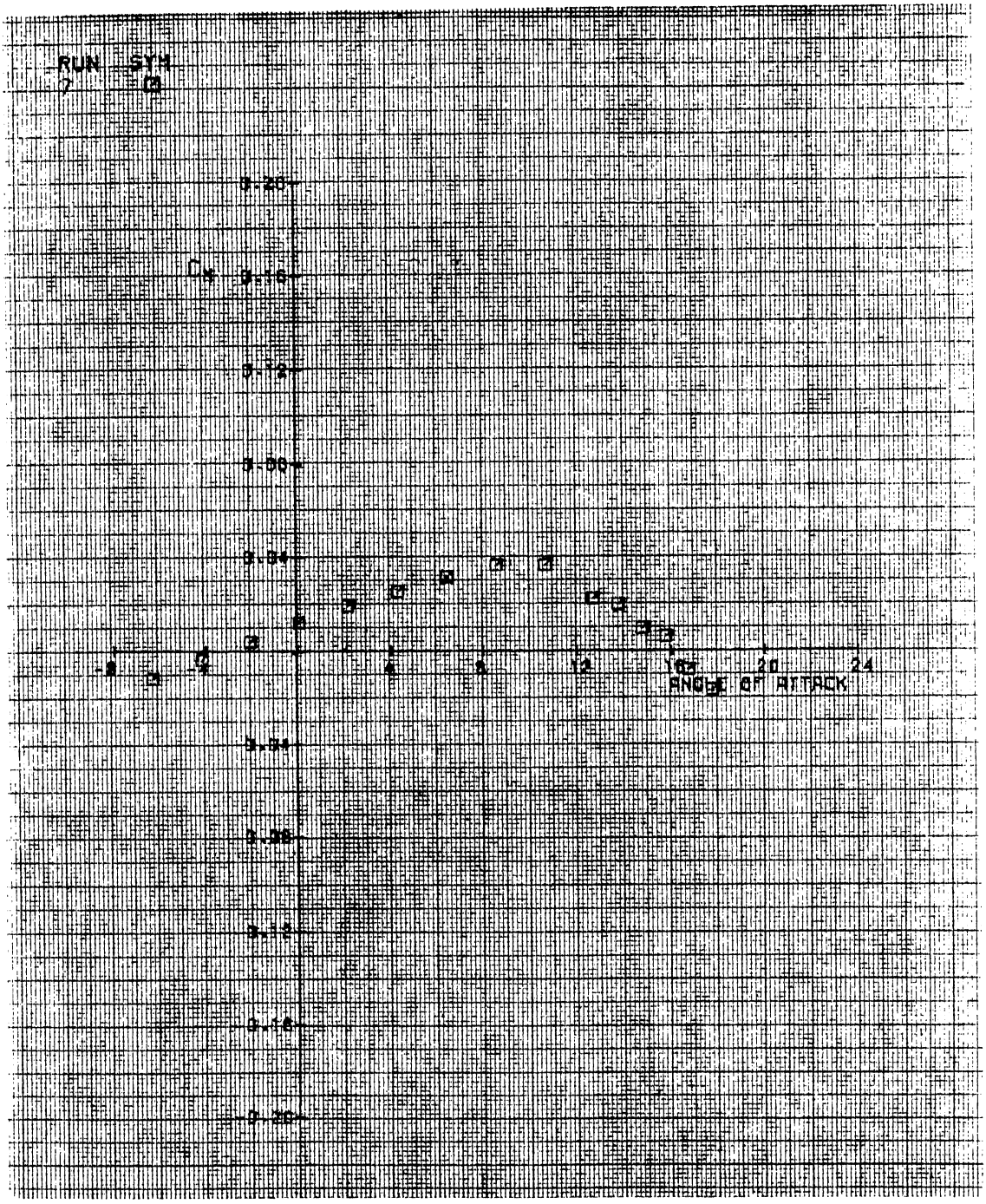

Figure 49. Run 7. Cm vs Alpha

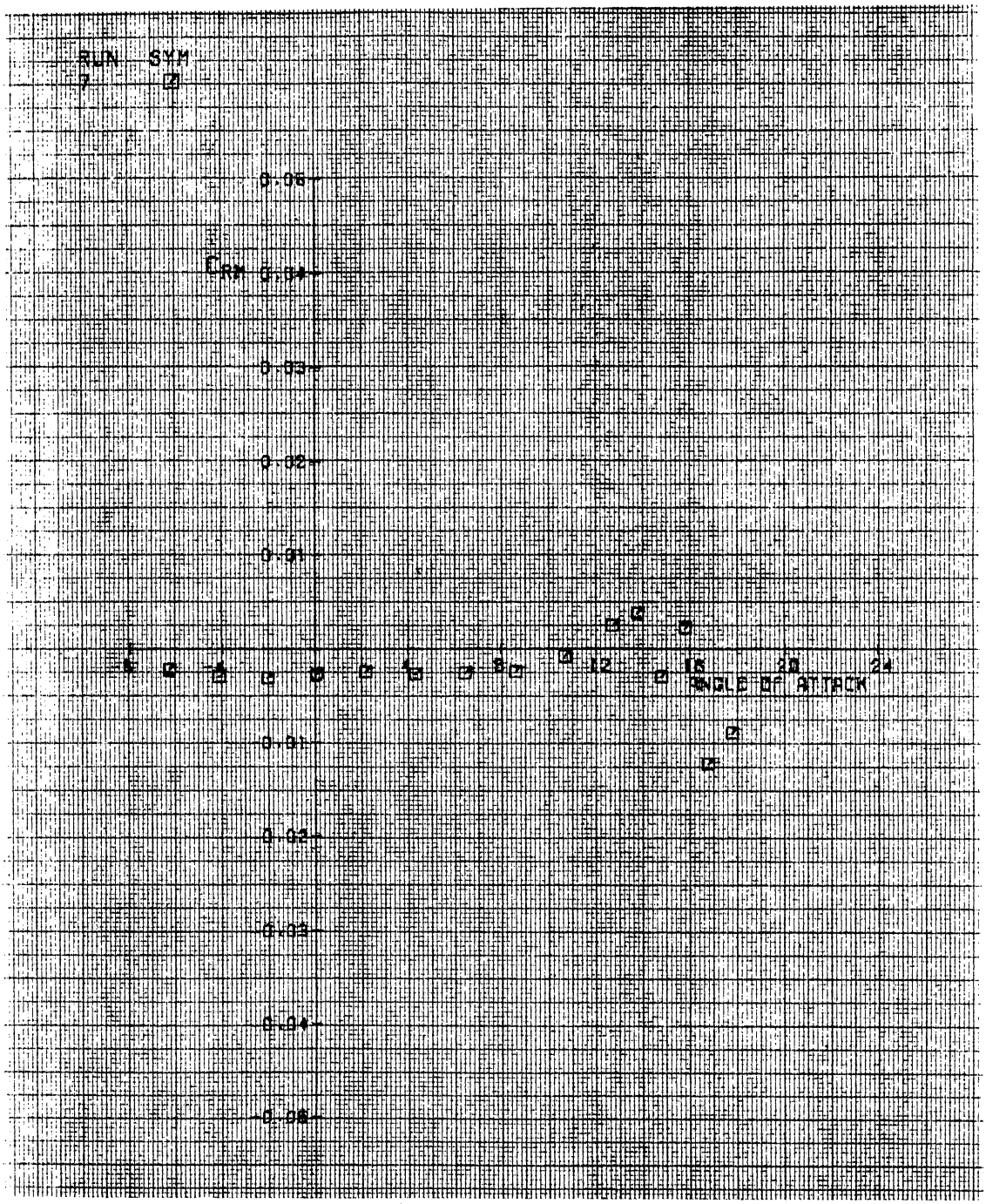

Figure 50. Crm vs Alpha

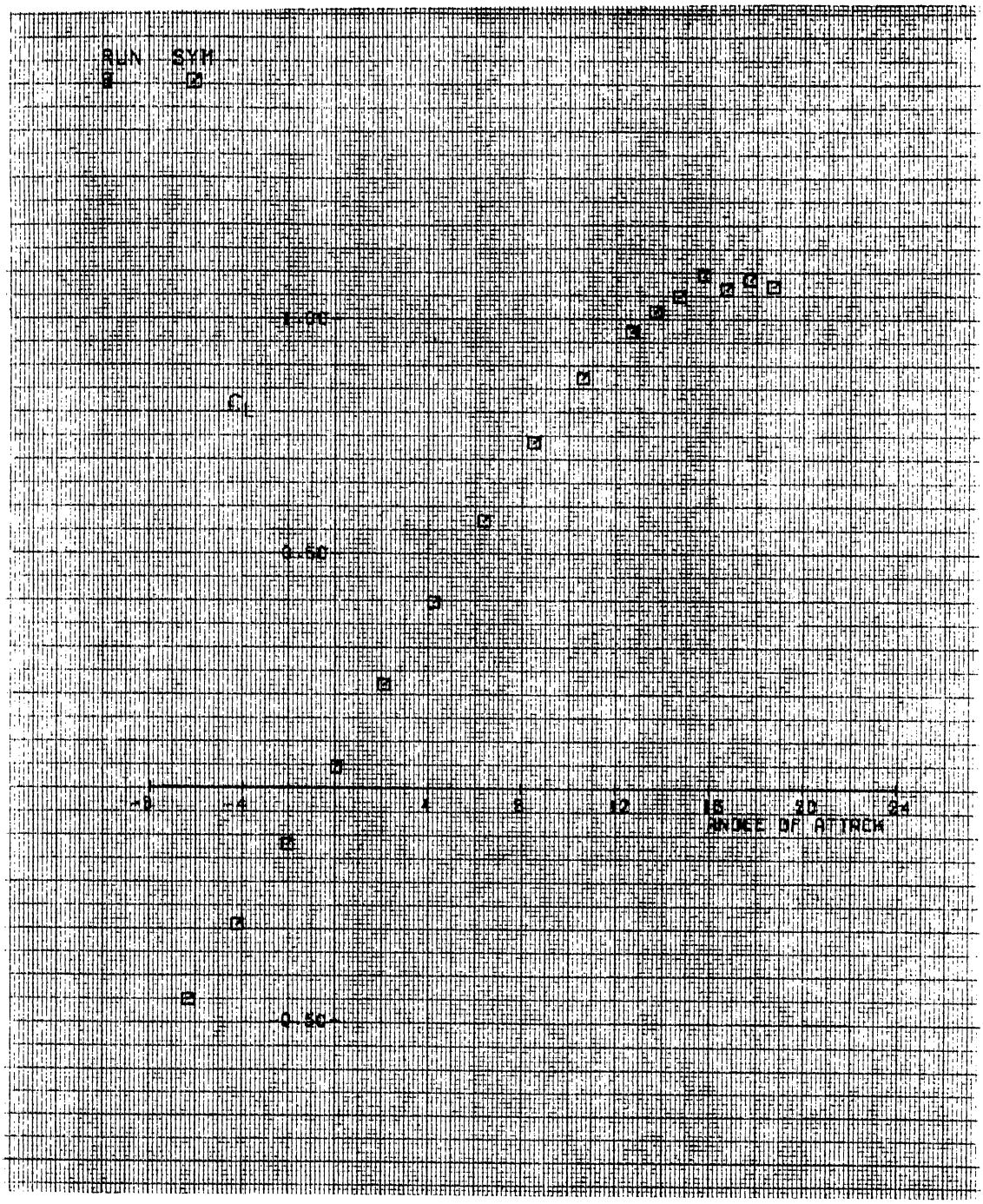

Figure 51. Run 8. Cl vs Alpha

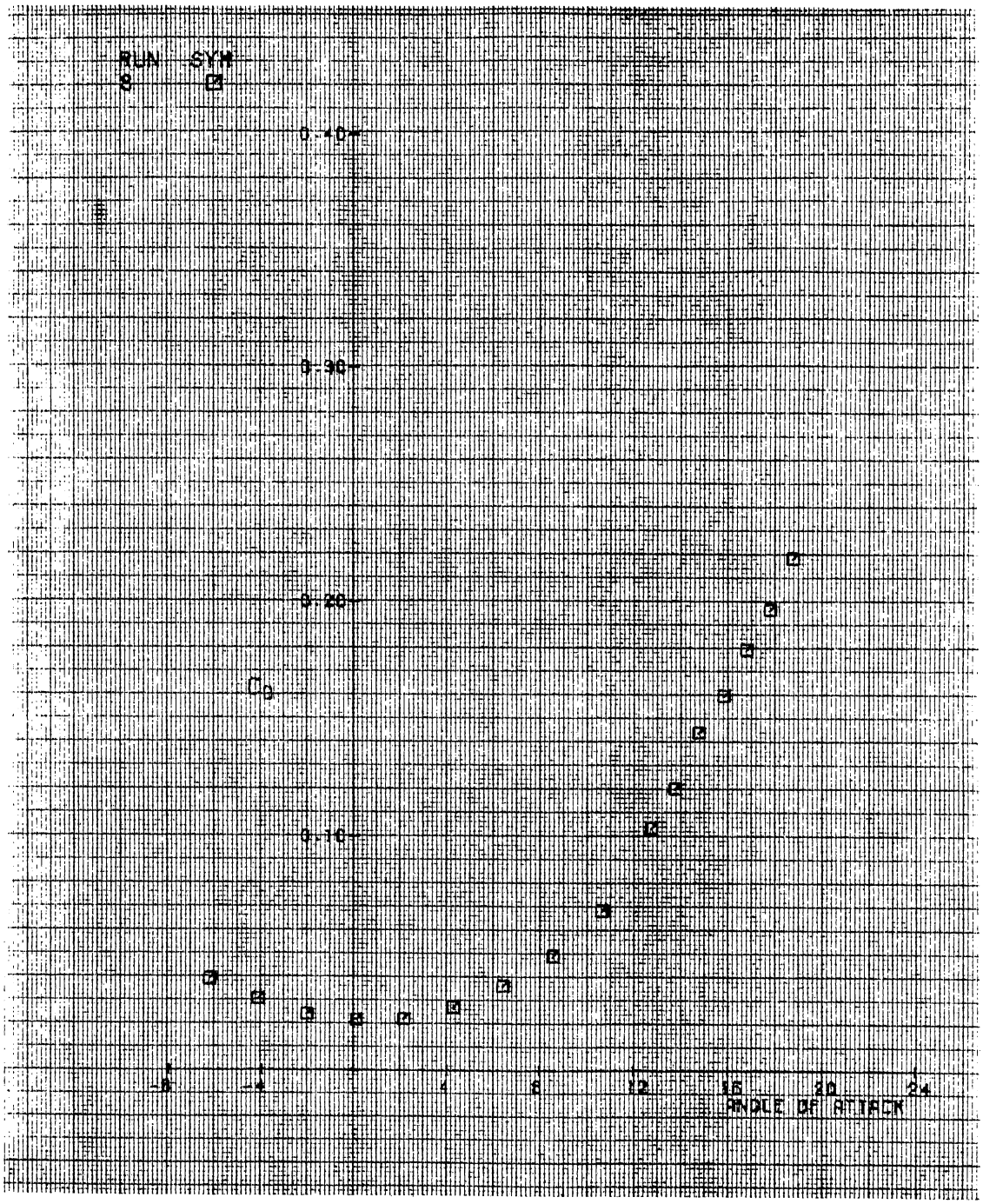

Figure 52. Run 8. Cd vs Alpha

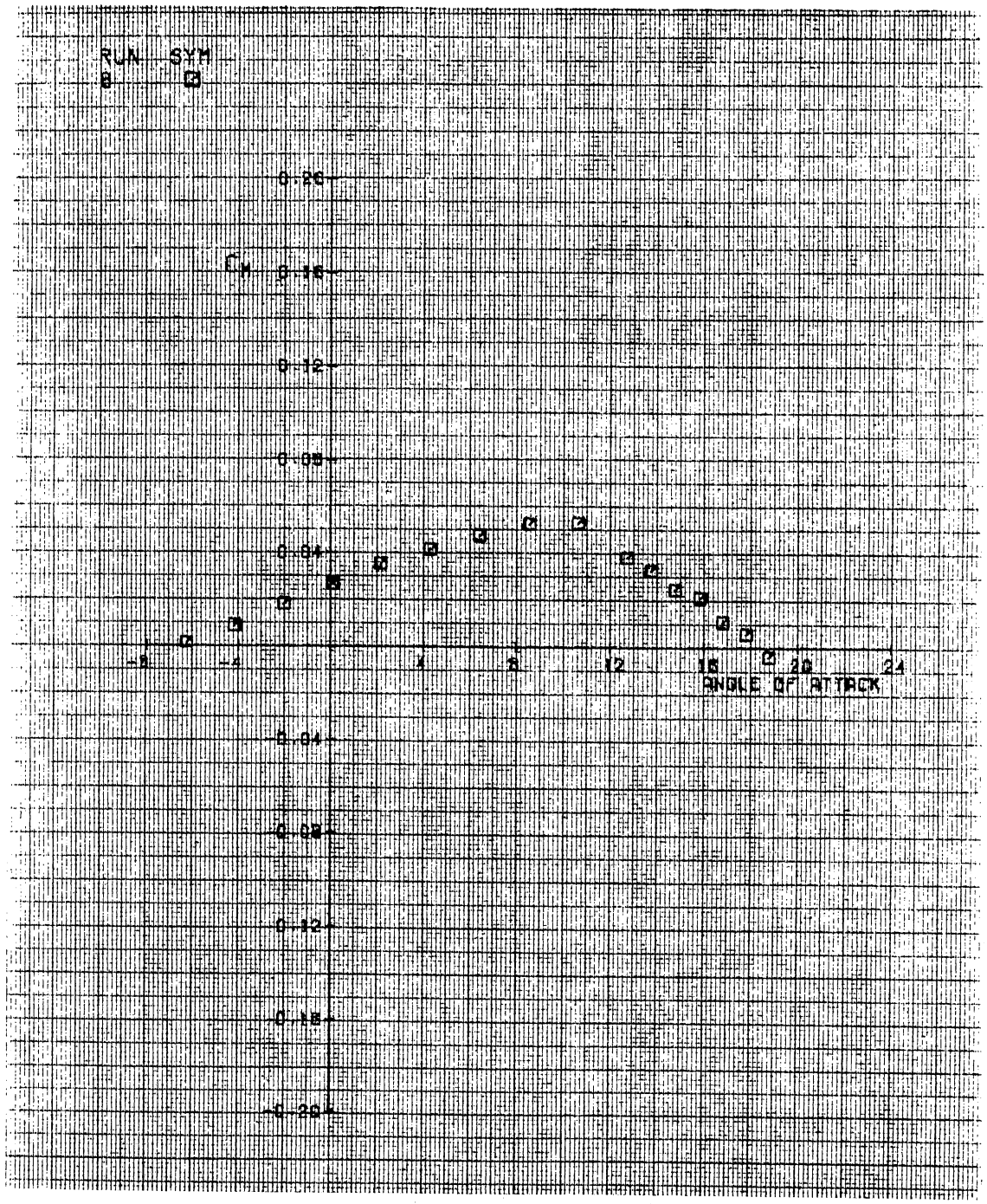

Figure 53. Cm vs Alpha

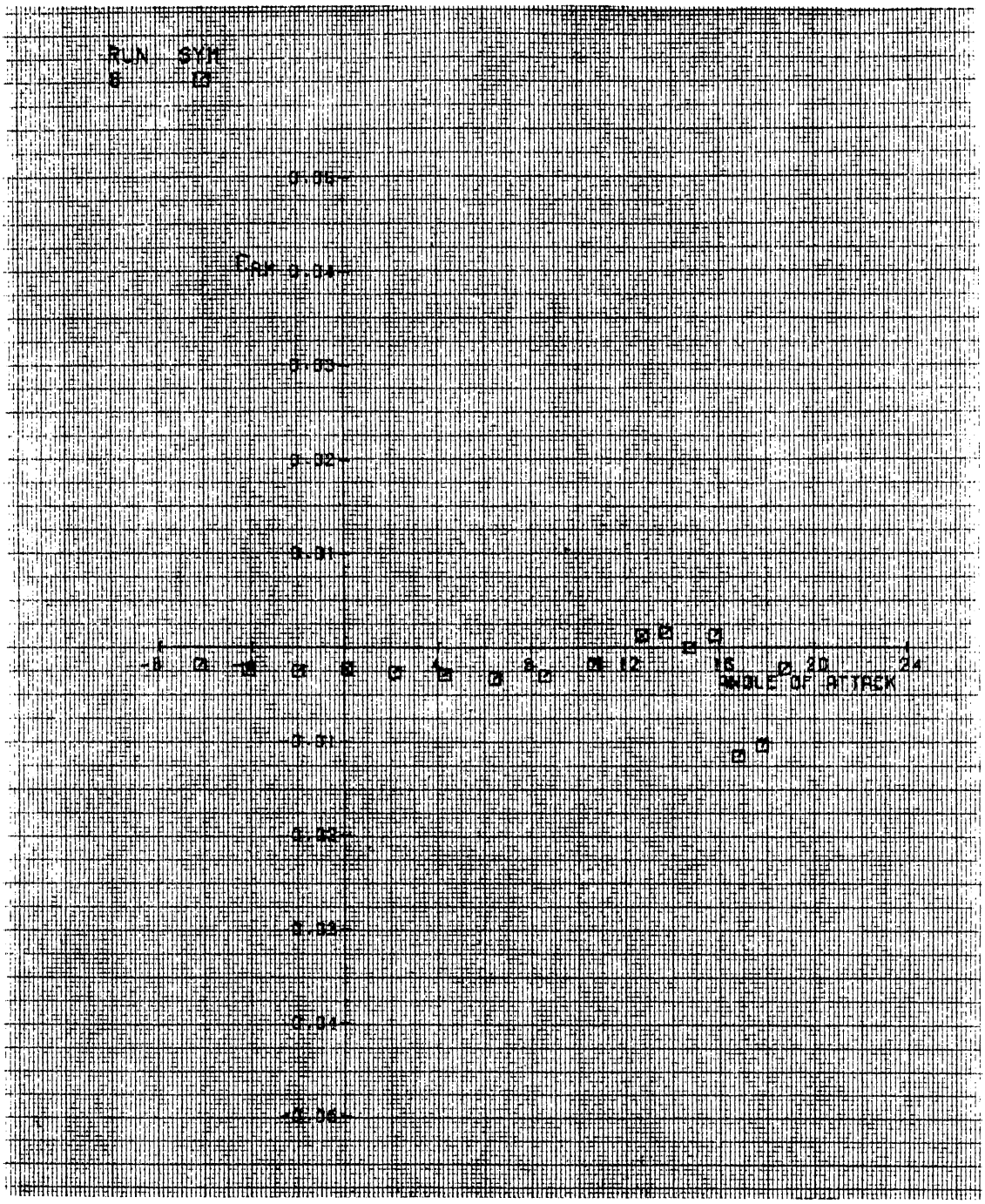

Figure 54. Run 8. Crm vs Alpha

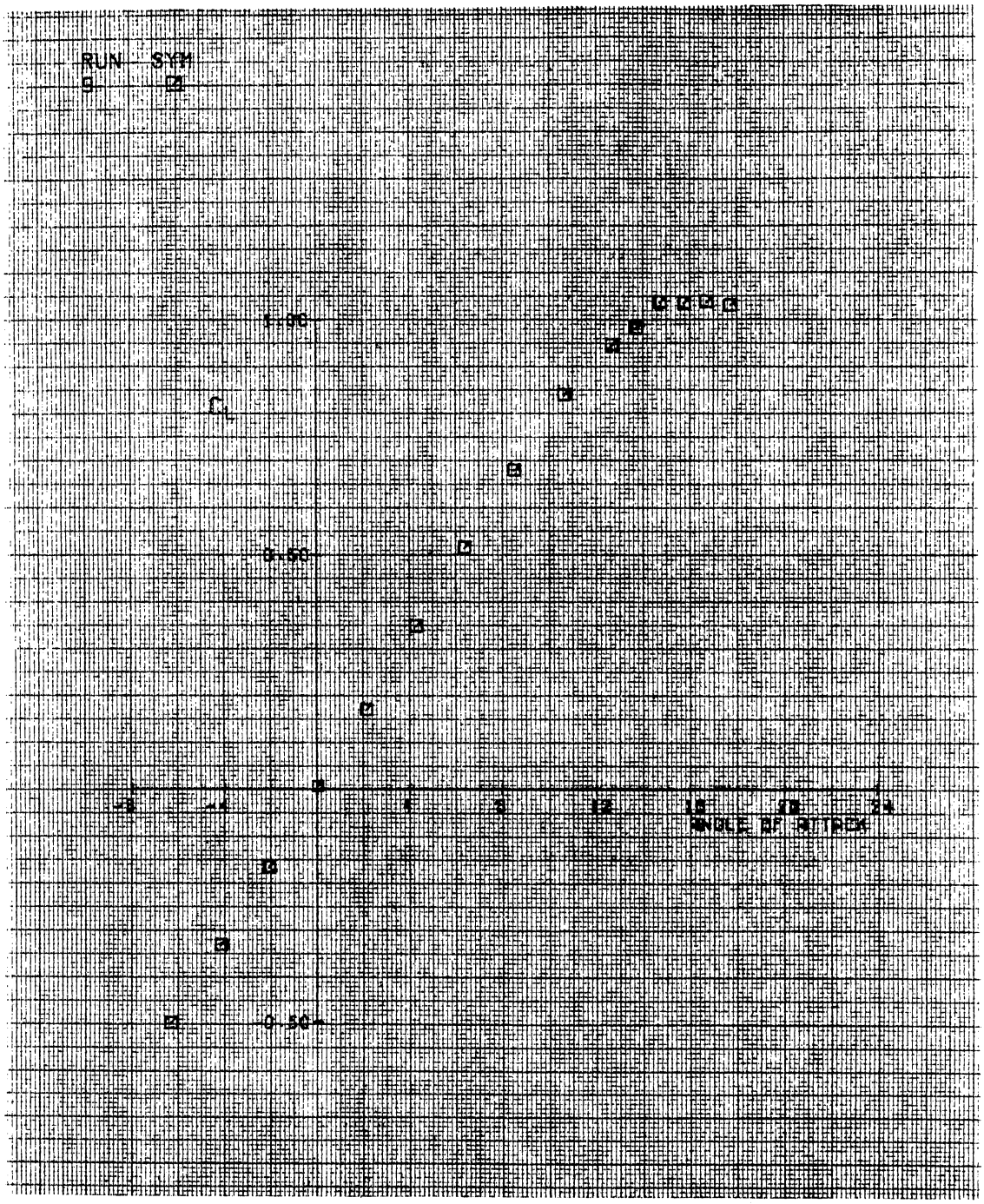

Figure55. Run 9. Cl vs Alpha

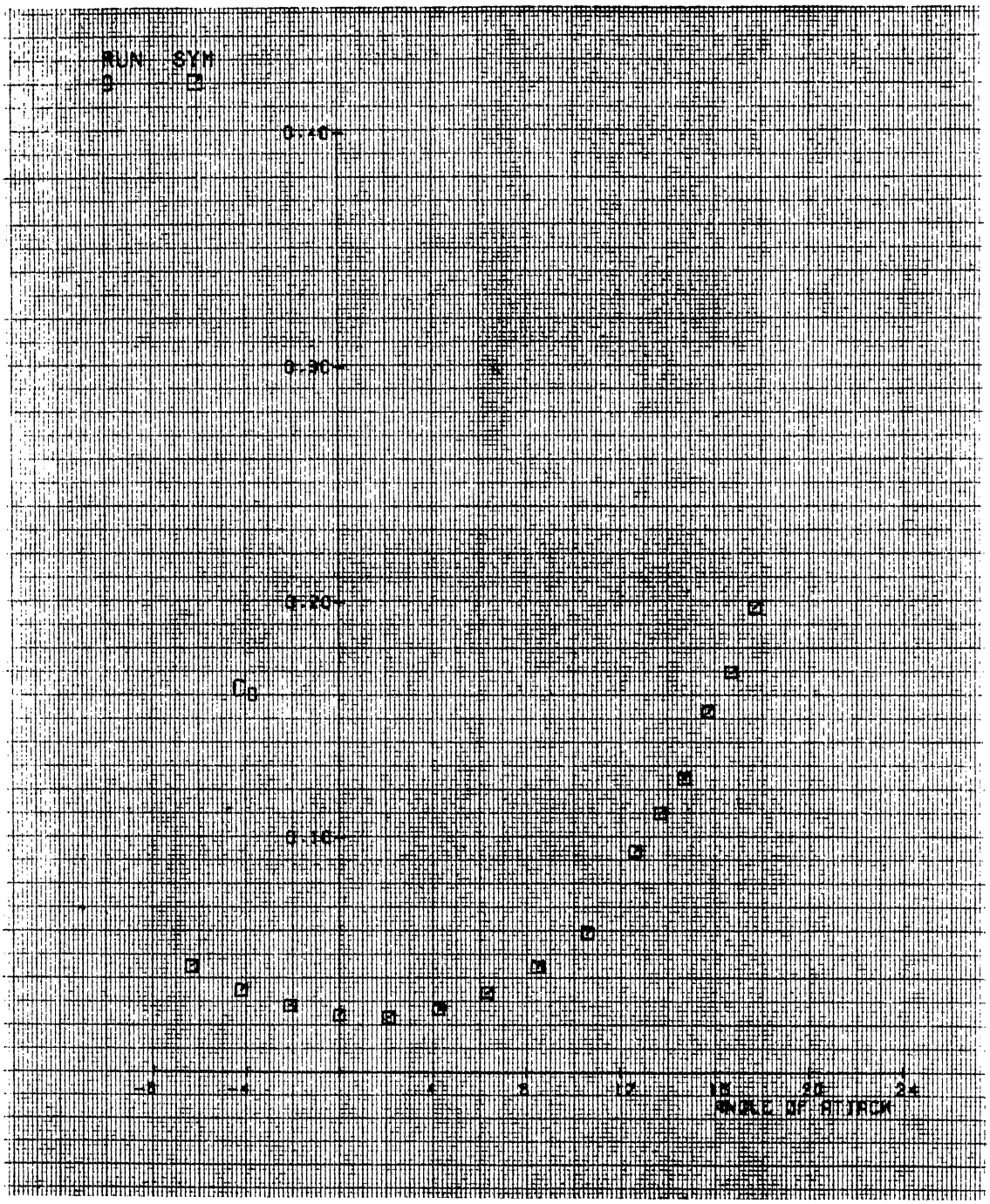

Figure 56. Run 9. Cd vs Alpha

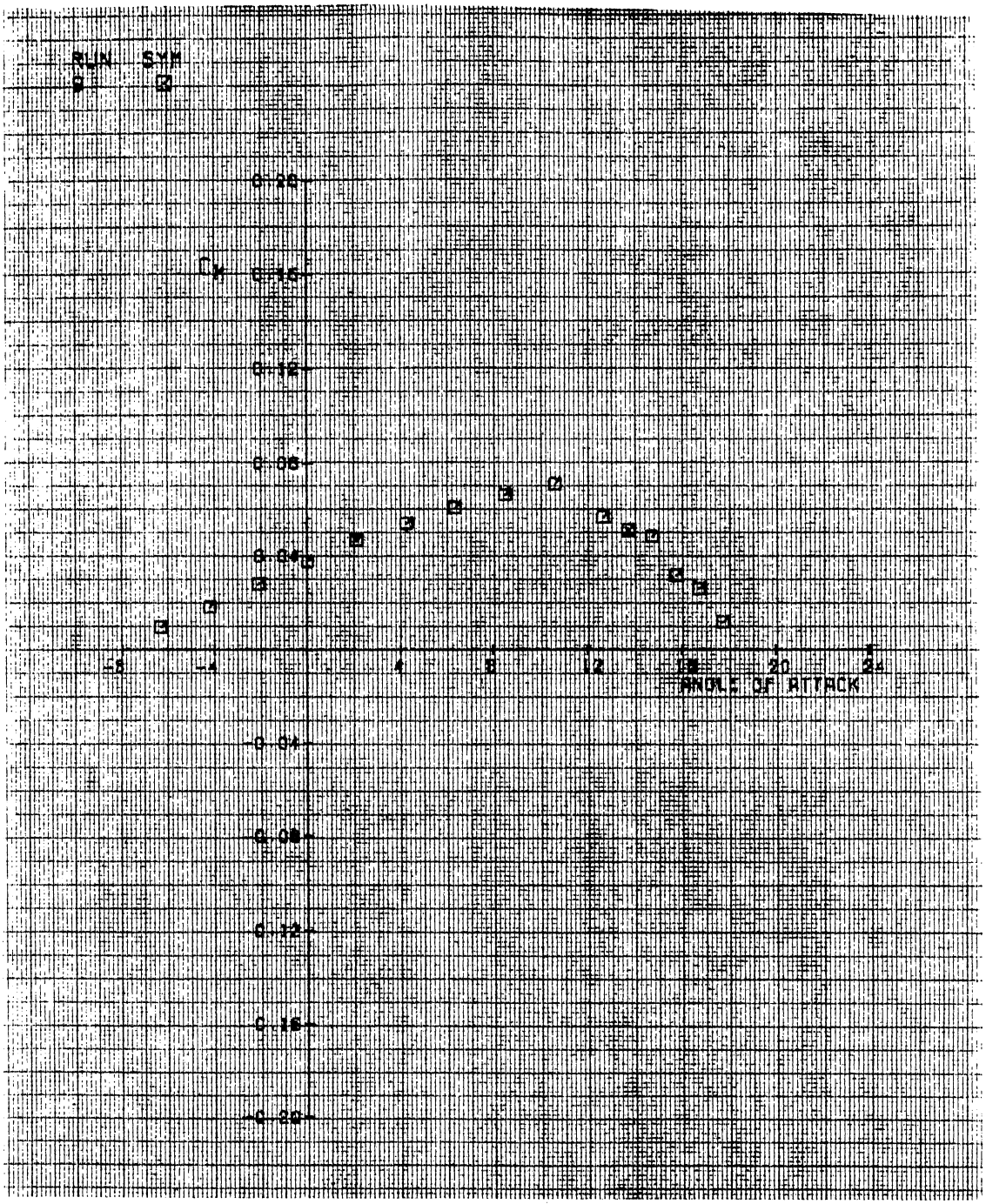

Figure 57. Run 9. Cm vs Alpha

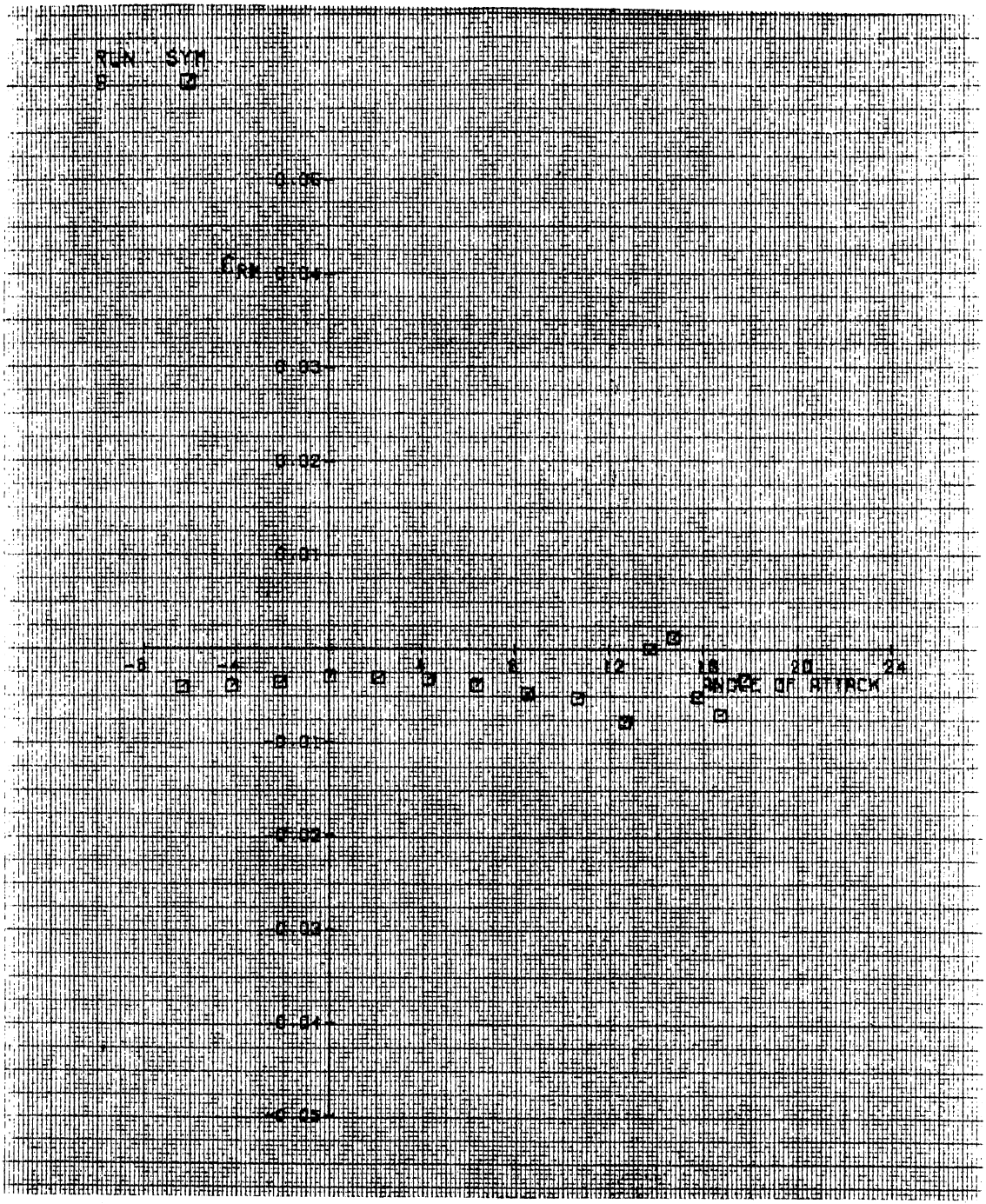

Figure 58. Run 9. Crm vs Alpha

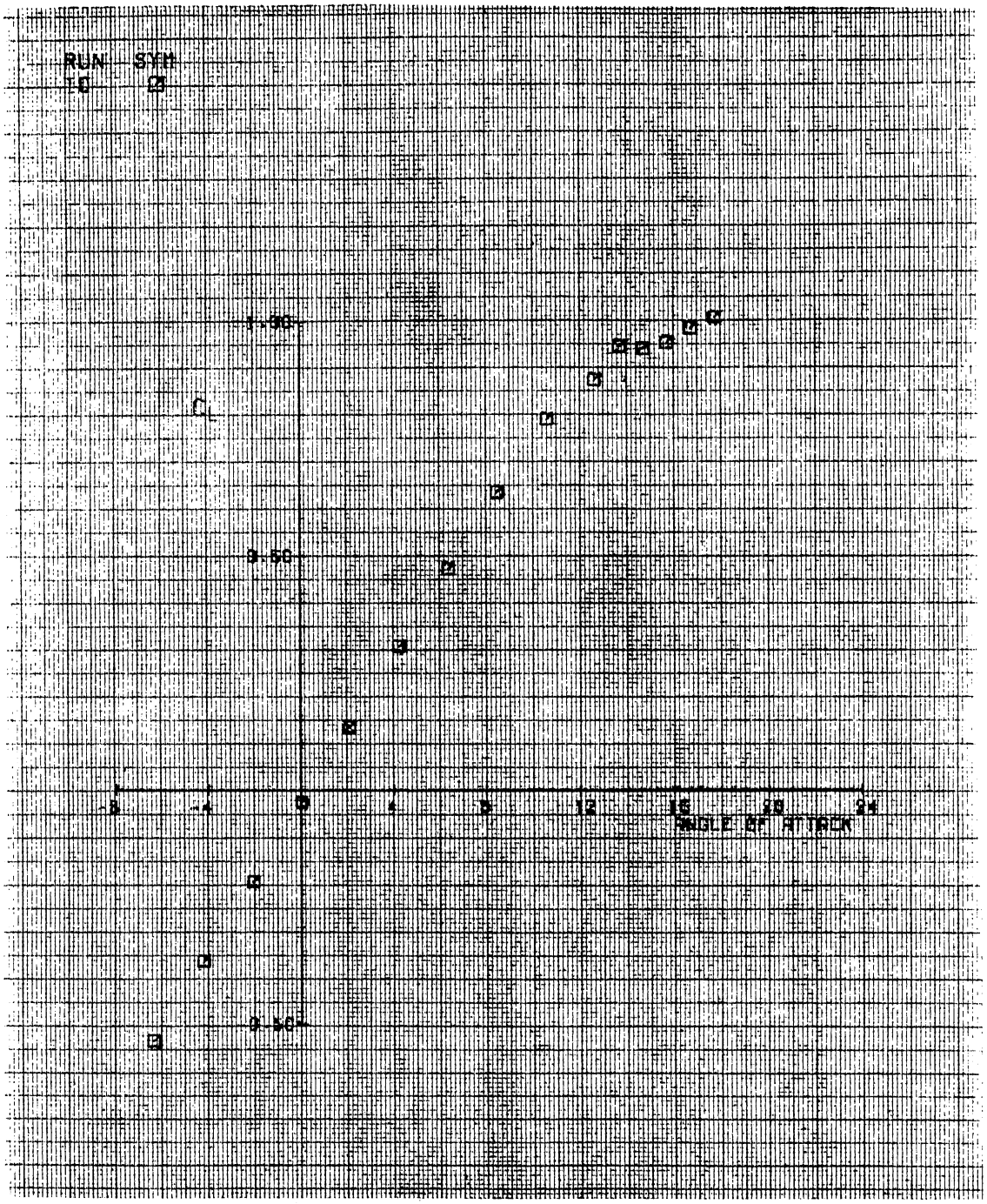

Figure 59. Run 10. Cl vs Alpha

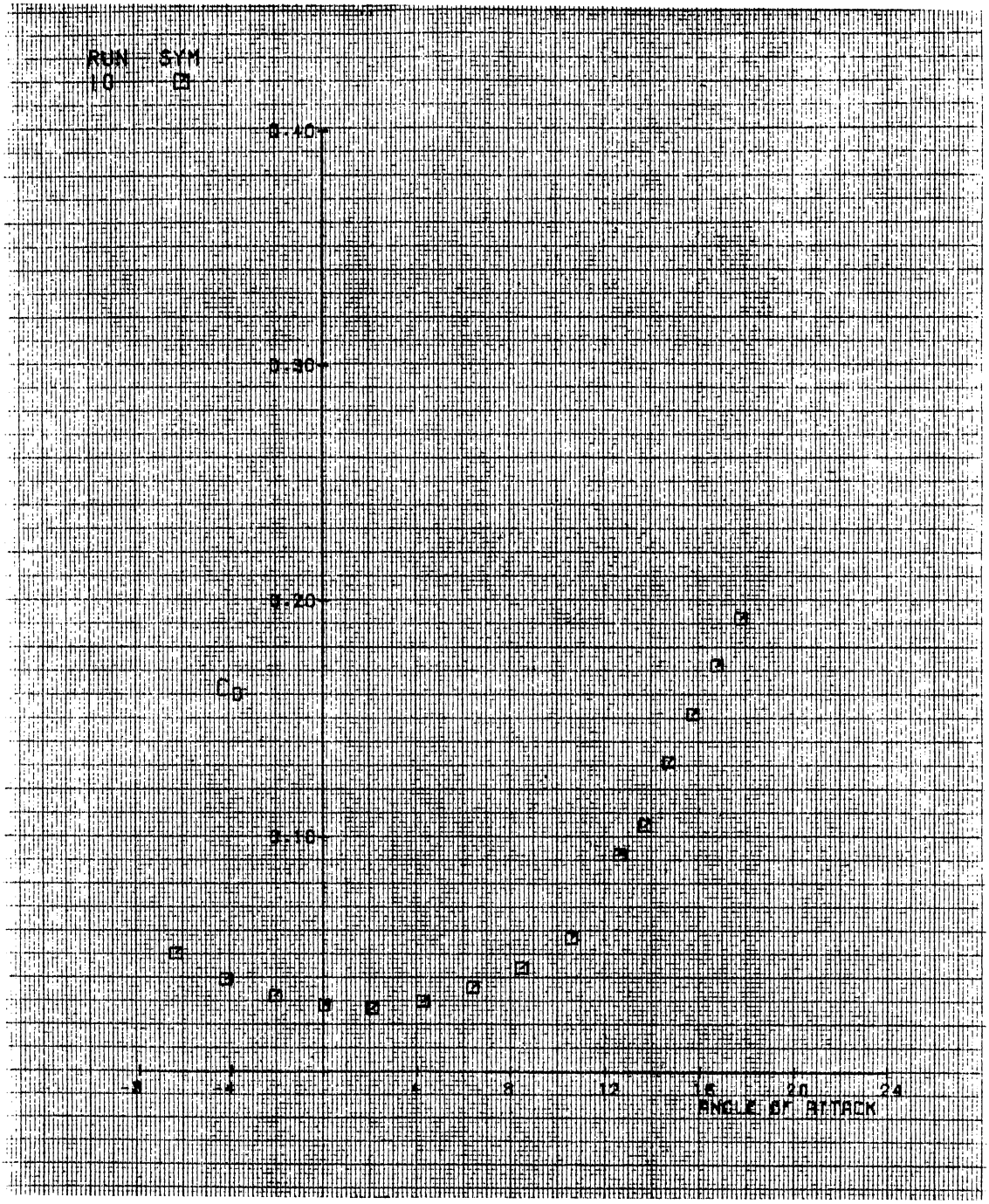

Figure 60. Run 10. Cd vs Alpha

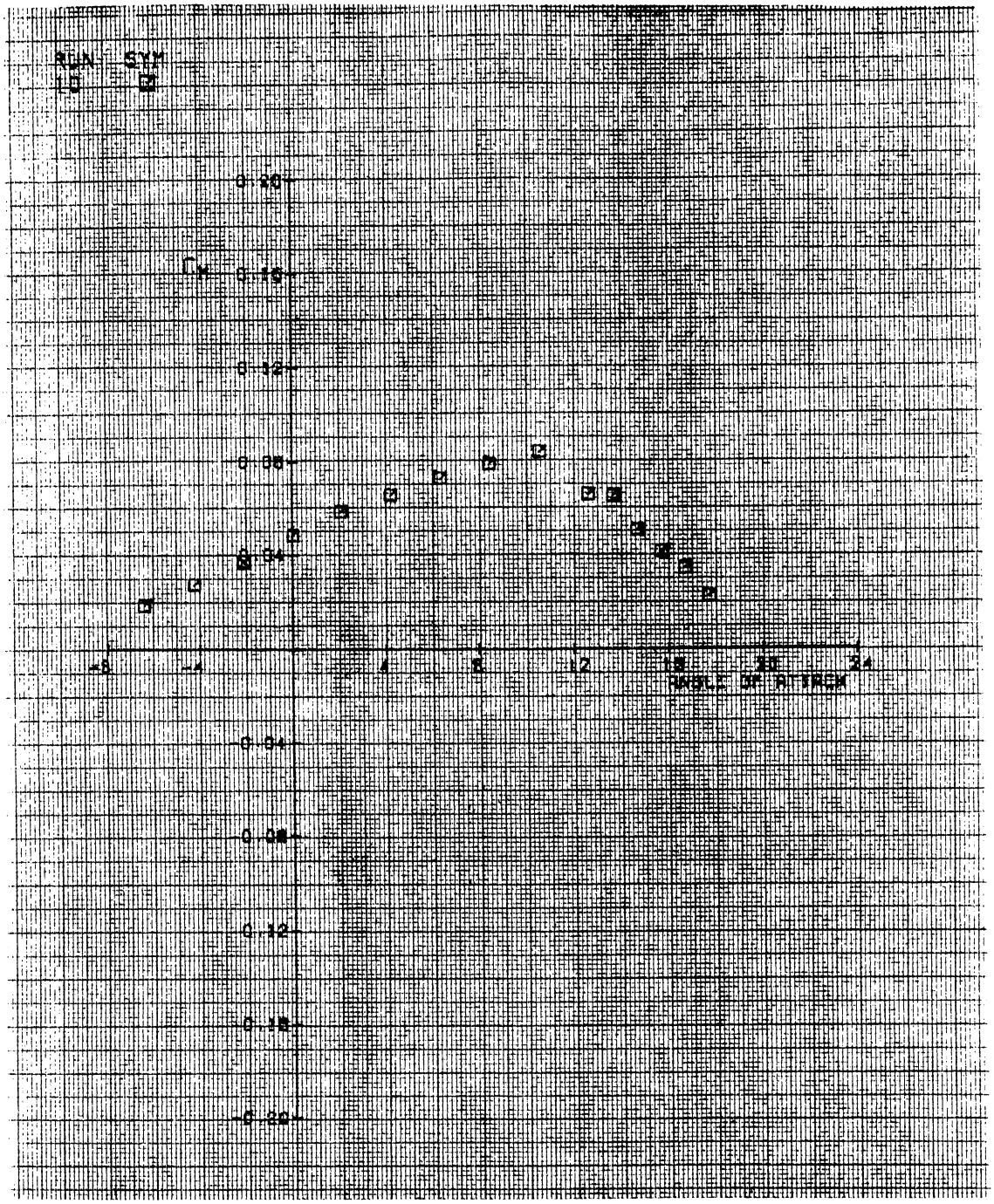

Figure 61. Run 10. Cm vs Alpha

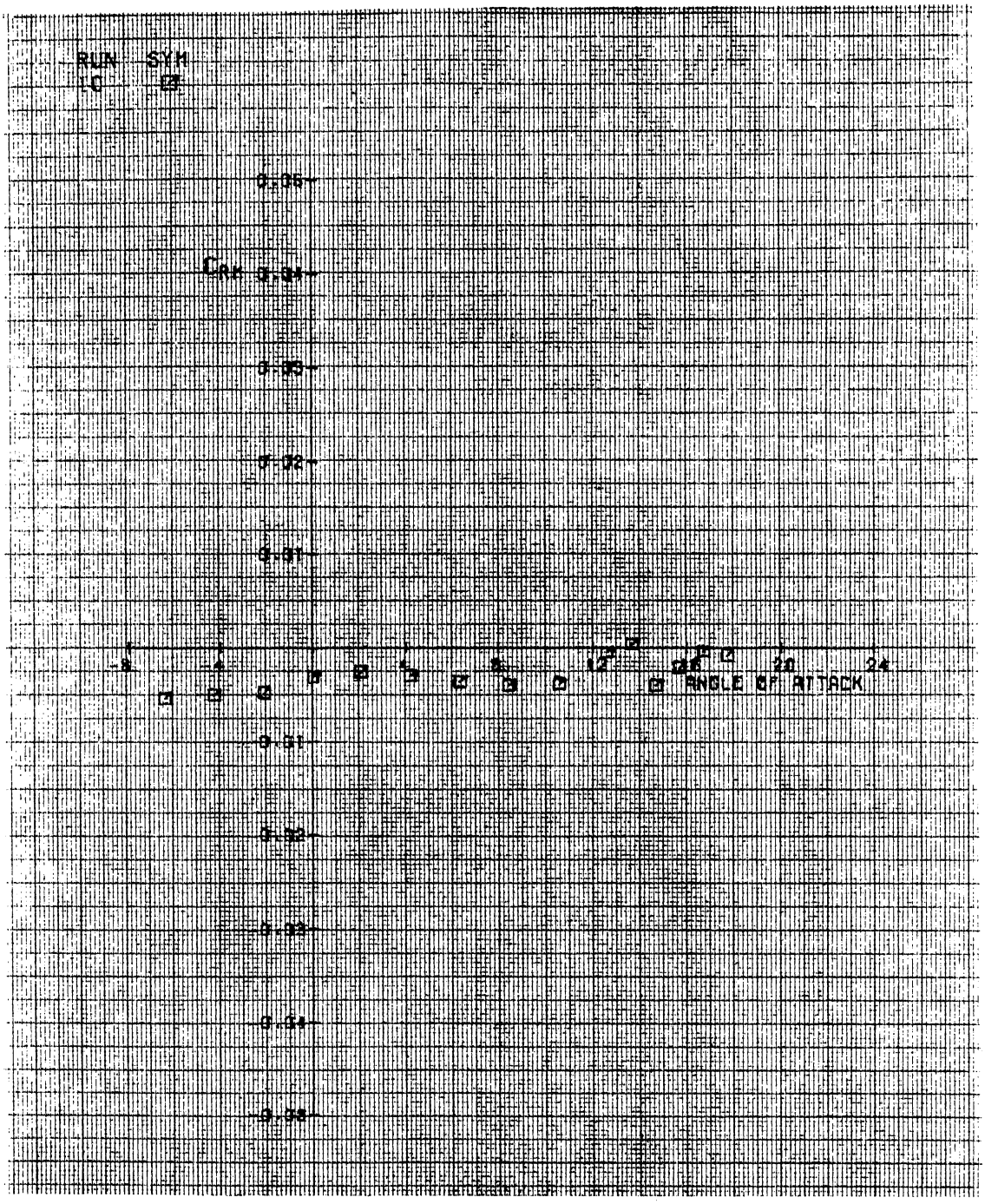

Figure 62. Run 10. Crm vs Alpha

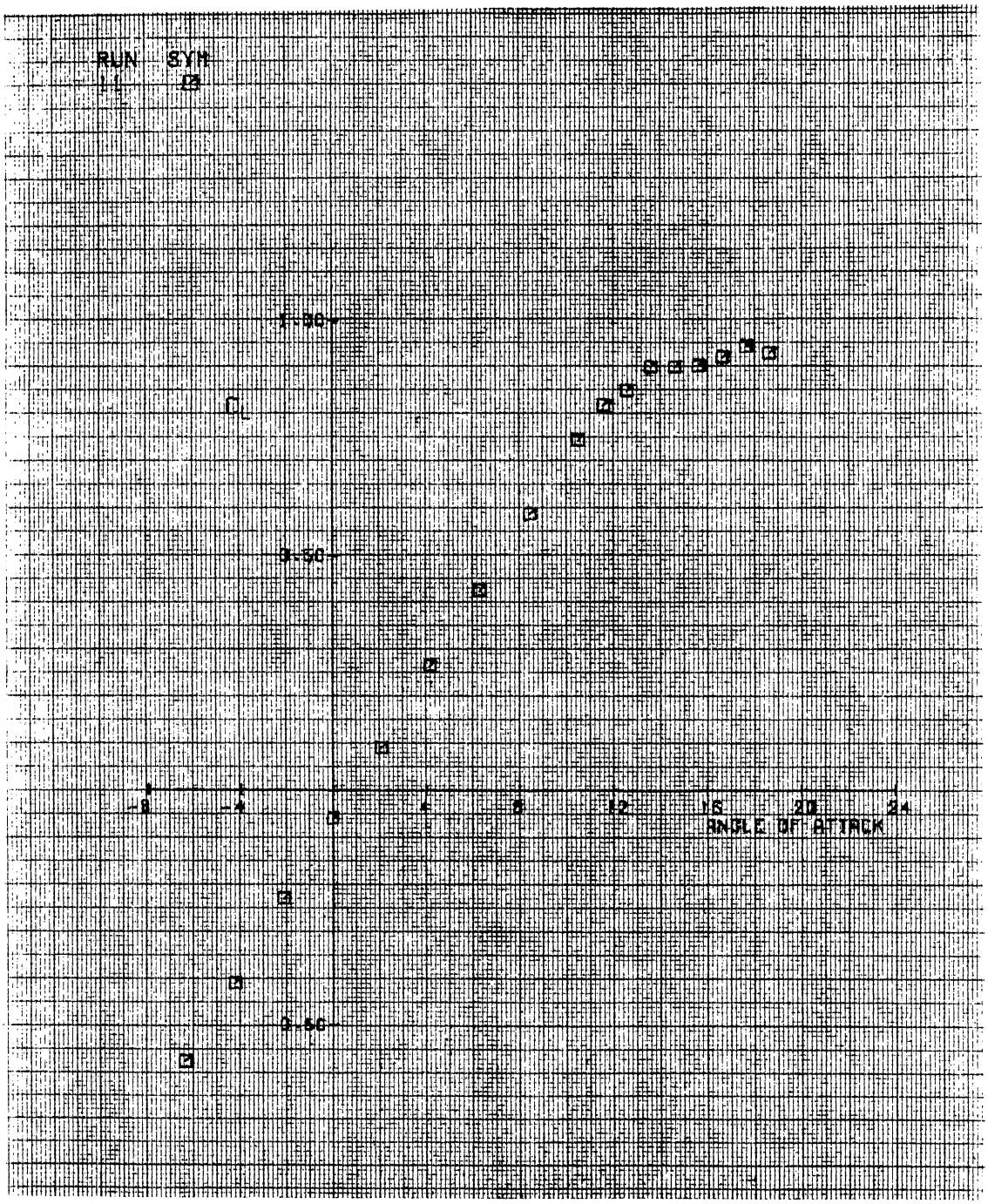

Figure 63. Run 11. Cl vs Alpha

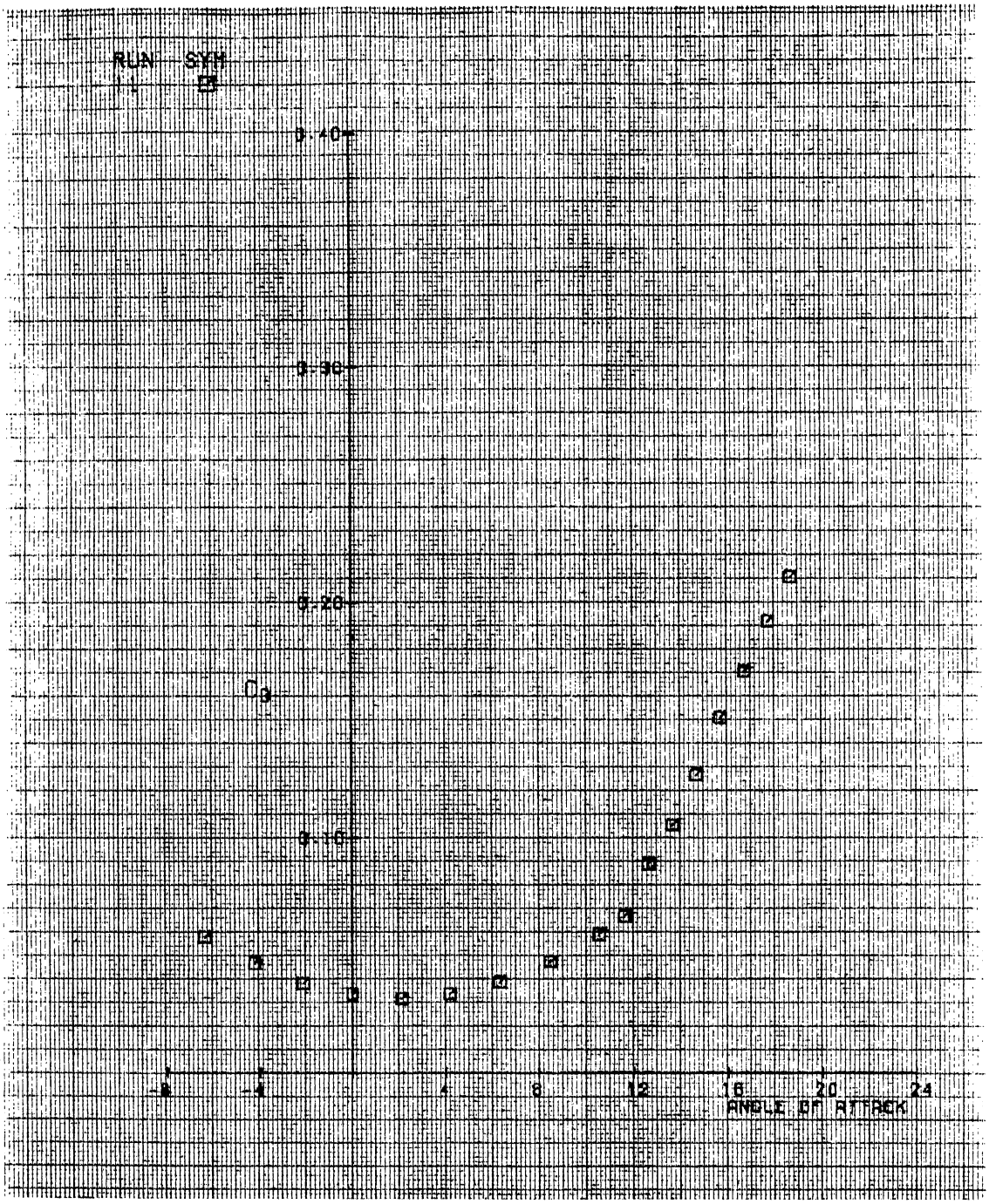

Figure 64. Run 11. Cd vs Alpha

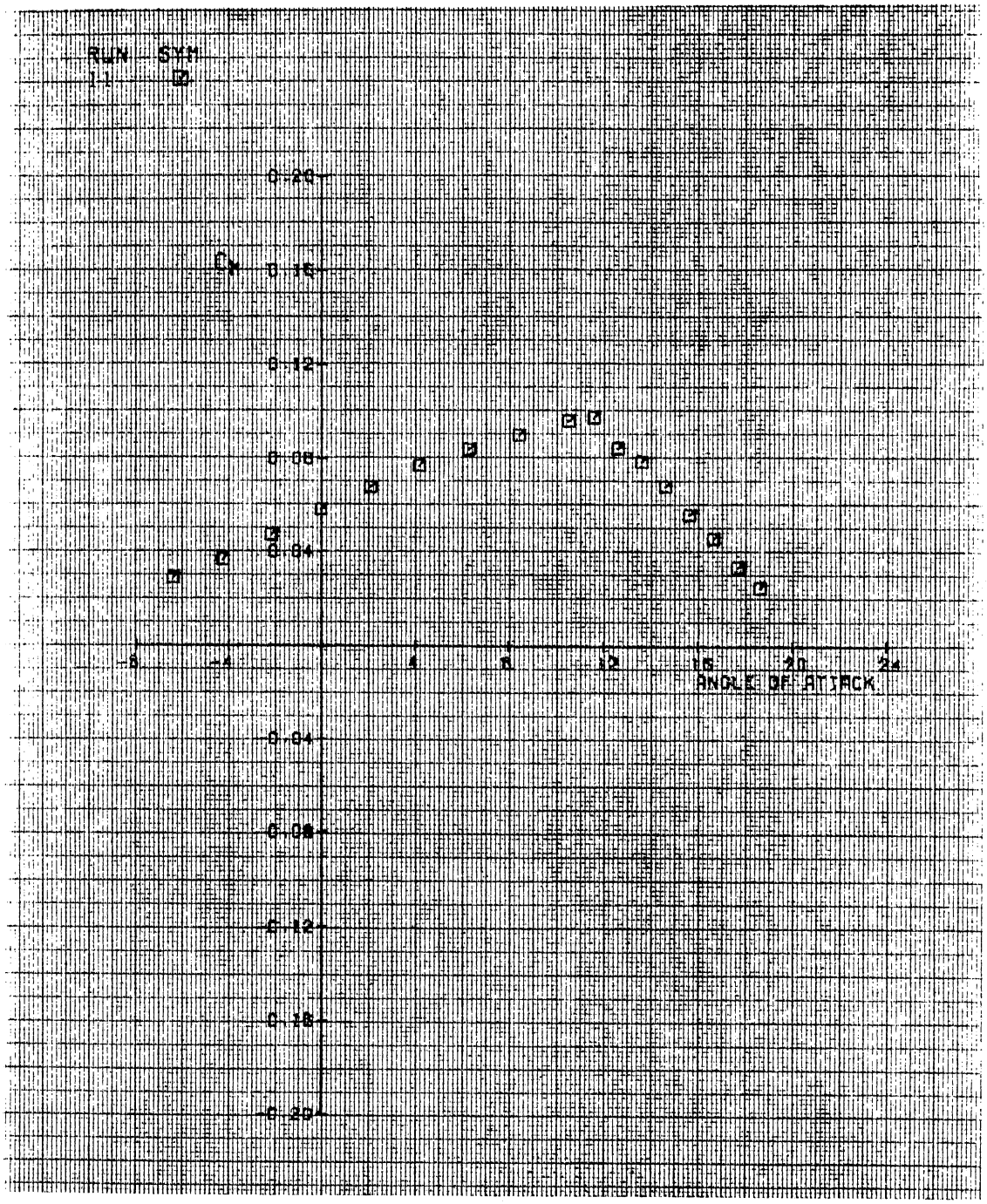

Figure 65. Run 11. Cm vs Alpha

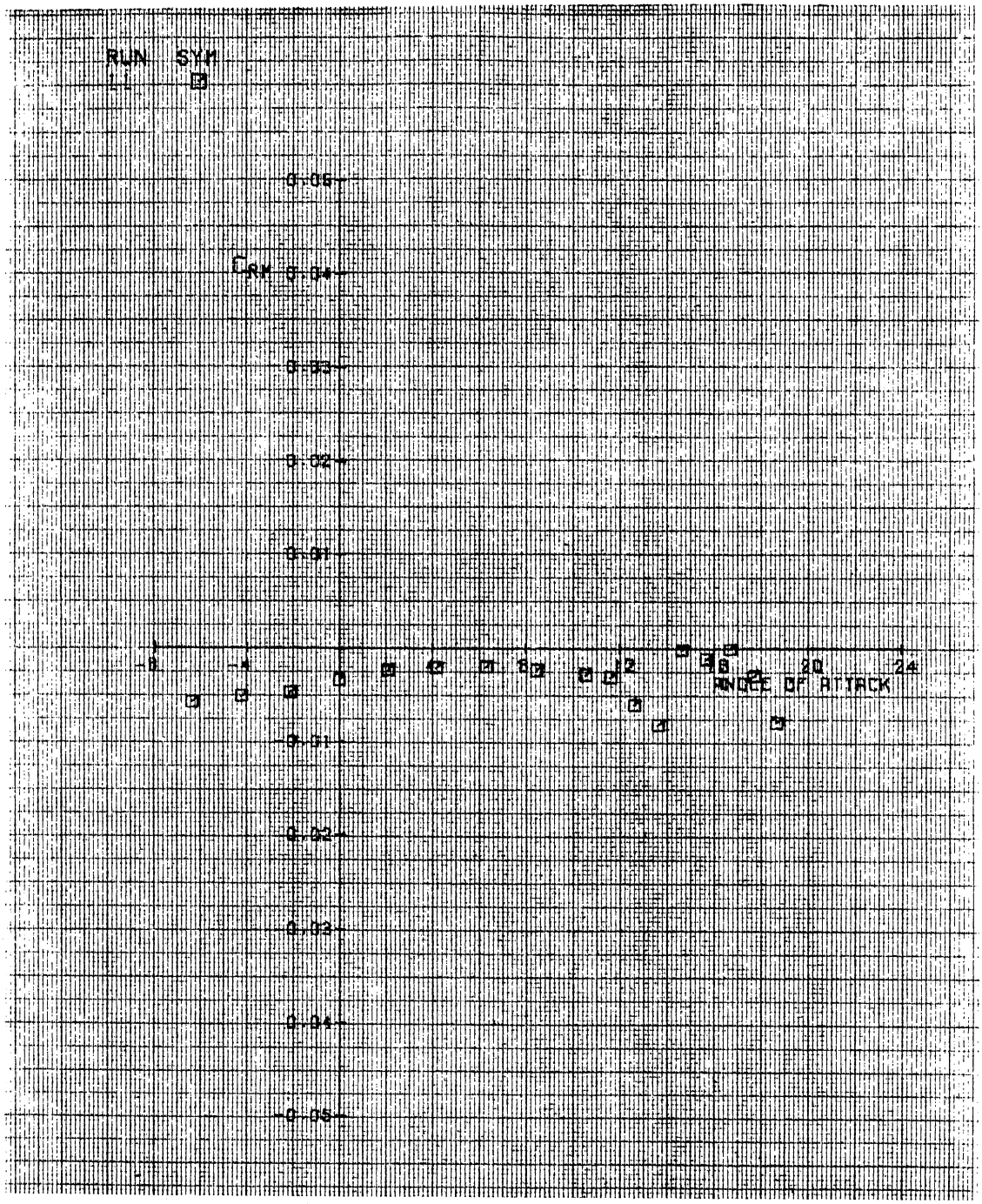

Figure 66. Run 11. Crm vs Alpha

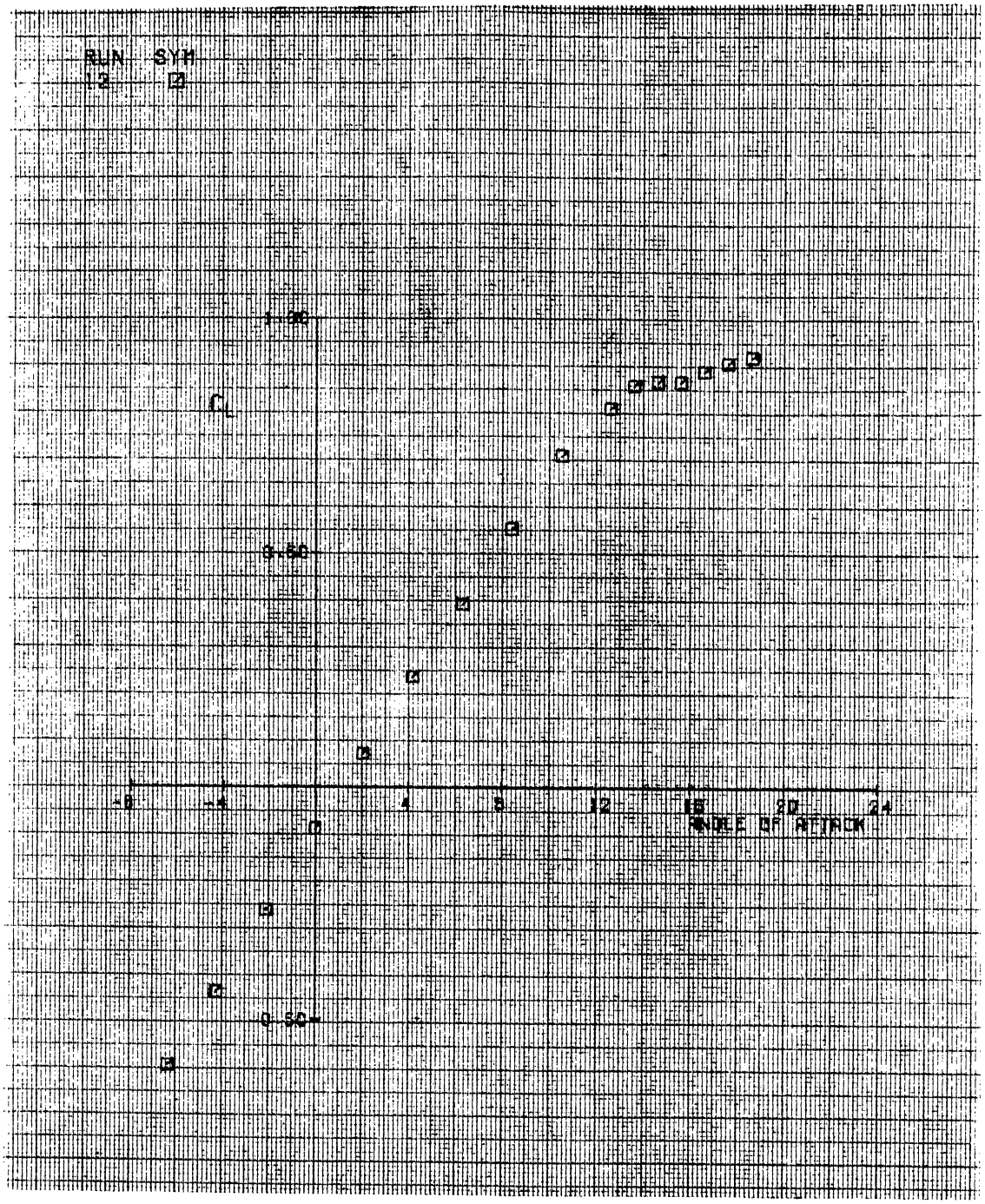

Figure 67. Run 12. Cl vs Alpha

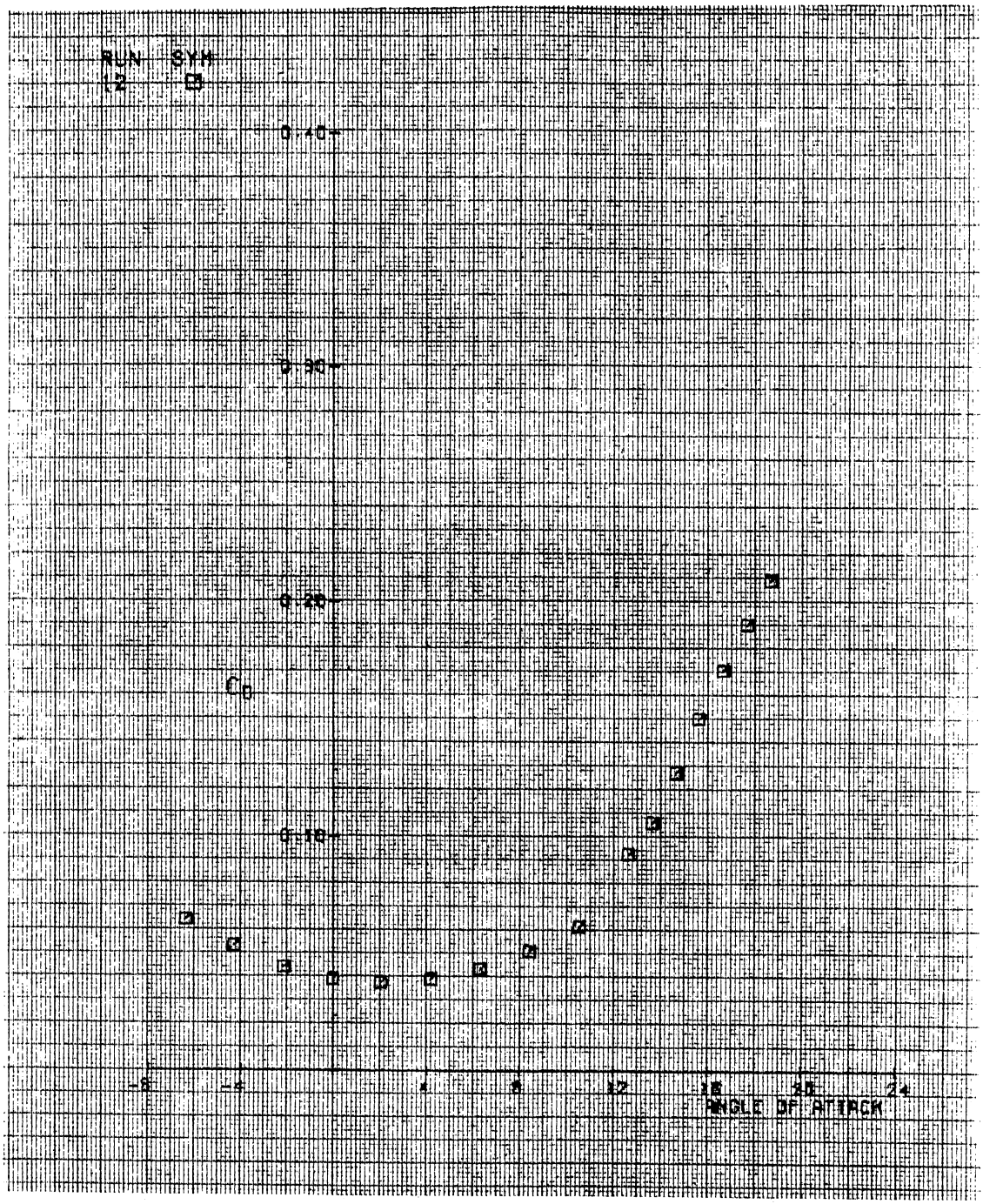

Figure 68. Run 12. Cd vs Alpha

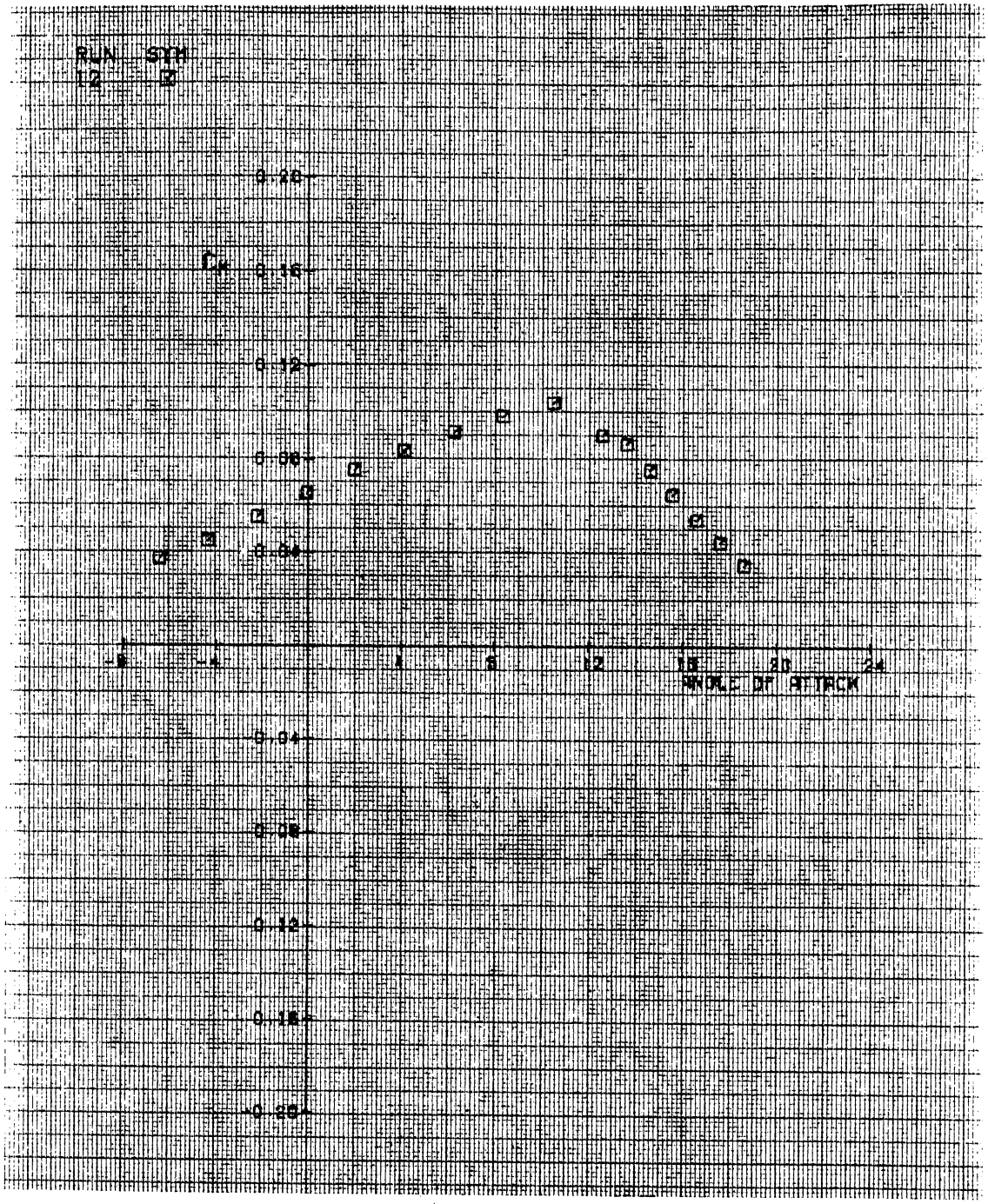

Figure 69. Run 12. Cm vs Alpha

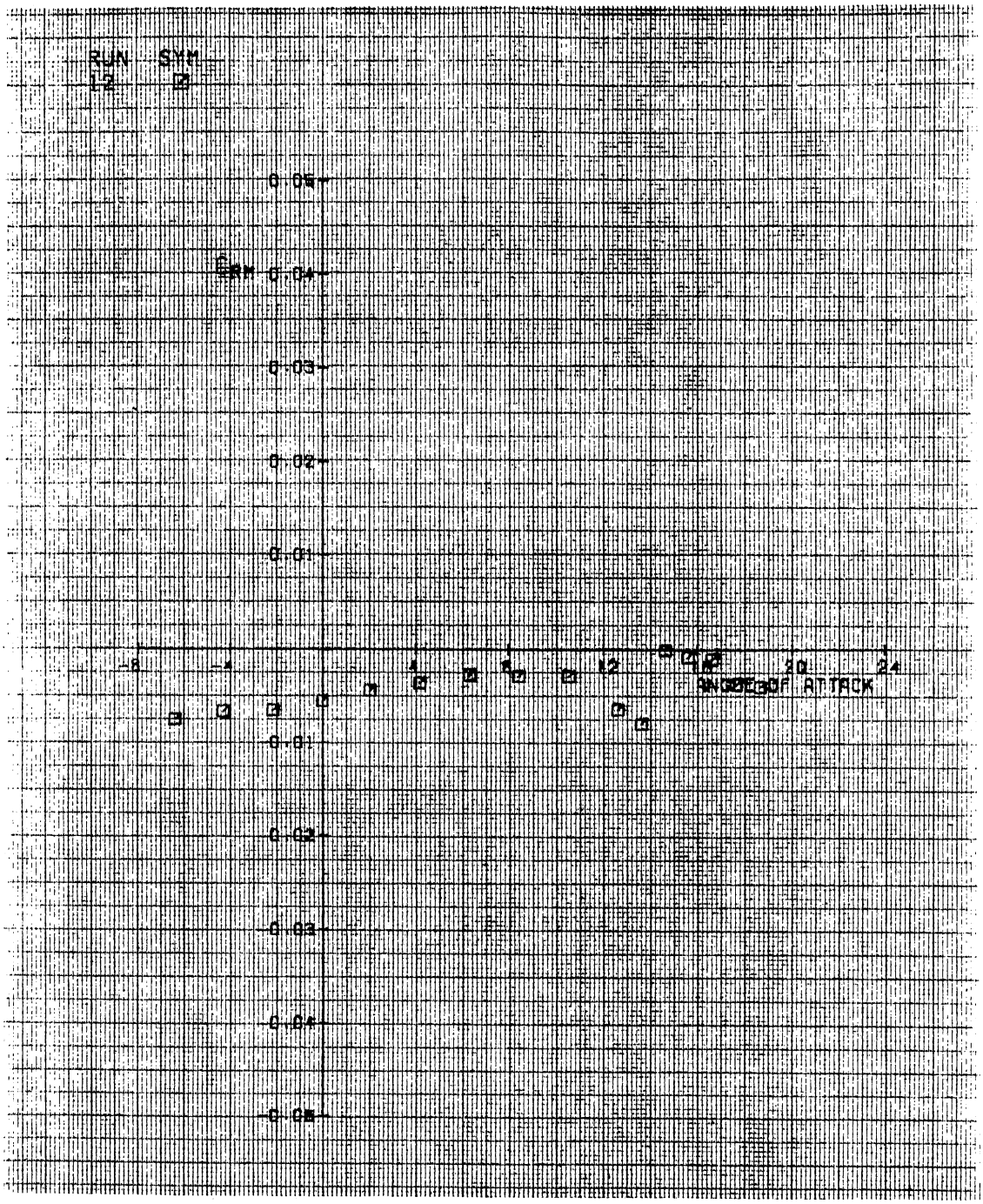

Figure 70. Run 12. Crm vs Alpha

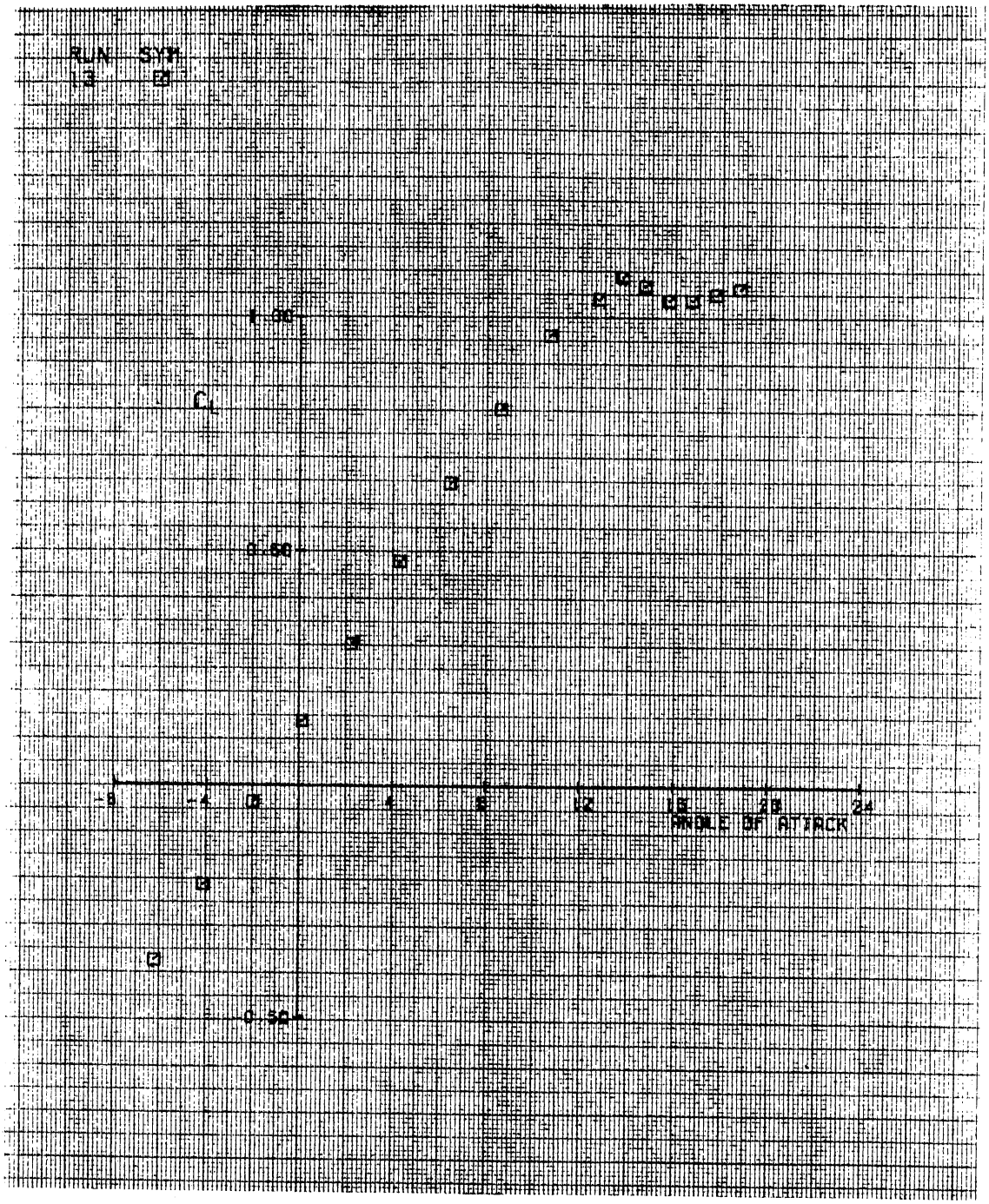

Figure 71. Run 13. Cl vs Alpha

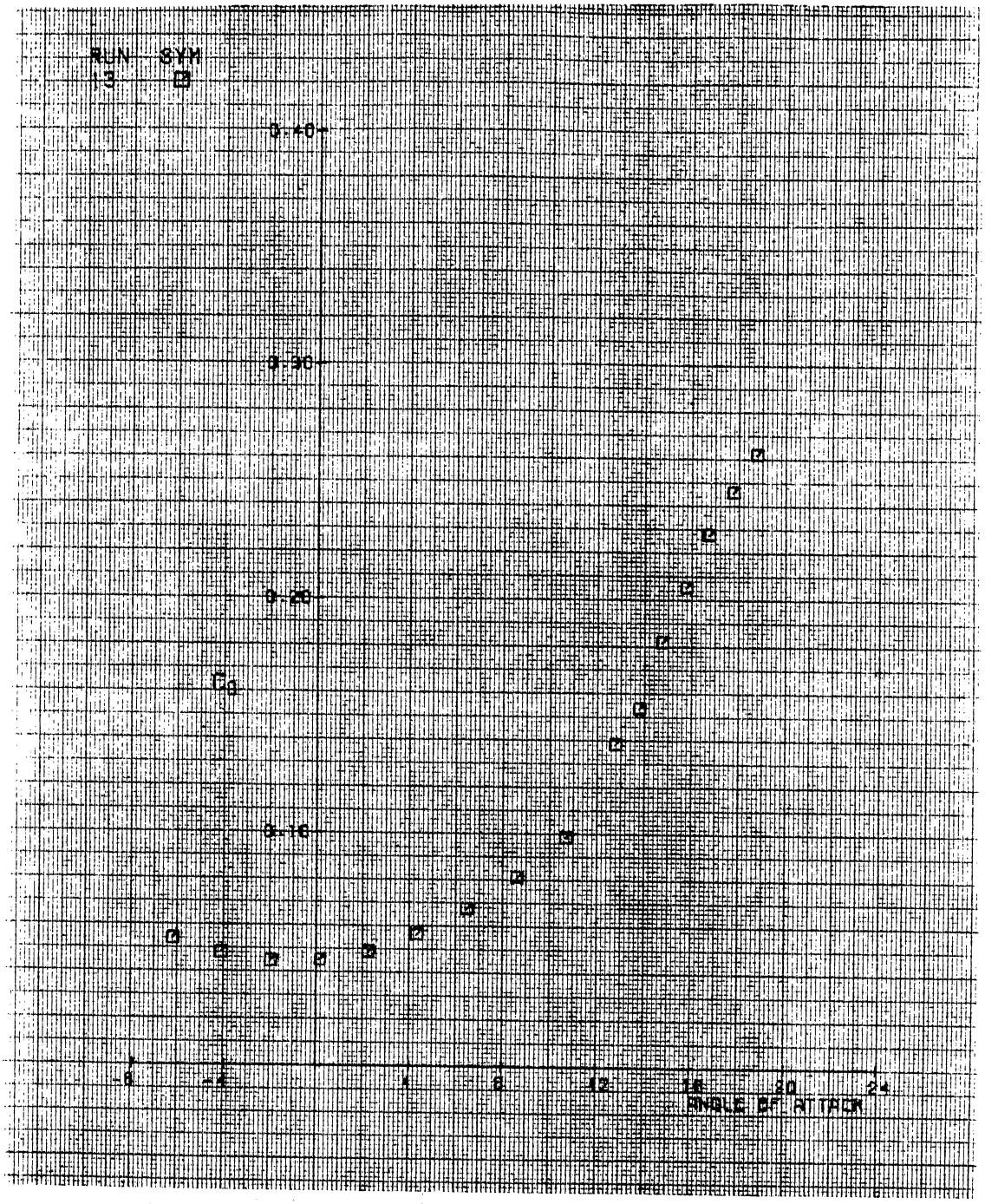

Figure 72. Run 13. Cd vs Alpha

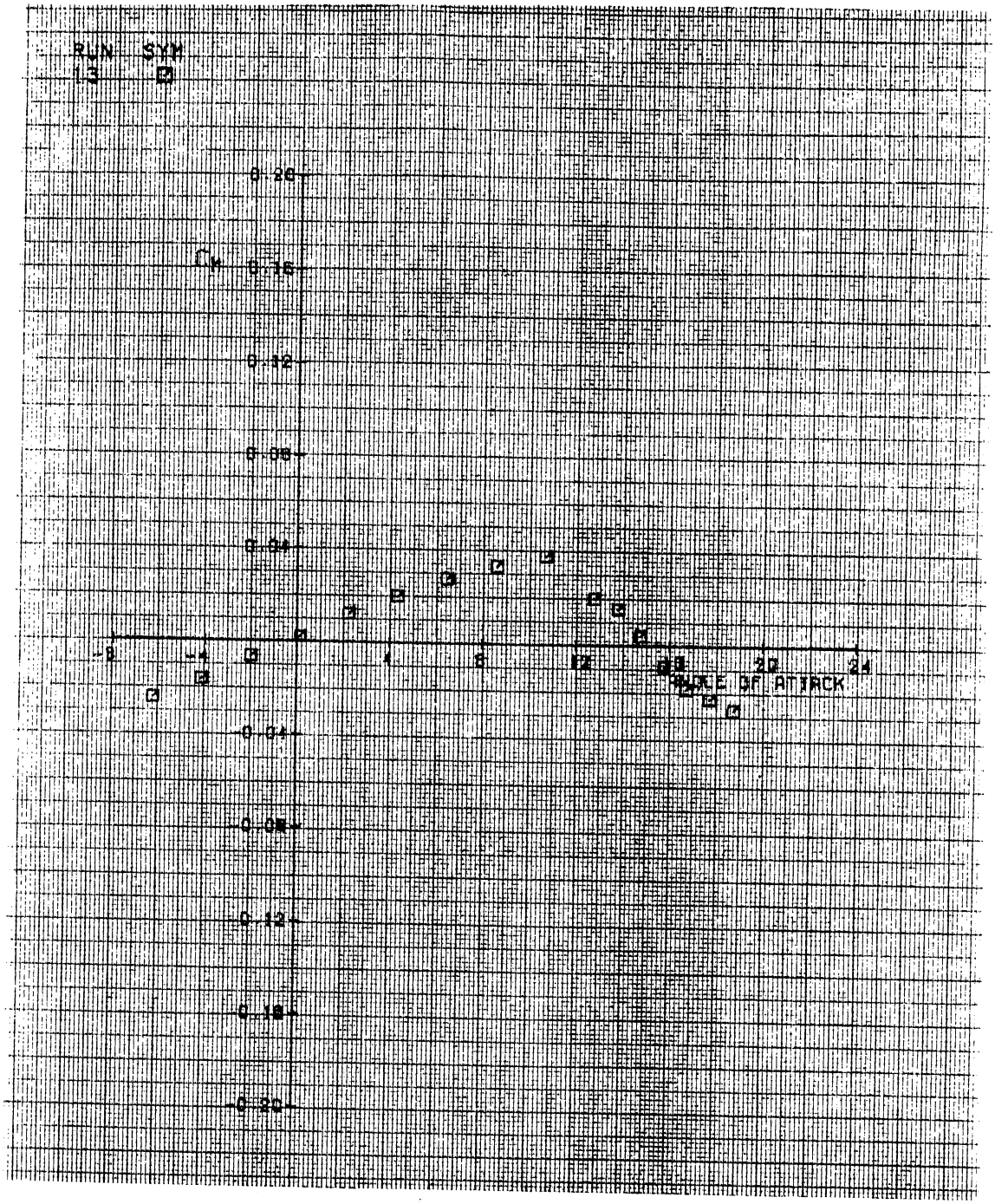

Figure 73. Run 13. Cm vs Alpha

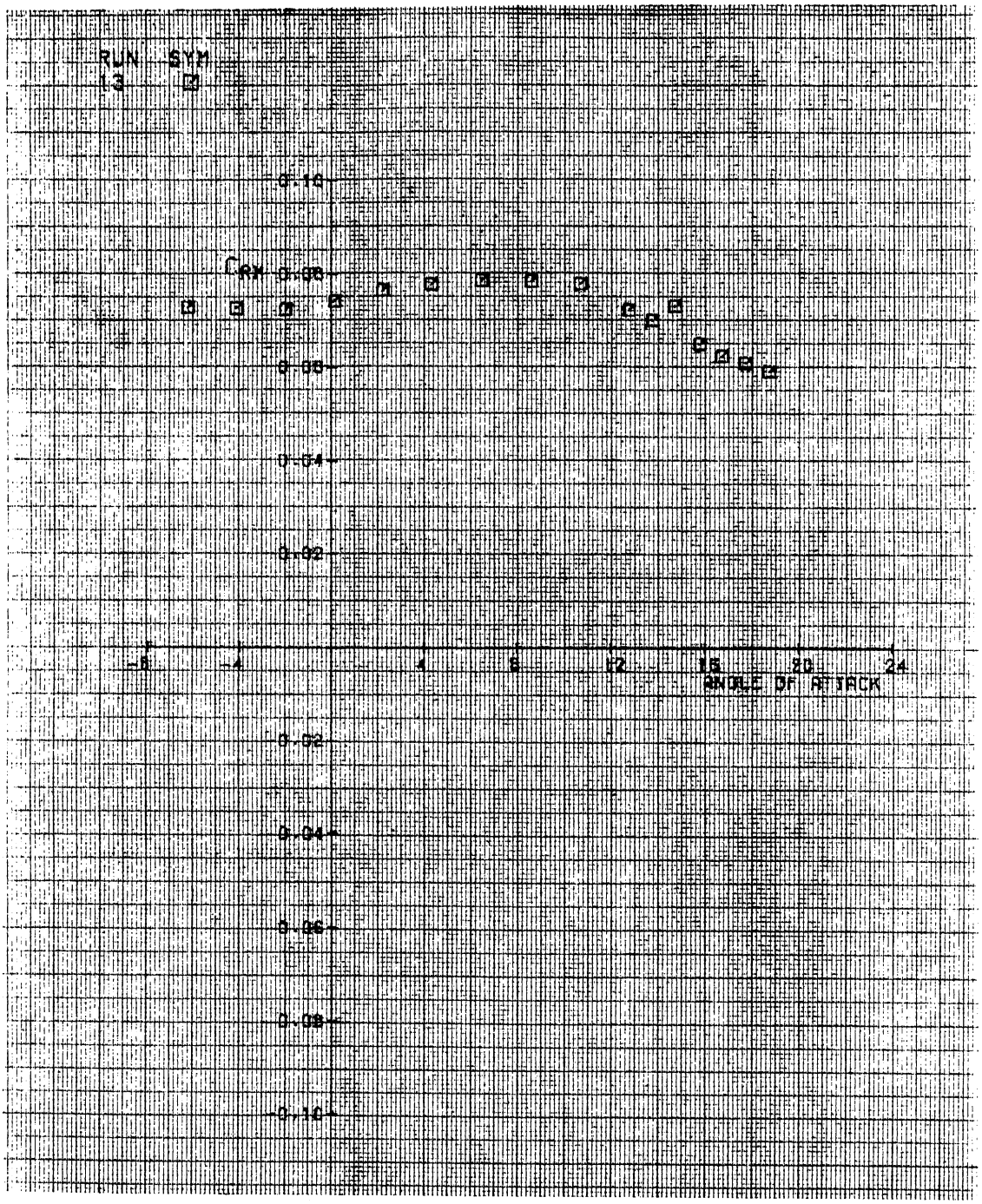

Figure 74. Run 13. Crm vs Alpha

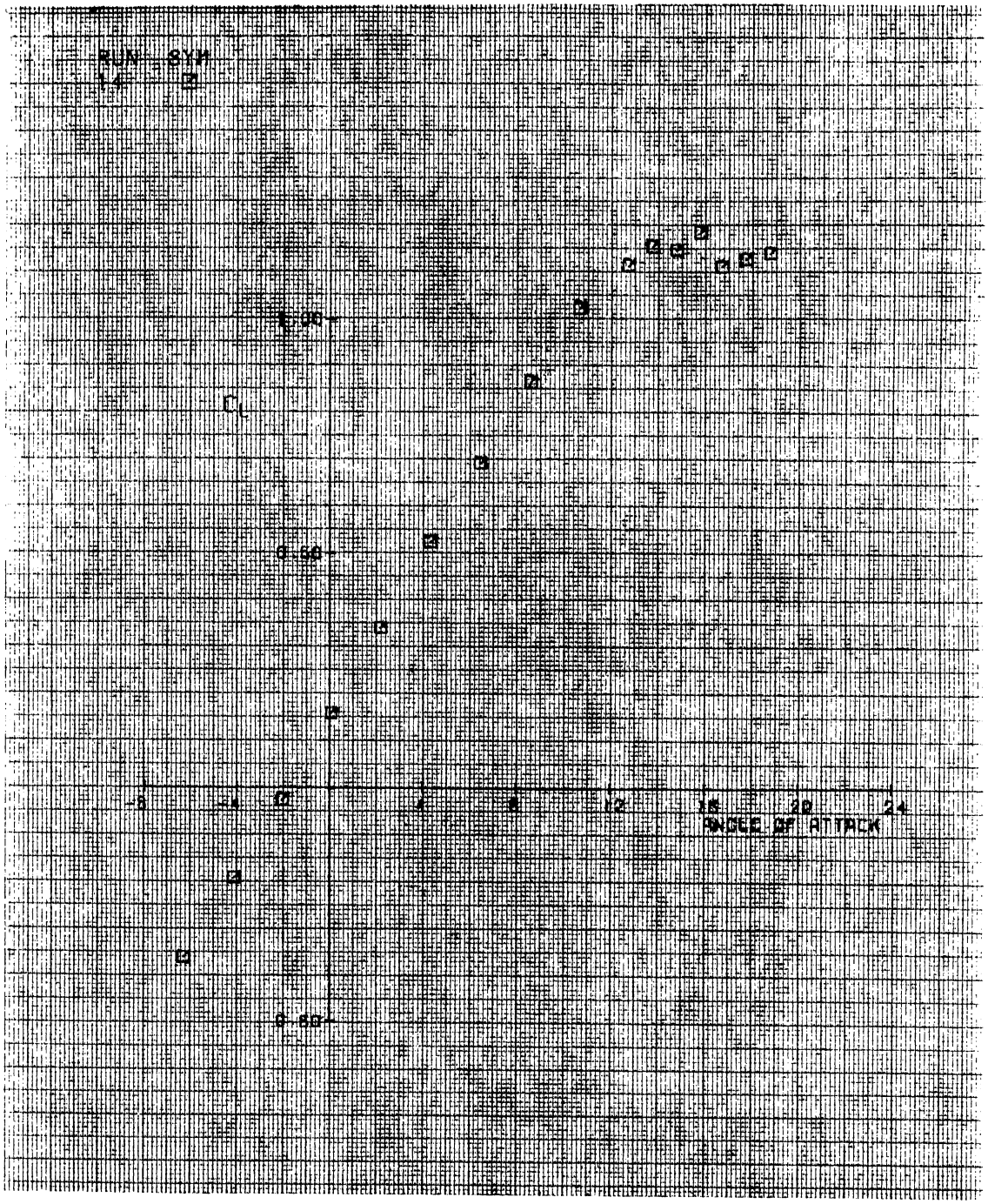

Figure 75. Run 14. Cl vs Alpha

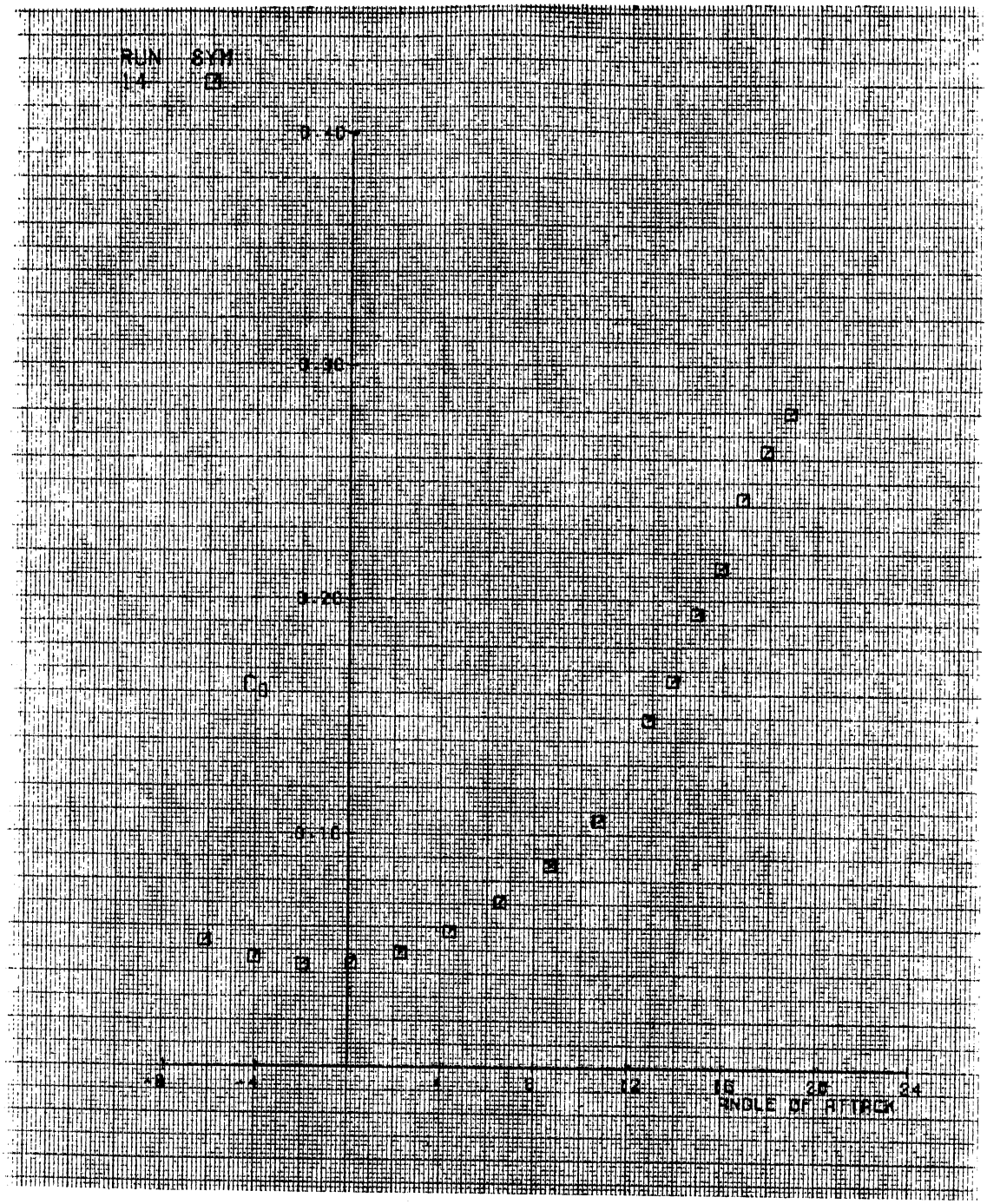

Figure 76. Run 14. Cd vs Alpha

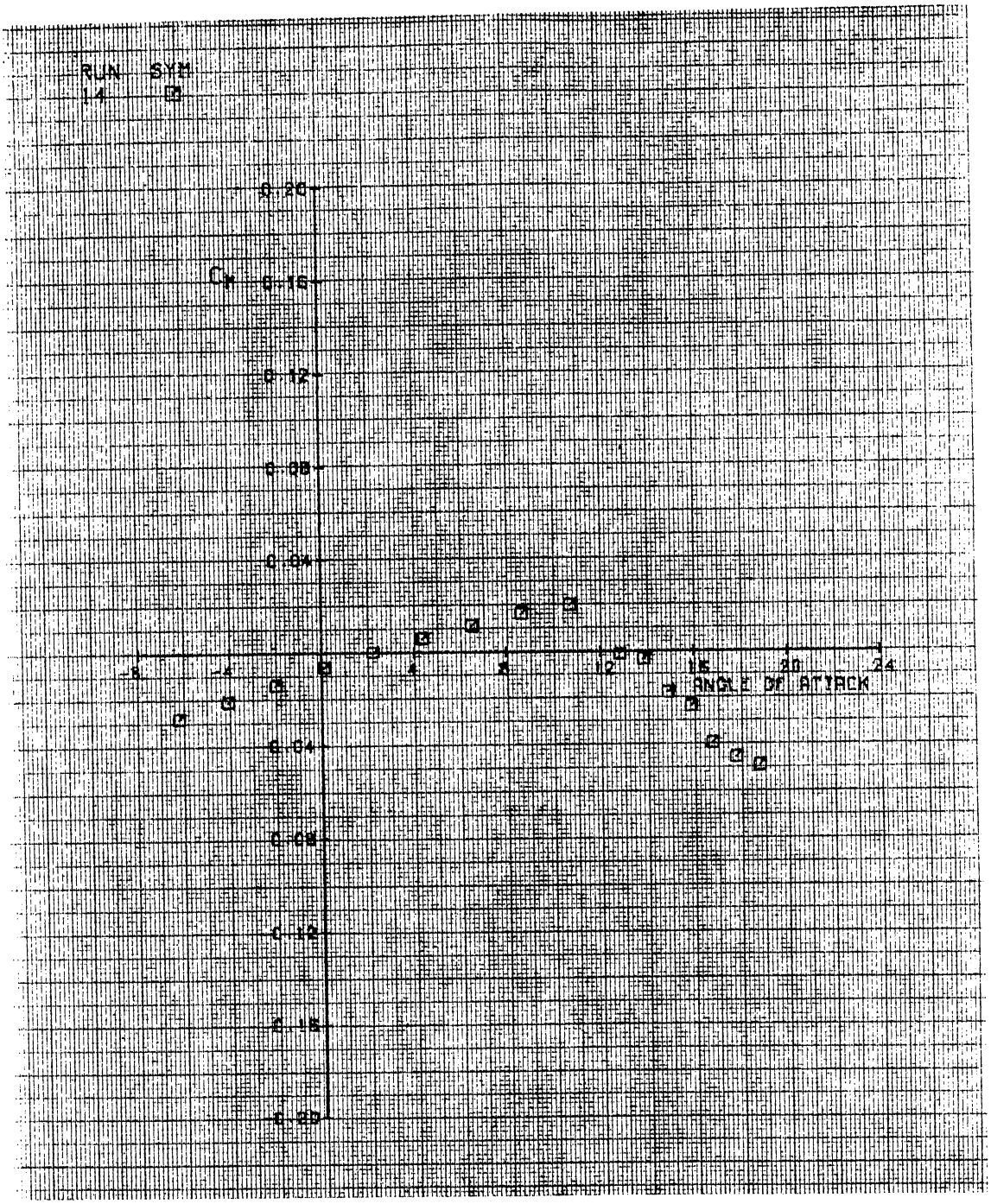

Figure 77. Run 14. Cm vs Alpha

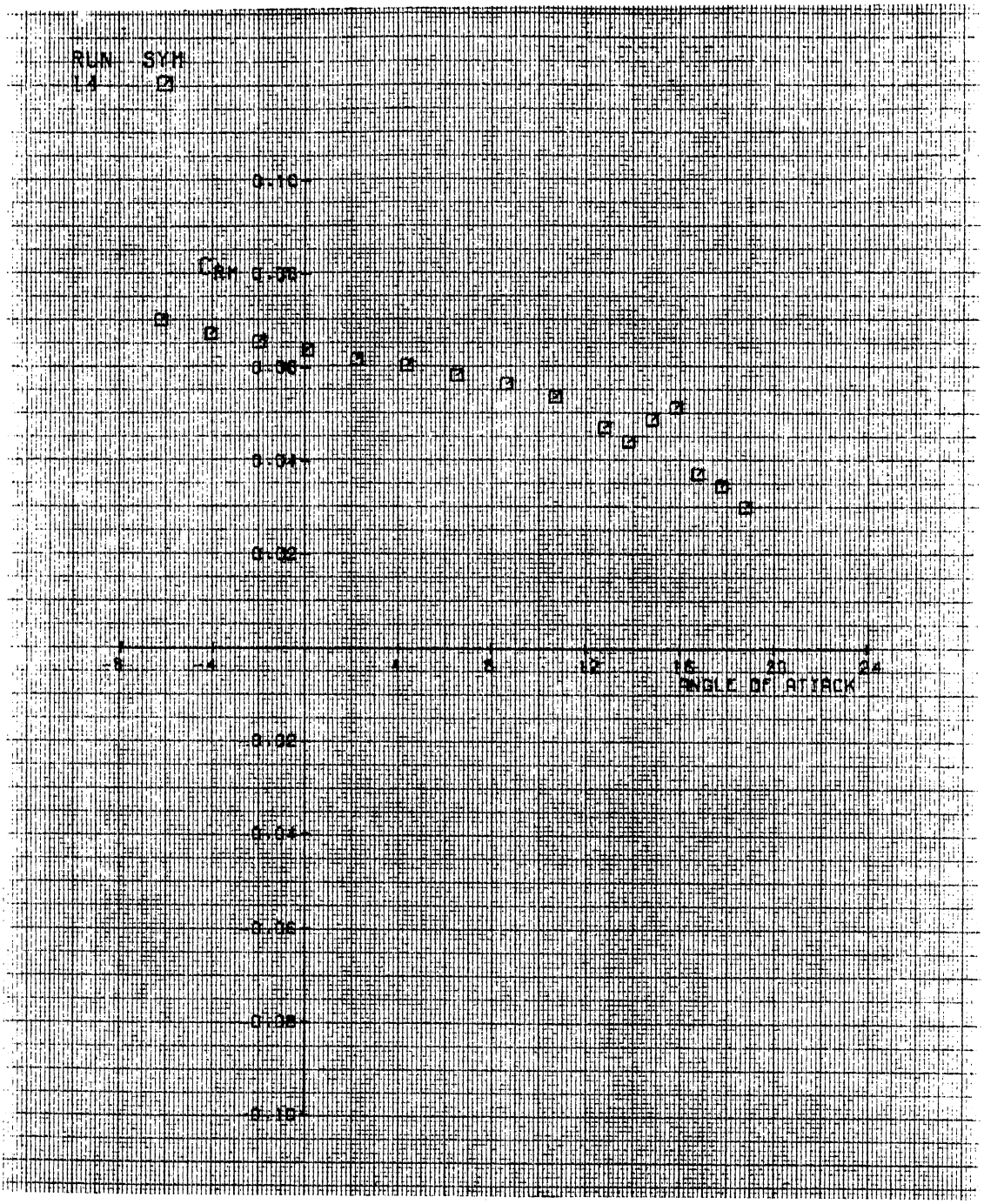

Figure 78. Run 14. Crm vs Alpha

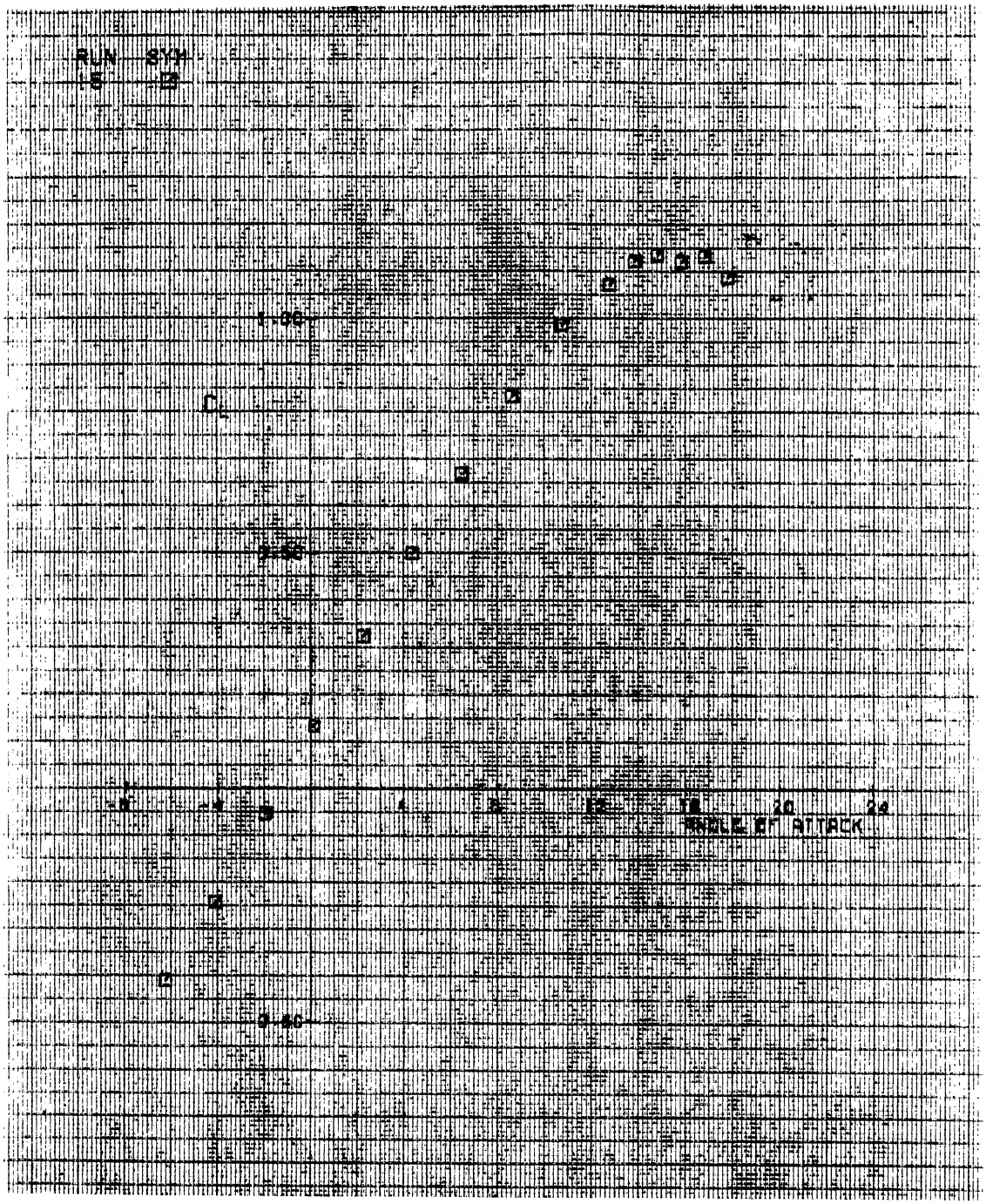

Figure 79. Run 15. Cl vs Alpha

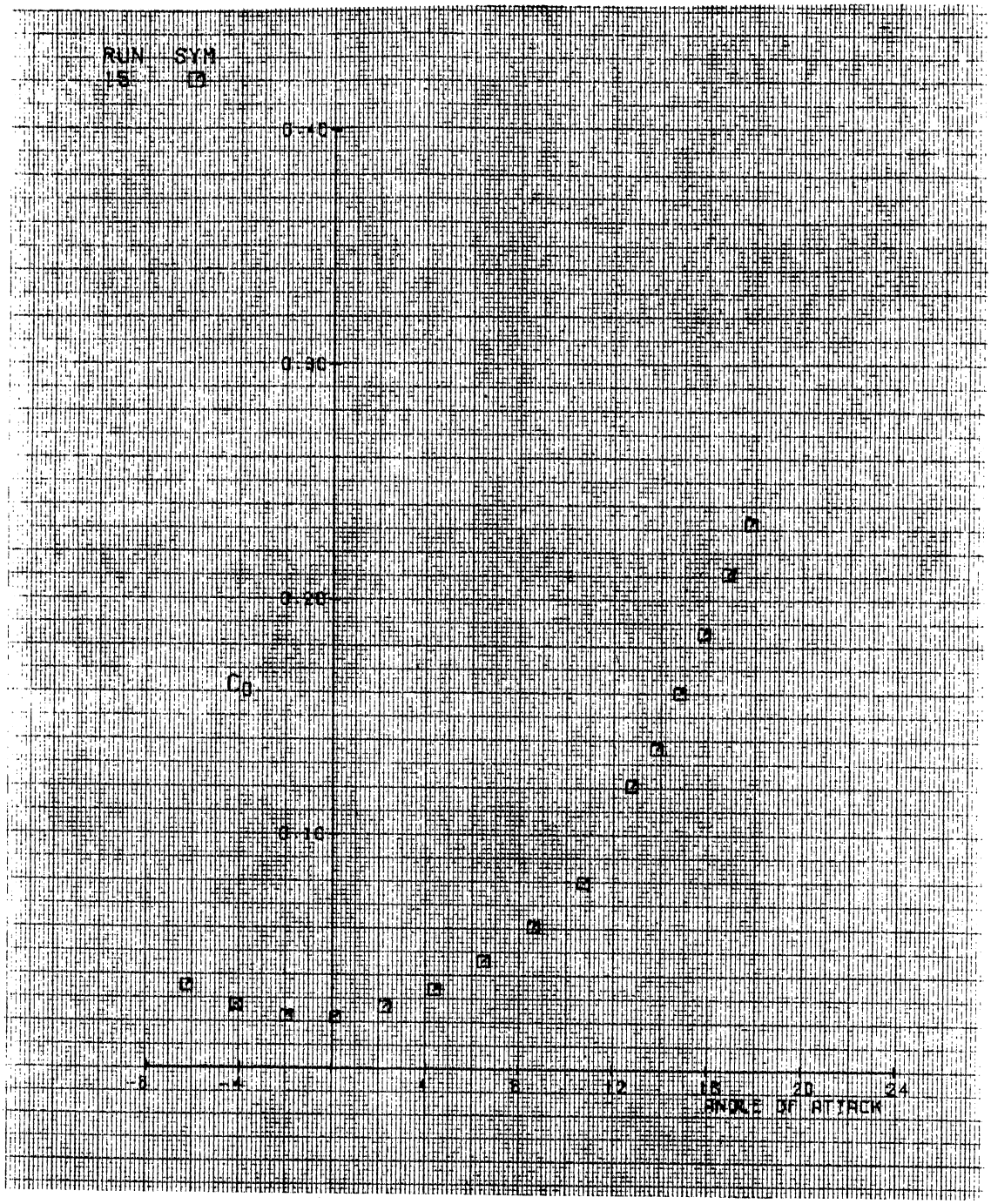

Figure 80. Run 15. Cd vs Alpha

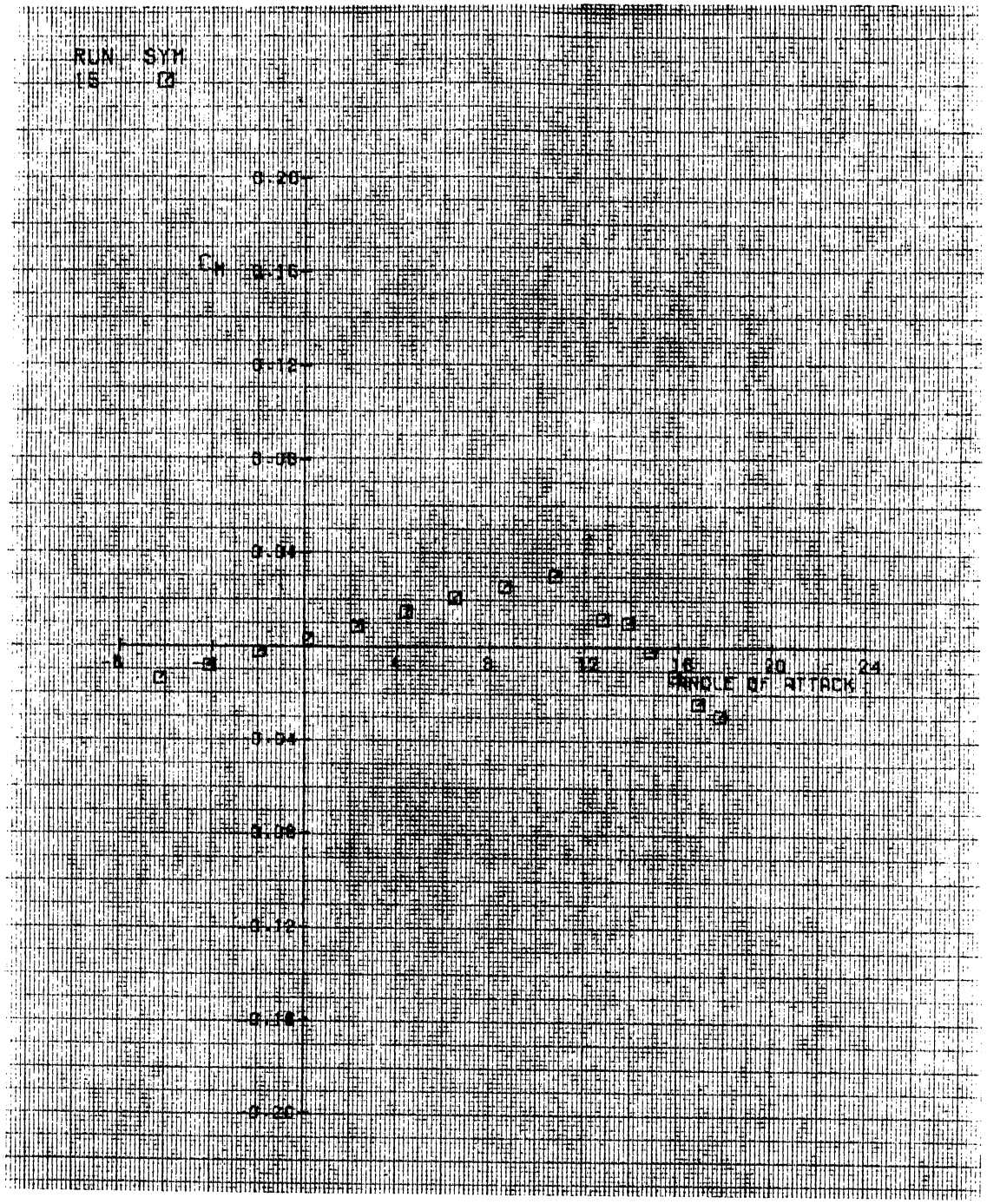

Figure 81. Run 15. Cm vs Alpha

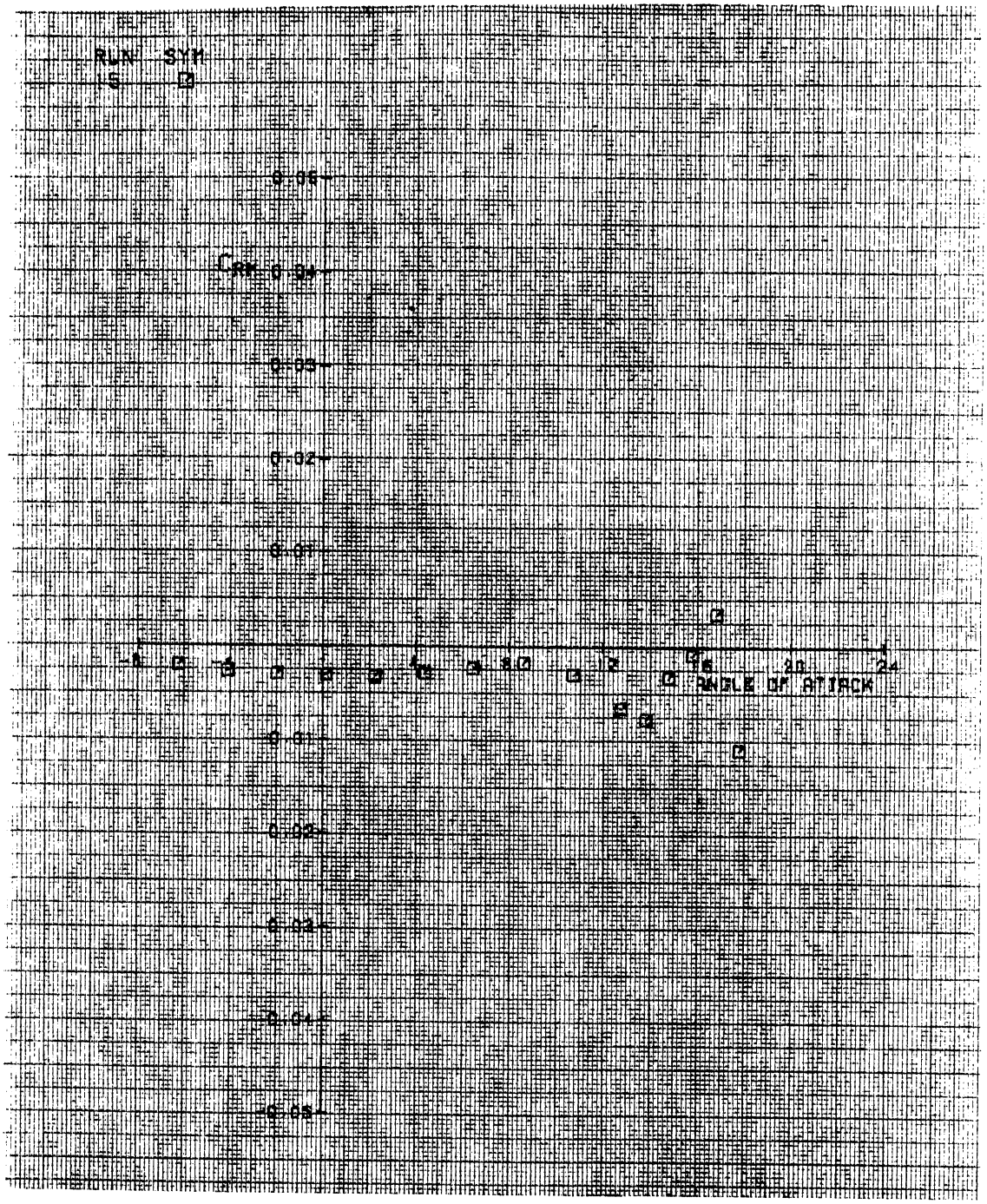

Figure 82. Run 15. Crm vs Alpha

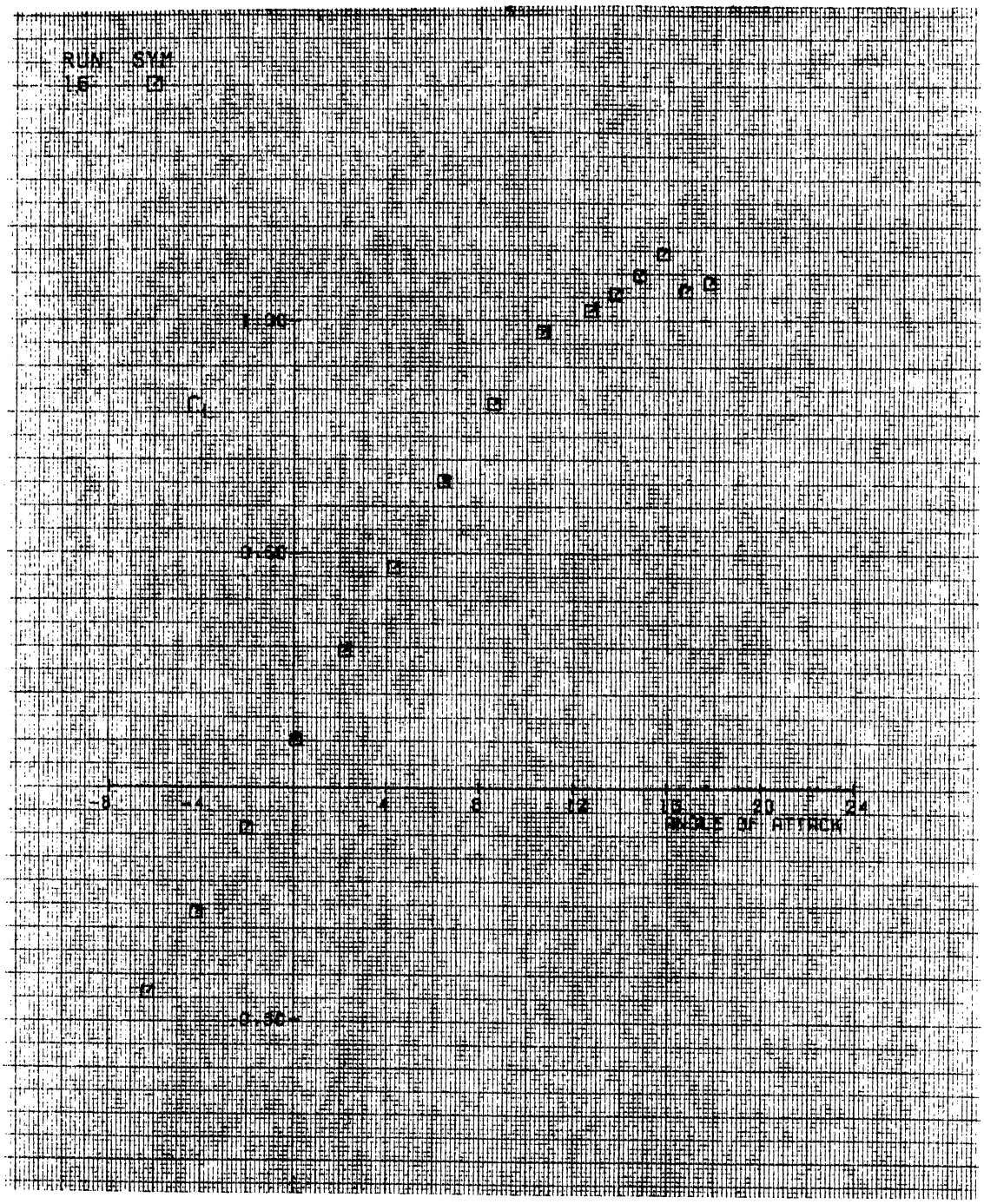

Figure 83. Run 16. Cl vs Alpha

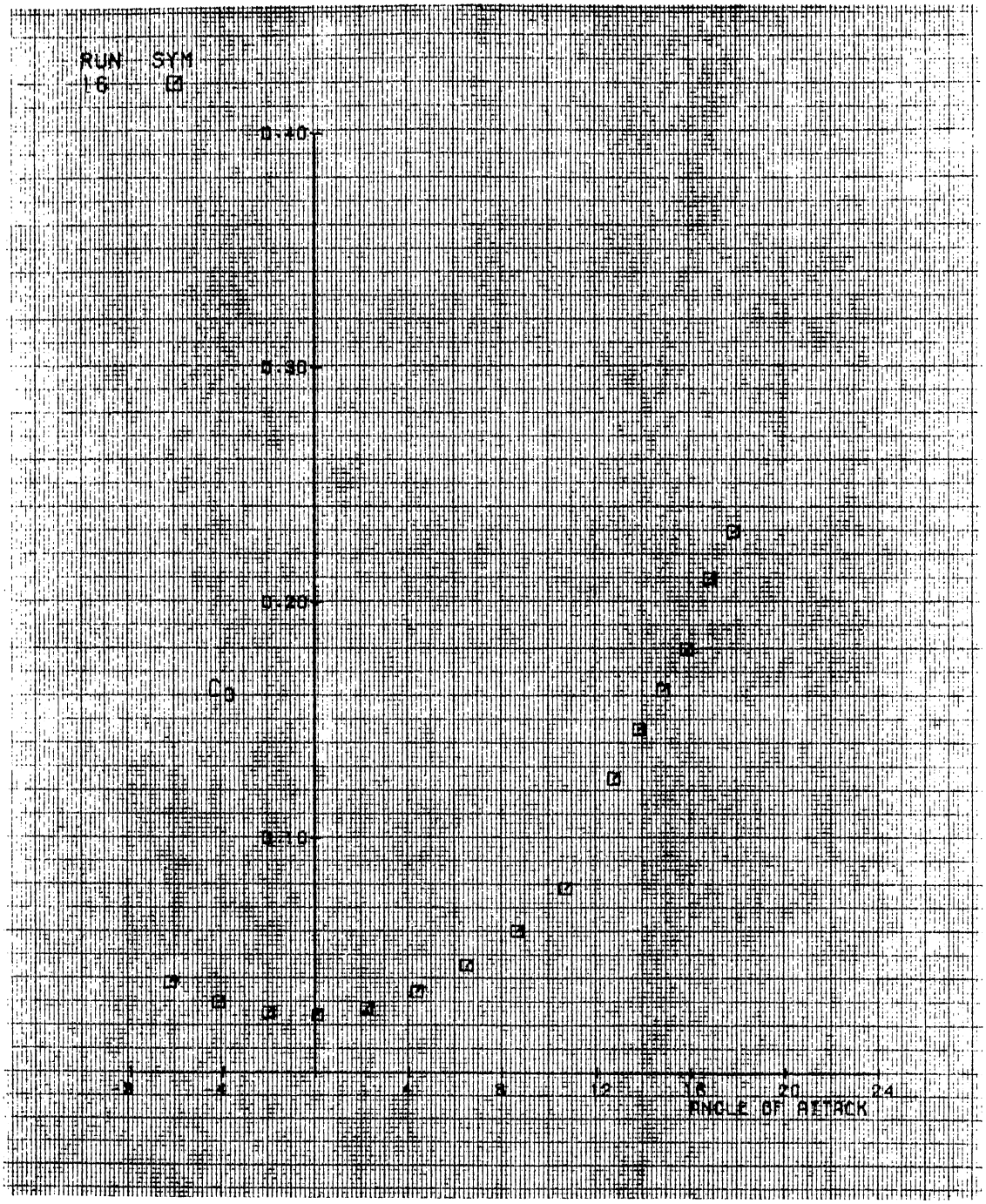

Figure 84. Run 16. Cd vs Alpha

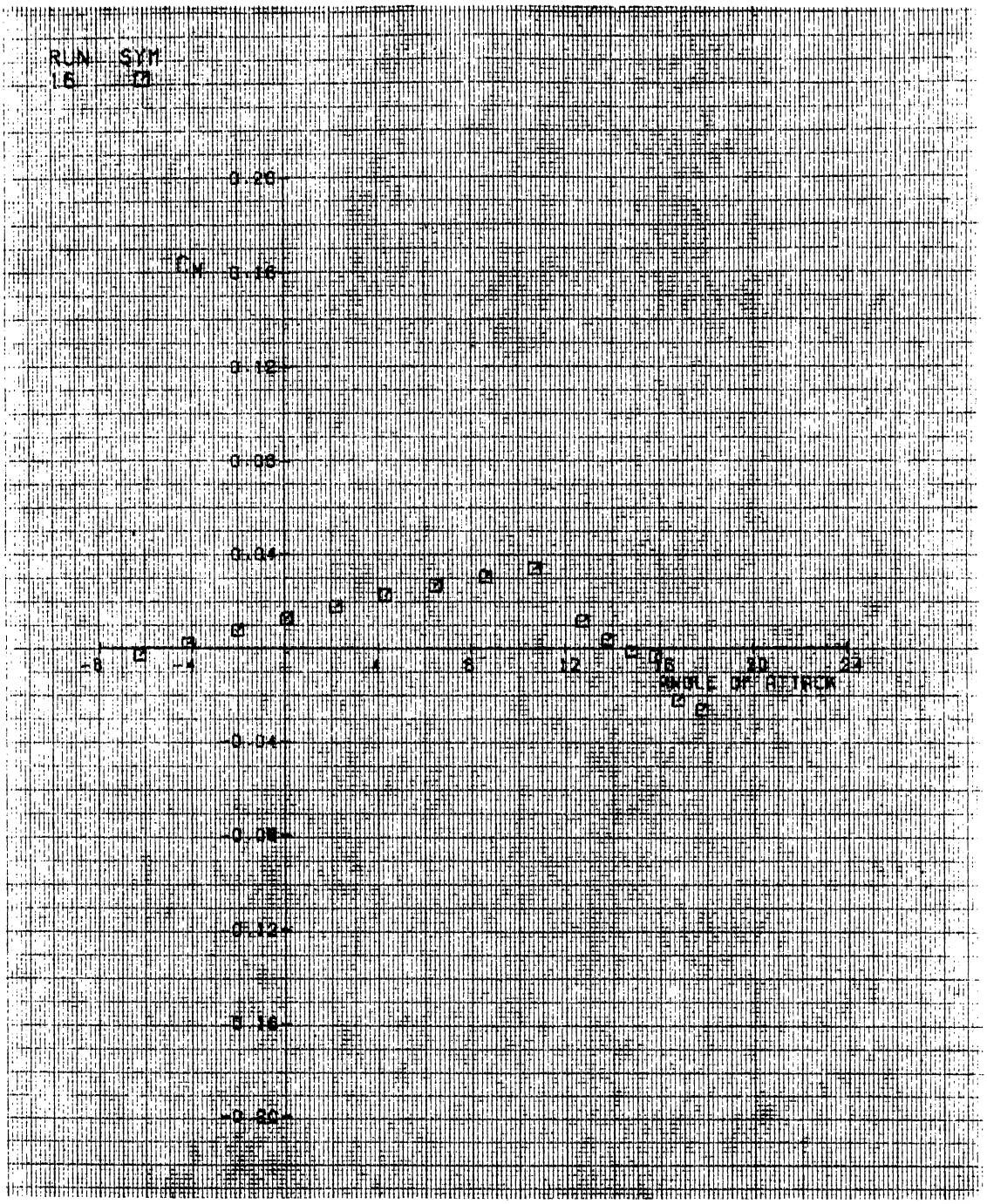

Figure 85. Run 16. Cm vs Alpha

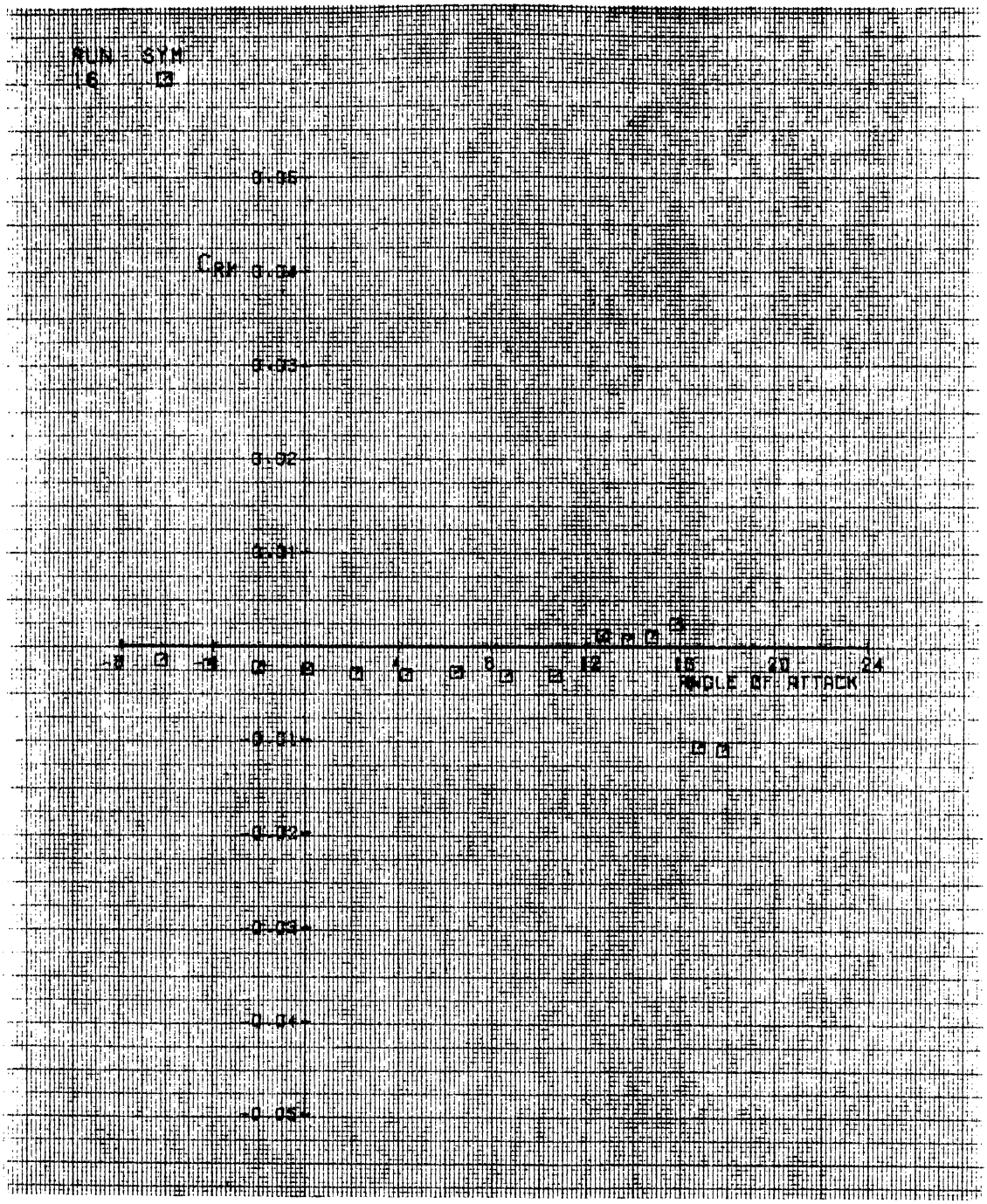

Figure 86. Run 16. Crm vs Alpha

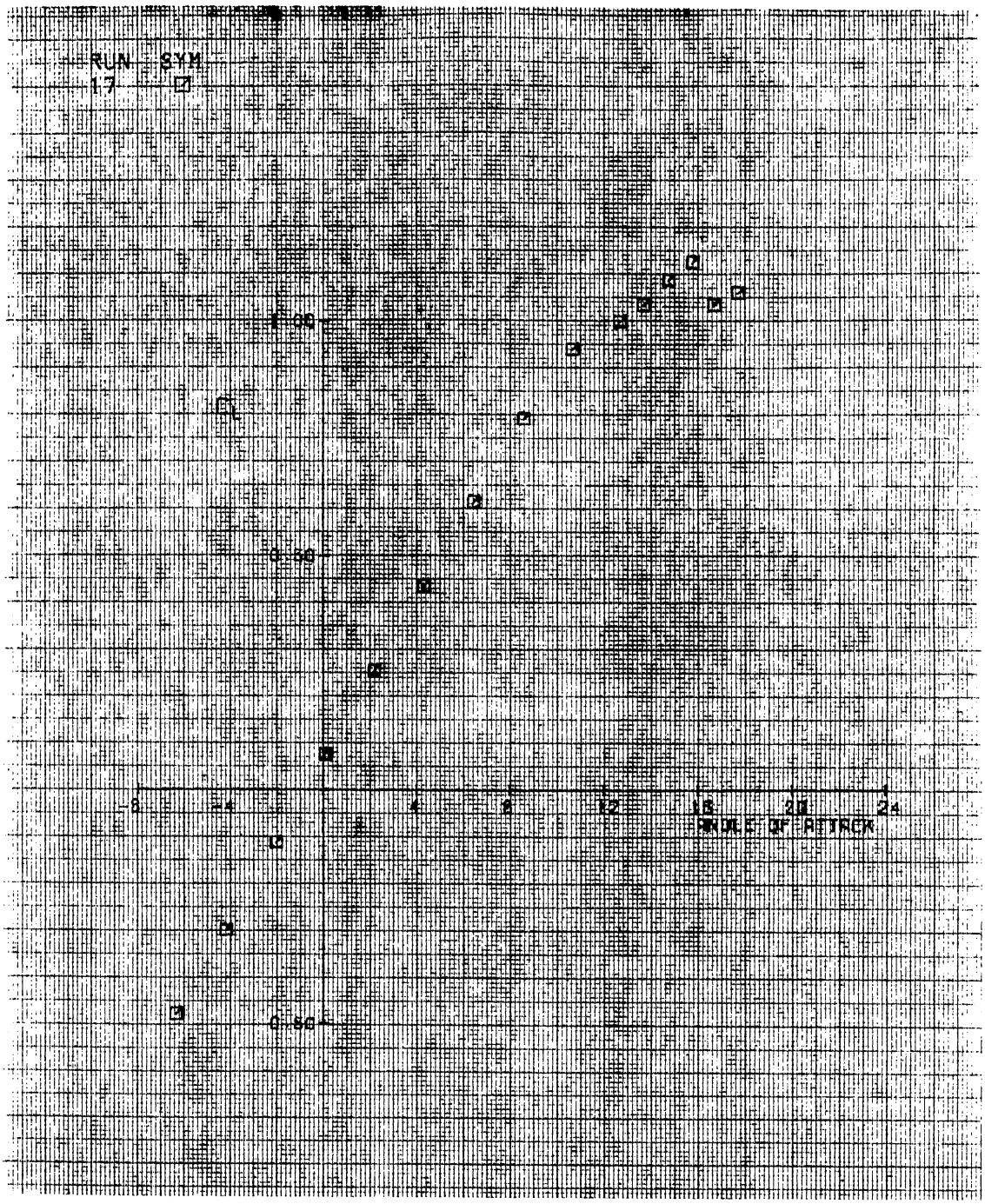

Figure 87. Run 17. Cl vs Alpha

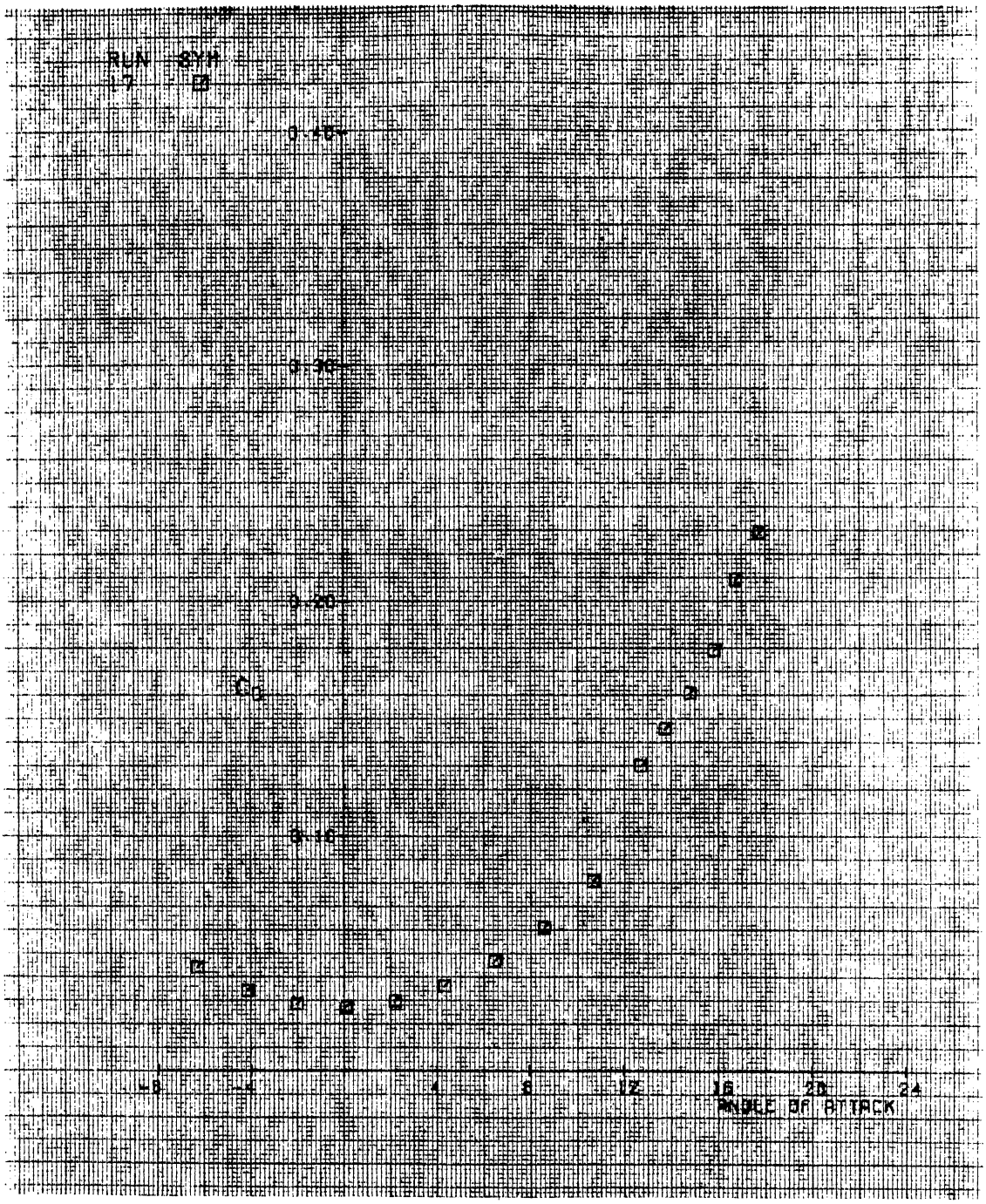

Figure 88. Run 17. Cd vs Alpha

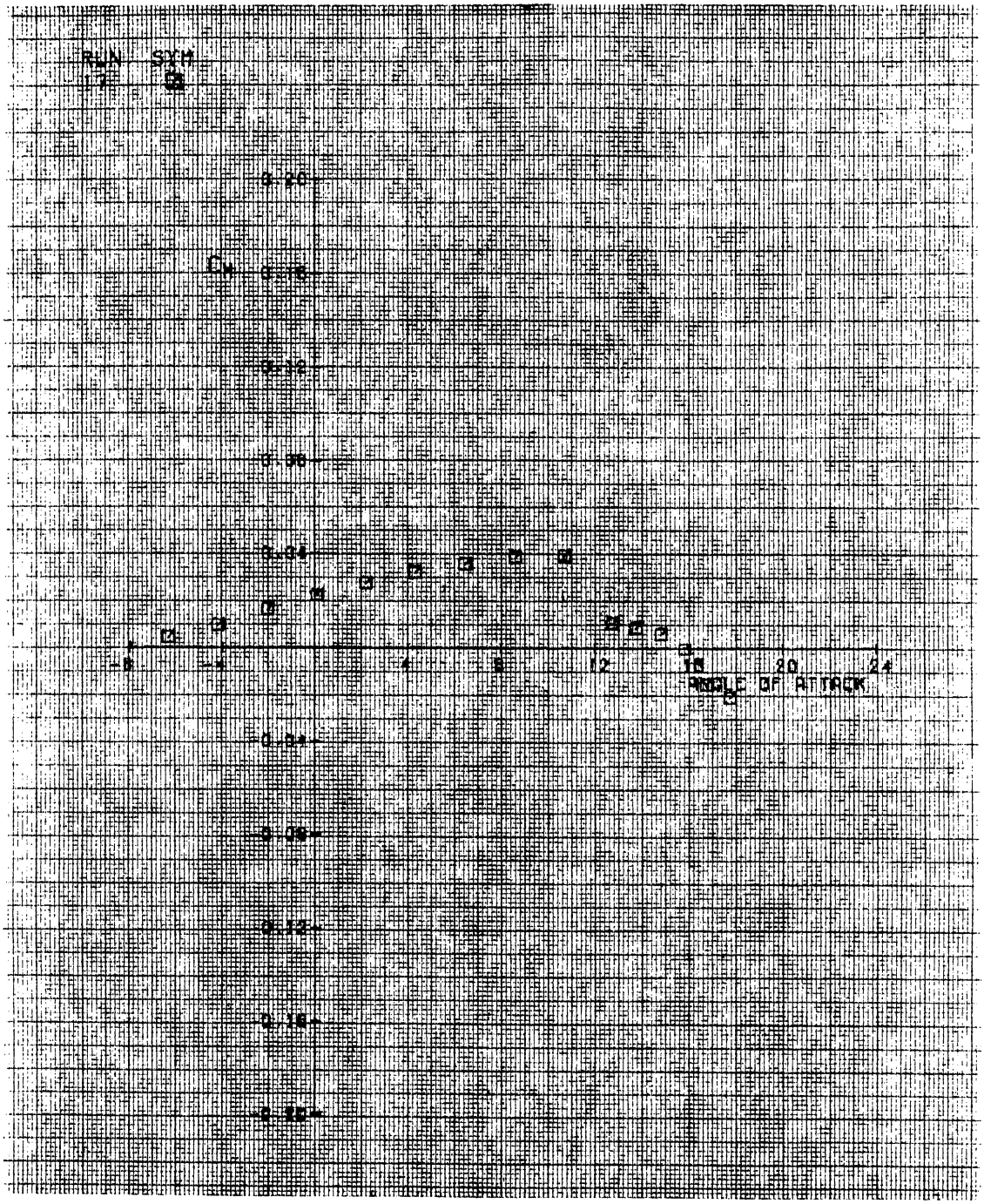

Figure 89. Run 17. Cm vs Alpha

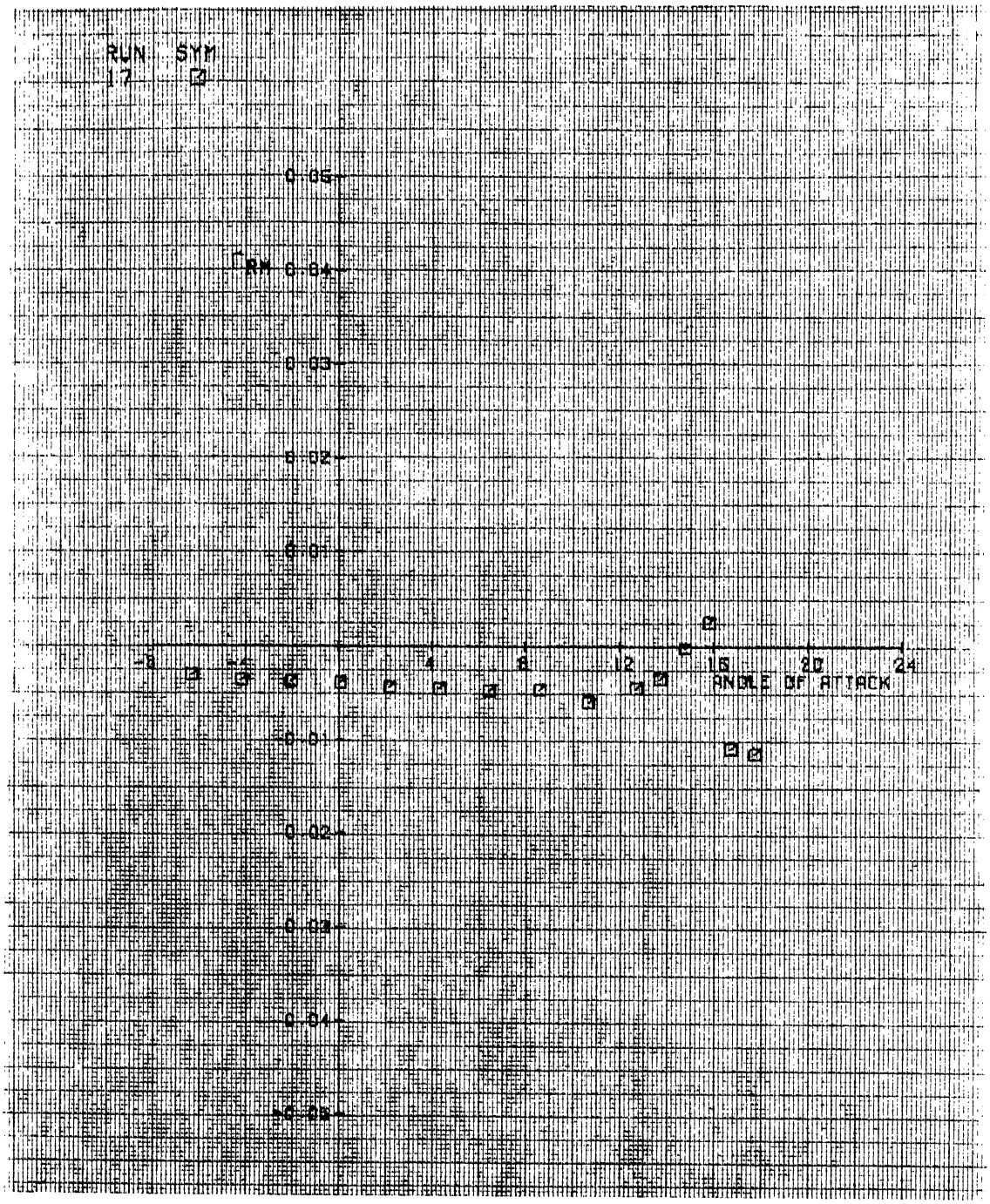

Figure 90. Run 17. Crm vs Alpha

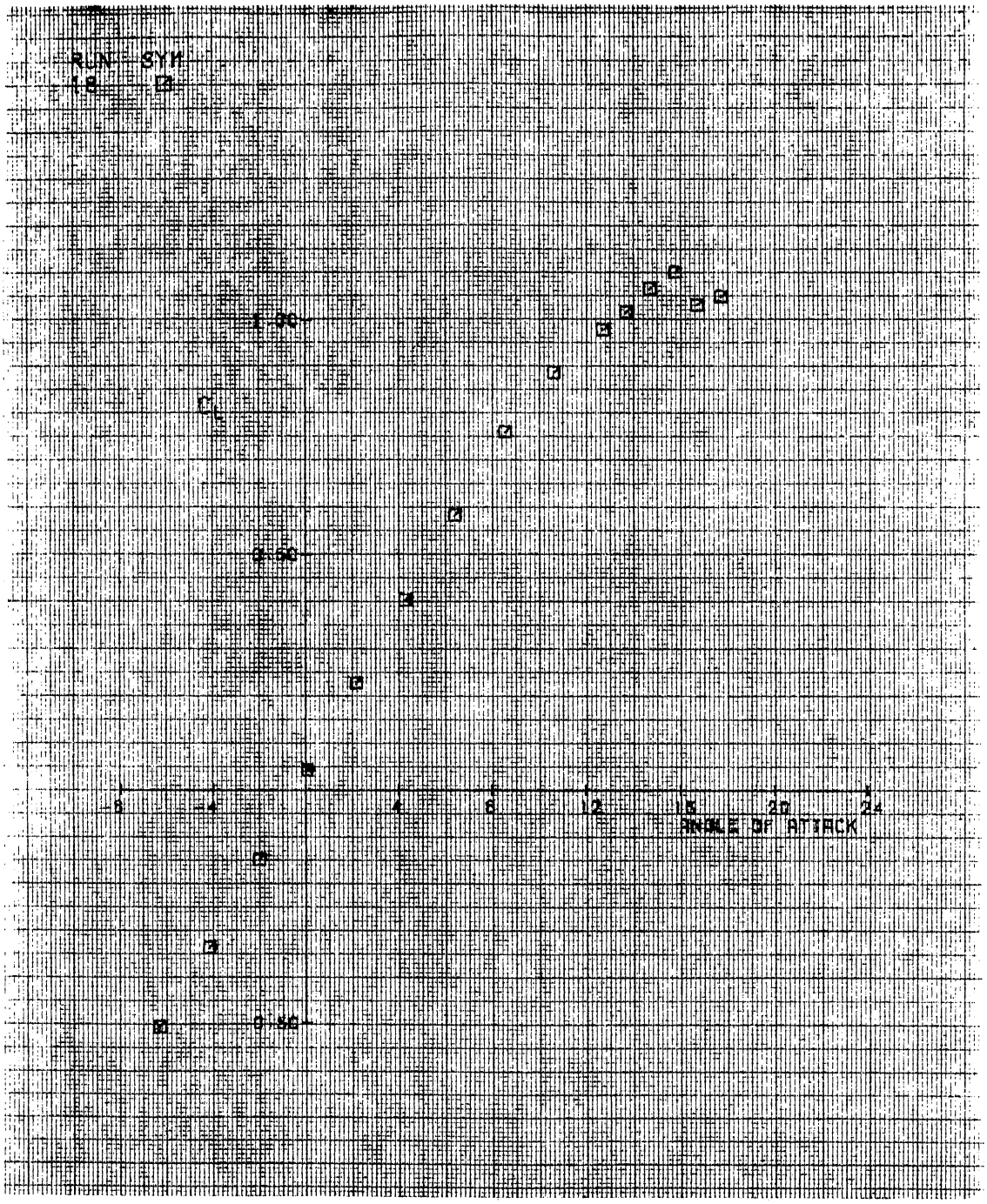

Figure 91. Run 18. Cl vs Alpha

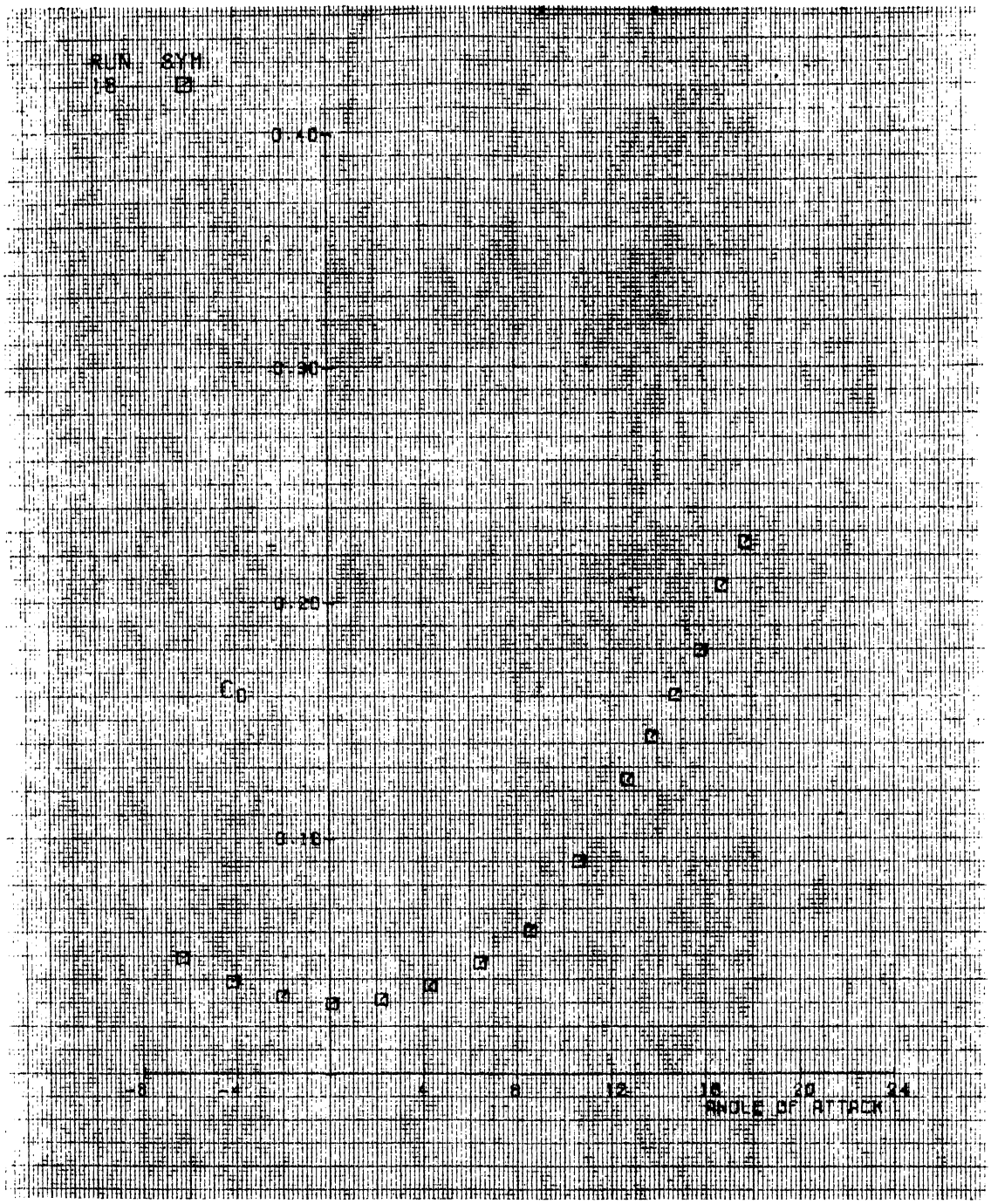

Figure 92. Run 18. Cd vs Alpha

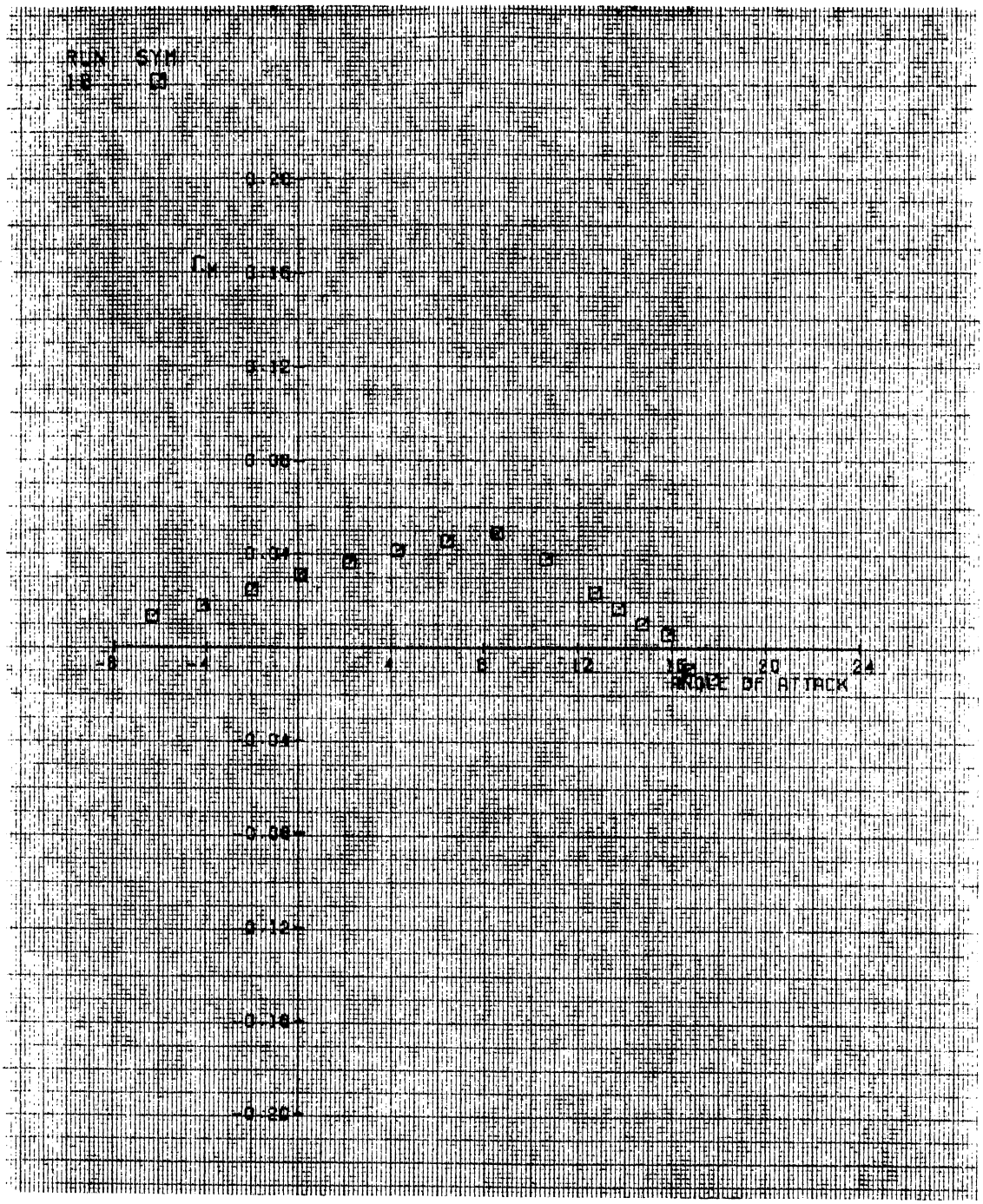

Figure 93. Run 18. Cm vs Alpha

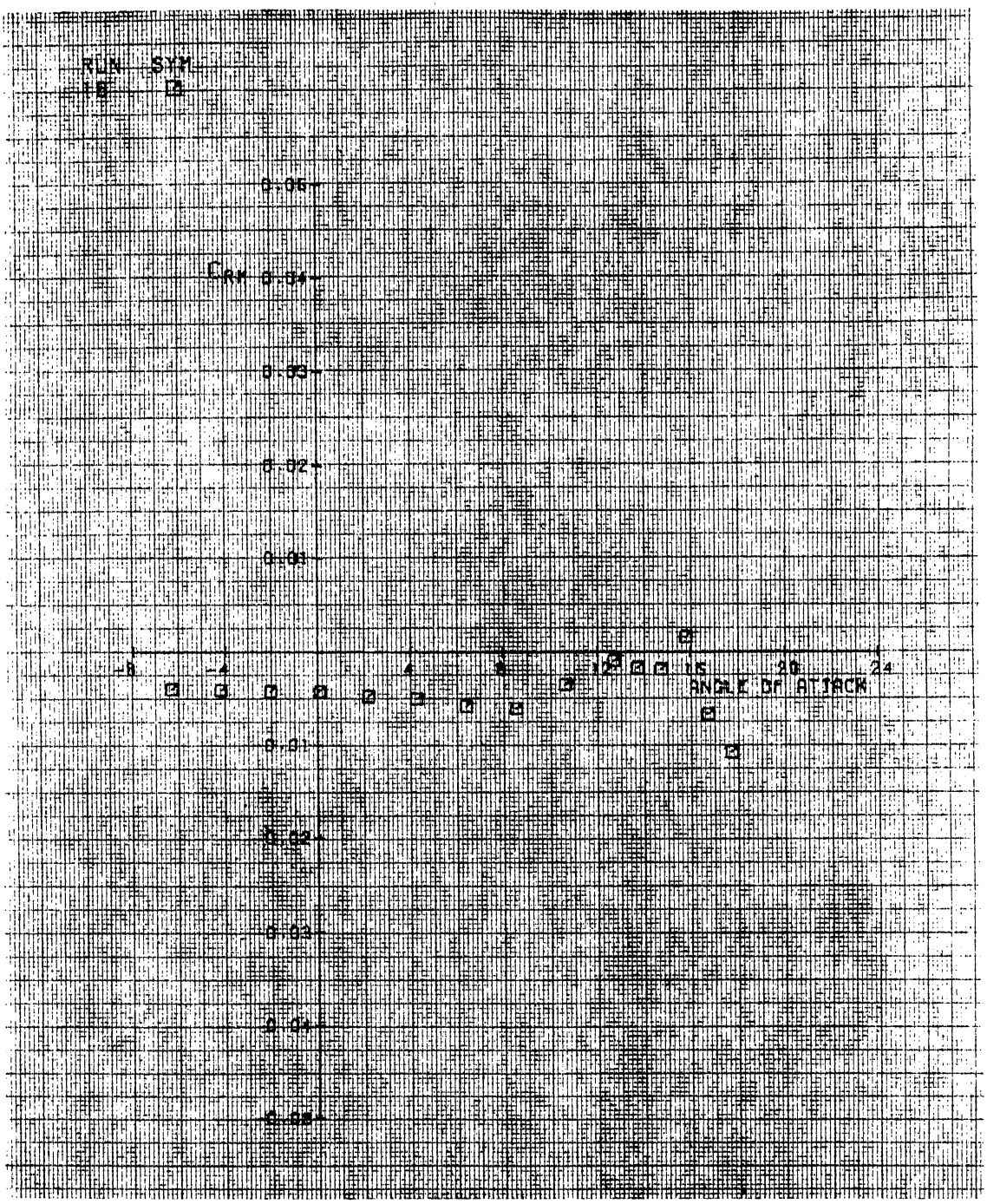

Figure 94. Run 18. Crm vs Alpha

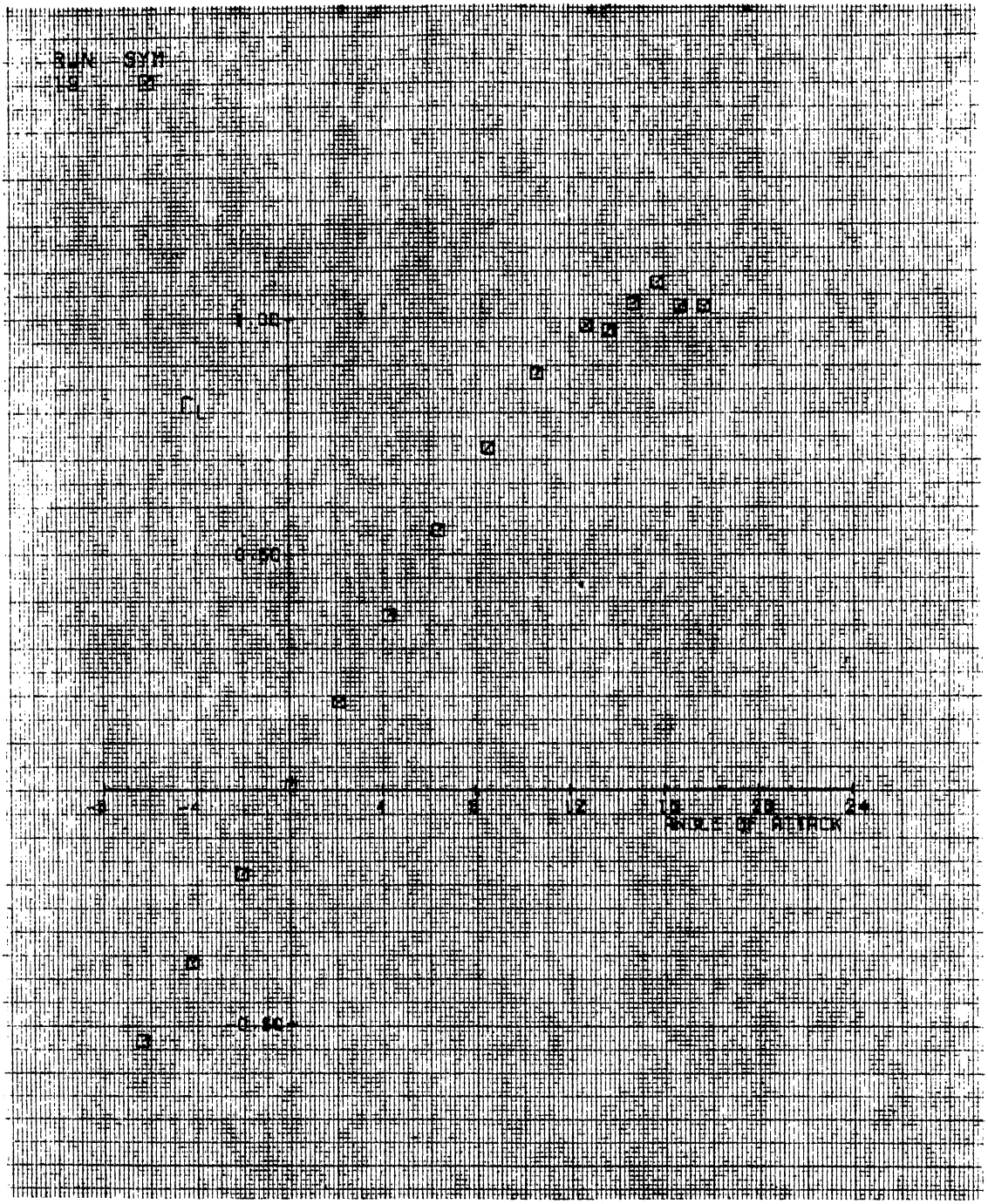

Figure 95. Run 19. Cl vs Alpha

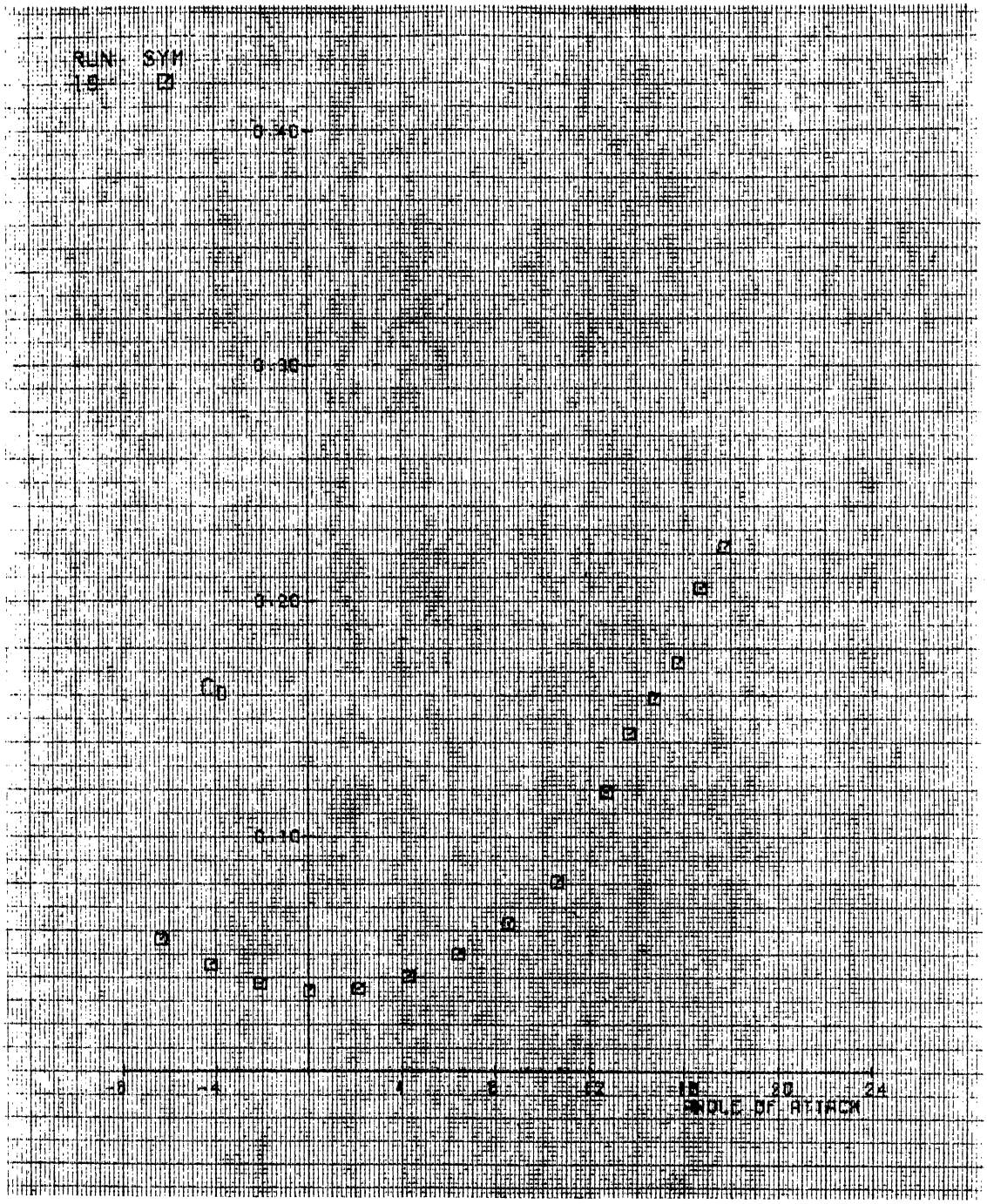

Figure 96. Run 19. Cd vs Alpha

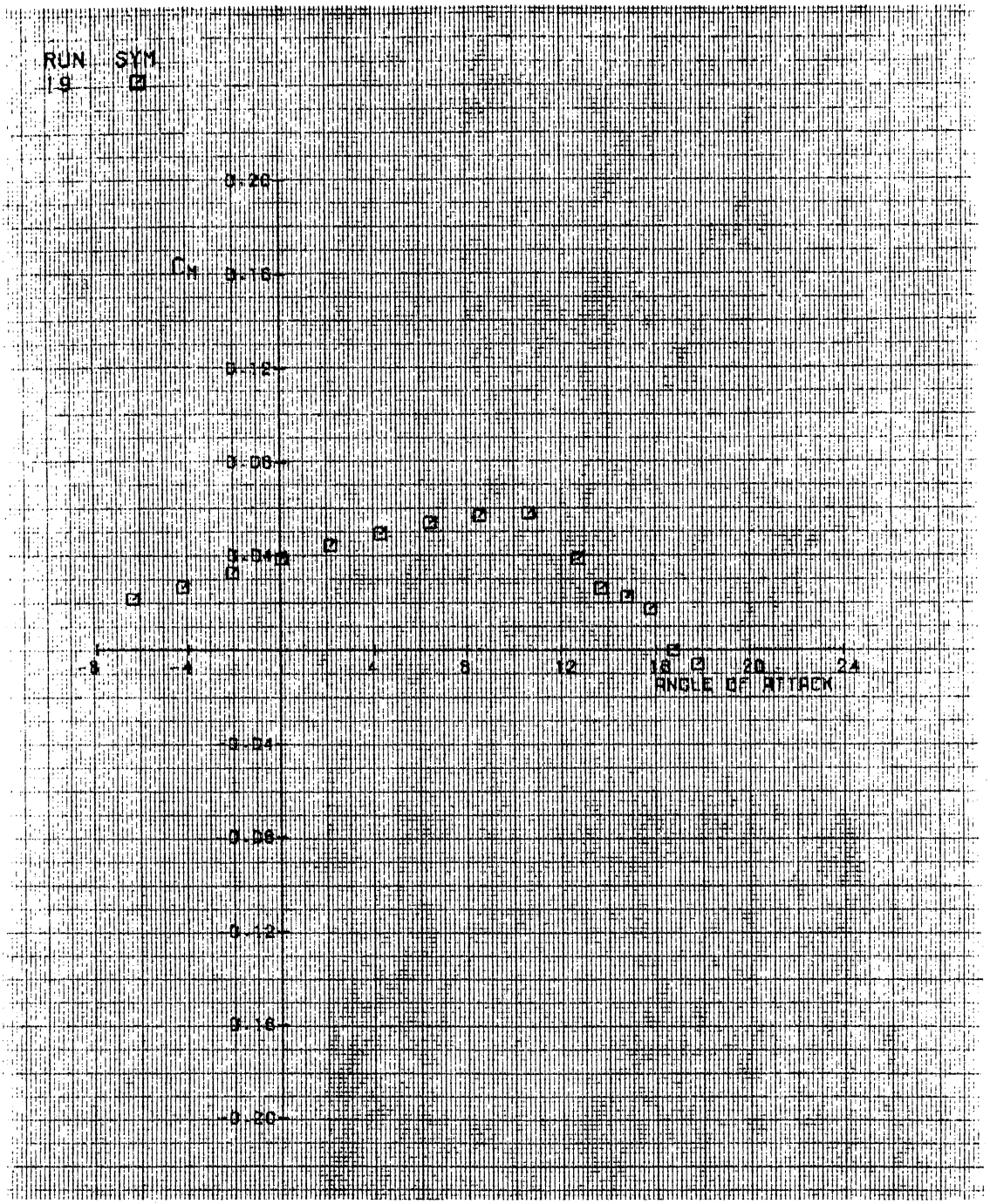

Figure 97. Run 19. Cm vs Alpha

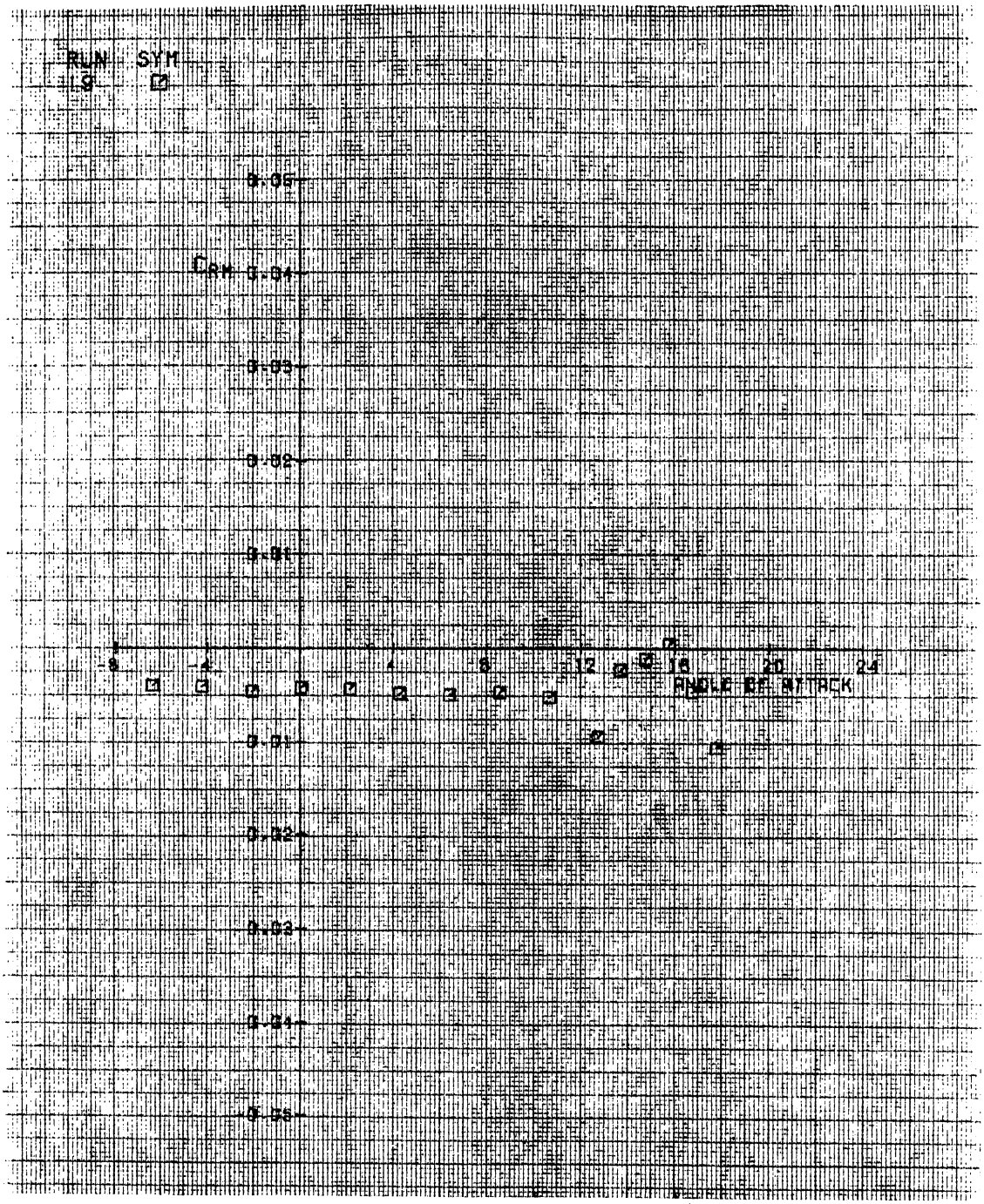

Figure 98. Run 19. Crm vs Alpha

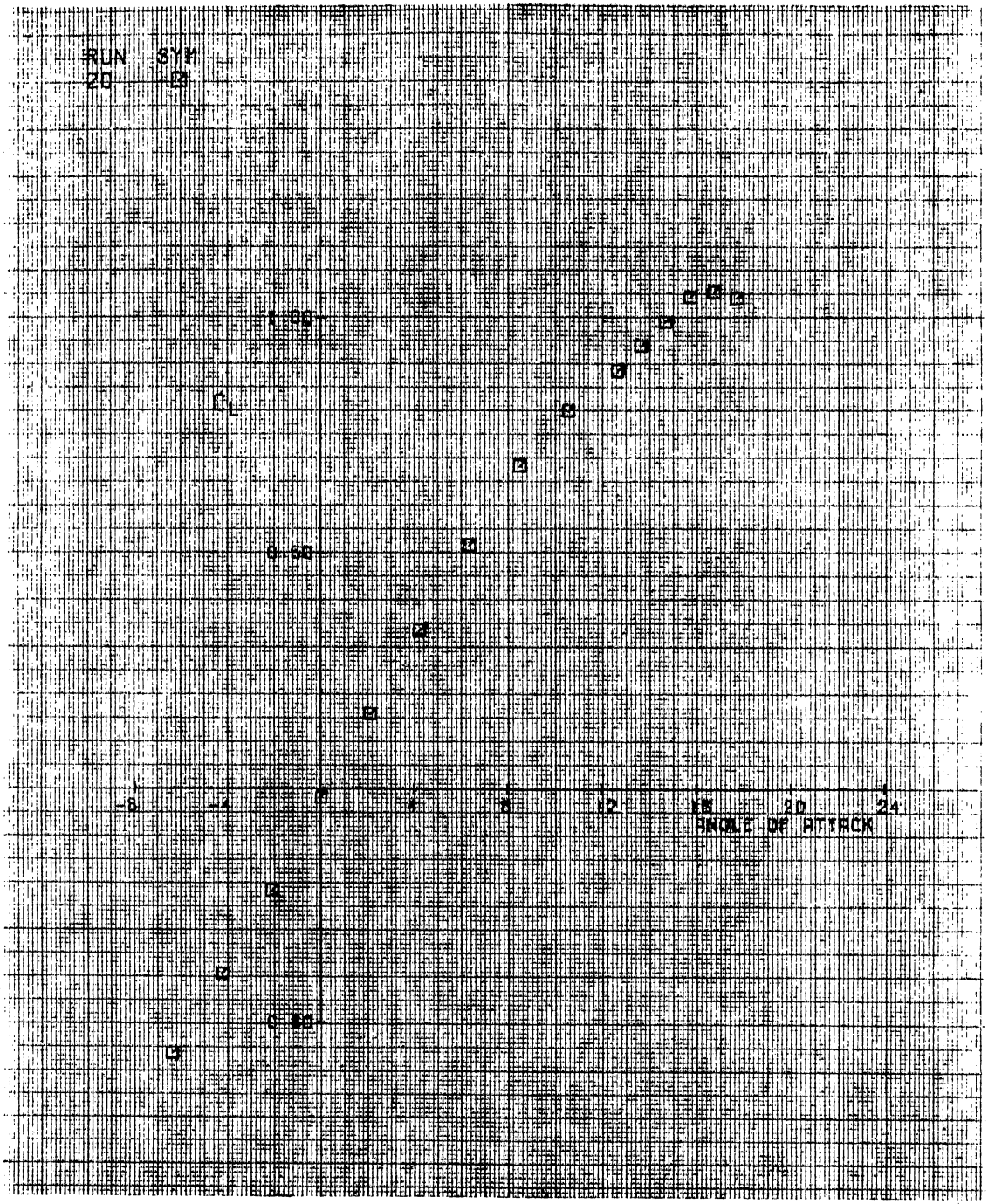

Figure 99. Run 20. Cl vs Alpha

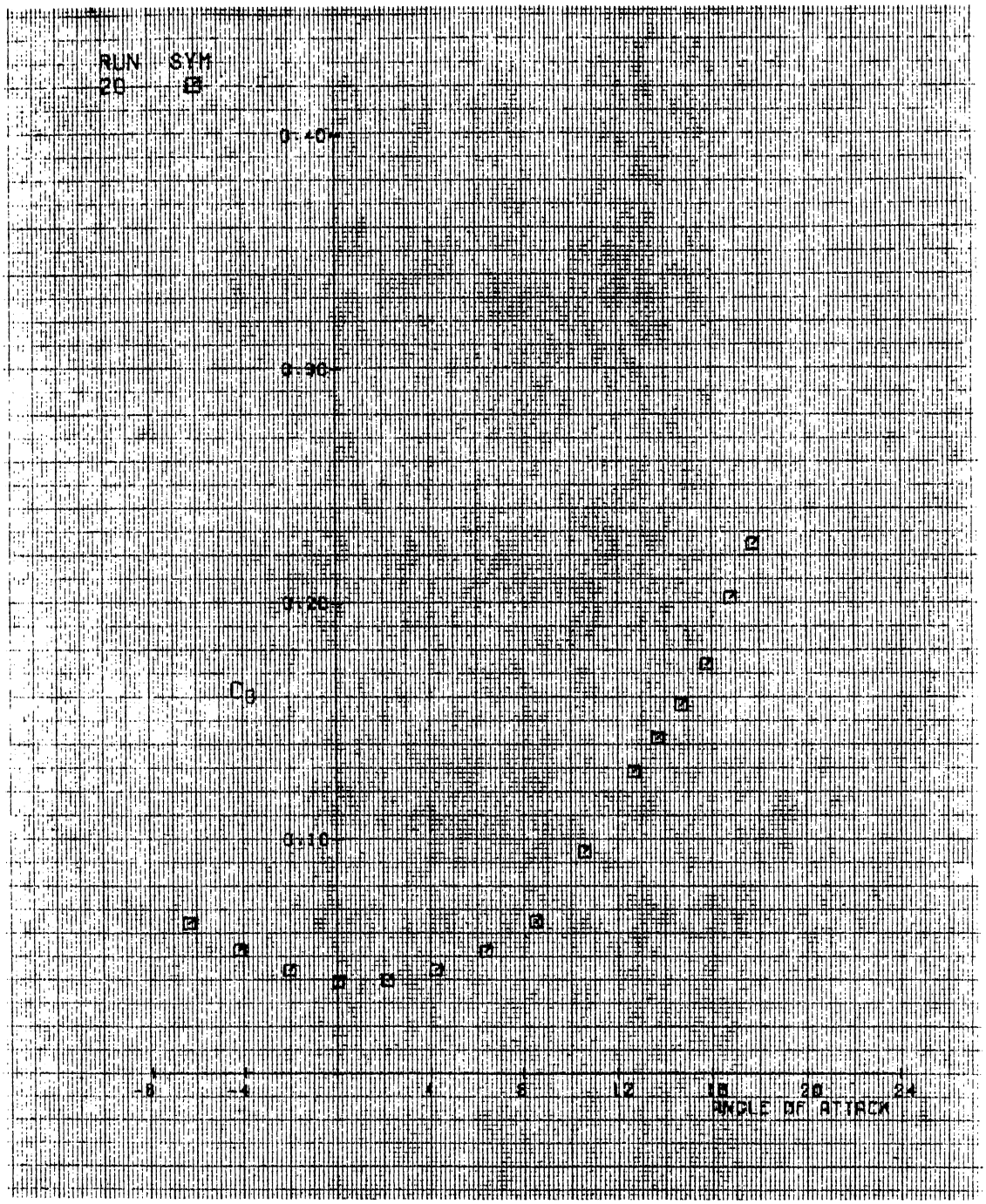

Figure 100. Run 20. Cd vs Alpha

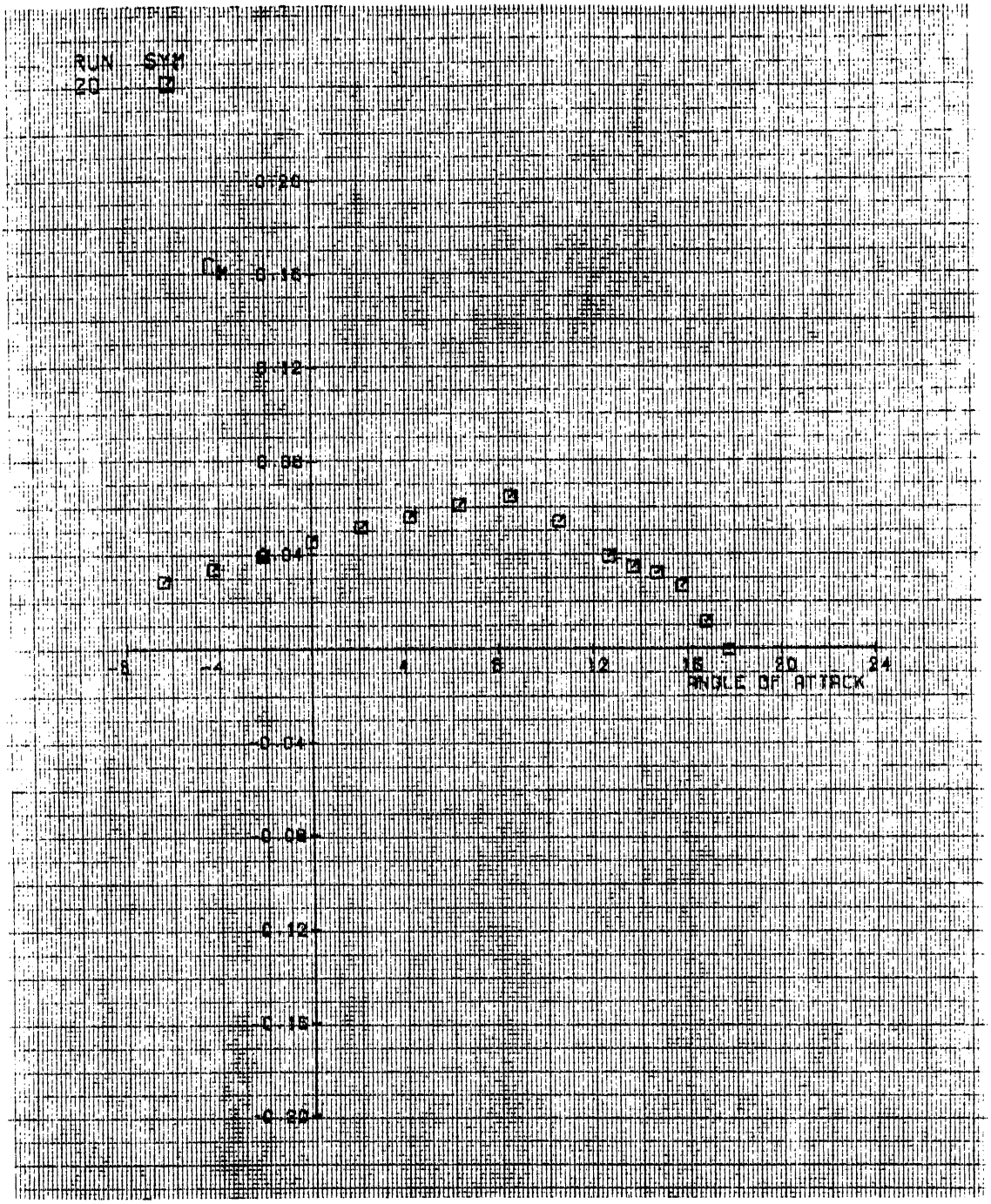

Figure 101. Run 20. Cm vs Alpha

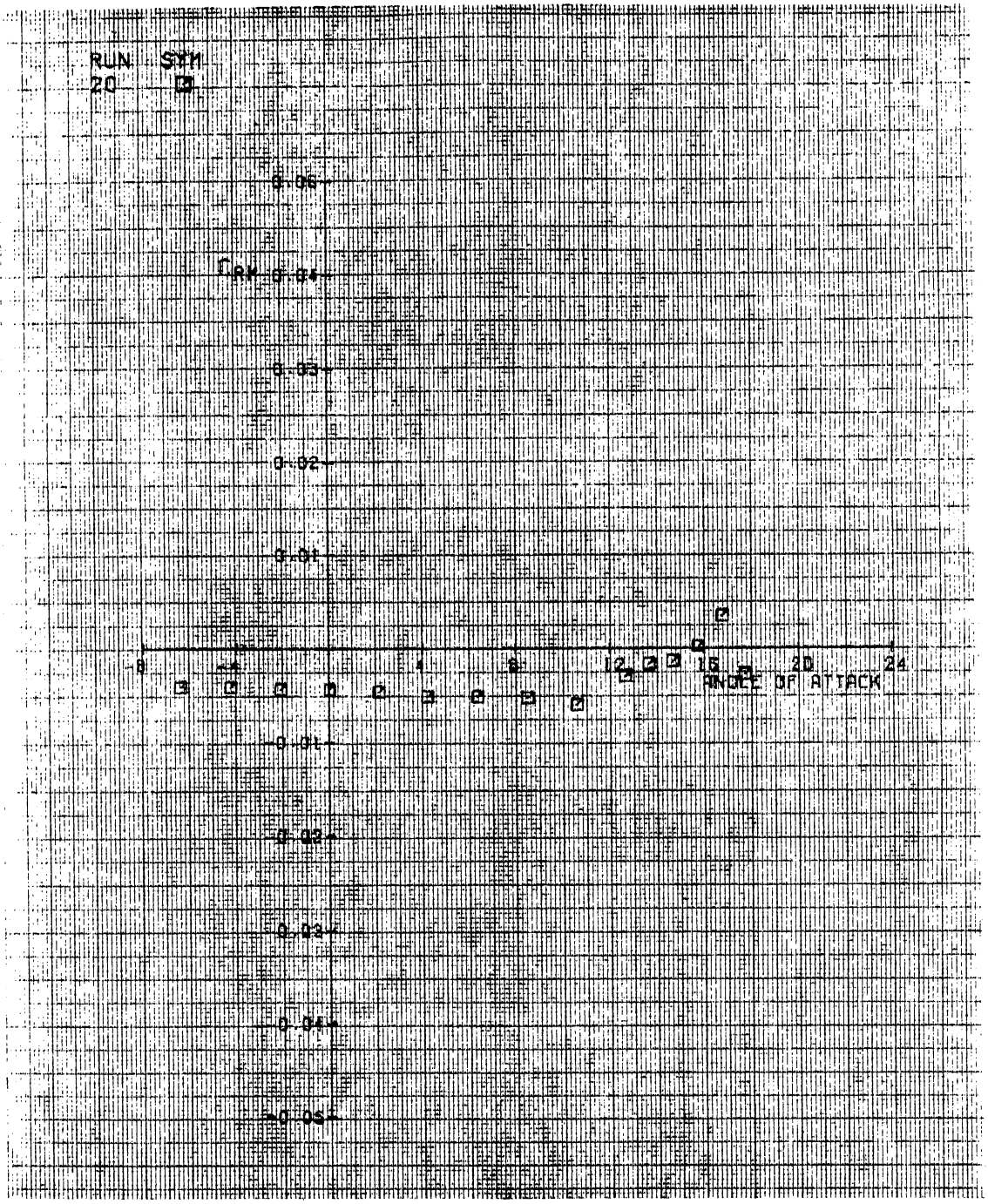

Figure 102. Run 20. Crm vs Alpha

VITA 2

Gary L. Kreps

Candidate for the Degree of

Master of Science

Thesis: AN AILERON DESIGN TO COUNTER ADVERSE YAW

Major Field: Mechanical Engineering

Biographical:

Personal Data: Born in Bristow, Oklahoma, October 18, 1948, the son of Bill J. and Edna V. Kreps. Married to Judy A. Charlson on October 20, 1973.

Education: Graduated from College High School, Bartlesville, Oklahoma in May 1966; received a Bachelor of Science degree in Mechanical and Aerospace Engineering from Oklahoma State University in July 1970; completed the requirements for the Master of Science degree at Oklahoma State University in July 1985.